TESIS DE LA UNIVERSIDAD DE ZARAGOZA

2019

36

Airama Albisa Novo

Advances in particle engineering for pharmaceutical applications

Departamento

Ingeniería Química y Tecnologías del Medio Ambiente

Director/es

Sebastián Cabeza, Víctor
Meireles-Masbernat, Martine
Piacentini, Emma

EXTRACTO

ISSN 2254-7606

Prensas de la Universidad Universidad Zaragoza

ISSN 2254-7606

Universidad Zaragoza
1542

Tesis Doctoral [Extracto]

ADVANCES IN PARTICLE ENGINEERING FOR PHARMACEUTICAL APPLICATIONS

Autor

Airama Albisa Novo

Director/es

Sebastián Cabeza, Víctor
Meireles-Masbernat, Martine
Piacentini, Emma

UNIVERSIDAD DE ZARAGOZA

Ingeniería Química y Tecnologías del Medio Ambiente

2018

Advances in particle engineering for pharmaceutical applications

A thesis submitted to obtain the degree of doctor, presented by

Airama Albisa Novo

Reduced Version

Zaragoza, 2018

Advances in particle engineering for pharmaceutical applications

A thesis

Prepared in the framework of

Erasmus Mundus Doctorate in Membrane Engineering to obtain multiple Doctorate degrees issued by

University of Zaragoza, Chemical and Environmental Engineering Department and Nanostructured Films and Particles (NFP) from Nanoscience Institute of Aragon (INA).

University of Calabria and Institute on Membrane Technology (ITM)

Université Toulouse III Paul Sabatier, Laboratoire de Génie Chimique de Toulouse (LGC).

Supervisors:

Dr. Victor Sebastian, Professor of Department of Chemical and Environmental Engineering and Aragon Nanoscience Institute, University of Zaragoza

Dr. Emma Piacentini, Researcher of Institute on Membrane Technology, National Research Council, University of Calabria

Dr. Martine Meireles, Researcher of Laboratoire de Génie Chimique, University of Toulouse - Paul Sabatier

Dr. Victor Sebastian Cabeza, Professor in the of Chemical & Environmental Engineering Department at the University of Zaragoza

INFORMS

That the thesis report entitled:

"Advances in particle engineering for pharmaceutical applications"

Has been elaborated by the student **Airama ALBISA NOVO,** under my supervision in cotutelle with the professors Dr. Emma Piacentini from University of Calabria and Dr. Martine Meireles from University of Toulouse. and **I AUTHORIZE** the presentation of this document

And for the record, I sing this document in Zaragoza _____ of _____ 2018

Dr. Victor Sebastian Cabeza, profesor del Departamento de Ingeniería Química y Tecnología del Medio Ambiente de la Universidad de Zaragoza

INFORMA

Que la memoria titulada

"Advances in particle engineering for pharmaceutical applications"

Ha sido elaborada por la estudiante **Airama Albisa Novo,** realizada bajo mi supervisión y en cotutela con los profesores Dr. Emma Piacentini de la Universidad de Calabria y Dr. Martine Meireles de la Universidad de Toulouse.

Y para que así conste, firmo este certificado en Zaragoza _____ of _____ 2018

Fdo. Dr Victor Sebastian Cabeza

Director del estudiante en la Universidad de Zaragoza

Departamento de Ingeniería Química y Tecnología del Medio Ambiente

Dr. Emma Piacentini, Researcher in Institute on Membrane Technology (ITM-CNR) at University of Calabria

INFORMS

That the thesis report entitled:

"Advances in particle engineering for pharmaceutical applications"

Has been elaborated by the student **Airama ALBISA NOVO,** under my supervision in cotutelle with the professors Dr.Victor Sebastian Cabeza from University of Zaragoza and Dr. Martine Meireles from University of Toulouse. and **I AUTHORIZE** the presentation of this document

And for the record, I sing this document in Rende (CS) _____ of _____ 2018

Dr. Emma Piacentini, investigador in Instituto de Tecnología de la Membrana (ITM-CNR) de la Universidad de Calabria.

INFORMA

Que la memoria titulada

"Advances in particle engineering for pharmaceutical applications"

Ha sido elaborada por la estudiante **Airama Albisa Novo,** realizada bajo mi supervisión y en cotutela con los profesores Dr. Victor Sebastian Cabeza de la Universidad de Calabria y Dr. Martine Meireles de la Universidad de Toulouse.

Y para que así conste, firmo este certificado en Rende (CS) _____ of _____ 2018

Fdo. Dr. Emma Piacentini

Director del estudiante en la Universidad de Calabria

Instituto de Tecnología de la Membrana (ITM-CNR)

Dr. Martine Meireles, Researcher from Laboratoire de Génie Chimique at University of Toulouse

INFORMS

That the thesis report entitled:

“Advances in particle engineering for pharmaceutical applications”

Has been elaborated by the student **Airama ALBISA NOVO,** under my supervision in cotutelle with the professors Dr. Emma Piacentini from University of Calabria and Dr. Victor Sebastian Cabeza from University of Zaragoza and **I AUTHORIZE** the presentation of this document

And for the record, I sing this document in Toulouse _____ of _____ 2018

Dr. Martine Meireles, investigador de Laboratoire de Génie Chimique en la Universidad de Toulouse

INFORMA

Que la memoria titulada

“Advances in particle engineering for pharmaceutical applications”

Ha sido elaborada por la estudiante **Airama Albisa Novo,** realizada bajo mi supervisión y en cotutela con los profesores Dr. Emma Piacentini de la Universidad de Calabria y Dr. Victor Sebastian Cabeza de la Universidad de Zaragoza.

Y para que así conste, firmo este certificado en Zaragoza Toulouse _____ of _____ 2018

Dr. Martine Meireles

Director del estudiante en la Universidad de Toulouse

Laboratoire de Génie Chimique

Acknowledgments

Last three year of this journey has been a great adventure. I wish to thank various people for their contribution to this project.

First of all, I want to thank to Erasmus Mundus Doctorate in Membrane Engineering (EUDIME) commission for grating me the scholarship to giving this phD. Especially, to Dr. Efrem Curcio and Dr. Enrico Drioli.
I would like to express my deep gratitude to Dr Victor Sebastian, Dr Emma Piacentini and Dr Martine Meireles, my research supervisors, for their patient guidance, enthusiastic encouragement and useful critiques of this research work.

I would also like to thank to the professors and researchers in University of Zaragoza. Professor Jesús Santamaria for give me the opportunity to work in NFP group. Thanks to all professors: Manuel, Reyes, Nuria, Jose Luis, Silvia, Marta, Pilar. Also, to all the postdocs, predocs and students, Roberta Manno, Cris, Kike, Fernando, MariCarmen, Gracia, Laura Español, Laura Uson, Carlos Bueno, Teresa, Vanesa, Adrian, Clara, Sara, Martha, Nuria, Martin, Maria, Dany, Giuseppe Tizio, Nidia. Also to SEM technicians: Carlos, Teo, Laura, Gala and Eugenio from the HPLC. To my friends Jorge, Diego, Sergio, Pilar, Lilliane.

My grateful thanks are also extended to the professors and researcher in University of Calabria. Dr. Lidietta Giorno for welcoming me in Institute on Membrane Technology and thank to all there, Fabio (for his support in membrane emulsification), Giuseppe Vitola, Giuseppe Ranieri, Francesca Militano, Leo D'Agostino, Alessandra, Sara, Nunzia, Carmen, Teresa, Rosalinda. Also, to friends in from other research groups that I meet there: Patricia Ayala, Paulina, Osvaldo, Edo Sanchez, Gaby, Diana Castiglioni, Alexander, Yairis, Fanny, Margarita, Diana Coello, Gloria, Vale Vale, Beatrice, Jack, Simona, Jimena Gómez, Isabel Navarro, Paul Manu, Paul Romero, Estela Narvaez, Gaston Chamba, John Marcos, Denia Cid, Celeste Garfrett, Tarteel, Maria Cristina Salatino, Parsu Reddy, Marco Rodrigo, Patricia Puspitaloka.

I would also like to extend my thanks to professors and researchers in University of Toulouse. Thank you to Dr. Pierre Aimar for welcoming in LGC group. To Dr. Kevin Roger for their support in the investigation and the colleges there: Marina, Leo, Pedro Oliveira, Asiel Hernández, Freddy Duranio Martì, Jesús Villalobos, Jr Brou, Lauren Amh, Leticia Vitola Pasetto and also to friends Camila, Cristopher, Jaime, Benja. To the EUDIME family: Magda, Mariella, Pritam, Abayneshy, Usman, Parashuram, Roberto, Sergio, Lakshmeesha, Zamidi, Mohamed Yahia, Azam, Alessio, Ahmet, Ramato, Izabella, Nayan, Efrem Curcio

Last but not the least, I would like to thank my family, because they was always supporting me from the distance, my mother Maria, my father Benito, my brother Beny and the rest of family: Maria Teresa, Monica, Carlos, Zenia, Juan, Joana, Carmen, Junior and new members family Alexandra and Maria Fernanda. My Cuban family in Zaragoza Yarelis, Javier, Sarita, María Fernanda y Leyre. My Spanish family in Zaragoza, specially to Sergio for all love and support in during this time, Fidel, Maria Jesus, Merche, Miguel, Jr Miguel, Jose Javier, Maria Jose, Inés y Lucía.

Summary

The present thesis entitled "*Advances in particle engineering for pharmaceutical applications*" has been performed under the Erasmus Mundus Doctorate in Membrane Engineering (EUDIME), (FPA 2011-0014), funded by European Union. The three partners involved are part of EUDIME consortium:

1. University of Zaragoza, Chemical and Environmental Engineering Department and Nanostructured Films and Particles (NFP) from Nanoscience Institute of Aragon (INA).
2. University of Calabria and Institute on Membrane Technology (ITM)
3. Université Toulouse III Paul Sabatier, Laboratoire de Génie Chimique de Toulouse (LGC).

Biodegradable nano/microparticles have extensive value as vehicles for drug delivery and form the basis of several therapies approved by the US Food and Drug Administration. One of the hurdles to overcome in the use of those materials as drug delivery vectors is their availability at industrial scale. Innovation in process technology is required to translate laboratory production into mass production while preserving their desired characteristics.

The transition between proof of concept and application in drug delivery system is not a simple task being the main reason that only a few drug delivery system products arrive to the market. (Wen, Jung, et Li 2015). Different challenges need to be overcome to meet the specific requirements of reproducibility, energy consumption, control of toxicity, environmental impact and productivity required for industrial application (Wood-Black 2014). Moreover there is a need for methodologies as basis for the scaling up of processes.

The main goal of this work is to develop a methodology for the production of a variety of particles (nano and microparticles). The synthesis mechanisms will be based on emulsification and nanoprecipitation by using two promising production approaches, membrane and millifluidic devices.

The specific goals to achieve are:

- Development of nano and micro emulsification techniques to produce nano/micro particles based on membrane emulsification and millifluidic devices.
- Control and tune the size distribution of particles according to the therapeutic target application (including administration route, biodistribution, target organ).
- Assessment of the proper drug encapsulation/loading to the required sustained release achieve a good control on the rate of drug release as well as on the burst release to improve the sustained drug delivery.
- Study of drug release pharmaco-kinetics in physiological conditions.
- Study the sustainability of the particle production process.

A complete overview of the spectrum of products that have been produced by using membrane and millifluidic based process combined with opportune secondary reaction are reported in Table 1.

Table 1: Spectrum of process performance with membrane and millifluidic devices.

	Chapter 2	**Chapter 3**	**Chapter 4**	**Chapter 5**
	Nanoprecipitation assisted by millifluidic system	**Nanoprecipitation assisted by membrane**	**Membrane emulsification / solvent diffusion method**	**Membrane emulsification/ glutaraldehyde crosslinking**
Polymer	PLGA-PEG	PLGA-PEG	PLGA-PEG	PVA
Drug	Dexamethasone (hydrophobic drug)	Dexamethasone (hydrophobic drug)	Dexamethasone (hydrophobic drug)	Catechol (hydrophylic drug)
Dispersed Phase (Stream 1)	Acetone	Acetone	Ethyl Acetate	Water
Continuous Phase (Stream 2)	Water	Water	Water	Isooctane
First Step	Nanoprecipitation using microchannels	Nanoprecipitation using membrane pores	O/W Membrane Emulsification	W/O Membrane Emulsification
Second Step			Solvent diffusion method	Glutaraldehyde crosslinking

The thesis is structured into one introduction chapter (**Chapter 1**), four experimental chapters (**Table 1: Chapter 2-5**), conclusion (**Chapter 6**) list of references and the appendix.

Chapter 1 provides a review of the state-of-the art of drug delivery systems including their production. The chapter is divided in three parts. First, the controlled release mechanism and the materials frequently used in drug carriers manufacturing will be described. Secondly, the different available methodologies able to control the main features of particulate systems for drug delivery will be highlighted. Finally, the specific challenges for the transition from the proof of concept to the application in drug delivery for particles manufacturing will be pointed out.

Chapter 2 study the PLGA-PEG nanoprecipitation using a millimixer device. Nanoprecipitation is highly attractive for nanoparticles production due to the low energy input required. The main challenge in polymeric NPs production by nanoprecipitation process is to achieve a fine control of the mixing processes

for large-scale production. The strategy is based on an adequate composition of two different streams in terms of PLGA-PEG and acetone mass fraction based on the specific ternary phase diagram of PLGA-PEG polymer/acetone/water. Then the effect of phase composition on morphology, particle size (Z-Average) and particle size distribution (PDI) of nanoparticles was studied. Regarding the encapsulation of the drug inside of the nanoparticles a first step was achieved by the construction of the ternary phase diagram of the DEX/acetone/water and the quaternary phase of PLGA-PEG/DEX/Water/Acetone. The drug encapsulation efficiency and drug loading efficiency were investigated and correlated with the quaternary phase diagram maximizing EE and DLE.

Chapter 3 studies the production of dexamethasone-loaded PLGA-PEG nanoparticles by membrane-assisted nanoprecipitation. Membranes are being increasingly used as the system of choice for scaling up the production of emulsions and particles. However, few examples are reported in literature on the use of membranes to assist nanoprecipitation process. The chapter will show the potentially of the use of membrane to develop a scalable continuous process suitable for the formulation of PLGA-PEG nanoparticle as drug delivery carriers. Process development and drug release aspects have been studied because considered essential regarding a potential clinic translation and industrial scale production.

Chapter 4 demonstrates the sustainable production of PLGA-PEG microparticles by membrane emulsification/solvent diffusion. The sustainability assessment of the process was evaluated by considering the properties of the polymeric particles produced (size, size uniformity, and drug encapsulation efficiency) together with the energy consumption. To determine the green impact of the particles production method proposed, the metric based on the Green Aspiration Level™ (GAL) was used. The impact of solvents used for polymer dissolution (EA or DCM), fluid-dynamic and operative conditions applied during membrane emulsification and solidification steps, respectively, were investigated.

Chapter 5 presents the production of Catechol encapsulated PVA particle by W/O membrane emulsification/crosslinking. Encapsulation of hydrophilic and/or amphiphilic small molecules is challenging due to the partitioning of drug from the polymeric phase into the external phase before solidification of the particles. In this chapter the encapsulation efficiency and drug loading efficiency of Catechol, a hydrophilic biomolecule, in PVA particles have been studied. Process development, drug release aspects and cytotoxicity have been assessed because are considered essential for the potential clinic translation and industrial scale production of drug delivery systems.

Chapter 6 contains the main conclusions of this thesis.

Finally, bibliography referenced throughout the document is shown and the appendix, where some important supplementary information is added

EUDIME project has an interdisciplinary characteristic demanding the collaboration of researchers from different scientific branches and institutions. Among them, I wish to highlight the collaboration with:

- University of Zaragoza: I have worked for 16 months in the design of polymeric materials, selection of drug related to biomedical applications, toxicity test, drug delivery and materials characterization.
    - Dr. Victor Sebastian (Professor of Department of Chemical and Environmental Engineering and Aragon Nanoscience Institute)
    - Dr. Jesus Santamaria (Professor of Department of Chemical and Environmental Engineering and Aragon Nanoscience Institute)
    - Dr. Manuel Arruebo (Professor of Department of Chemical and Environmental Engineering and Aragon Nanoscience Institute)
    - Dr. Gracia Mendoza (Researcher of Center for Biomedical Research of Aragon (CIBA))
- University of Calabria: I have worked in the design of membrane emulsification process for 11 months.
    - Dr.Emma Piacentini (Researcher of Institute on Membrane Technology, National Research Council, University of Calabria)
    - Dr. Lidietta Giorno (Director of Institute on Membrane Technology, National Research Council, University of Calabria)
    - Dr. Fabio Bazzarelli (Researcher of Institute on Membrane Technology, National Research Council, University of Calabria)
- University of Toulouse: I have worked in phase solubility diagrams and the design of millifluidic process for 9 months.
    - Dr.Martine Meireles (Researcher of Laboratoire de Génie Chimique, University of Toulouse - Paul Sabatier)
    - Dr. Kevin Roger (Researcher of Laboratoire de Génie Chimique, University of Toulouse -Paul Sabatier)

Resumen

La presente tesis titulada “Avances en la ingeniería de producción de partículas para la aplicación farmacéutica” ha sido realizada bajo el programa EUDIME (del inglés Erasmus Mundus Doctorate in Membrane Engineering, (FPA 2011-0014), subvencionado por la Unión Europea. Las tres universidades involucradas en esta tesis son parte del consorcio EUDIME:

1. Universidad de Zaragoza, Departamento de Ingeniería Química y Medio Ambiente y el Instituto de Nanociencia de Aragón (INA)
2. Universidad de Calabria y Instituto de Tecnología de la Membrana (ITM)
3. Universidad de Toulouse III Paul Sabatier, Laboratorio de Ingeniería Química de Toulouse (LGC).

Las nano/microparticles biodegradables tienen gran valor como vehículo para la liberación controlada de biomoléculas y son la base de muchas terapias aprobadas por la FDA (del inglés Food and Drug Administration) de Estados Unidos. Uno de los grandes problemas por solucionar en la utilización de estos materiales como vectores para la liberación de fármacos, es su disponibilidad a escala industrial. Por lo que, la innovación en procesos tecnológicos es requerida para lograr trasladar la producción a escala de laboratorio en producción a escala industrial, conservando sus características.

La transición desde la prueba de concepto y la aplicación en sistemas de liberación controlada no es una tarea fácil debido a lo cual solo un pequeño grupo de estos sistemas han llegado al mercado. (Wen, Jung, et Li 2015). Son diversos los retos que deben ser superados para lograr los requerimientos específicos de los sistemas de liberación contralada, como son reproducibilidad, consume de energía, control de toxicidad, impacto ambiental y productividad. (Wood-Black 2014). Además, existe la necesidad de metodologías como base para el escalado de los procesos.

El principal objetivo de este trabajo es el desarrollo de una metodología para la producción de variedades de partículas (nano and micropartículas). La síntesis estará basada en los procesos de emulsificación y nanoprecipitación; utilizando dos sistemas de producción muy prometedores, membrana y dispositivos de millifluidica.

Los objetivos específicos a llevar a cabo son:

- Desarrollo de técnicas de nano y micro emulsificación para la producción de nano / micro partículas utilizando emulsificación por membrana y dispositivos de milifluídica.
- Controlar y ajustar la distribución del tamaño de las partículas de acuerdo con la aplicación terapéutica (incluida la vía de administración, la biodistribución, el órgano diana).
- Lograr una adecuada encapsulación / carga del fármaco para la liberación sostenida requerida para un buen control sobre la velocidad de liberación del fármaco.

- Estudiar la farmacocinética de liberación de fármacos en condiciones fisiológicas.
- Estudiar la sostenibilidad del proceso de producción de partículas.

En la Tabla 1 se presenta una descripción completa de los productos que se han producido mediante el uso de procesos basados en membranas y dispositivos de milifluidica combinados con una reacción secundaria oportuna.

Table 1: Espectro de procesos de producción de partículas utilizando membranas y dispositivos de millifluidica.

	Capítulo 2	**Capítulo 3**	**Capítulo 4**	**Capítulo 5**
	Nanoprecipitación asistida por sistemas millifluidicos.	**Nanoprecipitación asistida por membranas**	**Método de emulsificación por membrana/ difusión de solvente**	**Método emulsificación por membrana/ entrecruzamiento utilizando glutaraldehído**
Polímero	PLGA-PEG	PLGA-PEG	PLGA-PEG	PVA
Fármaco	Dexametasona (fármaco hidrofílico)	Dexametasona (fármaco hidrofílico)	Dexametasona (fármaco hidrofílico)	Catecol (fármaco hidrofóbico)
Fase Dispersa (Corriente 1)	Acetona	Acetona	Acetato de etilo	Agua
Fase Continua (Corriente 2)	Agua	Agua	Agua	Isooctano
Primera Etapa	Nanoprecipitación utilizando microcanales	Nanoprecipitación utilizando poros de la membrana	O/W Emulsificación por membrana	W/O Emulsificación por membrana
Segunda Etapa			Difusión del solvente	Entrecruzamiento utilizando glutaraldehído

La tesis está estructurada con un capítulo introductorio (**Capitulo 1**), cuatro capítulos experimentales (**Tabla 1: Capítulo 2-5**), conclusión (**Capítulo 6**) lista de referencias y los anexos

El **Capítulo 1** provee una revisión del estado del arte de los sistemas de liberación controlada incluyendo su producción. Este capítulo esta' dividido en tres partes. Primero, se describe el mecanismo de liberación controlada y los materiales más frecuentes utilizados para producir estos sistemas. En segundo lugar, se

destacan las diferentes metodologías disponibles para producir los sistemas particulados para la administración de medicamentos. Finalmente, se señalan los desafíos específicos para la transición de la prueba de concepto a la aplicación la manufactura de partículas para sistemas de liberación controlada.

El **capitulo 2** estudia la nanoprecipitación del PLGA-PEG utilizando un dispositivo de millimezclado. La nanoprecipitación es un proceso altamente atractivo para la producción de nanopartículas debido al bajo consumo energético que requiere. El principal desafío en la producción de nanopartículas poliméricas utilizando el proceso de nanoprecipitación es lograr un control fino de los procesos de mezcla para la producción a gran escala. Esta estrategia se basa en encontrar una composición adecuada de dos corrientes diferentes como son el PLGA-PEG y fracción másica de acetona utilizando el diagrama de fase ternario del polímero PLGA-PEG / acetona / agua. A continuación, se estudió el efecto de la composición de fase sobre la morfología, el tamaño de partícula (Z-average) y la distribución del tamaño de partículas (PDI) de las nanopartículas. La encapsulación del fármaco dentro de las nanopartículas se logró estudiar mediante la construcción del diagrama de fases ternarias de DEX / acetona / agua y la fase cuaternaria de PLGA-PEG / DEX / agua / acetona. Se investigo' la eficiencia de la encapsulación y la capacidad de carga y se correlacionaron con el diagrama de la fase cuaternaria que maximiza EE y DLE.

El **capítulo 3** estudia la producción de nanopartículas de PLGA-PEG cargadas con dexametasona mediante nanoprecipitación asistida por membrana. Las membranas se utilizan cada vez más para los escalados de la producción de emulsiones y partículas. Sin embargo, pocos ejemplos se informan en la literatura sobre el uso de membranas combinadas con proceso de nanoprecipitación. El capítulo muestra el potencial del uso de las membranas para desarrollar un proceso continuo y escalable para la formulación de nanopartículas de PLGA-PEG. Los aspectos del desarrollo de procesos y la liberación de fármacos se han estudiado debido a que se consideran esenciales para la aplicación del del potencial clínico y la producción de las nanopartículas a escala industrial.

El **Capítulo 4** muestra la producción sostenible de micropartículas de PLGA-PEG por emulsificación por membrana / difusión de disolvente. La evaluación de sostenibilidad del proceso se realizó considerando las propiedades de las partículas poliméricas producidas (tamaño, uniformidad y eficiencia de encapsulación) junto con el consumo de energía. Para determinar el impacto verde del método de producción de partículas propuesto, se utilizó la métrica basada en método GAL (del inglés Green Aspiration Level ™). Se investigó el impacto de los disolventes utilizados para la disolución del polímero (EA o DCM), la dinámica de fluido y condiciones operacionales aplicadas durante la emulsificación por membrana y las etapas de solidificación, respectivamente.

El **Capítulo 5** presenta la producción de partículas de PVA encapsuladas con Catechol mediante W/O emulsificación por membrana /entrecruzamiento utilizando glutaraldehído. La encapsulación de moléculas pequeñas hidrófilas y / o anfifílicas es desafiante debido a la dispersión del fármaco desde la fase polimérica a la fase externa antes de la solidificación de las partículas. En este capítulo, se han estudiado la eficiencia de encapsulación y la capacidad de carga del Catechol, una biomolécula hidrófila, en partículas de PVA. Se han evaluado el desarrollo del proceso, los aspectos de liberación del fármaco y la citotoxicidad porque se consideran esenciales para el desarrollo de partículas con potencial clínico potencial, así como en su producción a escala industrial.

El **Capítulo 6** contiene las conclusiones fundamentales de la tesis.

Finalmente, se muestra las citas bibliográficas referenciadas durante todo el documento y se desglosan los anexos, donde importante información complementaria es añadida. El proyecto EUDIME tiene unas características interdisciplinarias por lo que demanda la colaboración de investigadores de diversas ramas e instituciones. Debido a esto, quisiera resaltar la colaboración con:

- Universidad de Zaragoza: He trabajado por 16 meses en el diseño de materiales poliméricos, la selección del fármaco, análisis de toxicidad, ensayos de liberación controlado y caracterización de materiales.
    - Dr. Victor Sebastian (Profesor del Departamento de Ingeniería Química y Ambiental e investigador del Instituto de Nanociencia de Aragón)
    - Dr. Jesus Santamaria (Profesor del Departamento de Ingeniería Química y Ambiental e investigador del Instituto de Nanociencia de Aragón)
    - Dr. Manuel Arruebo (Profesor del Departamento de Ingeniería Química y Ambiental e investigador del Instituto de Nanociencia de Aragón)
    - Dr. Gracia Mendoza (Investigador Centro de Investigación Biomédica de Aragón (CIBA))
- University of Calabria: He trabajado en el diseño del proceso de emulsificación por membrana por 11 meses.
    - Emma Piacentini (Investigador del Instituto de Tecnología de la Membrana, Consejo Nacional de Investigación, Universidad de Calabria)
    - Dr. Lidietta Giorno (Director del Instituto de Tecnología de la Membrana, Consejo Nacional de Investigación, Universidad de Calabria)
    - Dr. Fabio Bazzarelli (Investigador del Instituto de Tecnología de la Membrana, Consejo Nacional de Investigación, Universidad de Calabria)

- University of Toulouse: He trabajado en la construcción de los diagramas de fases y el diseño del proceso de millifluidica por 9 meses.
    - Martine Meireles (Investigador del Laboratorio de Ingeniería Química de Toulouse (LGC), Universidad de Toulouse III Paul Sabatier)
    - Dr. Kevin Roger (Investigador del Laboratorio de Ingeniería Química de Toulouse (LGC), Universidad de Toulouse III Paul Sabatier)

Sommario

Il presente lavoro di tesi intitolato “Advances in particle engineering for pharmaceutical application” è stato condotto nell’ambito del dottorato “Erasmus Mundus” in “Membrane Engineering” (EUDIME), (FPA 2011-0014), finanziato dall’Unione Europea. Le tre istituzioni coinvolte sono parte del consorzio EUDIME:

1. Universitá di Saragozza, Dipartimento di Ingegneria Chimica e Ambientale, gruppo di Particelle e Films Nanostrutturati (NFP) dell’Istituto di Investigazione di Aragonia (INA)
2. Universitá della e Instituto per la Tecnologia delle Membrane (ITM)
3. Universitá di Toulouse II Paul Sabatier, Laboraorio di Ingegneria Chimica di Toulouse

L’impiego di nano/microparticelle biodegradabili come sistemi di veicolazione di farmaci ha ricevuto un crescente interesse ed è alla base di diversi sistemi terapeutici approvati dall’Agenzia per gli Alimenti e i Medicinali statunitense. Una delle principali limitazioni all’uso di questi materiali come sistemi di veicolazione di farmaci è la loro produzione su scala industriale. Nuove strategie nel processo produttivo infatti sono necessarie per trasferire i risultati ottenuti su scala laboratorio nella produzione su larga scala mantenendo invariate le proprietà che il prodotto finale deve possedere sulla base dell’applicazione finale cui è destinato.

Il passaggio dalla “prof of concept” all'applicazione come sistemi di somministrazione di farmaci non è cosa semplice, come dimostrato dal fatto che sul mercato arrivano solo alcuni dei prodotti studiati (Wen, Jung, et Li 2015). Diverse sfide devono essere ancora superate per soddisfare requisiti specifici di riproducibilità, consumo energetico, controllo della tossicità, impatto ambientale e produttività richiesti per l’applicazione a livello industriale (Wood-Black 2014). In particolare, sono richieste metodologie avanzate per la produzione su larga scala di tali particelle.

Il principale obiettivo di questo lavoro di tesi è lo sviluppo di una metodologia per la produzione di particelle dell’ordine dei nanometri fino a pochi micron basata sull’emulsificazione e la nanoprecipitazione usando due promettenti approcci, la tecnologia a membrana ed i sistemi microfluidici.

Gli obiettivi specifici da raggiungere sono i seguenti:

- Sviluppare tecniche di nano/micro emulsificazione per produrre nano/microparticelle basate sull’emulsificazione a membrana e su sistemi microfluidici.
- Controllare e modulare la distribuzione delle particelle in base all’applicazione terapeutica specifica (considerando la via di somministrazione, la biodistribuzione, l’organo bersaglio).
- Ottenere l’appropriato incapsulamento del farmaco per il suo rilascio prolungato ed ottenere un efficiente controllo sulla velocità di rilascio del farmaco.
- Studiare la cinetica di rilascio del farmaco in condizioni fisiologiche.

- Studiare la sostenibilità del processo di produzione di particelle prodotte come sistemi di rilascio di farmaci.

Una panoramica completa delle diverse particelle prodotte e dei metodi impiegati per la loro produzione (incluse le reazioni secondarie necessarie alla solidificazione delle particelle liquide in forma di emulsioni) è riportata nella Tabella 1.

Tabella 1: Metodi di produzione di partielle polimeriche impigati nel presente lavoro di tesi.

	Capitolo 2	**Capitolo 3**	**Capitolo 4**	**Capitolo 5**
	Nanoprecipitazione attraverso sistemi microfluidici	**Nanoprecipitazione attraverso membrana**	**Metodo di emulsificazione attraverso membrana/ diffusione del solvente**	**Metodo di emulsificazione attraverso membrana/ reticolazione del glutaraldehyde**
Polimero	PLGA-PEG	PLGA-PEG	PLGA-PEG	PVA
Dopante	Dexamethasone (dopante idrofobico)	Dexamethasone (dopante idrofobico)	Dexamethasone (dopante idrofobico)	Catechol (dopante idrofilico)
Fase Dispersa (Flusso 1)	Acetone	Acetone	Etilacetato	Acqua
Fase Continua (Flusso 2)	Acqua	Acqua	Acqua	Isoottano
Step 1	Nanoprecipitazione attraverso microcanali	Nanoprecipitazione attraverso i pori della membrana	O/W Emulsificazione della membrana	W/O Emulsificazione della membrana
Step 2			Metodo di diffusione del solvente	Reticolazione del Glutaraldehyde

La tesi è strutturata in un capitolo introduttivo (Capitolo 1), quattro capitoli relativi all'attività sperimentale (Tabella 1, Capitoli 2-5), un capitolo conclusivo (Capitolo 6), lista delle referenze e annex.

Nel **Capitolo 1** è stata condotta un'analisi dello stato dell'arte dei sistemi di rilascio di farmaci e dei metodi usati per la loro produzione. Il capitolo è diviso in 3 parti. Nella prima parte sono descritti i meccanismi alla base del rilascio del farmaco ed i materiali frequentemente impiegati nello sviluppo di sistemi carrier. Nella seconda parte, sono illustrate le diverse metodologie disponibili per controllare la produzione di

particelle. Infine, sono analizzate le specifiche sfide da affrontare per promuovere il passaggio dagli studi in laboratorio all'applicazione finale dei sistemi di rilascio controllato basati su particelle.

Nel **Capitolo 2** è stato studiato il processo di nanoprecipitazione del PLGA-PEG usando un millimixer device. Il processo di nanoprecipitazione è altamente attraente per la produzione di nanoparticelle grazie al basso consumo di energia. Il principale obiettivo da raggiungere nella produzione di nanoparticelle mediante nanoprecipitazione è ottenere un fine controllo del processo di miscelazione nella produzione su larga scala. Il processo è basato sull'adeguata composizione di due differenti flussi in termini di quantità di PLGA-PEG e acetone sulla base del diagramma a tre fasi PLGA-PEG/acetone/acqua. È stato quindi studiato l'effetto della composizione delle fasi sulla morfologia, la dimensione (Z-average) e la distribuzione della dimensione (PDI) delle nanoparticelle. Per quanto riguarda l'incapsulamento del farmaco, un primo risultato è stato raggiunto nella costruzione del diagramma di fase ternario DEX/acetone/acqua e quaternaio PLGA-PEG/ DEX/acetone/acqua. L'efficienza di incapsulamento e di carico del farmaco sono state studiate rispetto al diagramma quaternario al fine di ottenere i più elevati valori di EE and DLE.

Nel **Capitolo 3** è stata studiata la produzione di nanoparticelle di PLGA-PEG contenenti desametasone mediante nanoprecipitazione assistita da membrana. Le membrane vengono sempre più utilizzate come metodologie alternative nella produzione di emulsioni e particelle. Tuttavia, pochi esempi sono riportati in letteratura sull'uso delle membrane per promuovere il processo di nanoprecipitazione. Il capitolo mostrerà il potenziale uso delle membrane nello sviluppo di un processo continuo, scalabile, adatto per la formulazione di nanoparticelle di PLGA-PEG come sistemi di veicolazione di farmaci. Gli aspetti dello sviluppo del processo e del rilascio del farmaco sono stati anche studiati perché considerati essenziali per il potenziale utilizzo clinico e la produzione su scala industriale.

Il **Capitolo 4** dimostra la produzione sostenibile di microparticelle di PLGA-PEG mediante emulsificazione a membrana accoppiata a diffusione del solvente. La valutazione della sostenibilità del processo è stata valutata considerando le proprietà delle particelle polimeriche prodotte (dimensione, uniformità delle dimensioni e efficienza di incapsulamento del farmaco) insieme al consumo di energia. Per determinare l'impatto ambientale del metodo di produzione delle particelle proposto, è stata utilizzata la metrica basata sul Green Aspiration Level ™ (GAL). Sono stati anche studiati l'influenza del solvente utilizzato per disciogliere il polimero (EA o DCM), le condizioni fluidodinamiche e operative applicate durante gli step di emulsificazione a membrana e successiva solidificazione.

Nel **Capitolo 5** è presentata la produzione di particelle di PVA contenenti Catecolo mediante emulsificazione a membrana accoppiata a reazione di reticolazione di emulsioni acqua-in-olio.

L'incapsulamento di piccole molecole idrofile e / o anfifiliche è reso difficile dalla ripartizione del farmaco tra la fase polimerica e la fase esterna (idrofobica) prima della solidificazione delle particelle. In questo capitolo sono stati studiati l'efficienza di incapsulamento del catecolo, una biomolecola idrofila, nelle particelle di PVA. L'ottimizzazione del processo, gli aspetti del rilascio del farmaco e la citotossicità sono stati valutati perché considerati essenziali per la potenziale applicazione clinica di tali sistemi di somministrazione di farmaci e la loro produzione su scala industriale.

Il **Capitolo 6** contiene le principali conclusioni del lavoro di tesi.

Il **Capitolo 7** contiene.

Infine, la bibliografia usata come referenza in tutto il documento è presentata y gli annex, dove vengono aggiunte alcune importanti informazioni supplementari relative al lavoro sperimentale condotto.

Il progetto EUDIME ha un carattere interdisciplinare che richiede la collaborazione di ricercatori con esperienza in diversi settori ed appartenenti a diverse istituzioni scientifiche. Tra questi, desidero evidenziare la collaborazione con:

• l' Università di Saragozza dove ho lavorato per 16 mesi nella progettazione di materiali polimerici, selezione di farmaci correlati alle applicazioni biomediche, test di tossicità, somministrazione di farmaci e caratterizzazione dei materiali.

  - Dr. Victor Sebastian (Professore del Dipertimento di Ingegneria Chimica e Ambientale dell'Istituto di Investigazione di Aragonia)
  - Dr. Jesus Santamaria (Professore del Dipertimento di Ingegneria Chimica e Ambientale dell'Istituto di Investigazione di Aragonia)
  - Dr. Manuel Arruebo (Professore del Dipertimento di Ingegneria Chimica e Ambientale dell'Istituto di Investigazione di Aragonia)
  - Dr.sa Gracia Mendoza (Ricercatrice del Centro di Ricerca Biomedica di Aragonia (CIBA))

- L'Università della Calabria presso cui mi sono accupata del design del processo di emulsificazione a membrana per 11 mesi.
  - Emma Piacentini (Ricercatrice dell'Istituto per la Tecnologia delle Membrane, Consiglio Nazionale della Ricerca, Universitá della Calabria)
  - Dr.sa Lidietta Giorno (Direttrice dell'Istituto per la Tecnologia delle Membrane, Consiglio Nazionale della Ricerca, Universitá della Calabria)
  - Dr. Fabio Bazzarelli (Ricercatore dell'Istituto per la Tecnologia delle Membrane, Consiglio Nazionale della Ricerca, Universitá della Calabria)

• l'Università di Toulouse dove ho lavorato alla costruzione dei diagrammi di fase ed il design del processo microfluidico per 9 mesi.

- Martine Meireles (Ricercatrice del Laboratorio di Ingegneria Chimica, Universitá di Toulouse – Paul Sabatier)
- Dr. Kevin Roger (Ricercatore del Laboratorio di Ingegneria Chimica, Universitá di Toulouse – Paul Sabatier)

Résumé

La présente thèse intitulée « avancées en ingénierie des particules pour des applications pharmaceutiques » a été effectuée dans le cadre Erasmus Mundus Doctorate in Membrane Engineering (EUDIME), (FPA 2011-0014), financée par l'Union Européenne. Les trois partenaires impliqués font partie du consortium EUDIME :

1. Le Département d'Ingénierie Chimique et Environnementale de l'Université de Saragosse et le « Nanostructured Films and Particles » (NFP) de l'Institut de Nanosciences d'Aragon (INA).
2. L'Université de Calabria et l'Institut de Technologies Membranaires (ITM)
3. L'Université Toulouse III Paul Sabatier, Laboratoire de Génie Chimique de Toulouse (LGC).

Les nano/microparticules biodégradables ont une valeur importante en tant que vecteurs pour l'administration de médicaments et constituent la base de plusieurs thérapies approuvées par le « Food and Drug Administration » des Etats-Unis. Un des obstacles à surmonter dans le cadre de l'utilisation de ces matières comme vecteurs d'administration médicamenteuse est leur disponibilité à l'échelle industrielle. Une innovation dans la technologie du procédé est requise pour convertir une production en laboratoire en production de masse tout en préservant leurs caractéristiques voulues.

La transition entre la démonstration de faisabilité et l'application dans le système d'administration de médicament n'est pas une tâche simple, ceci étant la raison principale pour laquelle seul un faible nombre de produit de système d'administration de médicament arrive sur le marché (Wen, Jung et Li, 2015). Différents défis doivent être surmontés afin d'atteindre les contraintes spécifiques de reproductibilité, consommation énergétique, contrôle de toxicité, d'impact environnemental et de productivité requises pour une application industrielle (Wood-Black 2014). En outre, il existe un besoin de méthodologies servant de base pour l'augmentation d'échelle des procédés.

Le principal objectif de ce travail est de développer une méthodologie pour la production d'une diversité de particules (nano et microparticules). Les mécanismes de synthèse seront basés sur l'émulsification et la nanoprécipitation en utilisant deux approches de production prometteuses, des outils membranaires et de milli-fluidique.

Les objectifs spécifiques à atteindre sont :

- Le développement de techniques de nano- et microémulsification pour produire des nano/microparticules basées sur l'émulsification membranaire et des outils milli-fluidiques.
- Contrôler et régler la distribution en taille des particules selon l'application thérapeutique ciblée (incluant la voie d'administration, la biodistribution, l'organe cible).
- L'évaluation de l'encapsulation/charge du médicament correspondant au niveau requis de largage, pour acquérir un bon contrôle sur la vitesse d'émission du médicament ainsi que sur l'émission du « burst », afin d'améliorer la durabilité de l'administration du médicament.

- L'étude de la pharmaco-cinétique de l'émission du médicament dans des conditions physiologiques.
- L'étude de la durabilité du procédé de production de particules.

Une vue d'ensemble complète du spectre de produits qui ont été produits en utilisant des procédés basés sur les membranes et la milli-fluidique combinés avec une réaction secondaire opportune est donnée dans le tableau 1.

Tableau 1 : Spectre de performance du procédé avec des outils membranaires et milli-fluidiques.

	Chapitre 2	**Chapitre 3**	**Chapitre 4**	**Chapitre 5**
	Nanoprécipitation assistée par un système millifluidique	**Nanoprécipitation assistée par membrane**	**émulsification de membrane / méthode de diffusion du solvant**	**émulsification de membrane/ réticulation de glutaraldéhyde**
Polymère	PLGA-PEG	PLGA-PEG	PLGA-PEG	PVA
Médicament	Dexamethasone (médicament hydrophobe)	Dexamethasone (médicament hydrophobe)	Dexamethasone (médicament hydrophobe)	Catechol (médicament hydrophyle)
Phase dispersée (Courant 1)	Acétone	Acétone	Acétate d'éthyle	Eau
Phase continue (Courant 2)	Eau	Eau	Eau	Isooctane
Première étape	Nanoprécipitation en utilisant des micro-canaux	Nanoprécipitation en utilisant des pores membranaires	O/W émulsification membranaire	W/O émulsification membranaire
Deuxième étape			méthode de diffusion du solvant	Réticulation de glutaraldéhyde

La thèse est structurée en un chapitre d'introduction (**Chapitre 1**), quatre chapitres expérimentaux (**Tableau 1 : Chapitres 2 à 5**), une conclusion (**Chapitre 6**), une liste des références et les annexes.

Le **Chapitre 1** fournit une revue de l'état de l'art des systèmes d'administration de médicaments en incluant leur production. Le chapitre est divisé en trois parties. Tout d'abord, le mécanisme d'émission contrôlé et les matériaux fréquemment utilisés dans la fabrication de vecteurs de médicaments seront décrits. Ensuite, les différentes méthodologies disponibles capables de contrôler les principales caractéristiques des systèmes particulaires pour l'administration de médicaments seront mises en évidence. Enfin, les défis spécifiques pour la transition de la démonstration de faisabilité jusqu'à l'application dans l'administration de médicaments pour la fabrication de particules seront indiqués.

Le **Chapitre 2** étudie la nanoprécipitation PLGA-PEG en utilisant un outil de milli-mélange. La nanoprécipitation est hautement attractive pour la production de nanoparticules du fait du faible besoin nécessaire en énergie. Le défi principal dans la production de nanoparticules en polymères par des procédés de nanoprécipitation est de parvenir à contrôler finement les procédés de mélange pour une production à grande échelle. La stratégie est fondée sur une composition adéquate de deux différents courants en termes de fraction massique en PLGA-PEG et en acétone, basée sur le diagramme de phase ternaire spécifique au système polymère PLGA-PEG/acétone/eau. Par la suite, l'effet de la composition de phase sur la morphologie, la taille de particule (moyenne Z) et la distribution de taille de particule (PDI) des nanoparticules a été étudié. En considérant l'encapsulation du médicament à l'intérieur des nanoparticules, une première étape a été franchie avec la construction du diagramme de phase ternaire du système DEX/acétone/eau et du diagramme de phase quaternaire du système PLGA-PEG/DEX/eau/acétone. L'efficacité d'encapsulation du médicament et l'efficacité de la charge du médicament ont été investiguées et corrélées avec le diagramme de phase quaternaire en maximisant EE et DLE.

Le **Chapitre 3** étudie la production de nanoparticules de PLGA-PEG chargées en dexamethasone par nanoprécipitation assistée par membrane. Les membranes sont de plus en plus utilisées comme système choisi pour l'augmentation d'échelle de production d'émulsions et de particules. Néanmoins, peu d'exemples sont rapportés dans la littérature sur l'utilisation de membranes pour assister les procédés de nanoprécipitation. Le chapitre montre le potentiel de l'utilisation de membranes pour développer un procédé continu évolutif adapté à la formulation de particules de PLGA-PEG comme vecteurs d'administration de médicaments. Le développement du procédé et les aspects d'émission du médicament ont été étudiés parce qu'ils sont considérés comme essentiels en vue d'une potentielle mise en application clinique et production à l'échelle industrielle.

Le **Chapitre 4** démontre le caractère durable de la production de microparticules de PLGA-PEG par émulsification membranaire/diffusion de solvant. L'analyse de durabilité du procédé a été évaluée en considérant les propriétés des particules de polymères produites (taille, uniformité de taille, et efficacité d'encapsulation du médicament) en parallèle avec la consommation d'énergie. Pour déterminer l'impact environnemental de la méthode de production de particules proposée, l'échelle basée sur le « Green Aspiration Level™ » (GAL) a été utilisée. L'impact du solvant utilisé pour la dissolution du polymère (EA ou DCM), et les conditions hydrodynamiques et opératoires appliquées durant les étapes d'émulsification membranaire et de solidification, respectivement, ont été investigués.

Le **Chapitre 5** présente la production de particules de PVA encapsulées avec du catechol par émulsification membranaire/réticulation W/O. L'encapsulation de petites molécules hydrophiles et/ou amphiphiles est difficile à cause du partitionnement du médicament de la phase polymère vers la phase externe avant solidification des particules. Dans ce chapitre ont été étudiées l'efficacité d'encapsulation et l'efficacité de la charge du médicament du Catechol, une biomolécule hydrophile, dans des particules de PVA. Le développement du procédé, les aspects d'émission du médicament et la cytotoxicité ont été évalués car ils sont considérés comme essentiels pour une potentielle application clinique et une production à l'échelle industrielle de ces systèmes d'administration de médicaments.

Le **Chapitre 6** contient les principales conclusions de cette thèse.

Enfin, les références bibliographiques citées tout au long du document est présentée et les annexes, dans lesquelles des informations importantes supplémentaires sont ajoutées.

Le projet EUDIME présente un caractère interdisciplinaire requérant la collaboration de chercheurs de différentes branches scientifiques et institutions. Parmi celles-ci, je souhaite mettre en évidence la collaboration avec :

- L'Université de Saragosse : j'ai travaillé pendant 16 mois sur le design de matériaux polymères, le choix de médicaments reliés à des applications médicales, des tests de toxicité, l'administration des médicaments et la caractérisation des matériaux.
    - Dr. Victor Sebastian (Professeur du Département d'Ingénierie Chimique et Environnementale et de Institut de Nanosciences d'Aragon)
    - Dr. Jesus Santamaria (Professeur du Département d'Ingénierie Chimique et Environnementale et de Institut de Nanosciences d'Aragon)
    - Dr. Manuel Arruebo (Professeur du Département d'Ingénierie Chimique et Environnementale et de Institut de Nanosciences d'Aragon)
    - Dr. Gracia Mendoza (Chercheur du Centre de Recherche Biomédicale d'Aragon (CIBA))
- L'Université de Calabria : j'ai travaillé sur le design de procédés d'émulsification membranaire pendant 11 mois.
    - Emma Piacentini (Chercheur de l'Institute on Membrane Technology, National Research Council, Université de Calabria)
    - Dr. Lidietta Giorno (Directeur de l'Institute on Membrane Technology, National Research Council, Université de Calabria)
    - Dr. Fabio Bazzarelli (Chercheur de l'Institute on Membrane Technology, National Research Council, Université de Calabria)

- L’Université de Toulouse : j’ai travaillé sur les diagrammes de solubilité de phases et le design de procédés milli-fluidiques pendant 9 mois.
    - Martine Meireles (Chercheur du Laboratoire de Génie Chimique, Université de Toulouse -Paul Sabatier)
    - Dr. Kevin Roger (Chercheur du Laboratoire de Génie Chimique, Université de Toulouse - Paul Sabatier)

Contents

Chapter 1

Production of polymeric particles. State of the art and challenges

This chapter is adapted with permission of Bentham Science Publishers Ltd from A. Albisa et al, Polymeric Nanomaterials as Nanomembrane Entities for Biomolecule and Drug Delivery, Current Pharmaceutical Design, 23, October, 2016, 263–80. Permission conveyed through Copyright Clearance Center, Inc.

1.1 Introduction

Some of the most efficient therapeutic biomolecules and drugs possess a high potential for treatment of a wide variety of previously intractable human diseases. However the therapeutic efficacy of these drugs can be seriously hampered due to an uncontrollable list of shortcomings: low water solubility, unfavorable stability, short circulation time in plasma, rapid clearance from the human body by phagocytes, poor bioavailability, non-specific toxicity against normal tissue and cells, low cellular uptake and susceptibility enzyme degradation [1,2]. In addition, the drug administration system should reduce the side effects and the required number of dose administration, eliminating the need for an specialized intake [3]. For instance, numerous studies have attempted to deliver proteins and polypeptides by oral route [4] because it is the most accepted route by patients. However, the bioavailability of these therapeutic agents is poor and depends on the rapid degradation in contact with the gastrointestinal fluids. Then, it is necessary to design effective drug delivery platforms to circumvent the previous shortcomings and enable the development and commercialization of new classes of therapeutic molecules.

The intersection of medicine and nano/microparticles has originated new delivery platforms. In particular, the application of polymeric nano/microparticles as delivery systems is one of the most promising alternatives developed during the last years. Biodegradable materials at the nano/microscale enable the encapsulation of drug, improving their bioavailability and retention time. Systematic studies have been carried out in this topic on rational design, preclinical evaluation, manufacture and formulation validation, and clinical development of these new drug platforms. However, the use of high quantities of carriers can lead to problems of carrier toxicity, effects on metabolism, and difficulties in carrier eliminations [5]. It implies that the biomolecule encapsulation efficiency and loading must be as high as possible.

Basically, the structure of this nano/microparticles mimic the natural biological membranes, enabling a controlled mass transport for a limited time and as a function of their biodegradability properties. Drug are typically dissolved, attached or encapsulated throughout the polymer matrix and released into the environment via diffusion. The large surface-to-volume ratio of materials enables the release of the payload at feasible and clinically relevant time scales, which is highly convenient to exploit the therapeutic value of many promising drug. Then, these delivery systems can be considered as free-standing 3-D membranes where drug can be delivered at a certain rate in a time-controlled operation or even on demand if a stimulus is applied. The most important design

factors of materials for drug delivery include size, surface charge, biomaterials and chemistry, chemical components, toxicity and degradability. Biomaterials based-drug delivery systems have been used for the treatment of various diseases including [6]: bacterial, fungal, parasitic infections, ulcers, hypertension, angina, glaucoma, uveitis, asthma, cancer and neurodegenerative disease. These nano/micro particles can be administered intravenously, orally, percutaneously, ophthalmically, pulmonarily or transmucosally to nose and lungs [6].

This chapter provides a comprehensive review of the state-of-the art of drug delivery systems including their production and challenges. The chapter is divided in three parts. First, the controlled release mechanism in particulate systems and the materials frequently used in drug carriers manufacturing will be described. Secondly, the different available methodologies that enable to control the main features of particulate systems for drug delivery will be highlighted. Finally, the specific challenges required to assess the transition from the proof of concept to the application in drug delivery for particles manufacturing will be pointed out.

1.2 Controlled release of biomolecules in nano and microparticles

One of the main limitations of conventional therapeutic treatments is the patient self-control on dose administration. The patient himself is responsible for the proper carrying out of the prescribed regimen. It is a characteristic of self-administered conventional dosage forms that only a relatively short duration can be achieved with them. Figure 1.1A depicts the concentration of a biomolecule or drug at the site of activity after the immediate intake for a 8 hourly interval. It can be observed that the biomolecule concentration which produces beneficial effects without harmful side effects (therapeutic window) occurs in a limited portion of the treatment period. Consequently, the frequency of administration must be raised to three intakes per day, which could induce toxic effects with an over-dosage. The limited duration of action is directly connected with the characteristic delivery profile of conventional dosage forms where period of overdosage alternates with a period of under-dosage, and for only a relatively limited time an optimal concentration is maintained. In the other hand, Figure 1.1A also depicts the biomolecule concentration profile achieved with a controlled release system, where the concentration is within the therapeutic window for the overall majority of the 24 h treatment. When using bio-nanomaterials as nanomembrane entities for time controlled release, the need for an initial over dosage does not arise and significantly smaller amounts of substance are required to obtain completely continuous and effective drug levels. This

fact is even more interesting for the administration of drugs with a short biological half-life that remains unused for therapy.

The release pathways in nano/microparticle are complex and specially depend on the type of biomaterial and drug properties, as well as the media of release. The particle biodegradability after the drug release is an important consideration in order to select the proper biomaterial for any controlled release mechanism. Biomaterials that are naturally excreted from the body are desirable [3]. On the other hand, no degradable materials should be only acceptable in applications in which the delivery system can be recovered after the release. From a kinetic release perspective, it is necessary to highlight that each biomolecule requires a different controlled release mechanism , that on the other hand, should be coupled with the physicochemical properties of the bio-nanomaterial where is located prior the delivery.

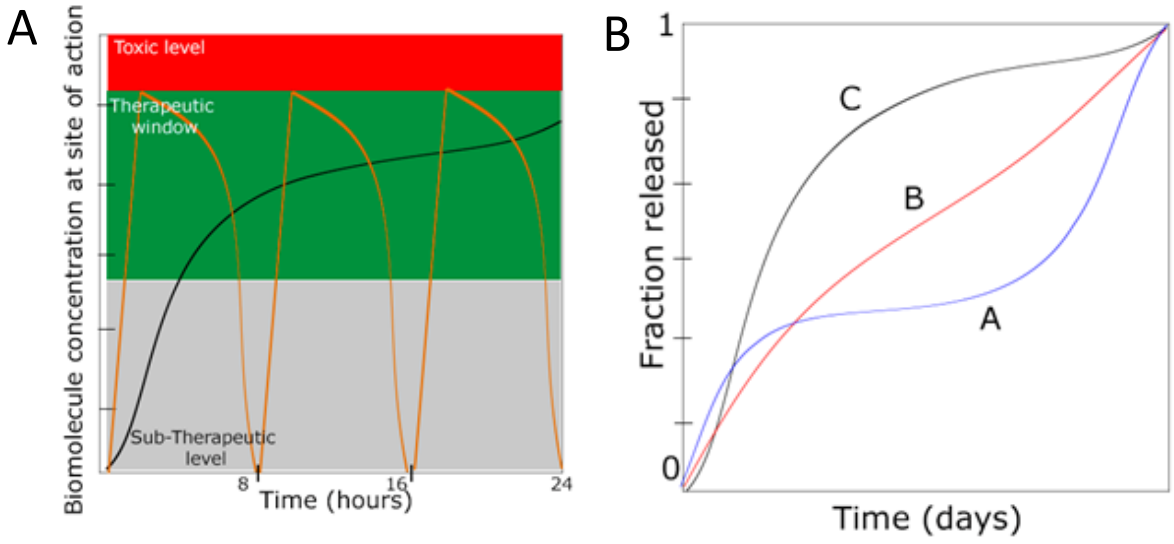

Figure 1.1 - A) Schematic of a biomolecule concentration at the site of therapeutic action. Therapeutic window and over/under dosage periods. Concentration profile after conventional delivery by a 8 hourly dose administration and using a controlled release by a bio-nanomaterial. B) Release profiles in nanomembrane entities:A- blue line depicts a three phase release, B- red line fits a burst and zero orden release and C- black line depicts a burst and a rapid phase II release. Figure reproduced with permission of Bentham Science Publishers Ltd from A. Albisa et al, Polymeric Nanomaterials as Nanomembrane Entities for Biomolecule and Drug Delivery, Current Pharmaceutical Design, 23, October, 2016, 263–80. Permission conveyed through Copyright Clearance Center, Inc

Generally, the release pathways can be classified into: delayed dissolution, solution flow control, stimuli-responsive delivery and diffusion controlled [3]. Delayed dissolution is achieved using a biomaterial matrix that dissolves at a slower rate than the drug itself. Solution flow control is conducted by an osmotic pressure gradient (osmotic pumping) across membrane pores. Stimuli-

responsive delivery implies that the payload is released as a respond of an extra- and intracellular biological stimuli. This mechanism is the most complicated, since it requires the presence of a sensor that detects the signal to stimulate the payload release and a membrane which can communicate with the sensor to start the release on demand. Finally, in diffusion-controlled release, biomolecules must be transported through tortuous pathways across the membrane.

In a diffusion-controlled release, drug has to pass through the polymeric shell, mimicking a 3D membrane, prior to reaching the surrounding medium. Release can occur by permeation through the shell, erosion of the shell or diffusion through pores (if existing). The mechanism of release is dominated by three stages [7]: (a) transport through water-filled pores, (b) transport through the polymer, and (c) due to dissolution or degradation of the encapsulating polymer (which does not require drug transport). Transport through water-filled pores is the most common way of delivery since the degradation rate is dependent on the type of biopolymer and the encapsulated drug are usually too large or hydrophilic to be transported through the polymer matrix [7]. Biomolecules are usually transported through water-filled pores by diffusion and convection, depending on a concentration and osmotic pressure gradient, respectively [7]. Polymer erosion and dissolution of polymer products by hydrolysis create pores. Erosion could preferentially occur in low molecular weight biopolymers, since a significant part of the polymer has a molecular weight just above the limit for water solubility. Small pores grow as contact with water by hydrolysis and subsequent erosion; finally, coalesce with neighboring pores enable form larger pores [8].

The classic three-phase release profile in a diffusion-controlled mechanism can be described as (Figure 1.1B):

Phase I- Burst release is usually attributed to non-encapsulated drug molecules located on the surface or in pores close to the surface easy accessible by hydration[9].

Phase II- Slow release phase, during which the drug diffuses slowly, either through the relatively dense polymer matrix or through the existing pores, while polymer degradation and hydration proceed.

Phase III- Fast release, this phase is often attributed to the onset of erosion.

However, the release profile could exhibit different patterns than the three-phase system, since payload release is usually a combination of complex processes (Figure 1.1B). For instance, the phase III is usually attributed to the onset of polymer erosion due to the degradation process, but it could also be attributed to the formation of cracks or just because the disintegration of the capsule. Also, the release rate can be decreased or even occur an incomplete release, due to payload interactions

such as the formation of physical or covalent aggregates [7]. Some variables related to the nanomembrane and media could also affect the release profile: porosity, tortuosity, swelling, polymer-biomolecule interaction, aggregation, deviations of pH, temperature, and redox potential. Then, it is difficult to draw some conclusion about the delivery performance just by the release profile, without considering some other physical and chemical factors [7].

The mass rate of permeation dM/dt of a drug molecule through a nanomembrane (polymer shell) can be written according to a mechanistic model of the first law of Fick under sink condition:

$$\frac{dM}{dt} = \frac{DKAC_d}{h}$$

The diffusion coefficient can be considered constant or time-dependent [10] due to the coexistence of a parallel diffusion path, across the polymer particle and its pores. In fact, the complexity in understanding the biomolecule delivery across the particle can be extended to the modelling study itself, where some models consider also the variation in particle size along the release [11] or even the presence of a permeability parameter to consider the formation of new pores after the biopolymer degradation [10]. Then, it can be drawn the conclusion that drug release could be affected by many processes simultaneously, which would be difficult to simulate, and the dominating mechanism may change with time. In addition, the biomolecule delivery can be also dependent from the surrounding media and the particles stability. If the particle mobility or mixing is not high enough, the concentration in the particle surrounding media can inhibit the release, following the well-known concentration polarization regime of membrane performance. This issue is typically more serious in hydrophobic biomolecule delivery, where the low water solubility can promote a fast achievement of saturation concentration [7]. On the other hand, if particles are not stable in the media, they tend to aggregate, decreasing the exposed surface area and reducing the delivery rate.

This thesis is based on the development of drug carriers for the delivery of two main biomolecules: dexamethasone and catechol. Their main properties as well as the specific requirement for their delivery in particulate materials will be described below.

1.2.1 Dexamethasone

Glucocorticoids are steroid hormones indicated for the treatment inflammatory disease. One of the first synthetic glucocorticoid is dexamethasone (DEX)[12,13]. Figure 1.2A shows dexamethasone molecule which it is obtained by modifying the structure of cortisol through the introduction of the 9-α-fluoro group and a 16-α-methyl substituent and an extra double bond between carbon 1 and 2

in the A-ring. DEX binds to glucocorticoid receptor more efficiently than cortisol; the presence of the fluorine atom makes it more lipophilic, while the methyl group bound to the carbon C-16 increases its affinity to the mineralocorticoid receptor [14]. Figure 1.2B shows chemical and physical properties of this molecule.

A

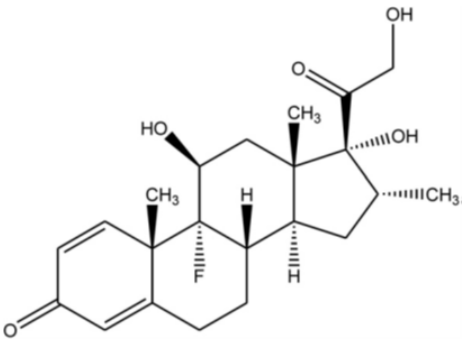

B

Property	Value
Formula	$C_{22}H_{29}FO_5$
Molar Mass	392.461 g/mol
Appearance	Colorless to white, odorless, crystalline solid.
Melting Point	504 to 507° F
Solubility in water	0.1mg/mL
Solubility in acetone	soluble
Solubility in ethyl acetate	4.1mg/g
Solubility in ether	Very soluble

Figure 1.2 A: Structure of dexamethasone. Adapted with from [14] with permission from Elsevier. B) Chemical and Physical Properties of Dexamethasone [13]

DEX is widely use in many biomedical applications, such as: cell culture, ophthalmology, proliferative vitreoretinopathy, subretinal neovascularization, arthritis and diabetic macular edema. The biological half-life of the dexamethasone is about 36 to 72 hours and need high doses of drug for reach its therapeutic level. Due to that serious side effects have been observed such as osteoporosis, high sugar concentration in the blood, hypertension and fluid retention. [15]. DEX has been encapsulated in some polymeric particle systems such as PLGA nano/microparticle [16–18], polycaprolactone implants [19] and chitosan films [20] reducing their spectrum of side effect and increasing the dexamethasone bioavailability [14]

1.2.2 Catechol

Catechol is a polyphenol compound with the molecular formula $C_6H_4(OH)_2$. Figure 1.3A shows their structure witch orthoisomer of three isomeric benzenediols. Catechol was first isolated in 1839 by H.Reinsch by dry distillation of catechin. Currently, it is produced industrially from phenol. It is mainly used as raw material for the synthesis of polymerization inhibitors, perfumes, drugs, pesticides and dyes. [21,22]. Figure 1.3B shows chemical and physical properties of this molecule.

A

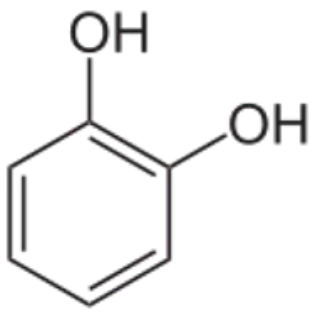

B

Property	Value
Formula	$C_6H_6O_2$
Molar Mass	110.1 g/mol
Appearance	white to brown feathery crystals
Melting Point	221 °F
Solubility in water	430 mg/mL
Solubility in ethyl acetate	Very soluble
Solubility in ether	Very soluble
Solubility in chloroform	Very soluble

Figure 1.3: A) structure of catechol B) Chemical and Physical Properties of Catechol [21,22]

Polyphenolic compounds have found to exhibit a wide range of biological activities including antioxidant, anti-inflammatory and neuroprotective effects. For catechol specifically, Zheng et.al found a correlation between their neuroprotective and anti-inflammatory effects with huge potentialities as anti-inflammatory drug [23]. Catechol are susceptible to oxidative deterioration, when exposed to oxygen, light, moisture, and temperature affecting their quality and shelf life. For this purpose, this biocomponent need to be encapsulated before their formulation as pharmaceutical products [24]. Catechol has been successfully encapsulated into carbon nanotubes [25], hyaluronic acid hydrogels [26] and PVA particules [27].

1.3 Polymers in Biomedical Applications:

Polymers represent the main and most promising class of biomaterials being extensively applied in multitude of biomedical applications, such as the controlled delivery of drug. This section provides a brief overview of the main properties and considerations of the most promising polymers applied as drug release system for drug delivery uses. According to the polymer source, polymers applied in biomedical applications, mostly biopolymers, can be classified into synthetic and natural (Figure 1.4).

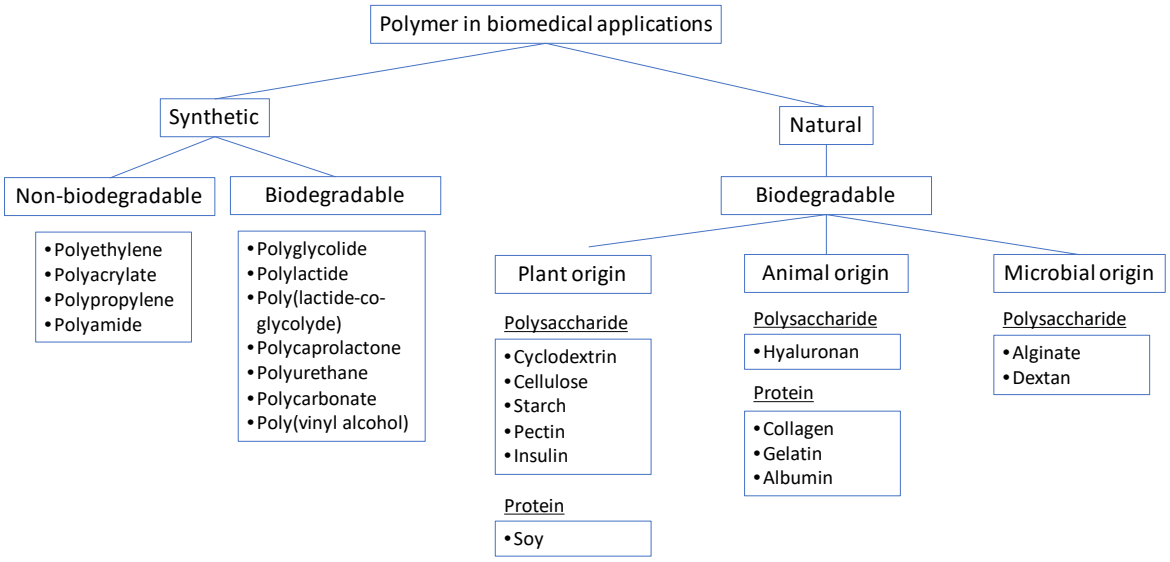

Figure 1.4.- Classification of polymers for biomedical uses: as nanomembranes for controlled delivery of biomolecules. Figure reproduced with permission of Bentham Science Publishers Ltd from A. Albisa et al, Polymeric Nanomaterials as Nanomembrane Entities for Biomolecule and Drug Delivery, Current Pharmaceutical Design, 23, October, 2016, 263–80. Permission conveyed through Copyright Clearance Center, Inc

1.3.1 Natural polymers in biomedical applications

Natural polymers are obtained primarily from plants, animal and microbial sources. These types of polymers are being used in a wide variety of biomedical applications due to their abundant availability, biodegradability, renewability and fewer toxic effect when compared with synthetic ones.

The natural polymers derived from plants, animals and microorganism can be classified according to their chemical structure into polysaccharides, polyesters and proteins (Figure 1.4):

Cyclodextrins are an example polysaccharide based polymers (plants source). Cyclodextrins are cyclic oligosaccharides with chemical stability in neutral and basic conditions, whereas they undergo non-enzymatic hydrolysis in acid conditions to yield glucose, maltose, and non-cyclic oligosaccharides [28]. On the other hand, chitosan is an example of polysaccharide based polymers (animals source). The most important properties comprise biodegradability, biocompatibility, microbicidal (reduces the infectivity of microbes) and mucoadhesive nature. This natural polymer is the most extensively investigated materials for pharmaceutical and biomedical applications, such as drug and gene delivery. It has been reported the encapsulation of a wide variety of biomolecules in chitosan nanoparticles: insulin [29], as well as antihormonal [30] and ocular drugs [31].Finally,

gelatin is one the most representative polymers derived from animals; in fact, it is produced from a partial hydrolysis of collagen existing in skin and bones. Gelatin structure consists of amino acids mainly glycine, proline and hydroxyproline. There are two main gelatin types, named as A-(or acid) type and B-(or alkaline) type [32]. Gelatin is an attractive polymer to control the release of drug due to its non-toxic, biodegradable, low-priced, bioactive and inexpensive properties. It has been reported the successful encapsulation of different biomolecules into gelatin nanoparticles (BSA [33] and several drugs (anticancer [34], anti-HIV [35], antimalarial [36]).

1.3.2 Synthetic polymers in biomedical applications

Synthetic polymers are one of the most promising biomaterials in the biomedical area since they can be artificially synthesized following an ease and low cost procedure. In addition, the versatility of synthetic polymers enables the fine tune of their physical, chemical, surface, morphology and biocompatibility [37]. According to the polymer stability in the living organism, synthetic polymers can be classified as non-biodegradable and biodegradable materials (Figure 1.4). The most commonly non-biodegradable polymers used in biomedical applications comprise polyethylene, polyacrylate, polysiloxane, polyamides and polypropylene. Biodegradable polymers are highly demanded due to the polymer was metabolized in the body after fulfilling its release purpose. In addition, it is desired that the polymer does not leave any trace to prevent the bioaccumulation. In fact, the general criteria for selecting a polymer for use as a biomaterial are to match the mechanical properties and the time of degradation to the needs of the delivery application [38]. The polymers should fulfill certain properties such as: a) do not induce an inflammatory/toxic response, b) have an appropriate shelf life, c) proper metabolization and d) should be easily sterilized.

Biodegradable synthetic polymers can be tailored to tune their mechanical properties and degradation kinetics. Biodegradation occurs either by abiotic reactions such us oxidation or hydrolysis where polymers fragmentize into lower molecular mass species, or by abiotic reaction where microorganisms chemically deteriorate polymer chains, and afterwards are bio-assimilated and mineralized [39]. The most used biodegradable synthetic polymers in drug delivery applications can be classified into poly(glycolic acid), poly(lactic acid) and their copolymers (Figure 1.4) [7]. Polyglycolic acid (PGA) is simple linear aliphatic polyester that degrades to glycolic acid (GA). The degradation of PGA to GA occurs by the scission of ester groups; afterwards GA can be resorbed through metabolic pathways. Polylactic acid (PLA) is more hydrophobic than PGA and can be copolymerized with PGA to produce Poly(lactide-co-glycolide)-PLGA. The ratio of PGA and PLA can

be varied to tune the properties of the polymer, for instance the degradation rate. PLA makes PLGA more hydrophobic, absorbs less water and then degrades more slowly. As a rule, higher content of PGA leads to quicker rates of degradation with an exception of 50: 50 ratio of PLA/PGA, which exhibits the fastest degradation [40]. On the other hand, PEG (poly ethylene glycol) is a hydrophilic and inert polymer that provides a steric barrier on the surface of the nanoparticles and minimizes their protein binding (opsonization). Adding PEG is useful to prolong NPs circulation (avoiding a fast clearance by macrophages) and to decrease premature drug release. Because of this, several copolymers of PLGA with PEG have been synthesized, encapsulating a wide variety of therapeutic drugs [41,42].

Polycaprolactone (PCL) is also a biodegradable polymer that degrades at a much lower rate than PLA. This fact makes PCL to be considered as a long-term drug delivery system. Polyurethane can be designed to be biodegradable, but the degradation products could be toxic, which unable its use as drug delivery carrier [43]. Regarding polycarbonate, these polymers possess ether and carbonyl groups than are susceptible of enzymatic degradation, producing non-toxic products [44]. Finally, polyanhydrides are together PLGA the synthetic polymers with the best control of drug delivery. They have two hydrolysable sites, whose degradation rates depends on the polymer composition. For instance, aromatic polyanhydrides will degrade slowly over a long period, while aliphatic polyanhydrides can fast degrade (days scale) [45].

Poly(vinyl alcohol) (PVA) is acknowledged to be one of few vinyl polymers that can have higher biodegradation rate. This is possible owing to the presence of hydroxyl groups which condition hydrophilic nature of this material [39,46] . It was concluded that the initial biodegradation step involves the enzymatic oxidation of the secondary alcohol groups in PVA to ketone groups. Hydrolysis of the ketone groups results in chain cleavage [47]

1.4 Drug Delivery Systems

Biomaterials can be assembled into drug delivery system with a permeable shell using a wide variety of procedures [48]. The high surface to volume ratio and the inherent properties of each biomaterial provide them unique properties: controlled/sustained release property, subcellular size and biocompatibility with tissue and cells, stable in blood, non-toxic, non-inflammatory, non-immunogenic, non-thrombogenic, do not activate neutrophils, biodegradable, avoid reticuloendothelial system and applicable to encapsulate several types of drugs and biomolecules such as proteins, peptides, or nucleic acids [49].

This section will focus in the last advances of the most valuable bio-materials applied as drug delivery system, as well as their impact on biomedicine and most important limitations.

1.4.1 Particles based on hydrogels

Since in 1960 Wichterle and Lim [50] reported the potential use of hydrophilic gels in biomedicine there was an exponential growth in this field of research. Hydrogels are three-dimensional, crosslinked networks of water-soluble polymers. In contrast with networks of hydrophobic cross-linked polymers, hydrogels can swallow high amounts of water or biological fluids (sometimes above 90% wt.). This property is due to the presence of hydrophilic groups (commonly -OH, -CONH-, -$CONH_2$- and SOH_3) attached to the polymer backbone, while the cross-links between network chains prevent the dissolution of the polymeric material in the aqueous medium.

Hydrogels can be classified depending on their origin source, polymer composition, network structure, change of polymer network, sensibility to stimulus, physical appearance and configuration (Figure 1.5). The origin source and polymer composition were describing above in this chapter (section 1.4.3). While synthetic polymer hydrogels present better structural and mechanical properties, natural polymer hydrogels show a high biocompatibility, biodegradability and better cell adhesion [51,52].

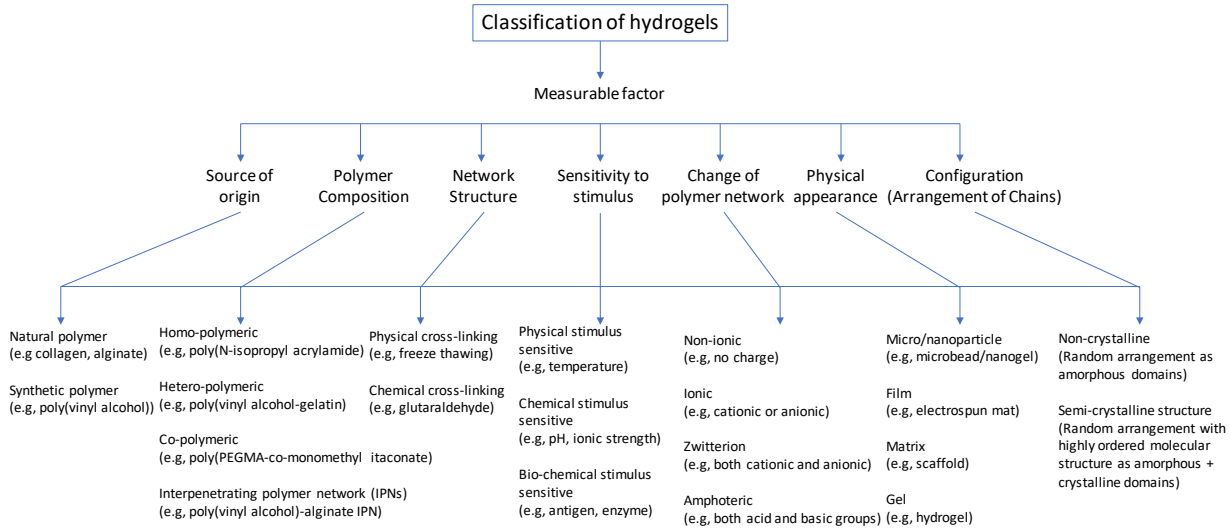

Figure 1.5: Classification of hydrogels. Reproduce from [52] with permission of Taylor & Francis

Hydrogels sensibility to stimuli can be classified based on the type of stimulus to which respond. Most common stimuli are those which responds to temperature [53], pH [54], electricity [55] or light [56], but also it was designed hydrogel nanomembarne entities capable to respond to other less common stimuli such as glucose [57], pressure [58] or specific ions and antigens [59]. An example

of the potential applicability of smart hydrophilic gels in biomedicine and drug controlled delivery is its use in the development of a self-regulated insulin delivery system. In 1980 Creque, Langer and Folkman demonstrate the possibility of release insulin from an ethylene-vinyl acetate matrix for a long time, controlled by the pH of the release medium [60]. Although this approach finally demonstrated to be incapable of controlling blood glucose in a physiological manner, a new active research is emerging. Nowadays a promising approach in glucose-responsive insulin delivery systems is trying to take advantage of the enzyme glucose oxidase that converts glucose to gluconic acid. Glucose oxidase is immobilized into the hydrogel structure promoting a microenvironmental pH decrease in contact with glucose. This pH decrease promotes insulin solubility, increasing the release rate. For example, an injectable glucose sensitive Dextran-chitosan and dextran-alginate based microgels was reported by Gu et al. [61] in recent years, demonstrating to be a feasible glucose-responsive insulin delivery systems. Smart hydrogels can be used not only as self-regulated delivery platforms but also as remotely triggered delivery systems. Timko et al. reported a themoresponsive nanogel based membrane combined with plasmonic nanoparticles as a subcutaneous reservoir for remotely triggered release of insulin or another drug [62].

Drug release from hydrogels can occur mainly by two different mechanisms: diffusion controlled and chemically controlled. Diffusion controlled is the most common release mechanism in hydrogels. Several models were proposed to describe diffusion through hydrogels [63,64]. A critical parameter that affects diffusion in hydrogels is the percentage of swelling, which is directly related to the amount of water imbibed in the structure and the diffusion rate. In diffusion-controlled release, the drug size should be smaller than the mesh size to allow diffusion through the matrix. In diffusion-controlled hydrogels, release is limited to short time spans and is concentration gradient dependent. Chemically controlled release in hydrogels has focused an enormous attention in recent years as a promising platform for drug delivery and tissue engineering due to the capacity to fine tune the release [65]. Release mechanism is determined by chemical reactions occurring in the hydrogel matrix, being the most common the cleavage of polymer chains by hydrolytic or enzymatic degradation or the reversible or irreversible reactions occurring between the polymer network and the releasable molecule. In many cases, release can be controlled by controlling bulk erosion or degradation as in biodegradable hydrogel scaffolds widely investigated for tissue regeneration [66]. Chemically controlled release enables a further release time than the diffusion controlled approach and generally produces a constant release rate. However, biomolecules should be larger than mesh size to be retained by polymeric matrix and avoid diffusion

Table 1.1 Examples of hydrogel for drug delivery.

Hydrogel Matrix	Biomolecule	Release Profile	Application	Structure	Reference
Collagen	Fibroblast Growth Factor	Fickian. Initial rapid and steady release within the first 7 days and then further sustained and steady release up to 30 days. 52%-76% (30 days)	Bone regeneration	Bulk	[59]
Chitosan-g-poly (acrylic acid)/attapulgite/sodium alginate	diclofenac sodium	pH controlled. 100% (2h) at pH7.4 50% (7h) at pH 6,8	Drug delivery	Beads	[60]
PNIPAM	Vitamin B12	Fickian + Pulsatile. Temperature controlled.	Drug delivery	Nanocomposite	[61]
Chitosan	Insulin	Glucose controlled: 40% (4h) Glucose=400mg/dl 10% (4h) Glucose=100mg/dl	Diabetes mellitus	Microparticles	[62]
Gelatin	Simvastatin	Sustained through matrix biodegradation. 100% (20 days)	Bone regeneration	Bulk	[67]
Carboxymethylpullulan	gentamycin	Fickian + biodegradation. Initial rapid and steady release. 65% (10h) 85% (40h)	Wound Healing	Film	[68]

1.4.1.1 Particles based on polyvinyl alcohol

Production of particles using poly(vinyl alcohol) (PVA) polymer was reported for the first time by Thanoo et.al in 1993 where aspirin, griseofulvin and nicotin were encapsulated into PVA particles. They observed that increase in the cross-linking density of the microspheres reduced the drug release rate considerably, suggesting that the release profile could be controlled by changing the cross-linking density. [69]. Morelli et.al produced acid sensitive particles by blending the PVA and

chitosan where up to 80% of cupper and 20% of sodium salicylate was released from the particles under acidic conditions while no significant release was finding under neutral conditions [70]. Similar pH-sensible behavior was determined by Hua et.al for diclofenac sodium encapsulated sodium alginate/poly(vinyl alcohol) hydrogel beads. Also, freeze-thawing process improved swelling behaviors providing a facile and effective method to improve the drug delivery system [71]. PVA hydrogel nanoparticle exerted a pronounced inhibition of nitric oxide synthesis by stimulated macrophages, thanks to that, it had an anti-inflammatory activity [72]. These examples corroborate the potentialities of particles based in polyvinyl alcohol as promising candidates for diverse biomedical applications.

1.4.2 Particles based on polyesters

The aliphatic polyesters, such as the poly(lactic acid)(PLA), poly(lactic-co-glycolic acid) (PLGA) and poly(ε-caprolactone) (PCL) are often used for pharmaceutical applications due to their biocompatibility and biodegradability. The biomolecule release mechanism presents in polyesters materials is a combination of degradation, erosion of the polymer and transport of the bioactive molecule (see Section 1.2). Biomolecule transport occurs following a diffusion process across the polymer matrix and the pores. Polyesters are depolymerized (degradation) in presence of water, but this phenomenon depends principally on the medium. The erosion is conducted according to different processes: surface-eroding and bulk-eroding. In surface-eroding, the polymer degradation rate in the surface is faster than the water penetration rate. On the contrary, in bulk-eroding process the water penetration rate in the surface is faster than the degradation rate. The erosion phenomena depend on the degradation, dissolution, and diffusion processes. Finally, the drug transportation has different stages, first it follows an “initial burst” release where high percentage of the drug is released in the initial early stage of the process. Later it can exhibit different release behaviors depending of the transport properties of the drug and the dynamic conditions of the degrading polymers. Payload release can be classified depending on the stage of the release as zero order, monophasic, biphasic and diphasic [73].

Bile et al. [74] stated an important correlation between surface morphology and drug delivery of PCL microparticles. A burst release was related to the drug located at the surface of the microparticles that was not retained by the encapsulation process and was deposited at the final drying step of the manufacturing process. The burst release was observed as soon as the microparticles were dispersed in water. On the other hand, hydrophobic PCL nanofibers

encapsulating the hydrophilic antibiotic drug tetracycline hydrochloride shown that the burst release of the drug was minimized by the transition to hydrophilic surface along the release time [75].

Particles based in PLGA based polymers are ones of the main polymer particles studied in this thesis and it is presented in detail in section 1.4.2.1

Table 1.2 summarizes the last advances in the use of polyester particles as biomolecule delivery system.

Type of Polymer	**Drug**	**Application**	**Encapsulation Efficiency, %**	**Size and Distribution**	**Release Profile**	**Ref**
Copolymer of poly(lactic acid) and poly(allyl ethylene phosphate) with cysteine or cysteamine–glutamic	doxorubicin (DOX)	Cancer treatment	31%	50-60nm	26-30% at 4days (depending conditions)	[76]
PLA: Poly (lactic acid) and PEG: Poly (ethylene glycol)	doxorubicin (DOX)	Drug Carrier for targeted drug delivery purposes	70-92%	High Polidispersity (210-470 nm)	The cumulative drug release of microspheres was rapid within 10 h and then followed a slower release rate. exponential model of the form kt^n (n=0,868)	[77]
PLGA 50:50 (153 kDa, or PLGA 75:25 (114 kDa)	Dexamethasone	Pediatric vascular and airway diseases	60% -l 80%	(50um-100um) Increase with destilation times	PLGA 75:25 (10%); PLGA 50:50 (20%) in all cases at 100 days	[78]
(PCL) MW 45,000 Da and 80,000 Da	cholecalciferol	Drug release	79-90%	22 -268um	2-12% at 1h(important role of microsphere surphase morphology)	[74]
PCL	tetracycline hydrochloride (TC)	Combination drug delivery and tissue engineering	11,5-19,2% (Depending of drug concentration)	Fiber Diameter 643um-825um Pore Diameter 450-158 (Depending of drug concentration)	20-60% at 2 days (Depending of drug concentration)	[75]

1.4.2.1 Particles based on PLGA polymers family

Drug delivery in PLGA nanoparticles can be tuned if the composition of lactic and glycolic acids is varied. The release rate is increased with the decrease of lactic acid monomer proportion due to the hydrophobicity increase of the matrix. The fastest degradation was achieved with PLGA 50% (PLA/PGA) (Fig. 1.6) [40]. Feng et al. [79] has studied the effect of encapsulating three different biomolecules (Bovine serum albumin-BSA 66 kDa, Lysozyme 13.4 kDa, and Vancomycin 1.45 kDa) and three formulations of PLGA-PEG polymer microspheres with different molecular weight (PLGA 9,5 kDa, 19,9kDa, 31,6kDa combined with PEG 5kDa). Drug release was firstly controlled by the initial burst diffusion, but the final release stage was controlled by a degradation/erosion process. The release profile of BSA was different than the ones with small molecular weight, being predominant the burst release respect to lag period as contrary to Vancomycin and Lysosime.

The effect of PLGA-PEG molecular weight in the biomolecule release pattern was also studied, highlighting a higher release rate in 9.5 kDa PLGA-PEG than with higher molecular weight due to its faster degradation and structure erosion. However, the contribution of the molecular weight of the drug has more significance influence in the biomolecule release that the PLGA-PEG molecular weight. Xu et al. [80] studied the influence of the surface density of PLGA-PEG on Paclitaxel drug release by blending various ratios of a diblock copolymer of PLGA and 5 kDa poly(ethylene glycol-PEG) (PLGA-PEG5k). The encapsulation efficiency and drug loading was found to be sensitive to the PEG content. The blended PLGA-PEG nanoparticles with PLGA-PEG experimented a more sustained release than PLGA ones, increasing the time to achieve 50% delivery from 1,5 to 6 days for PLGA and PLGA-PEG, respectively.

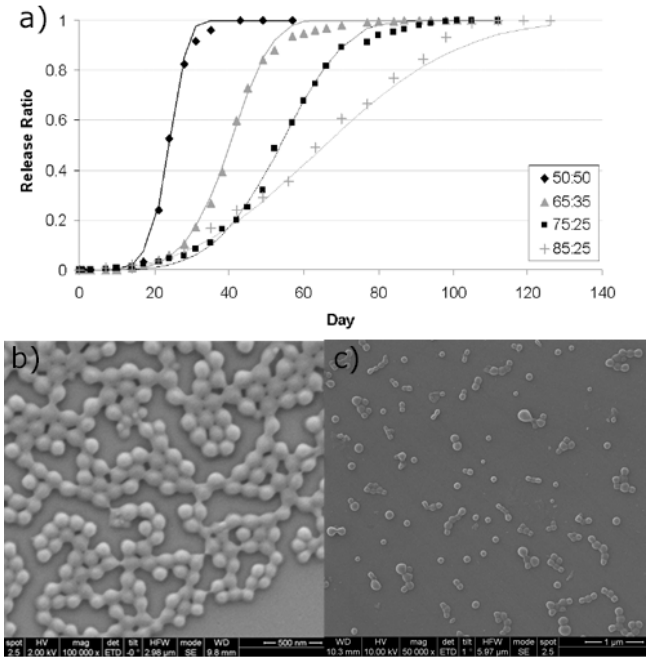

Figure 1.6.-a) Modeled in vivo release profiles for 50:50, 65:35, 75:25 and 85:15 poly lactic-co-glycolic acid. Notation 65:35 PLGA means 65% of the copolymer is lactic acid and 35% is glycolic acid. A biphasic release profile with an initial zero release period followed by a rapid drug release was observed. The profiles also shows increase in release rate with decrease in lactide to glycolide proportion. Reproduced with permission from [40] under CC license. b-c) SEM images of PLGA-PEG nanoparticles.

1.4.3 Lipid and Lipid-Polymer Hybrid particles

Lipids are amphiphilic molecules, which are constituted by a hydrophobic tail and hydrophilic head. Lipids can be assembled in contact with water, frequently in the form of liposomes. Consequently, liposomes are lipid vesicles that are structured as an aqueous core surrounded by a bilayer membrane (Figure 1.7). Some drugs are toxic and have a poor bioavailability after oral administration. These drawbacks can be overcome by the encapsulation of such drug in lipid nanoparticles, preventing its toxicity and improving its oral bioavailability [81]. Moreover, they can be formulated by an organic solvent free method [82].

In the past 20 years, it has been produced a wide variety of drugs encapsulated in liposomes for biomedical use [83]. The first liposomal pharmaceutical product (Doxil) was approved in 1995 by the Food and Drug Administration (FDA) for the treatment of acquired immune deficiency syndrome (AIDS) associated with Kaposi's sarcoma [84]. Other liposomal pharmaceutical formulations commercially available include: Ambisome (amphotericin B liposome for sever fungal infections) [85], DaunoXome (daunorubicin liposome, for blood cancer) [86], Visudyne (verteporfin liposome,

for age-related molecular degeneration) [87], Depocyt (cytarabine liposome, for neoplastic meningitis and lymphamatous meningitis) [88], DopoDur (morphine sulfate liposome, for pain) [89] and Marrqibo (vincristine sulfate liposome, for acute lymphoblastic leukemia) [90] . The last pharmaceutical product approved by the FDA (2015) was Onivyde (irinotecan liposome injection) in combination with fluorouracil and leucovorin, which is a liposomal formulation to treat patients with an advanced pancreatic cancer [91].

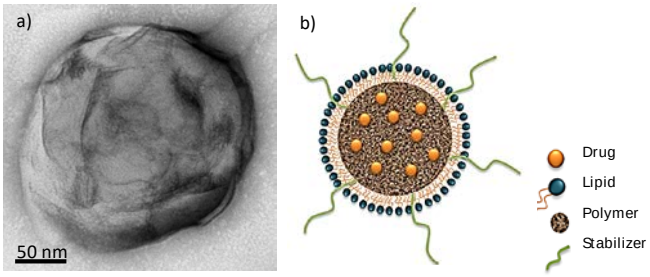

Figure. 1.7. a) TEM image of a lipid nanoparticle, the lipid nanoparticle was stained to contrast the lipid layer. b) Schematic illustration of a lipidpolymer hybrid nanoparticle.

1.4.4 Niosomes and Polymersomes particles

Considering the liposome structure model stated in the previous section, it is possible to substitute phospholipids for synthetic surfactant molecules to design a synthetic vesicle with a wall type bilayer membrane. Kunitake and Okahata [92] reported for the first time the synthetic bilayer membrane composed of a cationic dialkyldimethylammonium surfactant molecule. Since then, several synthetic surfactant molecules have been reported. These types of synthetic vesicles with surfactant non-ionic molecules are named niosomes. The niosomes can be formulated at relatively lower cost and high purity in comparison with liposomes and generally have better chemical stability (oxidation resistance) and can be functionalized by surface modification. On the other hand, the fast growth and the rising interest in vesicular system to use them as carrier of both hydrophilic and hydrophobic drugs, has resulted in the design of hybrid entities based on copolymers, names polymersomes. Polymersomes are more promising than liposomes due to their high membrane stability and low permeability. The properties of the membrane, such as permeability and stability, can be tuned and modulated by changing the species and lengths of copolymer blocks, resulting also in a variation of size and thickness. For instance the membrane thickness of liposomes is typically 4 or 5 nm, while the hydrophobic membrane thickness of polymersomes can be engineered to exceed 5 nm by simply varying the hydrophobic block molecular weight [93]. The rigidity and permeability of polymersomes can be also tuned by the modification of molecular building blocks. In comparison

with triblock copolymers, deblock copolymers have been proven to impose a compact bilayer structure, which is relatively rigid and less permeable than those of triblock copolymers [93].

According to literature, niosomes are widely applied in cosmetic since enhance the skin permeability of topically administered drugs, leading to increased bioavailability [94]. Niosomes are considered to promote cutaneous drug absorption via two mechanisms [94]: 1) niosomes modify the properties of the stratum corneum by reducing transepidermal water loss, which increases stratum corneum hydration and loosens its closely-packed cellular structure. 2) surfactants from the niosome shell serve as the matrix and the nanoscale size of the niosomes promote drug transfer across the stratum corneum (SC). Niosomes fuse with the lipids existing in the stratum corneum and the concentration gradient at the niosome-skin interface enable the drug permeation. There are published some review papers describing the main features of niosomes as well as drug loading efficiency [95].

Polymersomes are considered as new nanomembrane entities that circumvent some of the limitations of lipids nanoparticles: no ligand conjugation to prevent rapid blood clearance, critical assembly concentration and drug release difficulties. Polymersomes, as polymeric vesicles composed of amphiphilic copolymers, share with niosomes the same ability to encapsulate and release both water insoluble and soluble drug. However, the macromolecular nature of their building blocks enables to add new features including targeting, biodegradation and, more important, responsiveness [96]

1.5 Polymeric particles manufacturing methods

Particles manufacturing methods include the one-step and two-steps procedures (Figure 1.8). One-step methods are based on the precipitation of a polymer in conditions of spontaneous dispersion formation named nanoprecipitation or thanks to the self-assembly of macromolecules to form nanogels or by ionic gelation process where polyelectrolyte complexes are formed [97]. Contrary, in two-steps methods, a preliminary emulsification step is required to produce the liquid droplets that will be the template for the generation of the solidified particles by the appropriate secondary reaction step. The emulsification process can be carried out by using different emulsification systems such as high-pressure systems, high speed system, ultrasonic system, microfluid systems and membrane systems. Particle solidification could be achieved either by the precipitation (salting out, solvent diffusion and evaporation) or the gelation of a polymer (chemical or physical cross-linking).

Polymeric particles manufacturing methods

<table>
<tr><td rowspan="2">One step procedure
• Nanoprecipitation
• Self assembling macromolecules
• Ionic Gelation</td><td colspan="2">Two steps procedure</td></tr>
<tr><td>First Step: Emulsification</td><td>• High-pressure systems
• High speed system
• Ultrasonic system
• Microfluid systems
• Membrane systems</td></tr>
<tr><td></td><td>Second Step: Solidification</td><td>• Precipitation of the polymer from emulsion
  • Salting out
  • Solvent diffusion
  • Evaporation
• Gelation of the emulsion
  • chemical crosslinking
  • physical crosslinking</td></tr>
</table>

Figure 1.8. Overview of general methods for polymeric particles preparation. Box on the left (pink box): One step procedure. Boxes on the right: Two steps procedure where first step is emulsification (blue box) and second step is solidification (yellow box).

1.5.1 One step procedures

One step procedure are based on the precipitation of a polymer in conditions of spontaneous dispersion formation, thanks to the self-assembly of macromolecules or ion gelation method. [97]

A typical example of nanoparticle formation via self-assembly of macromolecules is the production of polyelectrolyte complexes nanospheres, also named nanoplexes. Polyelectrolyte are formed between polyamines and nucleic acids due to complementary charge annealing helping in the final structure of the nanospheres. [98].

Nanoparticles obtained from ionic gelation procedure are synthesized in totally aqueous media. They are included among the few organic solvent free methods. Ionic nanogels can be obtained from aqueous solutions of charged polysaccharides where small clusters are formed due to the presence of small ions of opposite charges. The small ions act as gelling agents [97,99,100]

The most widely used one step procedure method is nanoprecipitation and will be described below.

1.5.1.1 Nanoprecipitation

The nanoparticles obtained by the nanoprecipitation process are created after the dissolution of a solvent (p.e. Acetone) that is miscible with the non-solvent (p.e. Water). Nanoparticles are formed due to nucleation of small aggregates of macromolecules followed by aggregation of these nuclei.

The aggregation stops as soon as the colloidal stability is reached. The mechanisms involved in this process are the Interfacial turbulence and the diffusion-stranding. The interfacial turbulence involves the line between the two non-equilibrated liquid phases where appears a change of the physicochemical properties in order to compensate discrepancies in free energy. On the other hand; the diffusion-stranding mechanism is the spontaneous mixing process and it results in polymer partition into the aqueous non-solvent phase, which then aggregates into colloidal polymer particles upon solvent displacement [101]

Principal advantages of nanoprecipitations are:

- External energy input is not essential for the nanoparticle formation
- Works with modest equipment requirements and low energy costs
- Surfactants are not necessary.
- It is comparatively easy to influence the particle formation by changing concentration, solvent/non-solvent, and preparation technique.

Principal disadvantages of nanoprecipitations are:

- Water soluble drugs are usually poorly incorporated into the polymeric matrix
- The size and shape of the particles are hardly predicted.
- Difficult control on the mixing processes during nanoprecipitation

A central challenge in the development of polymeric nanoparticles by nanoprecipitation is the difficulty to control the mixing processes regulating dimensions and physicochemical properties of the nanoparticles with good accuracy[101]. Mixing control can be achieved by using stirred batch device, “T mixer” system, milli/microfluid system and membranes.

The stirred batch is normally used in lab scale, where a polymer solution is manually dispensed into a miscible non-solvent, following a procedure as simple as pipetting one liquid into another. This may be more than sufficient for a certain on–off, qualitative experiments, but for the scale up it is necessary the development of other systems [101]. One of the few scale up reactors published in the literature is reported in Galindo-Rodriguez work (Figure 1.9). The system consists in three reactors (R-N1, R-N2, R-N3) each one equipped with an axial impeller. The R-N1 and R-N3 reservoirs contain the aqueous and organic phases, respectively. Both phases are continuously supplied by independent peristaltic pumps (P1 and P2). The interesting point of this continuous system is a “Tee mixer” which serves to mix the two phases. In fact, when both phases come into contact in the central part of the “Tee mixer”, they diffuse into each other forming immediately the nanoparticles.

The raw nanoparticle dispersion is finally received in the main reactor (R-N2) and maintained under a gentle agitation. [102]

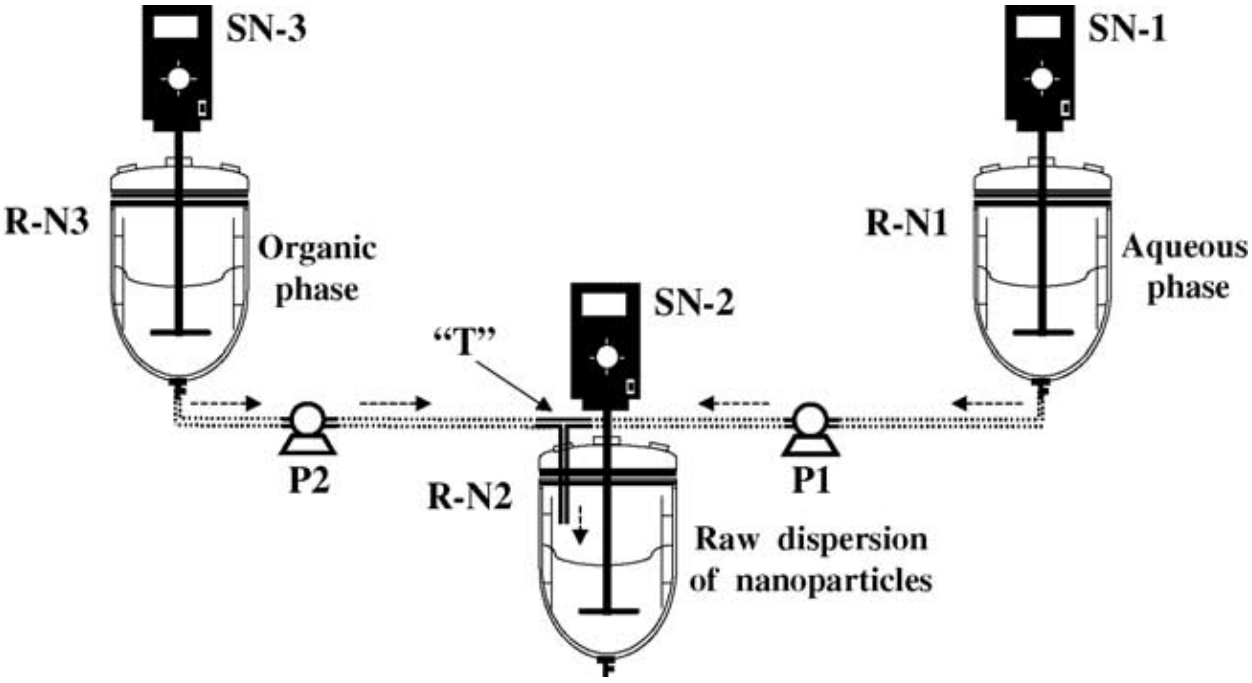

Figure 1.9. Set-up for the scaling-up the nanoprecipitation method. Abbreviations: SN-1, SN-2 and SN-3, stirrers (RW 20DZW.n stirrer, IKA Labortechnik, Staufen, Germany); R-N1, R-N2 and R-N3, 2.5 l reactors equipped with four baffles and an axial impeller; P1 and P2, peristaltic pumps; T, "Tee mixer". Reproduced from [102] with permission from Elsevier

1.5.1.1.1 Nanoprecipitation using Milli/Microfluidic devices

Production of nanoparticles by nanoprecipitation using microfluidics was for the first time reported by Karnik et.al [103] using a flow focusing microsystem designed by Knight [104]. Milli/Microfluidic systems are able to manipulate flows in the sub-ml/h, ml/h–l/h and 10–10,000 l/h ranges, respectively, thus covering the whole flow range up to the conventional mixers (Figure 1.10) [105]. Milli/microfluid system such as milli/micromixer can drastically reduce the mixing path resulting in a very fast mixing achieving within few milliseconds to microseconds. [106]. Mixing efficiency comparison was made by Schwolow et.al comparing different micromixer design such as flow focusing, interdigital multilamination, impinging jets and multi-inlet vortex [107]. This efficient mixing can be achieved by two ways: changing the flow rates ratio or modifying the configuration of the mixing; obtaining then, usually smaller particle size in comparison with conventional methods. [108,109]. Another advantage of the milli/micromixer is the ability to maintain the continuous production, obtaining same quality of the product during long time. Unfortunately, two

main disadvantages are presented in milli/micromixer: their relative low productivity due to the small internal volume and low flow rates being more appreciable in micromixer than in millimixer and blocking possibility by solid particle accumulation. [106]

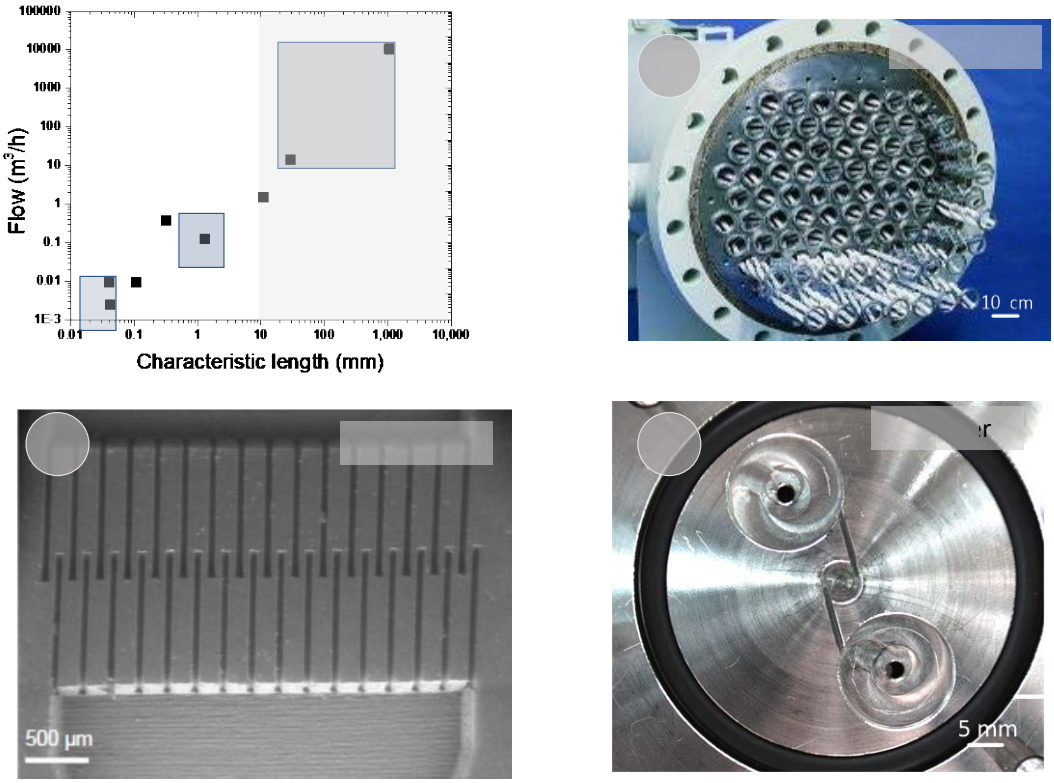

Figure 1.10. Micromixer , millimixer (laboratory-scale) and microstructured mixers (pilot-scale) close the gap to static mixers, yielding apparatus for a multi-scale concept. Graph flow vs characteristic length is reproduced from [110] with permission from Elsevier 1) Micromixer is reproduced with permission from [111] Copyright Clearance Center 2) Millimixer 3) Macromixer

1.5.1.1.2 Nanoprecipitation by using membrane systems

Production of nanoparticles by nanoprecipitation using membrane systems was for the first time reported by Charcosset et.al [112]. Nanoprecipitation of polymer involves membrane dispersion of the polymeric organic solution into aqueous solution. The unit operation of this technique is quite similar to membrane emulsification that it will presented below in this chapter (1.5.2.1 membrane emulsification). The difference is the complete solubility of organic solution and aqueous solution where the mixing has a vital performance. [113]. Jia et.al found how decreasing the pore size of the membrane from 30kDa to 10kDa, increases the flow Reynolds number and it favors the enhancement of micromixing efficiency [114]. This technique have been used to produce liposomes,

niosomes, micelles and polymeric nanoparticles. [113]. Only a few studies combine nanoprecipitation with membrane processing opening a new window on the application of membrane science in the last years.

1.5.2 Two steps procedure

1.5.2.1 First Step: Emulsification process

The process of converting two immiscible liquids into an emulsion is known as homogenization, and a mechanical device designed to carry out this process is named as homogenizer. [115]. They can be produced by using different emulsification systems such as high-pressure systems, high speed system, ultrasonic system, microfluidic systems and membrane systems showed in Figure 1.11.

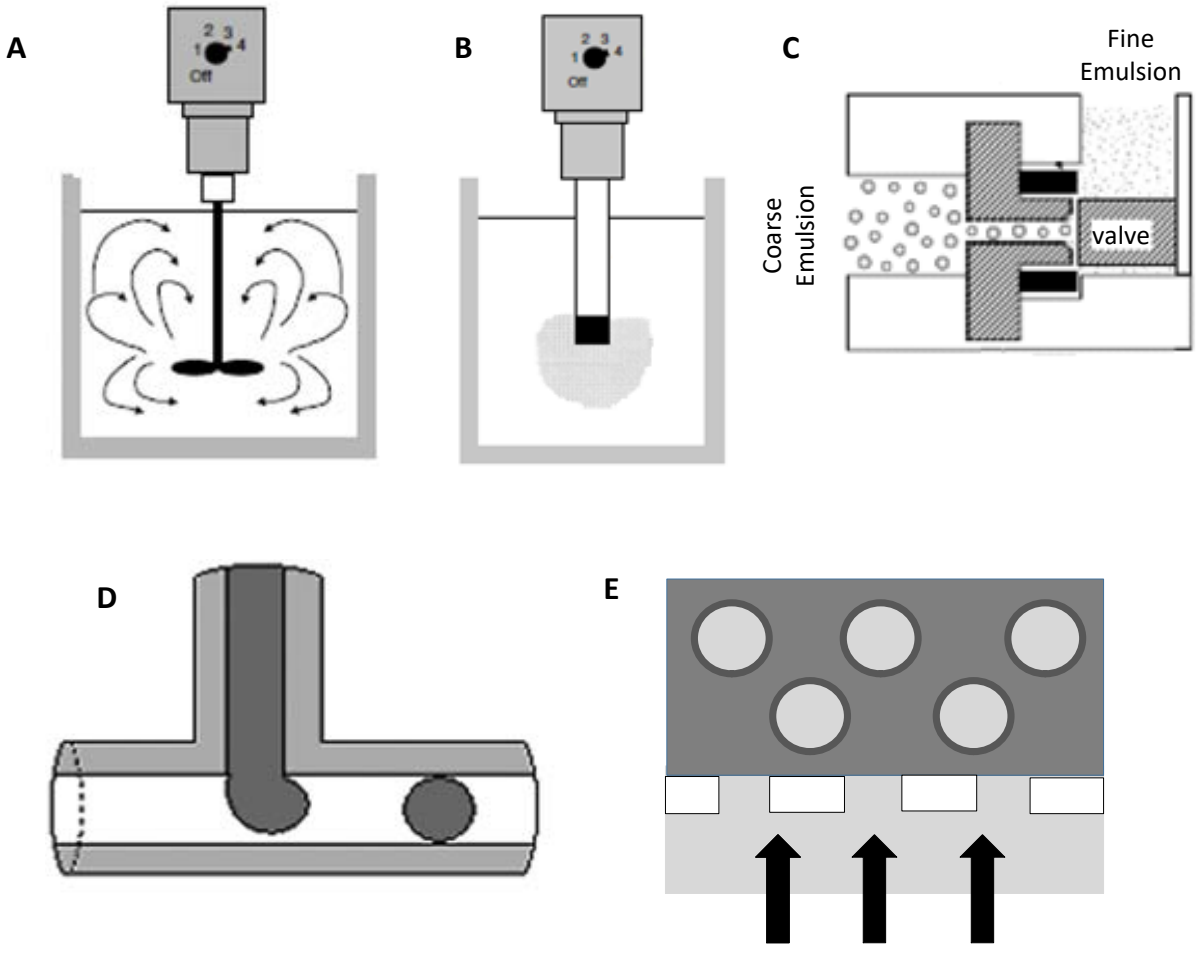

Figure 1.11. Emulsification devices. A) High-speed mixers B) Ultrasonic devise system C) High-pressure homogenization D) Microfluid systems E) Membrane systems. Reproduce from [115] with permission of Taylor and Francis Group LLC Books

High-speed mixers are the most commonly used method for directly homogenizing oil and aqueous phases in the lab scale formulation (Figure 1.11A). In a batch process, the oil, water, and other ingredients subjected to be homogenized are placed in suitable vessels, which can be as small as a few milliliters (for laboratory use) or as large as several tons (for industrial use) of liquid. The components are then agitated by a mixing head that rotates at high speed (typically up to 3600 r min^{-1}). [115]. This technique has been used for the production of microgels [116], capreomycin sulfate loaded PLGA particles [117] and solid lipid nanoparticles [118]

Ultrasound is also a powerful method of creating emulsions in immiscible systems (Figure 1.11B), due to transient collapse of the liquid–liquid interface [119]. The fundamental effect of ultrasound on a fluid is to impose an acoustic pressure (a sinusoidal wave dependent on time, frequency and the maximum pressure amplitude of the wave) [120]. This technique has been used in lab scale for encapsulating different drugs in particles, for example diclofenac sodium, dexamethasone in PLGA nanoparticle [121] and risperidone-loaded solid lipid nanoparticles [122]

High-pressure homogenization presented in Figure 1.11C. The droplet sizes of the coarse emulsion are reduced in a high-pressure homogenizer obtaining a fine emulsions with narrow distribution [123]. Pressure ranges between 20 and 4000 bar are necessary with the consequently high energy consume [124]. This technique has been used for producing particles using poly(D,L-lactide) (PLA) or PLGA [125], solid lipid nanoparticles from glyceryl behenate [126] and lecithin [127] using risperidone as model drug [122].

Microfluidic system and membrane systems will be described below.

1.5.2.1.1 Microfluidic emulsification

Microchannel emulsification technique was initially proposed by Kawakatsu [128] and it is an advanced emulsification technique capable of generating uniform droplets, with low coefficient of variation. Droplet generation by microchannel emulsification is performed via microchannels array consisting of parallel channels (Figure 1.12A) which generally enables the production of single micrometer-sized droplets with a relatively low throughput capacity [129]. A microchannel chip with asymmetric through-holes is presented in Figure 1.12B and it is capable of producing more stably monodisperse droplets with considerable high throughput capacity, which has been scaled up to 1.4 L/h of monodisperse emulsion droplets [130,131].

Geometric junction is the simplest microfluidic structure where a continuous phase is introduced from the one channel and the dispersed phase stream through other channel used for th generation

of droplets in different configurations e.g T junction (Figure 1.12C) and Y junction (Figure 1.12D) [132]. Flow focusing designs are also developed and presented in Figure 1.12E where dispersed phase (liquid A) flows through the middle channel and the continuous phase (liquid B) flows through the two outside channels. Both phases are forced to flow through a small orifice producing droplets [133].

The microchannel emulsification approach usually requires an energy input of 10^3–10^4J/m^3 [134]. The reason for this low force requirement is because droplet generation by microchannel emulsification is a very mild process that does not require any forced flow of the continuous phase, based on the spontaneous generation driven by the interfacial tension [135]. Emulsions produced via microchannel emulsification technique have many advantages over conventional emulsions in terms of their stability against coalescence due to Ostwald ripening since all the droplets are uniformly sized.

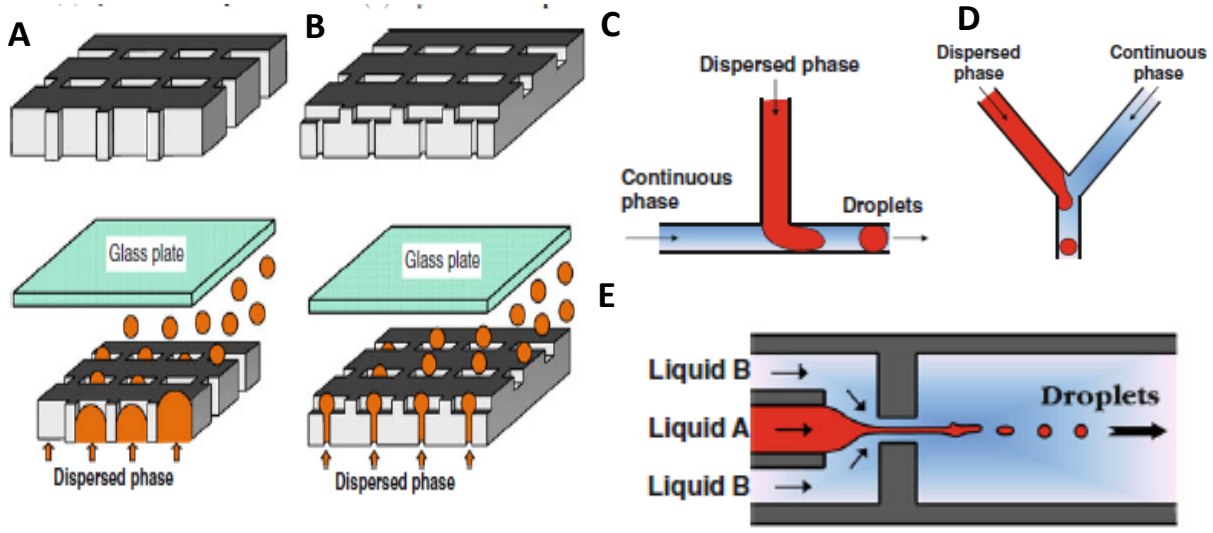

Figure 1.12 Microfluid emulsification designs A) Symmetric microchannel plate B) Asymetrix microchannel plate C) T juction D) Y juction E) microfluid flow focusing. Reproduced from [133] with permission of Springer Science and Bus Media B V.

1.5.2.1.2 Membrane Emulsification

The membrane emulsification process provides suitable solutions for pharmaceutical particles generation at different levels [136]:

- Bench and lab scale testing of formulation can be performed to produce particles and emulsions with tuned structure and functional properties.

- Large scale production of emulsions and particles can be carried out by transferring meaningful laboratory data for process scale-up.
- Continuous manufacturing process can be developed by connecting in series the membrane emulsification plant with a reactor to achieve simultaneous drop generation and chemical/ physicochemical reaction in the produced emulsion.

Membrane emulsification devices designed for small-scale testing are commercially available to establish the effectiveness of the membrane-based method in association with the desired formulation.

Shirasu-porous-glass (SPG) is a special kind of porous glass, obtained by phase separation of a primary CaO–Al2O3–B2O3–SiO2 type glass, made of Shirasu (volcanic ash from the southern part of Kyushu island), calcium carbonate and boric acid. [137]. Microengineered membranes are microfiltration membranes with a controlled pore geometry and spatial arrangement manufactured by semiconductor fabrication methods. Typical microsieves used in membrane emulsification are nickel microengineered membranes manufactured using UV-LIGA process, silicon nitride Aquamarijn TM, microsieves fabricated by reactive ion etching (RIE), stainless steel membranes fabricated by pulsed laser drilling or end-milling and single crystal silicon microchannel arrays fabricated by deep reactive ion etching [113]. Advantages of SPG membrane over microengineered membranes are in higher porosity, more versatile surface chemistry that can be used to modify the pore walls, broader range of pore sizes available, and lower fabrication costs. [113]

Membrane emulsification droplets are produced in situ by injecting a pure liquid (the dispersed phase) through the membrane into a second immiscible liquid (the continuous phase). Hydrophobic and hydrophilic membranes are needed to produce water in-oil (W/O) and oil-in-water (O/W) emulsions, respectively. At low production rates, droplets can be formed in the absence of any shear on the membrane surface, solely by the action of interfacial tension. At small interpore distances the push-off force as a result of droplet–droplet interactions on the membrane surface may assist in droplet detachment. To obtain uniform droplets at commercially viable throughputs, shear stress is generated at the membrane surface, usually using a cross-flow (Fig. 1.13A), pulsed flow (Fig. 1.13B), rotating membrane (Fig. 1.13C) or vibrating membrane set up (Fig. 1.13D) [133]

Using this technique have been fabricated gel microbeads, solid lipid particles, micro/nanospheres, liquid-core/polymer-shell capsules, porous particles, colloidosomes from polymer like chitosan, alginate, PCL, PLGA, PLA and gelatin [136]

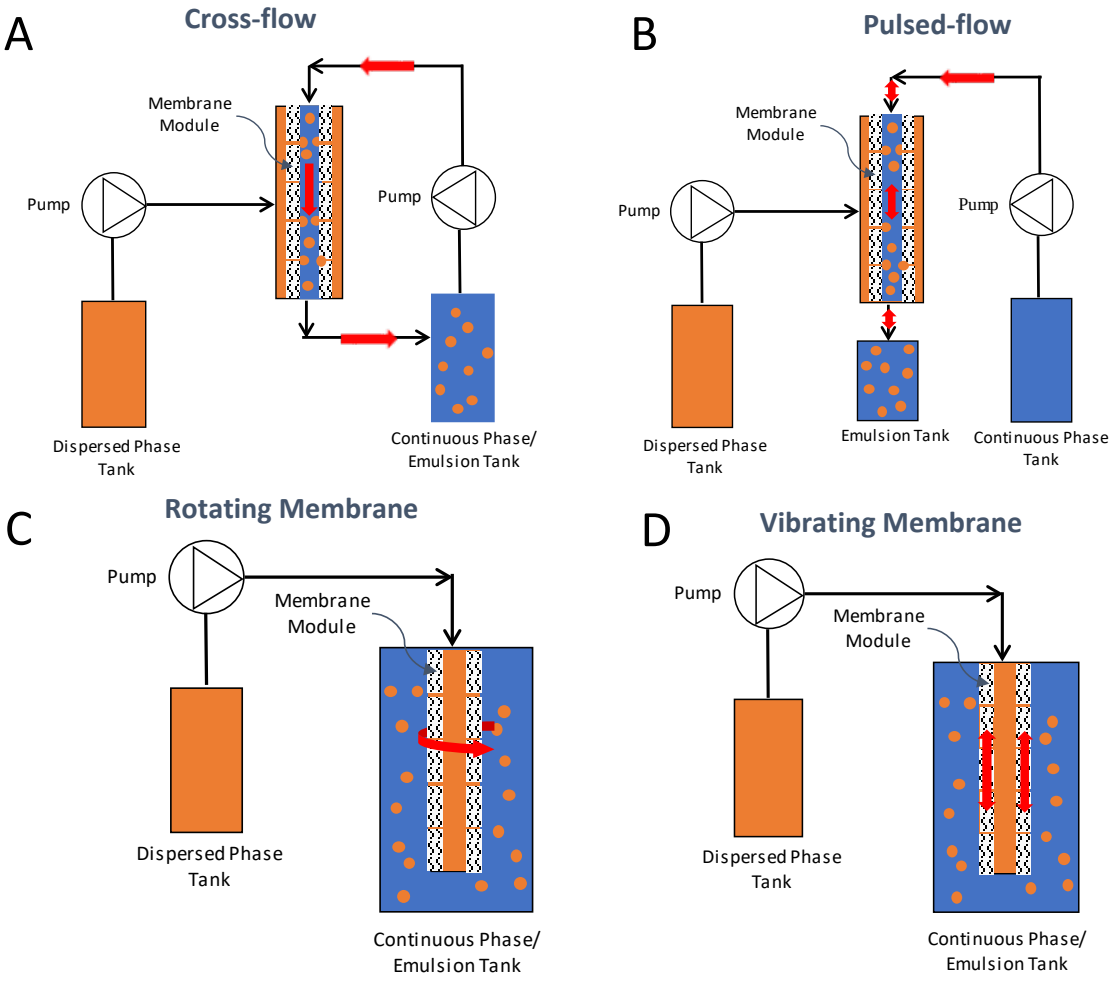

Figure 1.13: Membrane emulsification set up designs A) cross-flow B) pulsed flow C) rotating membrane D) vibrating membrane.

1.5.2.2 Second Step: Solid particle formation

The process of converting the emulsion into a solid particle is known as solidification procedure, and the process is controlled fundamentally by the physics-chemical properties. In general, the unit operation of this second step gives its name to the method [97]. Solidification process can be classified depending of the chemical process by precipitation of the polymer from emulsion (salting out, solvent diffusion, evaporation); gelation of the emulsion (chemical crosslinking, physical crosslinking) [97,138] Both methods, precipitation and gelation, will be will be described below.

1.5.2.2.1 Precipitation of the polymer from emulsion

Production of particles by solvent evaporation was reported for the first time by Vanderhoff in 1979 [139]. Depending of the type of solvent the process can be classified as solvent evaporation method

(when the solvent used to prepare the emulsion is insoluble in water)[140], solvent diffusion method (when the solvent used to prepare the emulsion is partly soluble in water) [141] and salting out method (when a high concentration of salt or sucrose is added performing a strong salting-out effect in the aqueous phase and improving the precipitation of the polymer) [138].

Concerning to solvent diffusion method, once the emulsion is formed, the droplets can be then diluted in water and the interaction between the emulsion droplets and the dilution phase is referred to as a "modification of phase equilibrium and solvent diffusion", which leads to polymer precipitation since the polymer is dispersed in the aqueous solution. [142]

The diffusion process consists of three stages (Figure 1.14). Stage A). At the beginning, when the dispersed phase is rich in solvent, the solvent diffusion rate F1 into the continuous phase is greater than the solvent evaporation rate F2. So, the continuous phase becomes rapidly saturated with solvent. Consequently, the concentration of solvent inside the continuous phase Cs reaches the solubility (maximum concentration). This stage is very short with a duration of several seconds. Therefore, it can be neglected. One way to control this stage is saturated the continuous phase with the solvent. Stage B: The quantity of solvent evaporated is compensated with solvent diffused into the continuous phase and Cs remains constant. The duration of this stage depends on the initial quantities of the dispersed phase and of the continuous phase. Stage C: The diffusivity of solvent in the dispersed phase decreases with an increase in polymer concentration. [140]

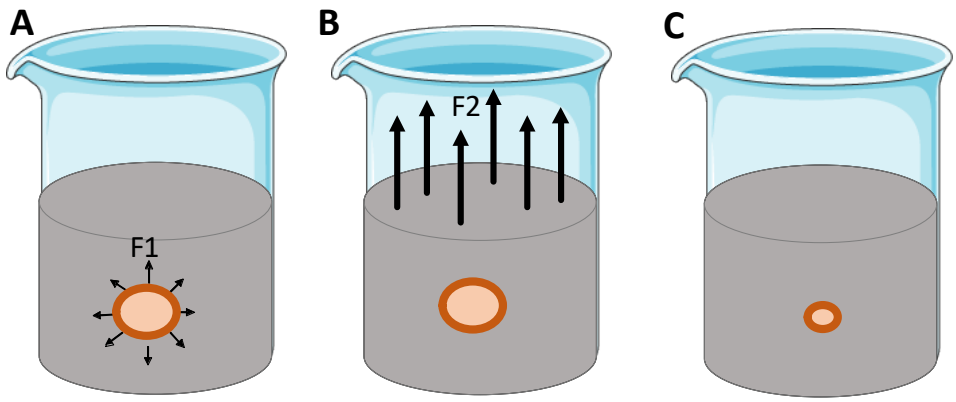

Figure 1.14: Diagram of solvent diffusion method A) The solvent diffusion rate F1 into the continuous phase is greater than the solvent evaporation rate F2 B) The quantity of solvent evaporated is compensated with solvent diffused C) Diffusivity of solvent in the dispersed phase decreases with an increase in polymer concentration.

The particle size is manly controlled by the emulsification step than the solvent diffusion step, however, some parameters need to be studied in this step such as: volume of water for dilution,

temperature of added water, rate of water addition for the dilution and stirring rate during the diffusion. [143,144].

1.5.2.2.2 Gelification process

Other methods to produce particles from emulsion are to crosslink the polymer dissolved in the emulsion droplets. This method can be applied for producing hydrogels, (explained in section 1.4.1). Preparation techniques adopted are physical crosslinking (e.g., freeze-thawing), chemical cross-linking (e.g., glutaraldehyde, GA), grafting polymerization, and radiation cross-linking. Such modifications can improve the mechanical properties and viscoelasticity for applications in biomedical and pharmaceutical fields [51]. The present thesis will be focus on the chemical crosslinking.

This process involves the introduction of the new molecules between the polymeric chains producing a cross-linked chain (Figure 1.15). The cross-linker can be a glutaraldehyde, epichlorohydrin, etc. One example is the hydrogel prepared using polyvinyl alcohol using glutaraldehyde as a cross-linker. [52]. Chemical-stabilization of hydrogels can result in potential cytotoxicity of materials as well as a loss of activity of immobilized proteins on the other hand hydrogel physical gels can be less stable during long time [145]. The crosslinking reaction is carried out in presence of an acid as a catalyst (Fig 1.15). The proposed mechanism for acid catalytic reaction involves the transfer of proton to or from a substrate molecule. [146]

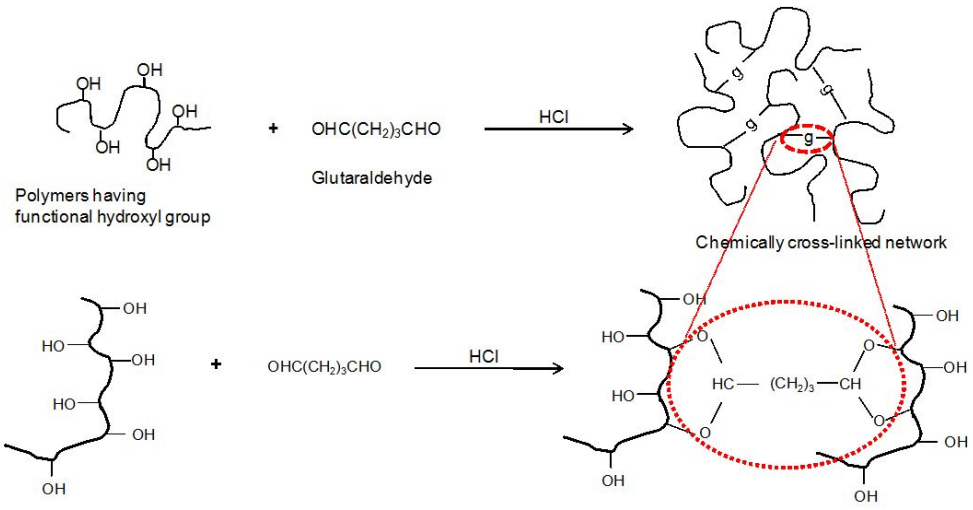

Figure 1.15: Schematic illustration of using chemical cross-linker to obtain cross-linked hydrogel network. Reproduced with permission from [51] under CC license

1.6 Challenges on the transition from the proof of concept to the application in the drug delivery particles manufactory.

The transition between proof of concept and application in drug delivery systems is not a simple task being the main reason that only a few drug delivery system products arrive to the market. [147]. Different challenges need to be introduced to answer to the specific requirements of energy consumption, toxicity, environmental impact, scalability and productivity needed for industrial application[148]. In this section, these aspects will be highlighted.

1.6.1 Process scalability

Particle production of polymeric particles are normally developed using "batch to batch" reactors, finding later big problems in the scale up [149]. Ortiz de Solosano et al. found how a scale up to a factor of 20 (150 and 300 mL) increase the particle size and heterogenicities of PLGA particles (from 0.4±0.1um to 1,2± 0.3um) using emulsification by sonification. These results corroborate that the emulsification process works well for small volume batches, but scale-up is difficult. [111]. Batch-to-batch processing have also problems of reproducibility and controllability, in terms of morphological and physicochemical properties. Consequently, the development of new technologies tackling some of these challenges could significantly accelerate the clinical translation of nanomedicines[111,149] Micro/Millireactors constitute perhaps the enabling technology of highest potential for particle production as such have been proposed to overcome the inherent discontinuity of typical batch discontinuous reactors. The scale up is also possible increasing the number of modules to adapt to the specific process requirements rather than custom design for each application typical of traditional reactors. Scaling by "numbering up" (arraying parallel microreactors) reduce financial risk, which is especially important in emerging areas such as particle production. [149]

Membrane emulsification is advantageous for the production of emulsions with a high dispersed to continuous phase ratio and it is suitable for large-scale production in continuous or semi-continuous mode. An automatic shirasu Porous Glass (SPG) membrane emulsification equipment for large-scale production with temperature and parameters of production process control systems is commercialized by Zhongke Senhui Company give. [136]. It was demonstrated that an industrial-scale membrane emulsification device was capable of formulating mineral Marcol 172 oil in water emulsions producing 1.2kg/L. [150]. Scaling through modulation is normally suggested (i.e. using

multiple membrane tubes). However, a discussion has been focused on simply using a higher membrane surface area in conjunction with larger vessels. This may be cheaper from a capital cost perspective rather than purchasing multiple smaller membrane tubes. [150].

Thanks to the advantages of membranes and micro/millireactors mentioned above those homogenization devices have been selected for our studies.

1.6.2 Energy consumption

Energy saving is a key parameter for the selection of the most suitable method for particle production at large scale. The emulsification step process represents the higher energy consumption in particles production [124]. Figure 1.16 shows a plot of mean droplet size produced by homogenizers as a function of the energy density required. Homogenizers vary considerably in the range of energy densities that they are capable of generating, and in the efficiency of these energy levels at disrupting emulsion droplets. High-speed mixers are only suitable for preparing emulsions with relatively large droplet sizes ($d > 5$ µm), whereas the other major types of homogenizers can be used to prepare smaller droplets. High pressure homogenization, high speed mixer and ultrasonic device needs high amount of energy to produce the emulsion due to the high shear stress necessary to produce emulsions with narrow size distribution. While membrane and microchannel emulsifications are able to produce emulsions with narrow droplet size distributions and the fact that they are highly energy efficient because much less energy is lost due to they are low shear stress devices [115].Considering the high energy efficiency of the membrane and microchannel devices, they were selected as the proper homogenizer devices for the production of particles in this thesis.

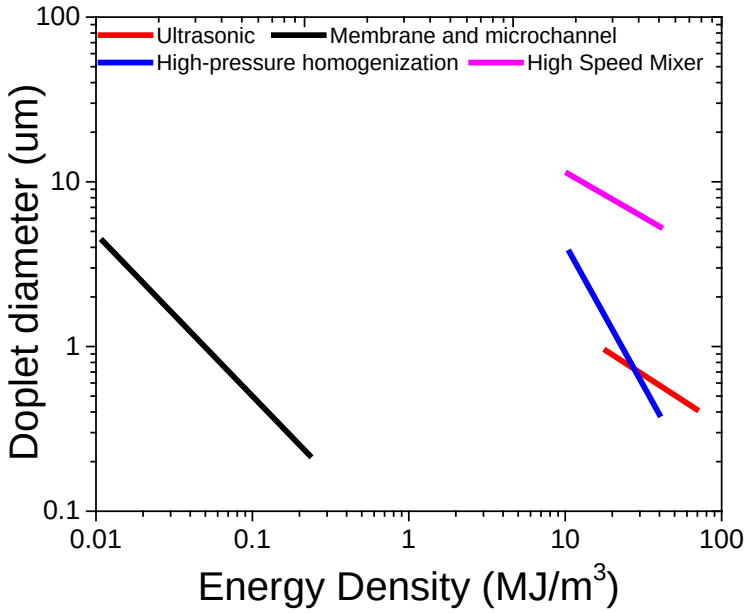

Figure 1.16: Comparison of homogenization characteristic of different mechanical homogenizers variation of mean droplet size with energy input. The precise relationship for a given device depend on the specific characteristic of the emulsion and homogenizer. Adapted from [115] with permission Taylor and Francis Group LLC Books

1.6.3 Safety and toxicity

To use the potential of drug delivery systems, it is required to also consider their safety and toxicological issues. Good manufactory processes establish the safety of raw materials, materials used in the manufacturing of drugs, and finished drug products. [151]. Then, polymer and solvents used in the production of particles need to be safe. PLGA-PEG and PVA are FDA-approved polymers, used for the preparation of drug delivery systems with proved low toxicity. [40,152,153]. The regulatory bodies of the European Union, Japan and USA regulate and classified as following [154]

- Class 1 solvents: Solvents to be avoided

Known human carcinogens, strongly suspected human carcinogens, and environmental hazards.

- Class 2 solvents: Solvents to be limited

Non-genotoxic animal carcinogens or possible causative agents of other irreversible toxicity such as neurotoxicity or teratogenicity. Solvents suspected of other significant but reversible toxicities.

- Class 3 solvents: Solvents with low toxic potential

Solvents with low toxic potential to man; no health-based exposure limit is needed. Class 3 solvents have PDEs of 50 mg or more per day.

- Class 4 solvents: Solvents for which No Adequate Toxicological Data was Found

The specification for the drug delivery system formulation should be set based on its qualification/biological safety level (toxicity studies) [151,155]. In vitro toxicity of particles in cultured cells is essential to fully understand the mechanisms of action of drug delivery formulations on biological systems. On the other hand, animal toxicity assessment tests can be time consuming and costly but provide useful and important information regarding formulation-associated toxicity. In addition, animal studies are important since several studies have shown that in vitro results alone do not always translate into in vivo results. The FDA guidelines need to be considered for preclinical studies of drug formulations planning in-vitro and in-vivo studies [156] Biocompatibility polymer (PVA and PLGA-PEG) and low toxic solvents (acetone and ethyl acetate - Class 3) are selected in this thesis to minimize the toxicity of the produced particles.

1.6.4 Regulatory aspects

For drug products to be marketed, they must be approved by the regulatory body. Regulatory agencies will not only consider clinical benefits and risks but will also focus on ensuring consistent quality and therapeutic performance of drug products. [147] . Regulation of drug products has been in a changing and evolutive path since International Conference on Harmonisation of Technical Requirements for Registration of Pharmaceuticals for Human Use started in the early 90s and the regulatory environment around the development of nano/microparticle has been under increased challenge. [157].

For drug delivery systems using complex formulation designs and manufacturing processes, the task of ensuring consistent quality becomes more challenging than traditional simple dosage forms. [147]. Specifications of these products are divided in two categories: Standard specifications (appearance, pH, osmolarity, residual solvent, sterility, pyrogen free, drug potency and drug-related substances) and drug delivery system-specific (particle size, percent "free" vs. encapsulated, zeta potential, phase transition, morpohology) [158,159]

1.6.5 Sustainability and green chemistry

Increased environmental awareness and pressure from legislators to curb emissions and improve energy efficiency by adopting greener technologies has markedly characterized the beginning of 21th century [160]. Unfortunately, pharmaceutical industry is the higher manufacturing contamination source having an attention point in the ACS GCI Chemical Manufacturer's Roundtable. Sheldon et al made a comparison between different industry segment

(oil refining, bulk chemical, fine chemical and pharmaceuticals). The highest ratio between among of product for annum and Environmental factor (kg waste per kg product) was found for pharmaceutical manufacture industry [161]

Green Chemistry can be considered as a series of reductions (Figure 1.17). These reductions lead to the goal of triple botton-line benefits of economic, environmental and social improvement. Waste reduction allow costs saving considering that it is becoming more expensive the waste disposal, especially hazardous. Energy and material consumption represent a large portion of process cost. These reductions also lead to environmental benefit in terms of both feedstock consumption and end-of-life disposal. Also, an increasing use of renewable resources will render the manufacturing industry more sustainable. [162]

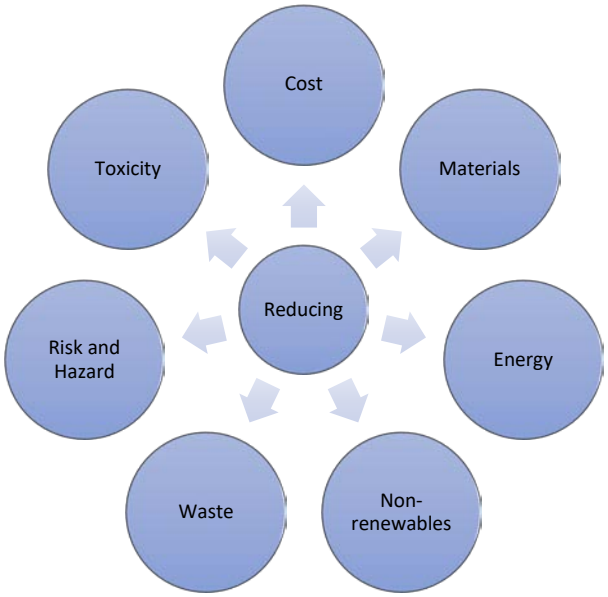

Figure 1.17. “Reducing”: The heart of Green Chemistry.

Numerous metrics have been formulated over time and their suitability has been discussed in extension. The problem observed is that the more accurate and universally applicable the metric devised, the more complex and unemployable it becomes. [160]. This thesis uses these concepts in combination with the particle production for evaluate the sustainability of the drug-loaded particle production process.

GlaxoSmithKline (GSK) has develop a carbon efficiency method where stoichiometry of reactants and products are included. Carbon efficiency is defined as the percentage of carbon in the reactants that remain in the final product following the equation 1.1 [163]

Equation 1.1 $\%\ \text{Carbon efficency} = \frac{\text{Amount of carbon in product} * 100}{\text{Total carbon present in reactants}}$

Atom Economy was developed by Barry Trost in 1991 [164] calculating the amount of reactants that remain in the final product. For a generic multistage reaction, the atom economy is as follows [160]:

$\mathrm{A} + \mathrm{B} \rightarrow \mathrm{C}$

Equation 1.2 $\%\ Atom\ Economic\ = \frac{\mathrm{M.W._C}}{\mathrm{M.W._A} + \mathrm{M.W._B}}$

Where A and B are reaction reagent and C is the product and MW is molecular weight of the components. The drawback of atom economy is that assumptions have to be made, where solvents are ignored. [160]

The E factor is a simple analysis used to calculate the greenness of a process. Process waste was determined via complete E factor calculation based on a simple mass-balance [165]. Two factors were determined: simple E factor (sEF) and complete E factor (cEF) (in which solvent and water consumed during the process are also included) using equation 1.3 and equation 1.4, respectively, adapted to the specific case of particle production:

Equation 1.3: $\mathrm{sEF}\ = \frac{\sum \mathrm{m(Raw\ Materials)} + \sum \mathrm{m(Reagents)} - \mathrm{m(Product)}}{\mathrm{m(Product)}}$

Equation 1.4: $\mathrm{cEF} = \frac{\sum \mathrm{m(Raw\ Materials)} + \sum \mathrm{m(Reagents)} + \sum \mathrm{m(Solvents)} + \sum \mathrm{(Water)} - \mathrm{m(Product)}}{\mathrm{m(Product)}}$

Where Σm(Raw Materials) represents the total raw material mass, Σm(Reagent) represents the total mass of the reagents used in the process and m(Product) represent the mass of product.

The process mass intensity (PMI), calculated as the ratio of the total mass of materials to the mass of the product, has been selected from ACS Green Chemistry Institute Pharmaceutical Roundtable as indicator of sustainability for the pharmaceutical sector:

Equation 1.5: $\mathrm{PMI} = \frac{\sum \mathrm{m(\ Materials\ \ input)}}{\mathrm{m(Product)}} = \ \mathrm{cEF} + 1$

Where the Σm(Materials input) includes the total mass of imput materials and m(Product) represent the mass of product.

Constable et.al made a comparison between the different methods revealing that atom economy and Carbon efficiency may be useful as an organising concept or in combination with other metrics due to solvent and inorganic compounds are ignored. While mass intensity and E factor may be usefully expressed as mass productivity, and as such, seems to be more broadly understood by business managers. The E factor and PMI can be used interchangeably in the Green Aspiration Level™ methodology. [160,163]

Chapter 2

Preparation of drug-loaded PLGA-PEG nanoparticles by nanoprecipitation based on microfluid devices

2.1 Introduction

Polymeric nanoparticles for drug delivery have been highly investigated in recent years [6,166–168]. They present many advantages: i) improving the solubility of drugs that normally dissolve poorly in water [169]; ii) modifying drug pharmacokinetics [170]; iii) increasing the drug half-life by reducing recognition and immunogenicity [171]; iv) targeting drugs to a specific diseased site and therefore reducing side effects [172]; and v) improving bioavailability and retention times [170][121,166,173]. Different techniques have been developed for the production of polymeric nanoparticles, e.g., nanoprecipitation, emulsion/solvent diffusion, emulsion/solvent evaporation, and salting-out [97,102,174]. Among them, nanoprecipitation has great potential due to its low energy consumption and simple processing method. The method describes a precipitation of a dissolved material into nanoscale particles after exposure to a non-solvent [101,175,176]. Under appropriate conditions, this process instantaneously generates a dispersion of small droplets or nanoparticles (NPs) with a narrow unimodal size distribution in the 50–300 nm range. This spontaneous process has been named the “Ouzo effect” and has been reported by first time by Vitale and Katz in 2003. [101,177–180]

A central challenge in the development of polymeric NPs by nanoprecipitation is the difficulty of controlling the mixing processes for regulating particle size and morphologies with good accuracy [101]. Here, milli/micromixers have high potential for easier control of the final particle properties due to their ability to accurately control mixing [106]. Table 2.1 shows different micromixer devices used for the production of drug-encapsulated particles, which show the potential of these devices for the production of NPs by nanoprecipitation. Millimixers have relatively higher productivity with respect to micromixers due to their bigger internal volume. Millimixers also present higher flow rates and lower possibilities of channels blocked by solid particle accumulation. [106].

Table 2.1: Production of nanoparticles by nanoprecipitation using different micro/millimixer devices

Polymer	Drug	Micro/millimixer Device	Application	Reference
poly(methyl methacrylate)	Ketoprofen	K-M steels micromixer	ophthalmologic	[109]
PLGA-PEG	Docetaxel	T-type Hydrodinamic Flow Focusing chip fabricated by standard micromolding process	Anticancer	[103]
PLGA-PEG	Doxrubicin	3D origami chip by bonding two polydimethylsiloxane layers after oxygen plasma	Anticancer	[181]
Polystryene	B-carotene	confined impinging jets micromixer micromixer fabricated by microdrilling	Food applications	[182]
PLGA-PEG	Docetaxel	Coaxial turbulent jet mixer fabricated by off-the-shelf components	Anticancer	[183]
Polaxamer 188	Meloxicam	Intensified micromixer based on a rotating surface	anti-inflammatory	[108]

As it was aforementioned in Chapter 1, microfluidic systems are a powerful tool to carry out a wide range of chemical reactions, and their use in the synthesis of NPs is attracting a remarkable interest. Thus, compared to conventional batch synthesis, microfluidic systems allow a precise control of the reaction conditions (reaction time, temperature, reactant concentration, and stoichiometry). Their high surface-area-to-volume ratios and mixing characteristics help to reduce or avoid temperature and concentration heterogeneities, decreasing NP polydispersity, and guaranteeing a specific composition and structure. Because of the accurate control and reproducibility of physicochemical properties achieved by microfluidic systems, they are considered as the technology of choice for mass production of nanomaterials. In this regard, controlled synthesis of polymeric NPs by rapid mixing is a novel research topic. However, besides the continuous production mode of microfluidic reactors, the throughput required to fulfil the clinical translation is still a challenge, and high-throughput procedures are highly desired. In this context, this work aims to study the feasibility of using a new millimixer device to increase the production throughput of PLGA-PEG nanoparticles loaded with DEX. Differently from micromixers, millimixer dimensions and design should promote to achieve an efficient passive mixing but decreasing the pressure drop. This fact should enable to operate at higher flow rates than the ones required with micromixers and then increase the

production throughput . The millimixer selected in this work was fabricated by LGC according to the design published by Johnson and Prud'homme (Johnson et Prud'homme 2003c). Considering that this type of millimixers was not previously applied in the production of nanoparticles by nanoprecipitation, this work aims to answer several key questions:

a) Is the mixing performance good enough to promote a molecular mixing of reagents?
b) Are millimixers able to tune the particle size and morphology of nanoparticles?.

In addition, encapsulation efficiency (EE) and drug loading efficiency (DLEs) have a significant relevance for pharmaceutical particles design being EE and DLEs a measure of the efficiency of the preparation method and the materials to incorporate the drug, respectively. [184]. Many parameters related to the operating variables and starting materials (such as polymer/drug/solvent/non-solvent system) influence the EE for the nanoprecipitation process (Table 2.2).

Table 2.2: Influence of operating variables and starting materials on EE for nanoprecipitation method. [142]

Variable	**Influence on EE**
Operating variables	
Stirring	Reducing stirring rate increases EE
Aqueous to organic solvent volume	Decreasing aqueous solution volume increases organic/aqueous solution ratio and decreases EE
Starting materials	
Drug nature	Hydrophilic molecules decrease EE
Drug initial amount	EE increases as drug initial amount increases up to a maximum value, when drug precipitation occurs.
Polymer nature	The stronger the drug–polymer affinity ,the larger the EE
Solvent nature	Significant influence on EE

Considering that, in the present work the ability of the millimixer studied to control the drug loading and promote a high encapsulation efficiency has been emphasized. In particular, first, the nanoprecipitation process of PLGA-PEG was studied by finding the area in the ternary phase diagram (PLGA-PEG/acetone/water) where the precipitation mechanism occurred for the NPs, which be

spheres with a narrow size distribution. Second, the EE and DLE were evaluated and then related to the quaternary phase diagram (PLGA-PEG/DEX/acetone/water).

2.2 Materials and Methods

2.2.1 Materials

The nanoprecipitation process is based on the proper mixing of four main materials: polymer, drug, solvent and non-solvent [101]. The PLGA-PEG polymer used in this study was Resomer RGP d 5055 (PLGA Mn 55kDa, lactide:glycolide 50:50, PEG Mn 5kDa, PEG wt% 5%, EVONIK, Germany). Dexamethasone (DEX) supplied by SIGMA–Aldrich was used as the model drug. Analytical grade acetone purchased from SIGMA-Aldrich was used as the organic solvent. Ultrapure water obtained from a Milli-Q purifier system (Millipore Corp., MA, USA) with a conductivity lower than 18.2 MΩ cm was used as the non-solvent.

2.2.2 Preparation of particles by nanoprecipitation using a millimixer device.

The PLGA-PEG polymer mass was dissolved in acetone (solvent) in order to obtain the desired polymer concentration. It was stirred by vortex for 10 min and used as Stream 1. Ultrapure water (non-solvent) was used as Stream 2. Stream 1 was modified by including DEX for the study of dexamethasone (DEX) encapsulation efficiency and drug loading efficiency. Stream 1 and Stream 2 were mixed using a millimixer device (manufactured at LGC, Toulouse, France) that was based on a design described by Johnson and Prud'homme [180].

Figure 2.1 shows the set-up, which includes two positive displacement pumps (Model: PHD 2000, Harvard Apparatus, Holliston, MA, USA) coupled with two plastic syringes (Plastipak, VWR, USA). Stream 1 and Stream 2 were pumped using a 10mL syringe and 50mL syringe, respectively. The stainless steel millimixer had two inlets and one outlet, in which its inlets were connected to the syringes and the outlet discharged the NPs solution to a collector flask using 1/16″ OD PTFE tubing. After the formation of NPs, the acetone was evaporated under continuous stirring (600 rpm) in an open flask for 3 hours and NPs were collected.

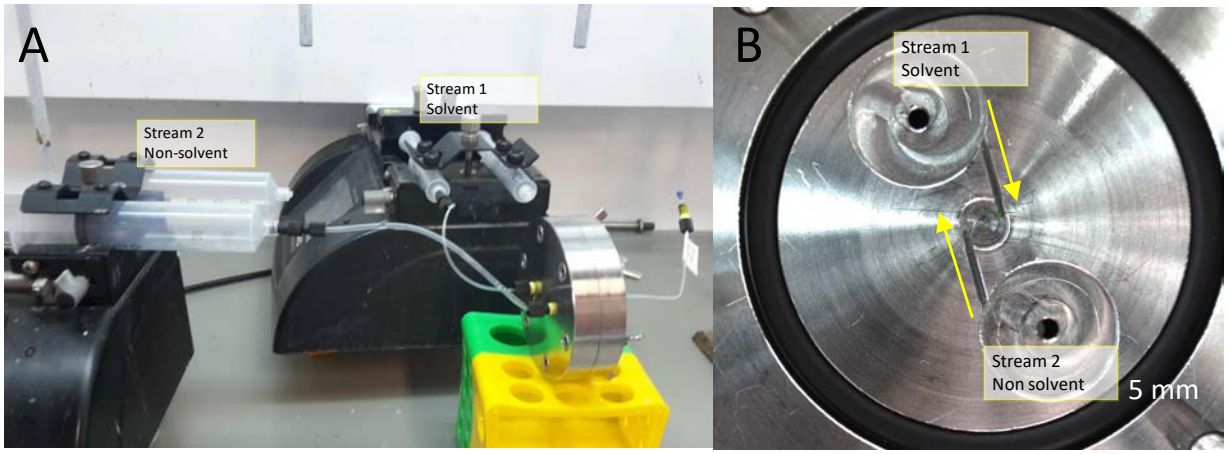

Figure 2.1: Micromixer setup. A) Syringe pump inlet, outlet and connections. B) Millimixer interior based on prescribed device [180].

Nanoprecipitation experiments were divided in 2 blocks; the first block used only PLGA-PEG polymer, and the second block used PLGA-PEG polymer and dexamethasone. During the first block, we prepared 8 formulations using PLGA-PEG polymer to explore the appropriate polymer and acetone mass fractions for inducing nanoprecipitation adequate for producing nanoscale particles with a narrow size distribution. Formulations with acetone mass fractions in the range 0.2 to 0.7 and PLGA-PEG mass fractions in the range $5.1*10^{-4}$ to 0.12 were selected. Flows were properly adjusted when the Stream 1 flow rate ($F_{stream1}$) was set between 11 – 90 mL/min, and the Stream 2 flow rate ($F_{stream2}$) between 25 – 100 mL/min; the PLGA-PEG polymer concentration ranged between 2 – 145 mg/mL. A summary of the operating flow rates and concentrations required to obtain the desired mass fractions for each formulation is reported in Appendix Table S2.1.

The second block included three sets of experiment. They are as follows.

Block 2 Experiment 1: Formulations for calculation of EE and DEL and correlation with precipitation curves. Here, formulations with acetone mass fractions in the range 0.08 to 0.4, PLGA-PEG mass fractions in the range $5.13*10^{-4}$ -$7.12*10^{-3}$, and DEX mass fractions in the range $2.56*10^{-4}$ -$3.57*10^{-3}$ were selected. Flows were properly adjusted when $F_{stream1}$ was set between 11.1 – 33.3 mL/min; $F_{stream2}$ between 50 – 100 mL/min; PLGA concentration between 2 – 20 mg/mL; DEX concentration between 1 – 10 mg/mL. The summary of operating flow rates and concentrations required to obtain the desired mass fractions for each formulation are reported in Appendix Table S2.2.

Block 2 Experiment 2: Influence of the contact time of DEX with PLGA-PEG nanoparticles.

The PLGA-PEG nanoparticles prepared by millifluidic device were produced using same protocol for the Block 1 experiment, which were later combined with powdered dexamethasone (DEX) to obtain

the final composition. The PLGA-PEG NPs were produced with $F_{stream1}$ = 22 mL/min, $F_{stream2}$ = 69 mL/min, and a PLGA-PEG concentration of 10 mg/mL. The PLGA-PEG NP solution was collected in a flask and 15 mg of the solution was weighted. 3.85mg of DEX was added to the weighted solution to obtain a DEX mass fraction of $2.55*10^{-4}$. The solution was continuously stirred at 600 rpm for 0.17 h, 0.5 h, 2 h, and 24 h.

Block 2 Experiment 3: Influence of PLGA-PEG mass fraction in the range $5.12*10^{-4}$ - $7.12*10^{-3}$.

The evaluation was conducted by increasing the PLGA-PEG concentration from 2 mg/mL to 28 mg/mL, for constant $F_{stream1}$ = 22 mL/min, constant $F_{stream2}$ = 69 mL/min, and using a DEX concentration of 1 mg/mL. The summary of flow rates and concentrations required to obtain the desired mass fractions for each formulation is reported in Appendix Table S2.3.

2.2.3 Study of mixing performance in the millimixer device using competitive chemical reactions.

Micro and millireactors have been frequently investigated by competitive chemical reactions in order to evaluate mixing time and mixing efficiency using well-defined kinetics as ‘‘chemical rulers’’. [107,185,186]. Second order competitive reactions are considered to determine the grade of mixing of reagents in the mixer. This grade of mixing can be quantified by the Damköhler number (Da), a dimensionless number used in chemical engineering to relate the chemical reaction timescale (reaction rate) to the transport phenomena rate (mixing time) occurring in a system:

Reaction 2.1 $\mathrm{A} + \mathrm{B} \overset{k1}{\rightarrow} \mathrm{Products}$ Fast

Reaction 2.2 $\mathrm{D} + \mathrm{B} \overset{k2}{\rightarrow} \mathrm{Products}$ Slow

A simple illustration on why these reactions are mixing-sensitive is given in Figure 2.2. In Figure 2.2A, the characteristic mixing time (t_{mix}) is smaller than the characteristic reaction time for the slow reaction (t_{rxn}). When Da << 1, the reaction kinetics approach the homogenous conditions. In addition, since k1 >> k2, the conversion of the reagent D is not detectable. In Figure 2.2B, the mixing time of the reactants is comparable to the characteristic reaction time and Da ≈ 1, resulting an unequal molar ratio to exist locally during the reaction. In the interfacial region, reagent A will immediately react with B, and leave reagent A depleted relative to D. Reagent D continues to diffuse toward B and increases its probability to react, resulting in a detectable conversion of reagent D as a marker allow characterizing the mixing [185].

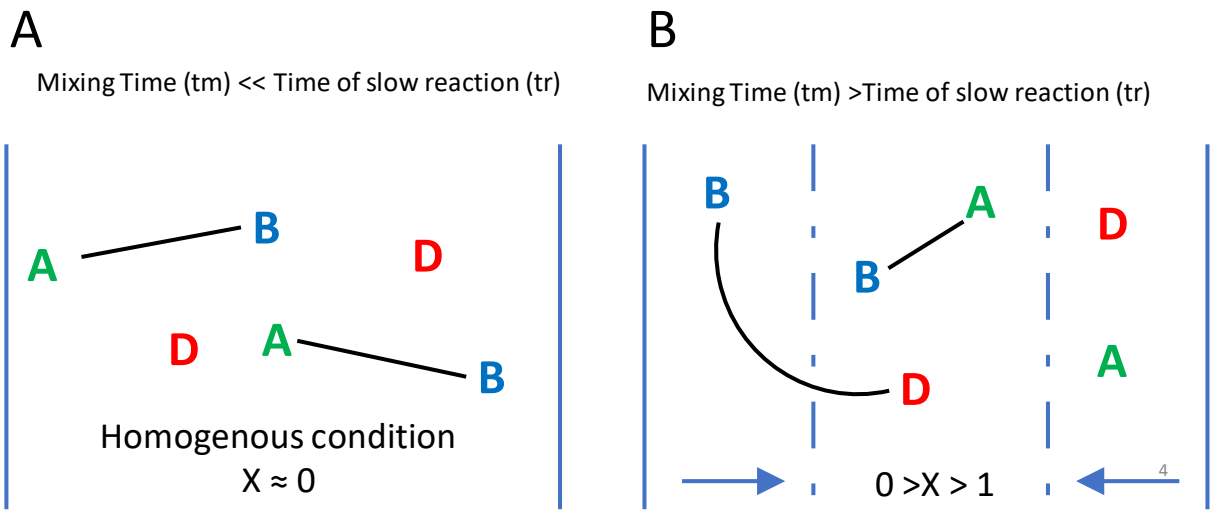

Figure 2.2: Representation of mixing effects on the product distribution of competitive reactions (Reaction 2.1 and 2.2 were A, B, C and D are reactants). A) Mixing is rapid enough to achieve homogeneous kinetics and undetectable conversion of the slow reaction. B) Mixing results in striations of reagent streams in the reaction (likely at incorrect volume ratios), and conversion of the slow reaction is detectable.

The fast reaction of this competitive reaction system is the neutralization of sodium hydroxide with a kinetic constant equal k1 =1.4*$10^8 m^3 \cdot mol^{-1} \cdot s^{-1}$ reported by Baldyga et al. [187].

Reaction 2.3 $OH^- + H^+ \rightarrow H_2O$ (A + B → Products FAST)

The slow reaction is the acid catalyzed hydrolysis of 2,2-dimethoxypropane (DMP) to form one mole of acetone and two moles of methanol

Reaction 2.4 $CH_3C(OCH_3)_2CH_3 + H^+ (+H_2O) \rightarrow CH_3COCH_3 + 2CH_3OH$ (D + B → Products SLOW)

DMP + H^+ (+H2O) → Acet + Meth

Johnson and Prud'homme reported a k2 value equal to 0.63 $m^3 \cdot mol^{-1} \cdot s^{-1}$ in the DMP reaction [185]

As discussed in Section 2.1.2, the millimixer set up consists of two inlet streams (Stream 1 and Stream 2) and one outlet stream. The flow rate ratio between the two inlet streams (S1/S2) was calculated using Equation 2.1:

Equation 2.1 $$S1/S2 = \frac{F_{Stream\ 1}}{F_{Stream\ 2}}$$

where $F_{stream\ 1}$ is the flow rate of Stream 1 (mL/min) and $F_{stream\ 2}$ is the flow rate of Stream 2 (mL/min). Two values for the ratio S1/S2 were studied, 1 and 0.11. For S1/S2 = 1 $F_{stream1}$ and $F_{stream2}$ were established in the range 0.1 – 50 mL/min. For S1/S2 = 0.11, $F_{stream1}$ ranged 0.11 - 11.1 mL/min while $F_{stream2}$ ranged 1 – 100 mL/min.

The Stream 1 component was HCl and the Stream 2 components were NaOH and DMP. Concentrations of HCl, NaOH and DMP were modified in order to have a fixed final composition before the reaction: C_{HCLo} = 100 mmol/mL, C_{NaOHo} = 105 mmol/mL, C_{DMPo} = 100 mmol/mL. To maintain S1/S2 = 1, the concentration of Stream 1 was combined with the concentration of Stream 2 to yield the following compositions: $C_{HCL,S1}$ = 200 mmol/mL, $C_{NaOH,S2}$ = 210 mmol/mL, and $C_{DMP,S2}$ = 200 mmol/mL. S1/S2 = 0.11 was maintained by having the compositions for Stream 1 and Stream 2 be $C_{HCL,S1}$ = 1000 mmol/mL, $C_{NaOH,S2}$ = 117 mmol/mL, and $C_{DMP,S2}$ = 111 mmol/mL. All initial solutions contained 25 wt % ethanol in deionized water and 90 mmol/mL NaCl. The outlet components were acetone, methanol, and the non-converted DMP.

Since the reaction rate constants in competitive reaction differ by many orders of magnitude and the fast reaction is essentially instantaneous relative to the mixing, the characteristic reaction time (reaction time scale of the system) can be expressed as the half-life of species H^+ ($t_{1/2}$) in a first order reaction of the slow reaction [188]:

Equation 2.2 $$t_{1/2} = \frac{\ln 2}{k * C_{HClo}},$$

where C_{HCLo} is the concentration of species H^+ present in the reaction and k is the rate constant. With the values reported above, i.e., C_{HCLo} = 100 mol/m^3 (100 mmol/mL) and k = 0.63 m^3·mol^{-1}·s^{-1}, we calculated $t_{1/2}$ = 11 ms.

Conversion of DMP (X_{DMP}) corresponds to the conversion of reagent D in the slow reaction and can help to characterize the mixing. The X_{DMP} calculation depends on the ratio between the concentration of DMP obtained after the reaction (C_{DMP}, mmol/mL), and the concentration of DMP at the beginning of the reaction (C_{DMPo}, mmol/mL) [107,185].:

Equation 2.3 $$X_{DMP} = 1 - \frac{C_{DMP}}{C_{DMPo}}$$

C_{DMPo} has a fixed value equal to 100 mol/m^3 and C_{DMP} was indirectly measured using the concentration of acetone at the end of the reaction ($C_{acetone}$) using Equation 2.4 and stoichiometry considerations. The volume at the end of the reaction is constant, which allows for the molar concentration to be added or subtracted.

Equation 2.4 $$C_{DMP} = C_{DMPo} - C_{acetone}$$

The concentration of acetone at the end the reaction was measured by a UV–VIS spectrophotometer (Model: UV1800, Shimazu, USA) operating at wavelength of 265 nm following the method developed by Barthauer et.al. [189] . The linear regression coefficient (R^2) determined in the range 5–100 mmol/L was equal to 0.985 (n=10).

The effect of the total flow on the conversion of DMP (X_{DMP}) using the S1/S2 ratios of 1 and 0.11 was studied and the results are reported in Figure 2.3. The total flow is the sum of $F_{stream1}$ and $F_{stream2}$, which progressively increased with the increase of both inlet flow streams. A value X_{DMP} = 0.65 ± 0.04 was obtained when the total flow was maintained below 20 mL/min. A decrease of X_{DMP} was observed when the flow was further increased from 20 mL/min to 110 mL/min, thereby presenting a similar tendency between curves for both S1/S2 (1 and 0.11). Considering the relation between good mixing and the nanoprecipitation process [101,106], it is recommended to work at X_{DMP} lower than 0.2 to maximize the mixing mechanism [180,185]. Thus, the necessary total flow rate to obtain an adequate mixing in the nanoprecipitation process using the millimixer device was deduced to exceed 60 mL/min, where $F_{stream\ 1}$ > 6 mL/min and $F_{stream\ 2}$ > 56mL/min.

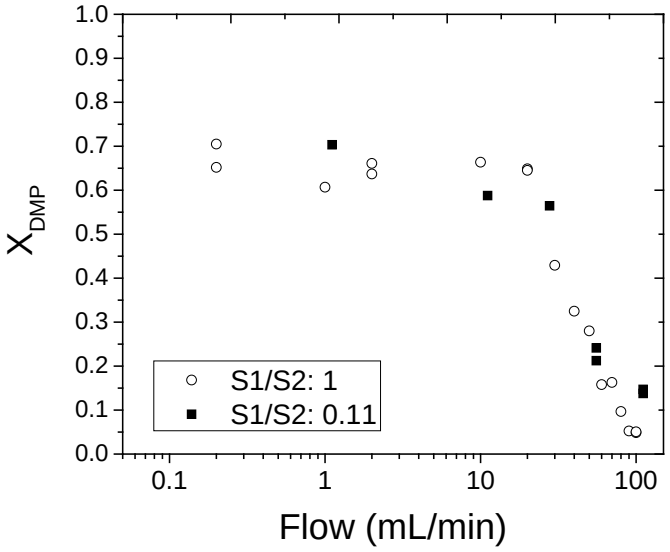

Figure 2.3: Experimental results for the conversion of DMP (XDMP) as a function of the total flow rate using S1/S2 ratios of 1 (open circle) and 0.11 (black square).

Particles were produced by nanoprecipitation using millimixer device considering the flow values established above (Appendix Table S2.1, Table S2.2 and Table S2.3). An exception was made for Samples 7 and 8 from Block 1 Experiment 1 (Appendix Table S2.1), where high $F_{stream1}$ (acetone volume flow) and high compositions were necessary. (Sample 7: [$f_{acetone}$ = 0.70, $f_{PLGA\text{-}PEG}$ = 0.01] and Sample 8 [$f_{acetone}$ = 0.7, $f_{PLGA\text{-}PEG}$ = 0.12]). For these cases, $F_{stream1}$ was set to 90 mL/min and $F_{stream2}$ to 25 mL/min to obtain S1/S2 = 3.6, in which a high overall flow at 115 mL/min (higher than 60 mL/min) was maintained.

2.2.4 Phase diagrams

Solubility boundary curves were obtained by a simple titration method reported by Aubry et.al. in 2009. The method is based on the precipitation of the solute (PLGA-PEG and/or DEX) by adding a mixture of solvent (acetone) and non-solvent (water), where dynamic light scattering (DLS) is used as an indicator of the precipitation [179].

Solutions with different concentrations were prepared by dissolving the solute (PLGA-PEG or DEX) in acetone with stirring by a magnetic bar at 300 rpm into an isothermal bath at 25 ^{0}C. A light scattering count rate onset of 100 was used to classify the samples either as transparent or cloudy using a VASCO$^{\gamma}$ Particle Size Analyzer for DLS (Cordouan Technologies, Pessac, France). Mass fractions of acetone, water and solute of the measured samples were plotted in a ternary phase diagram. The obtained solubility boundary curve divides the transparent samples from the cloudy samples. Two curves were obtained using PLGA-PEG and DEX as solutes.

2.2.5 Particle characterization

2.2.5.1 Particles analysis

Particle size and polydispersity (PDI) of the nanoparticles were measured by DLS. The software used to collect and analyse the data is NanoQ™ software. The measurements were made at a controlled temperature of 25°C. The Z-average diameter (Z-Average) and the polydispersity index (PDI) were obtained from the autocorrelation function using a refractive index of 1.55.

Morphological analysis of the NPs was carried out by scanning electron microscopy (SEM). Measurements were performed with an Inspect F50 (FEI, Eindhoven, Netherlands) at the LMA-INA-Universidad Zaragoza facilities; its operational voltage was 10–15 kV. The collected purified samples were stained by mixing 200 µL of NP colloids with 200 µL of phosphotungstic acid solution (75 mg/mL) for 1.5 h. The resulting dispersion was washed three times with Milli-Q water using a centrifuge at 3100 rpm. Finally, 10 µL of the resulting NP suspension was added on a glass slide, air-dried, and sputtered with platinum.

2.2.5.2 Encapsulation Efficiency and Drug Loading Encapsulation determination

The encapsulation efficiency (EE) and drug loading encapsulation (DLE) have been evaluated according to the following equations (Equation 2.4 and Equation 2.5):

Equation 2.5 $$EE = \frac{DEX_{encap}}{DEX_{total}} * 100$$

Equation 2.5 $$DLE = \frac{DEX_{encap}}{PLGA_{total}} * 100$$

where EE is the encapsulation efficiency (%), DEX_{encap} is the encapsulated dexamethasone mass (mg), DEX_{total} is the initial dexamethasone mass in the dispersed phase (mg), DLE is the drug loading efficiency (%) and $PLGA_{total}$ is the initial PLGA mass in the dispersed phase (mg).

The encapsulated DEX mass was determined by high performance liquid chromatography (HPLC) and following the method developed by Español et.al [121]. To evaluate these quantities, a known quantity of NPs was dissolved in acetonitrile, mixed for 1 hour with the internal standard (diclofenac sodium). Methanol was then added into the mixture and mixed in an ultrasonic bath for 15 minutes to enhance PLGA precipitation. The dispersion was centrifuged at 12,000 rpm for 20 minutes to remove the polymeric residue, and the supernatant was filtered using 0.22-µm PTFE syringe filters and placed in a vial for HPLC analysis. A reversed-phase C18 column (2.6 µm, 50x4.6mm Phenomenex kinetex) was used. The mobile phase was acetonitrile/water pH 3 (50/50 v/v). The flow rate was 0.4 mL/min and detection was performed at 260 nm by the UV detector. The linear regression coefficient (R^2) was determined in the range 0.01–30 µg/mL as 0.9993 (n=10).

2.3 Results and Discussion

This section is structured in two main subsections. The first subsection presents the results of nanoprecipitation using a millimixer device described in Section 2.2. Firstly, an adequate composition of two different streams in terms of PLGA-PEG and acetone mass fraction was determined to be based on the phase diagram of PLGA-PEG polymer/acetone/water. We then focused on the effect of phase composition within this on the morphology, particle size (Z-Average) and particle size distribution (PDI) of nanoparticles. The second part, concerns the encapsulation of the drug inside the nanoparticles. The ternary phase diagram of the DEX/acetone/water and the quaternary phase of PLGA-PEG/DEX/water/acetone were constructed. Lastly, the drug encapsulation efficiency and drug loading efficiency were investigated and correlated with the quaternary phase diagram to maximize EE and DLE.

2.3.1 Nanoprecipitation by using millimixer devices

2.3.1.1 Construction of phase diagram for PLGA-PEG polymer to find the adequate region of nanoprecipitation

Figure 2.4A shows the ternary phase diagram of the polymer/water/acetone system where compositions are plotted according to the final mass fraction PLGA-PEG (horizontal axis) and the mass fraction acetone (vertical axis). This diagram was obtained according to methods described in Section 2.2.4. The PLGA-PEG mass fraction is represented on the x-axis and is log-scaled in order to display the precipitation area.

As can be seen in Figure 2.4A, the PLGA-PEG solubility boundary (red line) has a convex shape and divides the transparent polymer solution (blue "X") from the cloudy polymer solution (blue open square). Hydrophobic characteristic of the polymer is verified due to the low amount of water necessary for the precipitation. Similar boundary was found by Aubry for polymethylmethacrylate using acetone as the solvent [179].

Next, nanoprecipitation experiments using millimixer system were performed for the PLGA-PEG /acetone composition, which are plotted in the red colour in Figure 2.4A. We confirmed the formation of nano- and microparticles for compositions well below the PLGA-PEG solubility boundary, which constitutes a phase separation region (Figure 2.4C). However, samples with compositions near the boundary present nano- and microparticles with heterogeneous shapes and amorphously-shaped polymers (They can be seen in Figure 2.4C for e.g., Sample 7 [$f_{acetone}$ = 0.70, $f_{PLGA-PEG}$ = $1*10^{-2}$] and Sample 8 [$f_{acetone}$ = 0.7, $f_{PLGA-PEG}$ = 0.12]), whereas, samples distant from the boundary are homogenous with nanoscale dimensions (in Figure 2.4C, e.g., Sample 1 [$f_{acetone}$ = 0.20, $f_{PLGA-PEG}$ = $5.1*10^{-4}$] and Sample 5 [$f_{acetone}$ = 0.20, $f_{PLGA-PEG}$ = $5.1*10^{-4}$]).

To elucidate these differences, a so-called "Ouzo" diagram for nanoprecipitation is represented in Figure 2.4B. To the best of our knowledge, no data are available in the literature for the ternary PLGA-PEG/acetone/water system. However, Beck-Broichsitter et al. determined a ternary diagram for the PLGA/acetone/water (containing 0.1 wt % of poloxamer 188) system at 25°C [178]. Beck-Broichsitter's use of the "Ouzo diagram" was considered here since the physicochemical properties of PLGA-PEG and PLGA are similar, especially the solubility and interaction parameters. These similarities for both polymers are expected to show similar behaviour in the same acetone/water ternary system [142]. Both solubility and interaction parameters (such as solvent-water and

polymer-solvent interaction) are reported to influence the phase mixing of the nanoprecipitation process [142].

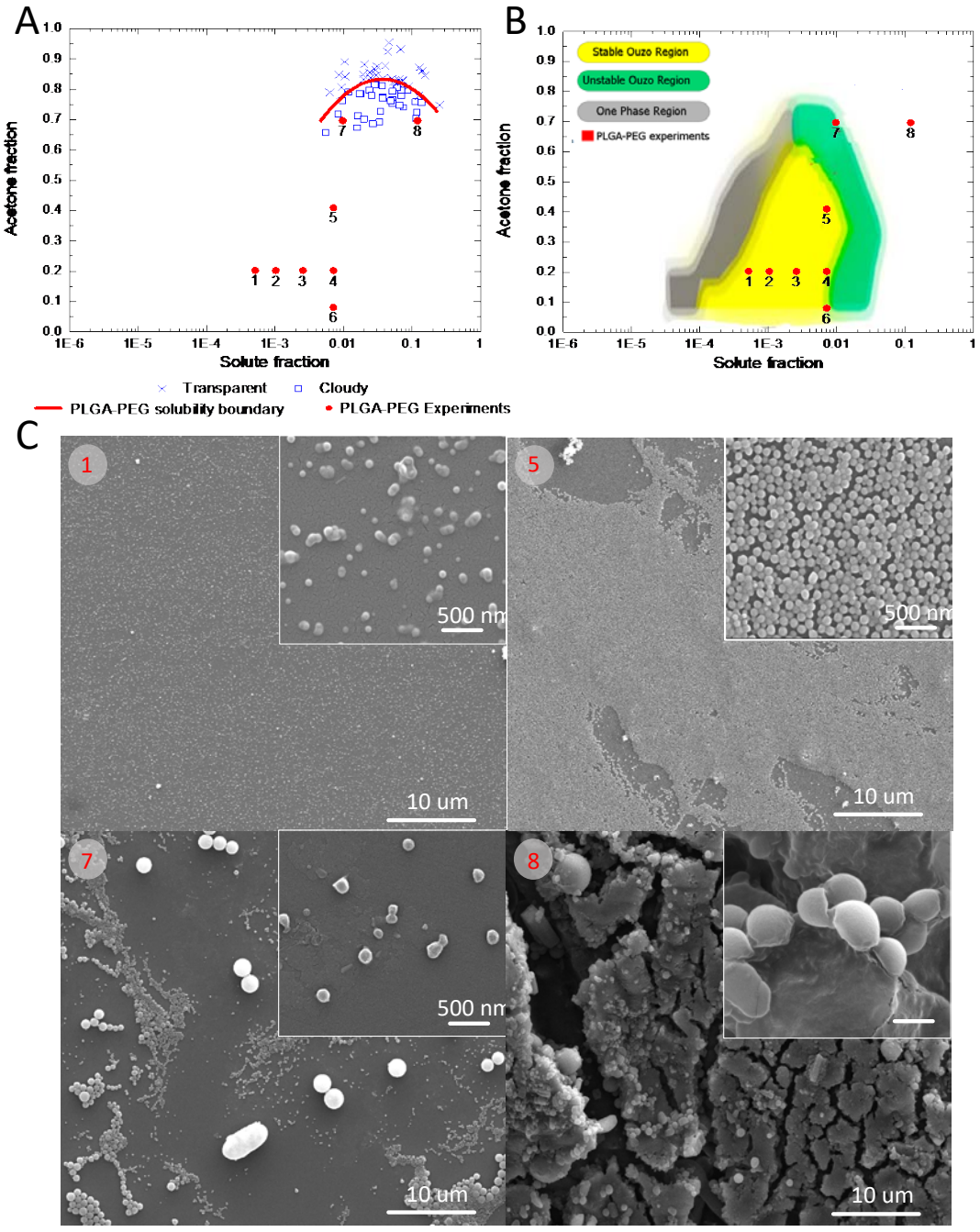

Figure 2.4: A) Phase diagram of PLGA-PEG/ acetone/ water; blue "X": transparent polymer solution; blue open square: cloudy polymer solution; red line: PLGA-PEG solubility boundary; red close circle: PLGA-PEG nanoprecipitation using millifluidic system experiments. B) Ouzo diagram obtained by Beck-Broichsitter et al. (2015) [178] in combination with our experimental data; grey colour area: one phase region; yellow colour area: stable ouzo region; green colour area: unstable Ouzo region;

red close circle: PLGA-PEG nanoprecipitation using multifluidic system experiments. C) SEM images of PLGA-PEG nanoparticles produced by nanoprecipitation using multifluidic system experiments. Sample 1 [$f_{acetone}$ = 0.20, $f_{PLGA\text{-}PEG}$ = 5.1*10^{-4}]; Sample 5 [$f_{acetone}$ = 0.20, $f_{PLGA\text{-}PEG}$ = 5.1*10^{-4}]; Sample 7 [$f_{acetone}$ = 0.70, $f_{PLGA\text{-}PEG}$ = 1*10^{-2}] ;and Sample 8 [$f_{acetone}$ = 0.7, $f_{PLGA\text{-}PEG}$ = 0.12].

Three regions have been identified (Figure 2.4B): a single-phase region (grey colour), a stable "ouzo" region (yellow colour), and unstable "ouzo" region (green colour). A single-phase region corresponds with very low polymer mass fraction where no particles are detectable. The stable "ouzo" region corresponds to a medium polymer mass fraction where optimum conditions for nanoprecipitation are achieved. The unstable "ouzo" region correspond to high polymer fraction where polymer aggregation is present [178]. Particles obtained by the millifluidic system for compositions corresponding to these different regions of the diagram were characterized by SEM (Figure 2.4C). Sample 1 [$f_{acetone}$ = 0.20, $f_{PLGA\text{-}PEG}$ = 5.1*10^{-4}] is inside the stable Ouzo region; Sample 5 [$f_{acetone}$ = 0.20, $f_{PLGA\text{-}PEG}$ = 5.1*10^{-4}] and Sample 7 [$f_{acetone}$ = 0.70, $f_{PLGA\text{-}PEG}$ = 1*10^{-2}] are inside the unstable Ouzo region; Sample 8 [$f_{acetone}$ = 0.70, $f_{PLGA\text{-}PEG}$ = 0.12] is outside of the Ouzo diagram. Particles corresponding to compositions in the stable Ouzo region are homogenous and have spherical shapes, whereas particles corresponding to compositions in the unstable ouzo region are heterogeneous with spherical and oval shaped nano and microparticles. Conversely, formulations located out of the Ouzo diagram have very high polymer mass and exhibit amorphous polymer particles. The relation between the stable Ouzo region and the production of homogenous nanoparticles was reported for different polymers such as PLGA [178], polymethylmethacrylate [179] and polycaprolactone [190].

Although still controversial, the nanoprecipitation mechanism in the Ouzo domain is reported to occur in three stages: 1) a nucleus is formed by several unimers of polymer; 2) nuclei growth occurs through a diffusion-limited process by addition of more unimers and 3) the growth process ends as a result of the formation of a polymer brush layer on the nanoparticle surface [101]. In the unstable Ouzo region, the number of nuclei is very high due to the high amount of polymer; growth occurs mainly through random collisions of existing particles. The probability of collisions is proportional to the square of the number of particles and is assumed that each collision causes aggregation of the two particles involved. [191,192]. Conversely, the growth rate in the stable Ouzo region depends on the supersaturation and on the diffusion coefficient of the solute molecules. These factors for the growth help restrict particle size to the nanoscale with a homogenous particle size distribution [191]. The controlled growth of the nanoparticle inside of the stable ouzo region is further studied in the next section.

2.3.1.2 Effect of phase composition on the nanoprecipitation process

In Figure 2.4B, the red points labelled 1 to 6 represent the compositions used for millifluid experiments inside the stable Ouzo region. Samples 1 to 4 have a constant acetone mass fraction (0.2) and increasing PLGA-PEG mass fractions in the range $5.12*10^{-4}$ - $7.12*10^{-3}$. Samples 4 to 6 have a constant PLGA-PEG mass fraction ($7.12*10^{-3}$) and increasing acetone mass fractions in the range 0.08 - 0.4. Figure 2.5 shows how the particle size (gray bar) and PDI (white bar) depend on the PLGA-PEG mass fraction and acetone mass fraction. Particle size (Z-average) increases from 77 to 160 nm when the PLGA-PEG fractions increase from $5.12*10^{-4}$ to $7.12*10^{-3}$ using an acetone fraction of 0.2 (Figure 2.5A), which indicates a correlation between PLGA-PEG mass fraction and particle size. Conversely, the acetone fraction does not have any influence on the Z-Average when the acetone fraction increases from 0.08 to 0.4 using a constant PLGA-PEG fraction of $7.12*10^{-3}$ (Figure 2.5B). The PLGA-PEG and acetone fractions have no apparent influence on the PDI. These results corroborate the fact that particles obtained at the nanoscale inside the Ouzo region have a rather narrow particle size distribution (<0.1).

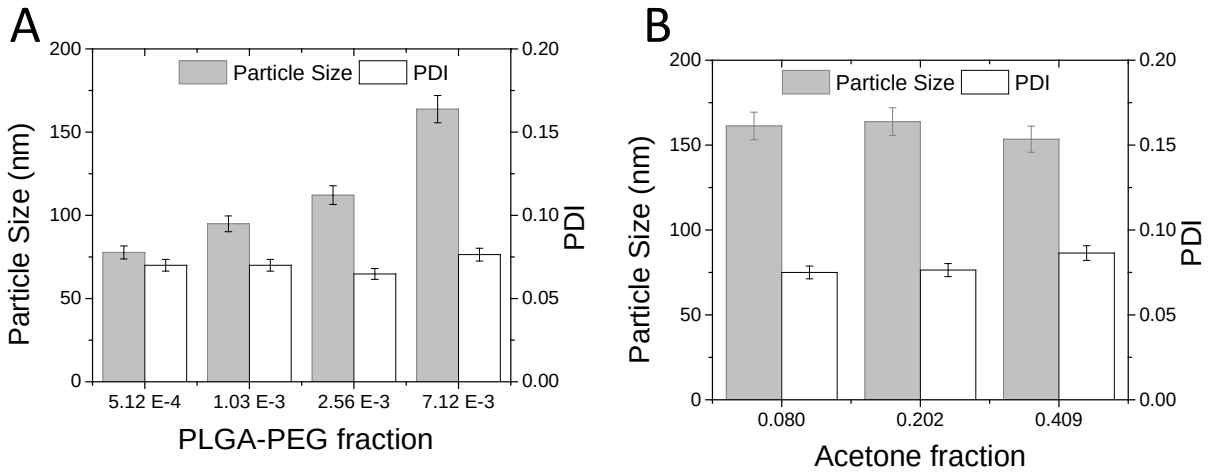

Figure 2.5: Particle size (gray bar) and particle size distribution (PDI, white bar) behavior in the nanoprecipitation using millimixer devices process A) Influence of PLGA-PEG fraction on the particle size and particle size distribution (growing effect); B) Influence of acetone fraction on the particle size and particle size distribution.

These results corroborate that the Ouzo domain is important for controlling the particle size in nanoprecipitation. Lebouille et. al reported a power law equation where particle size is proportional to the mixing time and polymer mass fraction [193]:

Equation 2.6 $$\text{Particle size (nm)} \propto (t_{\text{mix}} * f_{\text{polymer}})^{1/3},$$

where t_{mix} is the mixing time and $f_{polymer}$ is the polymer fraction and the particle size (Z-average) is measured by DLS. Equation 2.6 was used to fit our data, assuming perfect mixing from the kinetic studies described in Section 2.2. A mixing time t_{mix} = 11 ms was obtained and polymer mass fractions were estimated in the range $5.12*10^{-4}$ - $7.12*10^{-3}$.

Fitting our data with Equation 2.6 of the previous form led to a correlation factor of 0.9808. In our case, the Z-average is proportional to the polymer mass fraction via Equation 2.7:

Equation 2.7 Particle size (nm) = $318.52*(t_{mix}*f_{polymer})^{0.274}$.

The 0.274 exponent obtained from our date differs from the 0.33 exponent reported in Lebouille et.al. This difference may be due to the assumption of perfect mixing which was not completely fulfilled in our mixing device. However, the relation is evident, and corroborates the control of the growth rate for particle size by the mixing time observed in nanoprecipitation using the millimixer device.

2.3.2 Encapsulation efficiency and drug loading efficiency

2.3.2.1 Ternary phase diagram of the drug (DEX/acetone/water)

The relation between EE, DLE, and the quaternary phase diagram is studied in the current section. We start with the ternary phase diagram of the drug/water/acetone system Figure 2.6. The DEX solubility boundary was found using a titrating method with dexamethasone as with solute. This boundary has a sigmoidal shape and divides the transparent drug solution (red "X") from the cloudy drug solution (red square). In some compositions, dots of DEX were visibly observed in the transparent solution. They are represented on the boundary as open red square symbols. Maximum solubility is obtained in the water/acetone mixture where the DEX fraction is equal to 0.1 and acetone fraction to 0.7. Such behaviour is phenomenologically known for many macromolecular compounds, where some reactants dissolve in mixtures better than in pure solvents [194]. For example poly(vinyl chloride) is insoluble in acetone as well as in carbon disulfide, but is soluble in the mixture [195]. The opposite situation is also known; e.g., polyacrylonitrile is dissolved in pure malononitrile and N,N-dimethylformamide solvents, but the mixture of both solvents is not able to dissolve this compound. [194,196]. This phenomenon could be useful to precipitate dexamethasone in concentrations higher than 0.1 mg/mL. However, in principle, this gives rise to two solubility boundaries, one corresponding to the amorphous drug, and the other one to the crystalline drug. The solubility of the amorphous form is necessarily higher than that of the crystalline form. During a nanoprecipitation experiment, the fast kinetics of precipitation implies the formation of

amorphous particles, which may then recrystallize with time [197,198]. This can be the cause of the visual dots present in the transparent solution, where the equilibrium is not reached yet.

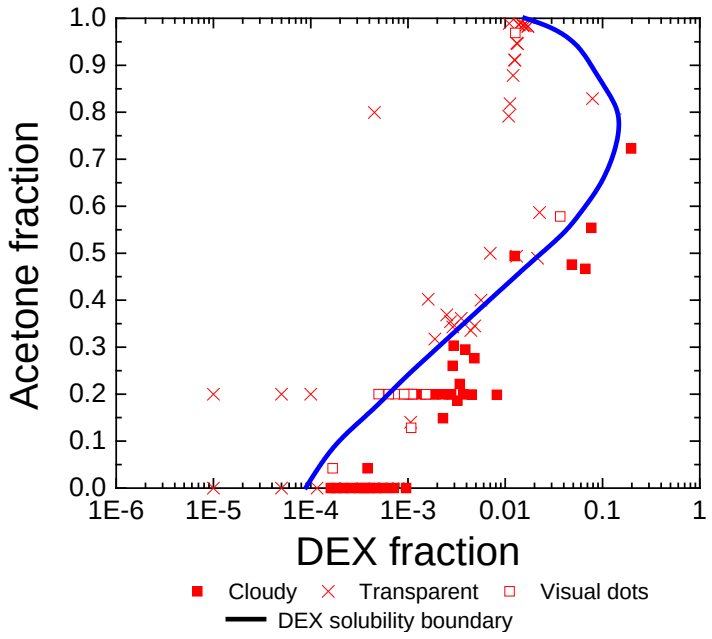

Figure 2.6: Phase diagram of DEX/ acetone/ water; red "X": transparent drug solution; red open square: visual dots observed in transparent solution; red close square: cloudy drug solution; blue line: dexamethasone solubility boundary.

2.3.2.2 Quaternary phase diagram (PLGA-PEG/DEX/acetone/water) and their correlation with EE and DLE

Phase diagrams for systems with four components can be represented conveniently as the sum of the two ternary phase diagrams. Figure 2.7A shows the quaternary system of PLGA/DEX/acetone/water. Compositions are plotted according to the acetone mass fraction (vertical axis) and the final solute mass fraction (horizontal axis). PLGA-PEG polymer and dexamethasone are solutes and their solubility boundaries were imported from Figures 2.4A and 2.6, respectively. The PLGA-PEG solubility boundary curve has a convex shape that is represented in red colour; the dexamethasone solubility boundary curve has a sigmoidal shape represented in blue colour.

Experiments of nanoprecipitation for the production of dexamethasone-loaded PLGA-PEG nanoparticles using millifluidic device were performed and labelled in Figure 2.7A as Sample 1 to 6. In all cases, PLGA-PEG concentrations correspond to the "phase separation region" preparation, which result in polymer nanoparticles. However, dexamethasone compositions have been chosen

to correspond to two main cases: (1) the dexamethasone mass fraction is in the solubility region of the diagram (Figure 2.7A Sample 4 - 6), and (2) the dexamethasone mass fraction is in its phase separation region (Figure 2.7A Sample 1 - 3). As reported in Table 2.3, when the dexamethasone mass fraction is in its solubility region, EE and DLE have an average of 10.23 ± 1.09% and 5.0 ± 0.5%, respectively. When the dexamethasone mass fraction is in the phase separation region, EE and DLE decrease to 4.2 ± 1.06% and 2.1 ± 0.52%, respectively. EE and DLE are thus more favoured if the dexamethasone mass fraction is located in its solubility region.

Figure 2.7B shows the SEM images of two representative formulations in both sides of the DEX solubility region. The formulation prepared in the DEX phase separation region is Sample 2 [$f_{acetone}$ = 0.20, $f_{PLGA\text{-}PEG}$ = $5.08*10^{-3}$, f_{DEX}= $2.55*10^{-3}$], which presents large hexagonally-shaped crystals of dexamethasone with microscale dimensions and spherically-shaped nanoparticles. On the contrary, the formulation prepared in DEX solubility region is Sample 6 [$f_{acetone}$ = 0.20, $f_{PLGA\text{-}PEG}$= $5.13*10^{-4}$, f_{DEX}= $2.56*10^{-4}$], which presents only spherically-shaped nanoparticles without crystals.

EE and DLE both collapse if dexamethasone precipitates, as observed for the case where crystallization of dexamethasone occurs in the bulk solution, and outside of the polymer particles. This result suggests a competition between molecular dispersion of the drug within the polymeric matrix and crystallization forces. Crystallization becomes the driving force and reduces the amount of drug encapsulated until an equilibrium between crystallization and DEX encapsulation is reached. [199].

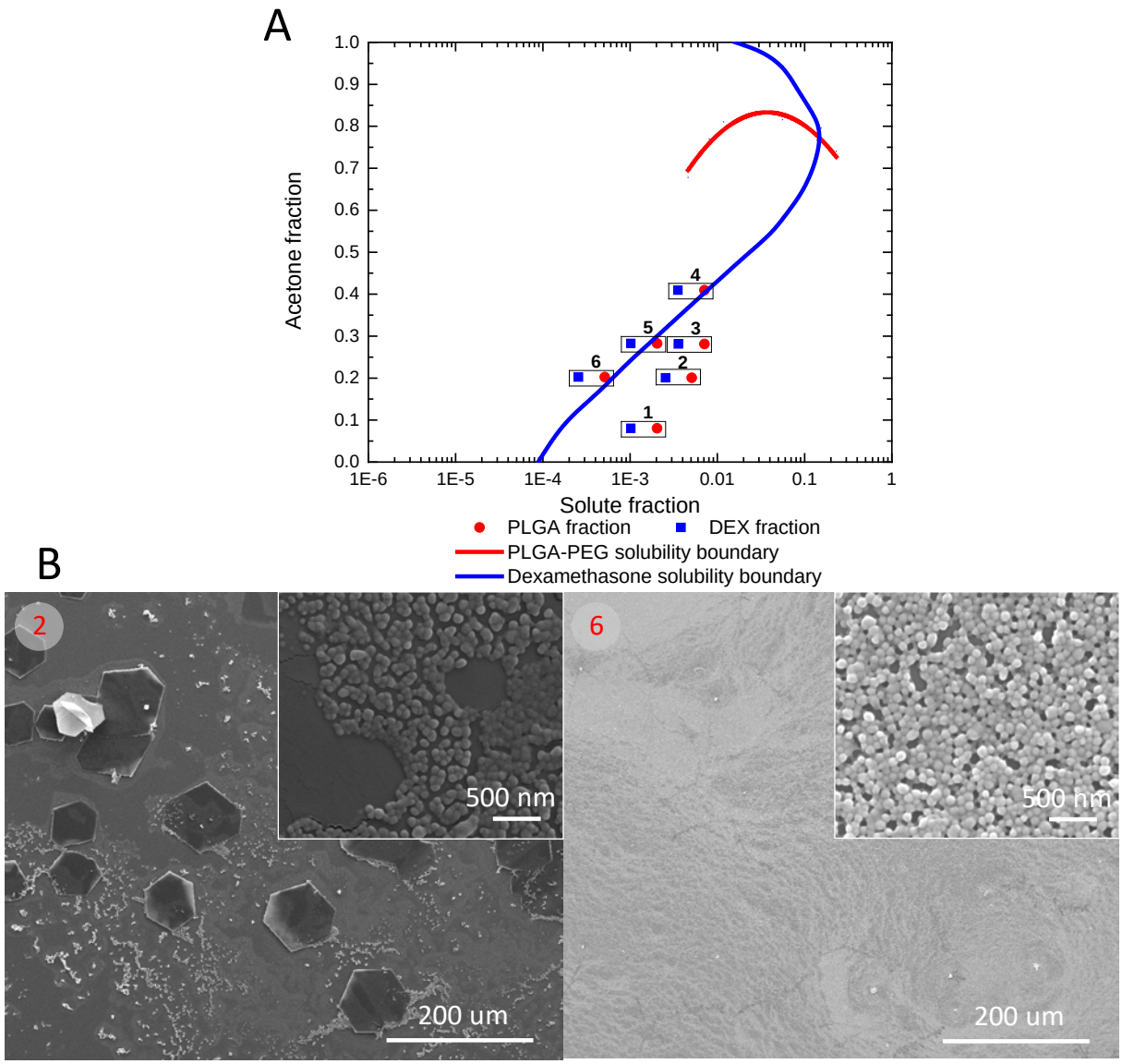

Figure 2.7: A) Quaternary phase diagram of PLGA-PEG/ DEX/ acetone/ water; red line: PLGA-PEG solubility boundary; blue line: DEX solubility boundary; black open square: Formulation of DEX encapsulated in PLGA-PEG nanoparticles produced by nanoprecipitation using multifluidic system experiments, combining PLGA-PEG polymer composition (red close circle) and DEX composition (blue close square); B) SEM images of DEX-loaded PLGA-PEG nanoparticles produced by nanoprecipitation using millifluidic device. Sample 2 [$f_{acetone}$ = 0.20, $f_{PLGA\text{-}PEG}$ = 5.08*10^{-3}, f_{DEX} = 2.55*10^{-3}], Sample 6 [$f_{acetone}$ = 0.20, $f_{PLGA\text{-}PEG}$ = 5.13*10^{-4}, f_{DEX} = 2.56*10^{-4}].

Table 2.3: EE, DLE, Particle size, and polydispersion of DEX-loaded PLGA-PEG nanoparticles plotted in Figure 2.7

	Data			Results			
Sample	**Acetone Fraction**	**PLGA-PEG Fraction**	**DEX Fraction**	**EE**	**DL**	**Part.Size**	**PDI**
	-	**-**	**-**	**%**	**%**	**nm**	**-**
1	0.08	$2.0*10^{-3}$	$1.02*10^{-3}$	4.9%	2.4%	116.32	0.12
2	0.20	$5.08*10^{-3}$	$2.55*10^{-3}$	4.8%	2.4%	134.56	0.10
3	0.28	$7.12*10^{-3}$	$3.57*10^{-3}$	3.0%	1.5%	163.82	0.08
4	0.41	$7.12*10^{-3}$	$3.54*10^{-3}$	10.6%	5.2%	153.48	0.09
5	0.28	$2.04*10^{-3}$	$1.02*10^{-3}$	11.1%	5.5%	105.28	0.12
6	0.20	$5.13*10^{-4}$	$2.56*10^{-4}$	9.0%	4.5%	77.72	0.07

The following experiment was performed to support the hypothesis that the encapsulation mechanism of dexamethasone is through solubilization in the polymer particles. PLGA-PEG nanoparticles were produced using a millifluidic device. Dexamethasone in powder form was added for a final composition corresponding to [$f_{acetone}$ = 0.20, $f_{PLGA\text{-}PEG}$ = $2.56*10^{-3}$, f_{DEX} = $2.56*10^{-4}$]. Dexamethasone and PLGA-PEG nanoparticles were left in contact for 0.17 h, 0.5 h, 2 h and 24 h. After their respective contact times, samples were collected and the EE and DLE measured. Figure 2.8 shows how EE (gray bar) and DLE (white bar) depend on the contact time between dexamethasone and PLGA-PEG nanoparticles. The values were compared with control data. The control sample had the formulation produced from a conventional method, where DEX and PLGA-PEG were solubilized together before producing the nanoparticles. The EE and DLE were found to be approximately constant (EE = 45.04 ± 2.42%; DLE = 4.74 ± 0.2%) as the contact time of dexamethasone was increased. A significance level of $p < 0.05$ was used as a threshold for statistical significance (Appendix Figure S2.1S-S2.2). For all times investigated, both encapsulation and drug loading efficiencies are close to the control sample and correspond to the precipitation of the polymer particles in the presence of dexamethasone. Results corroborate that the dexamethasone encapsulation mechanism occurs through solubilization into the polymer particles and does not co-precipitate together with the polymer. Also, PLGA-PEG particles precipitate faster than DEX, which favour the formation of separated crystals.

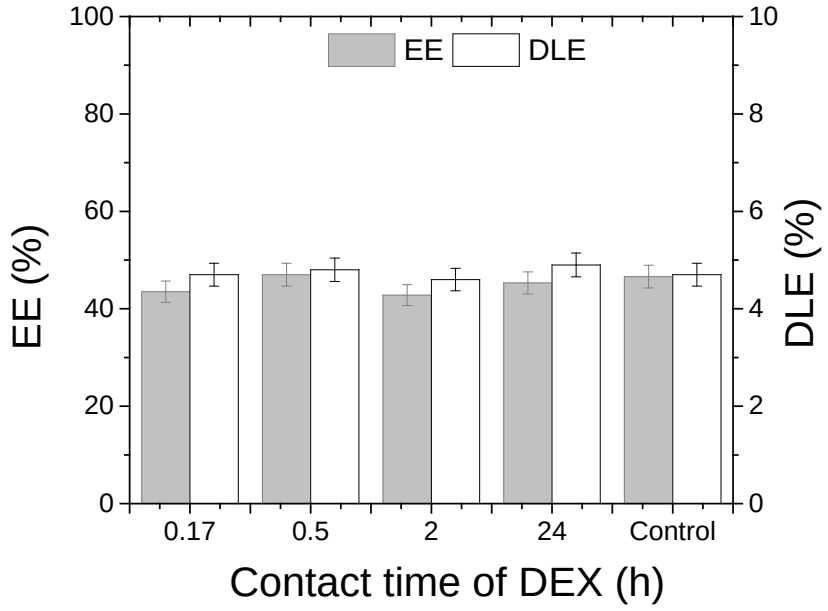

Figure 2.8: EE and DLE of DEX encapsulation in PLGA-PEG particles, where dexamethasone was added to a solution containing already precipitated polymer particles. Control formulation was made in a conventional method that involved solubilizing DEX and PLGA-PEG together prior to making the nanoparticles. EE (gray bar) and DLE (white bar).

Figure 2.9A shows the quaternary diagram. Figure 2.9B shows the EE and DLE results for DEX encapsulated in PLGA-PEG NPs where the DEX/PLGA-PEG ratio was changed from 50% to 4%. Solubility boundaries were extended (discussed above). We focus on the representation of a constant DEX fraction ($2.56*10^{-4}$, blue square) and the PLGA-PEG fraction increasing from $5.12*10^{-4}$ to $7.12*10^{-3}$ (red circle). Upon increasing the polymer amount, DLE is constant around 4.6%, and EE increases from 9.1% to 46.6% as $f_{PLGA\text{-}PEG}$ increases from $5.12*10^{-4}$ to $2.56*10^{-3}$, and the DEX/PLGA ratio decreases from 50% to 10%. This phenomenon can be explained by the need for the solubilized drug to find an equilibrium through adsorption/desorption with polymer matrix particles. The polymer fraction can change the inner structure of polymer particles, which change the final particle size as discussed in Section 2.1.1.2. Therefore, if the polymer content in the particle increases, the solubilized drug can be in contact with a growing number of adsorption sites until the EE and DLE maxima of 46.6% and 4.7%, respectively, are reached. By then, the DEX/PLGA ratio is 10% and $f_{PLGA\text{-}PEG}$ is $2.56*10^{-3}$. [142,200]. Once the DEX/PLGA ratio is reduced to 4% ($f_{PLGA\text{-}PEG} = 7.12*10^{-3}$), EE and DLE decrease to 43.5% and 2.2%, respectively. If the polymer concentration increases too much, a particle swelling may occur and induce a desorption phenomenon [142,200].

Our results are in agreement with the data reported in literature where an increase of EE was observed in PLGA nanoparticles obtained by nanoprecipitation using the drugs Flurbiprofen [201] and Cyclosporin A [202]. Specifically, for the dexamethasone, Campus et al. obtained an EE of 48% for dexamethasone-loaded PLGA nanoparticles. [18].

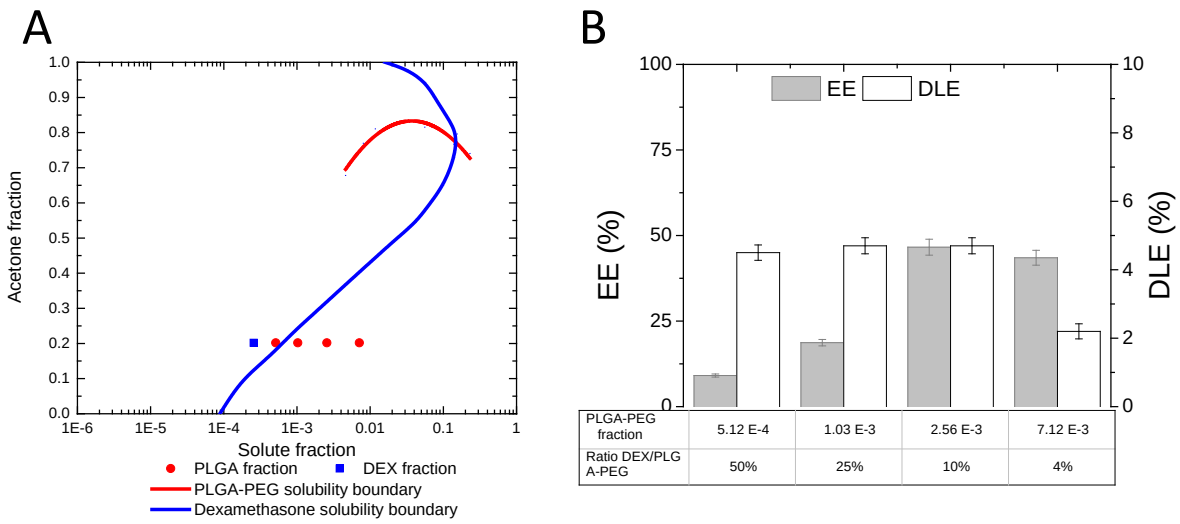

Figure 2.9: Influence of PLGA-PEG fraction and DEX/PLGA-PEG ratio on PLGA-PEG nanoparticles produced by nanoprecipitation using millifluidic device. A) DEX-loaded PLGA-PEG represented in quaternary diagram. Constant DEX fraction ($2.56*10^{-4}$) is represented by the blue square; increasing PLGA-PEG fraction is represented by red circles ($5.12*10^{-4}$- $7.12*10^{-3}$). B) EE (gray bar) and DLE (white bar).

2.4 Conclusion

In this chapter, the nanoprecipitation process using a millimixer based on a design by Johnson and Prud'homme [185] for the production of NPs was evaluated. First, we studied the nanoprecipitation process of PLGA-PEG by determining the precipitation mechanism through the ternary phase diagram (PLGA-PEG/acetone/water). We located the area where the precipitated particles are nanoscale, spherical, and have a narrow size distribution. The obtained PLGA-PEG nanoparticles range in size from 77 to 160 nm and have a PDI lower than 0.1.

We then evaluated the encapsulation efficiency (EE) and drug-loading efficiency DLE and correlated these variables with the quaternary phase diagram (PLGA-PEG/DEX/acetone/water). The encapsulation mechanism of dexamethasone occurs through solubilization in the polymer particles.

Maximum EE and DLE of 45.04 ± 2.42% and 4.74 ± 0.2%, respectively, were obtained when the DEX/PLGA ratio is 10% and $f_{PLGA\text{-}PEG}$ is $2.56*10^{-3}$.

In summary, we found that DEX/PLGA-PEG coprecipitation is not possible and thus does not permit DEX encapsulation. The dexamethasone encapsulation mechanism is occurs by solubilization of the drug in the polymer particles. In addition, PLGA-PEG particles precipitate faster than DEX, which promote the formation of separated crystals.

Chapter 3

Preparation of Drug-Loaded PLGA-PEG Nanoparticles by Membrane-Assisted Nanoprecipitation

3.1 Introduction

Polymeric nanoparticles (NPs) are intensely investigated due to their high potential, particularly, for diagnosis and drug-delivery applications [167]. They can be degraded in vivo, either enzymatically or by hydrolysis or both, to produce biocompatible, toxicologically safe by-products which are further eliminated by the normal metabolic pathways [40]. However, only a few of the drug-loaded nanoparticle systems investigated are able to reach the market. Among the main reasons for this are the difficulties regarding the scale-up of the manufacturing process, regulation standards and failure in clinical trials [149,157,203].

PLGA (poly-d,l-lactide-co-glycolide) is a FDA-approved polymer, used for the preparation of biodegradable nanosystems [40,152]. The rate of drug release from PLGA nanoparticles can be tuned by modifying the relative amount between lactic (PLA) and glycolic acids (PGA) in the polymer composition [40]. The release rate increases as the proportion of lactic acid decreases, due to the hydrophilicity increase in the matrix. The fastest degradation is achieved with PLGA 50% (PLA/PGA) [40,204]. On the other hand, PEG (poly ethylene glycol) is a hydrophilic and inert polymer that provides a steric barrier on the surface of the nanoparticles and minimizes their protein binding (opsonization). Adding PEG is useful to prolong NPs circulation (avoiding a fast clearance by macrophages) and to decrease premature drug release. Because of this, several copolymers of PLGA with PEG have been synthesized, encapsulating a wide variety of therapeutic drugs such as paclitaxel, dexamethasone or docetaxel [205,206].

Different production techniques (i.e. nanoprecipitation, emulsion/solvent diffusion, emulsion/solvent evaporation, salting-out, etc.) have been reported for the synthesis of PLGA-PEG nanoparticles [174,206–208]. Among them, nanoprecipitation is highly attractive due to the low energy input required. Generally, the nanoprecipitation process yields nanoparticles after mixing a solution of the polymer in an organic solvent (i.e., acetone), with a non-solvent (i.e., water), where the polymer is not soluble. Consequently, the resulting nanoparticles are quite sensitive to the mixing process and solvents miscibility. NPs are formed due to the nucleation of small aggregates of polymeric macromolecules (nuclei), followed by the aggregation of the formed nuclei to generate a stable polymer nanoassembly. The aggregation stage is suppressed as soon as colloidal stability is reached. [101]

The main challenge in polymeric NPs production by nanoprecipitation process is to achieve a fine control of the mixing processes. This is crucial in order to tune with good accuracy, the size and physicochemical properties of the nanoparticles [180,185]. Producing polymeric NPs by an approach

that meets clinics requirements remains highly challenging: it requires an independent operator, scalable and size-adjustable synthesis [111]. Typically, multistep batch laboratory procedures are not suitable for large-scale production due to the low reproducibility between batches [149]. A compromise often has to be accepted between the high throughput rates required and the ability to control the desired nanoscale features. Consequently, new technologies are required to overcome these challenges and significantly accelerate the clinical translation of nanomedicines [111,149].

The use of nanoprecipitation methods at industrial scale is still hindered by the lack of a robust technique able to translate the results from laboratory scale to mass production. Only few studies deal with the design of a reliable scale up of NPs production by nanoprecipitation [209]. Typically, a continuous system like a "T mixer" is used for large scale production where the two phases diffuse into each other forming the NPs. The work of [102] is a good example of this approach. However, the results achieved by these authors showed differences in terms of drug loading and particle size at laboratory scale and at pilot scale. Where higher turbulence generated in the continuous pilot scale mode is obtained (responsible of the drug diffusion in the external aqueous phase before the polymer chains aggregated to form the NPs) [102]. Automatically controlled devices, such as Semi-Automated Nanoprecipitation-System (SAN-System) and high-throughput dynamic light scattering (HT-DLS) have been advocated to enable a good control over processing parameters while following a high-throughput (HT) approach [101,209,210].

Membranes are being increasingly used as the system of choice for scaling up the production of emulsions and particles. Membrane emulsification, also combined with secondary solidification reactions, is a well-established technology with demonstrated scale-up capabilities [211–214]. However, the study of nanoprecipitation in combination with membrane processing (membrane-assisted nanoprecipitacion or MANA) has opened a new window on the application of membrane science in the last years (Table 3.1) [112,215–218].

Table 3.1 : Examples of membrane assisted nanoprecipitation:

Polymer	Drug	Membrane	Application	Reference
Polycaprolactone	Vitamin E	Kerasep ceramic membranes	antioxidant	[112]
Phospholipid	Vitamin E	Microengineered membranes	antioxidant	[217]
Polycaprolactone	spironolactone	Kerasep ceramic membrane	pediatric use	[218]
Polycaprolactone	rapamycin	flat SS membrane	organ transplant rejection	[219]
Polycaprolactone	-	disc-shaped membrane	-	[215]
Diblock copolymers poly(oligoethylene glycol acrylate)-b-poly(styrene) (POEGA-b-PSt)	-	Shirasu porous glass (SPG) membranes	-	[220]

In the present work, the production of PLGA-PEG NPs by MANA has been investigated for the first time. The scalability and reproducibility of the process was also studied. In this respect, our aim is to develop a scalable continuous system suitable for the formulation of PLGA-PEG NPs. Process development and drug release aspects that are essential regarding a potential clinic translation and industrial scale production was also studied. Dexamethasone has been selected as a model drug in view of its well-known properties as an anti-inflammatory and immunosuppressant corticosteroid widely used for the treatment of different pathologies including arthritis, allergy, joint pain, skin and eye disorders, leukemia, lymphoma, multiple myeloma, cancer-associated side effects, inflammation, and immune-system disorders. Being a hydrophobic drug, encapsulation is often proposed to increase its bioavailability [15]. In this work, we have evaluated the encapsulation efficiency and drug loading efficiency of dexamethasone in PLGA-PEG NPs as well as its delivery profile to unveil the release mechanism.

3.2 Materials and Methods

3.2.1 Materials

Poly[(D,L-lactide-co-glycolide)- co-PEG] diblock) (PLGA-PEG) polymer: RESOMER Select 5050 DLG mPEG 5000 (Diblock PLGA (50:50) PEG (5kDa, 5%)) were purchased from EVONIK Industries AG.

Pluronic F127 and Acetone were purchased from Sigma-Aldrich. Deionized water was used in all the experiments. All chemicals used were reagent grade.

3.2.2 Production of PLGA-PEG nanoparticles by membrane –assisted nanoprecipitation

A polymeric solution of PLGA-PEG (10 mg mL^{-1}) in acetone was used as organic solution (stream 1, S1) and Pluronic F127 in water (11.6 mg mL^{-1}) was used as aqueous solution (Stream 2, S2). For the study of dexamethasone encapsulation efficiency and release, the S1 was modified by including dexamethasone (PLGA-PEG at 10 mg mL^{-1} and dexamethasone at 1 mg mL^{-1} in acetone)

The preparation of polymeric nanoparticles was carried out by using a Shirasu porous glass (SPG, Miyazaki, Japan) hydrophilic tubular membrane. Membranes with a pore size of 1 and 0.2 um were tested. The effective membrane area was 31.3 cm^2. The schematic figure of the membrane apparatus used for nanoparticles preparation is illustrated in Figure 3.1. A pump was used to inject the stream 1 through the membrane pores. The stream 2 was pulsed back-and forward (pulsed cross-flow mode) at a fixed amplitude and frequency along the lumen side of the membrane by a programmable peristaltic pump (Digi-Staltic double-Y Masterflex® pump Micropump, model GJ-N23.JF1SAB1). The value of the amplitude was fixed at 4.7 10^{-2} m and the frequency was modified in the range between 1.48 and 3.57 Hz. The maximum shear stress (τmax) [Pa] is a function of the amplitude (a) and the frequency (f) of the pulsed flow according to equation 3.1 [221]:

Equation 3.1 $$\tau_{max} = 2\ a\ (\pi\ f)^{\frac{3}{2}}\ (\mu_c\ \rho_c)^{\frac{1}{2}}$$

Where τmax is the shear stress (Pa), α is the amplitude, f is the frequency, μc is the stream 2 viscosity (Pa s) and ρc is the stream 2 density (kg m-3).

The stream 1 flux (Jd) was determined by the volumetric flow, measuring the stream 1 consumption from the graduated feed cylinder. Jd (L h-1 m-2) is given by the following equation 3.2:

Equation 3.2 $$Jd = Qd / A$$

Where, Qd is the stream 1 flow rate (L h-1) and A is the membrane area (m-2). The stream 1 flow rate was varied between 9.6 10^{-3} and 6 L h^{-1} that corresponds to a stream 1 flux between 3 and 1917 $Lh^{-1}m^{-2}$. Polymeric NPs are formed after the controlled diffusion of the stream 1 into the stream 2 (Figure 1-b).

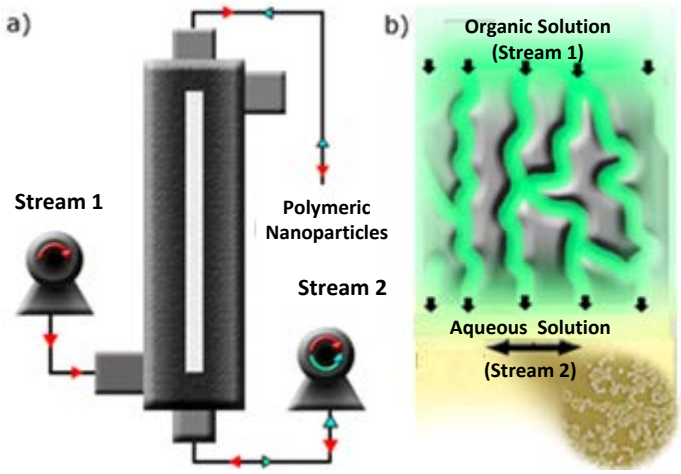

Figure 1. a) Membrane-assisted nanoprecipitation set-up. b) Schematic representation of nanoparticles production by nanoprecipitation at the membrane level (green colour refers to the polymer dissolved in the solvent, yellow colour refers to the antisolvent).

Different ratios of stream 1 volume /stream 2 volume (S1/S2) were tested in the range from 0.16 to 1.2. stream 1/stream 2 (S1/S2) ratio was calculated using equation 3.3. The S1 volume corresponds to the total volume of polymeric solution permeated trough the membrane at time t while the S2 volume was constant and equal to 50mL. As a result, the S1/S2 ratios increased as a function of time

Equation 3.3 S1/S2 ratio (t) = S1 Volume (t) / S2 Volume

At the end of each experiment, the produced droplets were collected and left under the fume hood for 3 hours to allow acetone evaporation. The resulting particles were centrifuged at 2100 g for 10 min, the supernatant was stored for further analysis and the pellet was lyophilized for 24h (0.01 bar, - 40oC) using a LyoAlfa 10/15 lyophiler from Telstar.

3.2.3 Production of PLGA-PEG nanoparticles by nanoprecipitation in stirred batch-type reactor

The nanoprecipitation process was carried out in a beaker (batch-type reactor) and mixing was produced by magnetic stirring (300 rpm) at room temperature. In this case, the organic solution was added into drop by drop. The composition of organic (stream 1, S1) and aqueous (stream 2, S2) solutions were the same as the one used for conducting the experiments with the MANA process.

A 150mL batch-type reactor was filled with 50 mL of S2 and the S1 volume was gradually added (from 16 mL to 55 mL) to obtain a S1/S2 volumetric ratios from 0.32 to 1.1. This procedure reproduces the conditions used by using the membrane equipment. For each S1/S2 volume ratio

studied, the produced droplets were collected and left under the fume hood for 3 hours to allow acetone evaporation. The resulting particles were centrifuged at 2100 g for 10 min and the pellet was lyophilized for 24h (0.01 bar, -40oC) using a LyoAlfa 10/15 lyophilazer from Telstar.

3.2.4 Particles characterization

3.2.4.1 Particle analysis

Particle size and polydispersity (PDI) of the nanoparticles were measured by Dynamic light-scattering (ZetaSize NanoZS, Malvern Instrument). The software used to collect and analyse the data was ZetaSizer Sofware 7.1 from Malvern. The measurements were made at a controlled temperature of 25°C. The Z-average diameter (Z-Average) and the polydispersity index (PDI) were obtained from the autocorrelation function using a refractive index of 1.55.

Morphological analysis of the nanoparticles was carried out by Scanning Electron Microscopy (SEM, Inspect F50; FEI, Eindhoven, the Netherlands) at the LMA-INA-Universidad Zaragoza facilities operated at 10–15 kV. Purified-collected samples were stained by mixing 200 uL of nanoparticles colloid with 200uL of phosphotungstic acid solution (75 mg/mL) during 1.5 hours. The resulting dispersion was washed three times with Milli-Q water using a centrifuge. Finally, 10 uL of resulting nanoparticles suspension was added on a glass slide, dried in air, and sputtered with platinum.

3.2.4.2 Encapsulation Efficiency and Drug Loading Efficiency

The encapsulation efficiency (EE) and drug loading efficiency (DLE) were calculated using an indirect method. The particles were separated from the liquid using Centrifugal Ultrafiltration Devices (Vivaspin) from Sartorius Stedim. DEX concentration in supernatant was measured directly after the centrifugation using HPLC analysis. DEX encapsulated was calculated by mass balance.

HPLC analysis was performed at 40 °C, using a reversed-phase C18 column (2.6 µm, 50x4.6mm Phenomenex kinetex) and eluted isocratically with acetonitrile/water (50/50 v/v). The flow rate was fixed at 0.4 mL/min and detection was obtained by UV detection at 260 nm. The linear regression coefficient determined in the range 0.01–30 µg mL-1 was 0.9993 (n=10).

The EE and DLE were calculated according to equations 4 and 5, respectively.

Equation 3.4 $EE = (DEX\ encap)/(DEX\ total)*100$

Equation 3.5 $DLE = (DEX\ encap)/(PLGA\text{-}PEG\ total)*100$

Where EE is encapsulation efficiency (%), DEX encap is Dexamethasone mass encapsulated (mg), DEX total is the Initial Dexamethasone mass in the stream 1 (mg), DLE is drug loading efficiency (%) and PLGA-PEG total is Initial PLGA-PEG mass in the stream 1 (mg)

3.2.4.3 In vitro drug release study

About 10 mg of lyophilized dexamethasone-loaded nanoparticles were transferred to the dialyzer and suspended in 200 uL of release media (0.1 M PBS pH 7.4) at 37ºC. The dialyzer was then introduced into an eppendorf vial containing release media (1 mL), which was stirred at 100 rpm using a magnetic stir bar. Dexamethasone release was assessed by intermittently sampling the contents of the release media, the buffer was replaced with fresh solution after sampling. Drug content during the release study was evaluated by HPLC using the same method described above.
The release profiles were evaluated by fitting the experimental data to equations describing different kinetic release. Linear regression analyses of the experimental data obtained from in-vitro drug release studies were made for four different models: zero order, first order, Korsmeyer–Peppas and Higuchi. A description of the method is reported in supporting information S3.

3.3 Results and Discussion

This section is structured in two main parts. The first deals with the investigation of the effect of streams composition, fluid dynamic conditions (organic solution flux and wall shear stress) and membrane pore size on the particle size and particle size distribution of PLGA-PEG nanoparticles produced by membrane-assisted nanoprecipitation. The second part includes the evaluation of encapsulation efficiency (EE), drug loading efficiency (DLE) and in vitro release of dexamethasone-loaded PLGA-PEG nanoparticles prepared by membrane-assisted nanoprecipitation.

3.3.1 Effect of phases composition

PLGA-PEG concentration was kept constant at 10 mg ml^{-1}, a sufficiently diluted concentration to result in polymer nucleation [222]. The amounts of PLGA-PEG, acetone and water were modified in order to identify the respective polymer, solvent and non-solvent amounts required to obtain stable colloidal formulations at the defined ouzo region [223]. The construction of “Ouzo diagram” represents a meaningful resource for nanoprecipitation. To the best of our knowledge, no data are available in the literature for the ternary system PLGA-PEG/Acetone/water. On the other hand, a ternary diagram for PLGA, acetone, and water (containing 0.1 wt % of poloxamer 188) system, at 25°C, was determined by Beck-Broichsitter et al [178]. This ouzo diagram has been used as a

reference in the present work to select the respective polymer, solvent and non-solvent amounts that resulted in nanoparticles production by solvent displacement. This assumption was considered correct because the physicochemical properties of PLGA-PEG and PLGA are similar, and then both polymers are expected to show a similar behaviour in the same acetone/water ternary system [142]. Both solubility and interaction parameters (such as solvent-water and polymer-solvent interaction) are reported to influence the phase mixing of the nanoprecipitation process [142]. PLGA-PEG mass fraction ($f_{PLGA\text{-}PEG}$) and solvent mass fraction ($f_{Acetone}$) studied in the present work were plotted together with the data obtained from the literature for PLGA in the ternary system water/acetone. Three regions have been identified: one phase region, stable ouzo region and unstable ouzo region (Figure 3.2) [178] obtained at different S1/S2 volumetric ratios while maintaining constant the PLGA-PEG amount.

Four samples were considered representative of the nanoprecipitation process: sample 1 ($f_{acetone}$: 0.20; f_{PLGA}: $2.5*10^{-3}$; S1/S2 ratio: 0.32); sample 2 ($f_{acetone}$: 0.35; f_{PLGA}: $4.5*10^{-3}$; S1/S2 ratio: 0.70), sample 3 ($f_{acetone}$: 0.49; f_{PLGA}: $6.1*10^{-3}$; ratio S1/S2: 1.22) and sample 4 ($f_{acetone}$: 0.7; f_{PLGA}: $9.7*10^{-3}$; S1/S2 ratio: 3). SEM images from samples 1-3 confirm the stability of the colloids formed in the stable "Ouzo" region (Figure 2). Those nanoparticles were uniform (PDI = 0.17 ± 0.05) and the particle size varied from 261 ± 28 nm to 390 ± 40nm. SEM images of the particles produced in the unstable "ouzo" region (sample 4) by nanoprecipitation, reveal the presence of a bimodal size distribution (PDI=0.5) with one population of particles in the range of 300 nm and the other in the range of 1000 nm. These results are in agreement with some previous systems not based on PLGA-PEG [179], where the production of monodisperse nanoparticles or a bimodal distribution of particles (nanoparticles + microparticles) was dependant on the location of synthesis conditions in relation to the stable and unstable ouzo regions, respectively. Data obtained in this work indicate that the PLGA-PEG nanoparticles can be produced by nanoprecipitation in the same range of acetone/water relative volume ratio as those reported for PLGA, thus validating the use of the diagram in figure 3.2 for our system. A S1/S2 ratio higher than 3 resulted in the production of microparticles in addition to nanoparticles as a result of an excess of dissolved polymer in water [178,179].

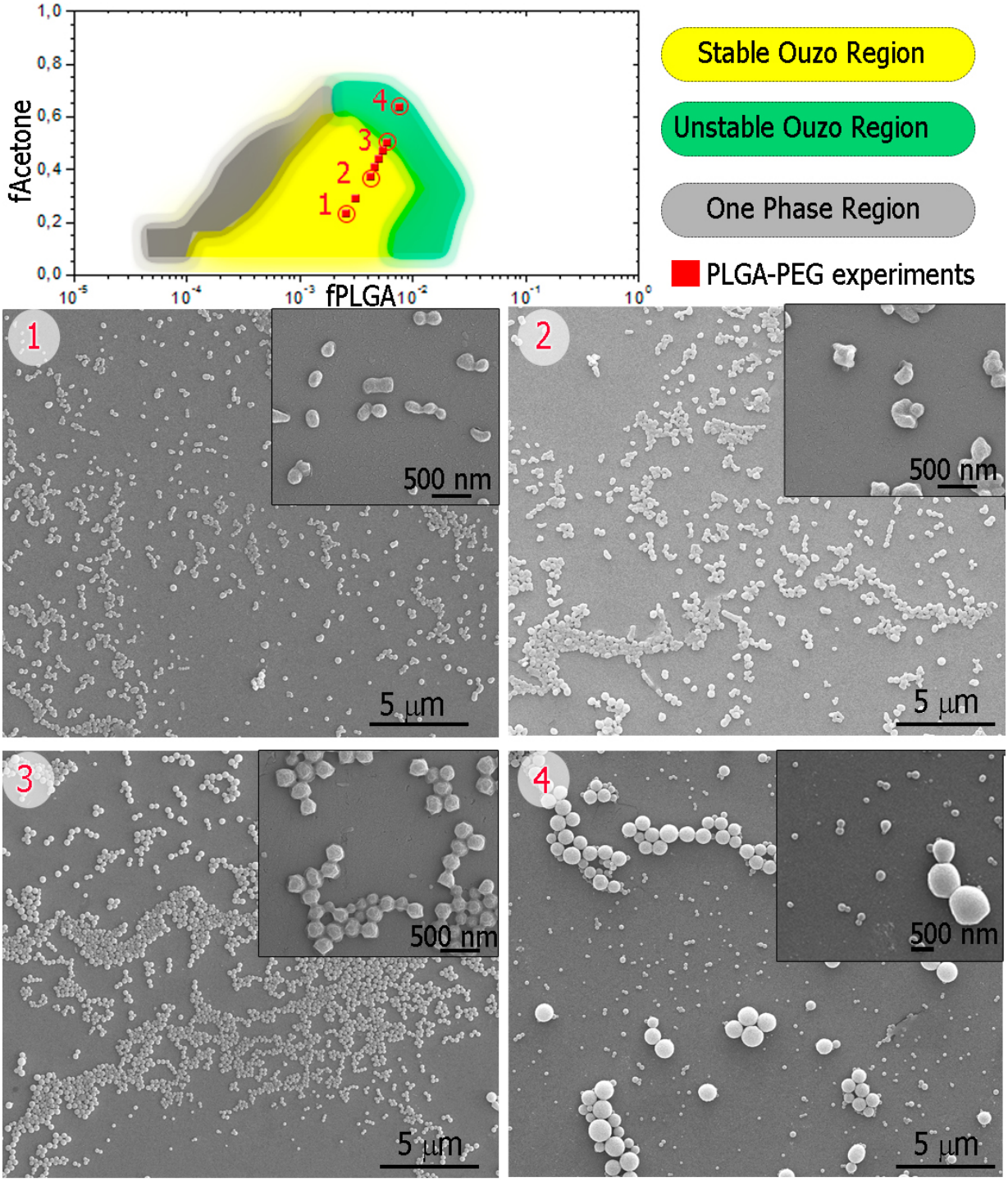

Figure 3.2. Location of the experimental points obtained in the present study for PLGA-PEG polymer (in red color) in the Ouzo diagram obtained by Beck-Broichsitter et al. (2015). SEM images of nanoparticles produced by nanoprecipitation membrane-assisted. Sample 1 (S1/S2 ratio: 0.32). Sample 2 (S1/S2 ratio: 0.70). Sample 3 (ratio S1/S2: 1.22). Sample 4 (S1/S2 ratio: 3).

The influence of the relative volume S1/S2 on particle size and polydispersity has been evaluated by two approaches: 1) pulsed cross-flow membrane-assisted method and 2) a conventional stirred batch-type method (Figure 3.3). In case of pulsed cross-flow MANA, an increase of nanoparticle size was observed in the range from 250 to 400 nm as a function of S1/S2 volumetric ratio increase. On the other hand, the PLGA-PEG NPs produced by nanoprecipitation in the conventional batch type reactor were not affected by the S1/S2 ratio and NPs with a diameter of 100 nm were produced throughout the range explored (Figure 3.3). The different trend can be explained by the different mixing at the micro-scale obtained by these production methods. Nanoprecipitation occurs in three stages: 1) a nucleus is formed by several unimers of polymer; 2) nuclei growth occurs through a diffusion-limited process by addition of more unimers and 3) the growth process ends as a result of the formation of polymer brush layer on the nanoparticle surface [101]. In MANA the polymer solution is continuously added into the non-solvent phase, and solvent/non-solvent mixing occurs at the pore level where the two phases are in contact. The rate of solvent exchange is very high due to the steep concentration gradient and the formation of nuclei start. As soon as acetone passes through the membrane pores, it gradually diffuses in the water, changing the composition of the S2. After nuclei formation, growth continues over time as the stream 1 continues to flow through the membrane pores to achieve the required S1/S2 volumetric ratio however, the fast initial decrease of polymer concentration prevents further generation of nuclei. The remaining dissolved polymer gradually precipitates over the nuclei formed as the counter-diffusion of water and acetone lowers its solubility. The final particle size is a result of a process of particle growth over the nuclei initially formed, rather than forming new entities. In contrast, the solvent-non-solvent mixing is instantaneous in batch nanoprecipitation, where the reagents were mixed by the vortex generated during the magnetic stirring. In this case the intense agitation accelerates the water-acetone mixing. As a consequence, all the nuclei are formed instantaneously, leading to a fast depletion of the polymer. In this case, the phase of gradual counter-diffusion of water and acetone does not exist and growth ends abruptly as soon as the polymer in the immediate vicinity of the nuclei has been used up. The resulting nanoparticles mean size was not a function of the mass fraction of acetone added. This observation was supported by the experiments carried out in batch process by simulating the conditions used in membrane experiments, where a volume of acetone (S1) from 16 to 55 mL was added drop-by-drop, in 50 mL of water to reach the desired S1/S2 volumetric ratio. In this case, similar results, in terms of particle size and PDI, were obtained in batch methodology by maintaining constant the S1 volume varying the S2 volume from 4.1 mL to 100 mL.

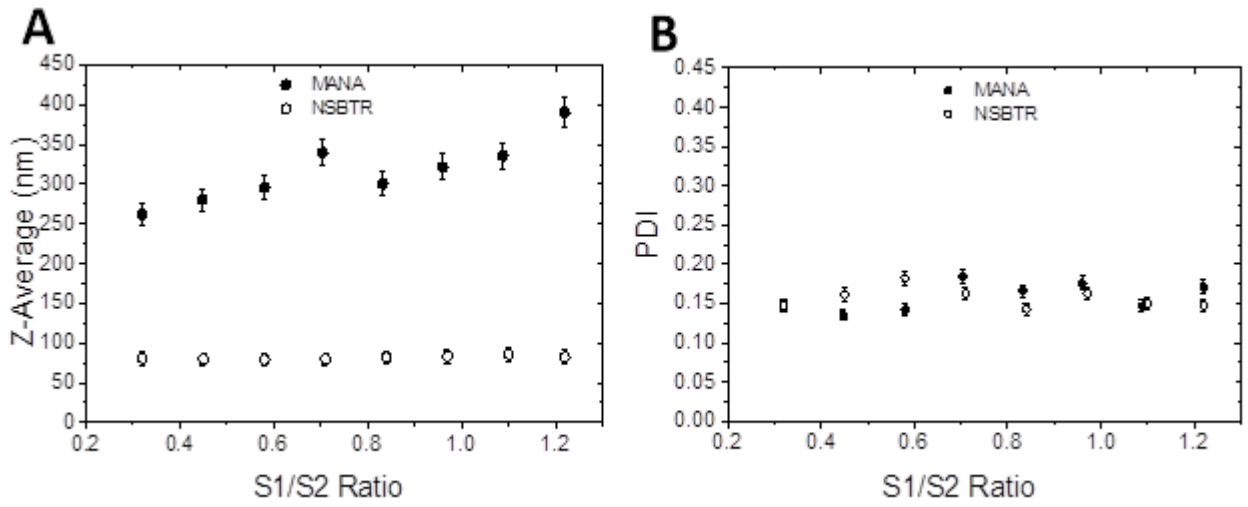

Figure 3: Influence of S1/S2 ratio on PLGA-PEG nanoparticles produced by using membrane–assisted nanoprecipitation approach (MANA) and nanoprecipitation in a stirred batch-type reactor (NSBTR) A) PLGA-PEG nanoparticles Z-Average; B) PLGA-PEG nanoparticles polydispersity index (PDI)

These results were in agreement with previous works that also reported the lack of influence of S1/S2 ratio on particles sizes when precipitation was carried out in a stirred batch reactor [142,224,225]. The different results on the influence of the relative amount of S1 and S2 on particle size in membrane and batch systems suggest that the main role of the membrane in nanoprecipitation is to govern the nuclei growing step by controlling the mixing of solvent with non-solvent at the pore level. A PDI lower than 0.2 was obtained in both membrane-assisted and batch nanoprecipitation. However, in MANA the growth process is characterized by the deposition of several polymer unimers on the same nucleus formed at nucleation stage [103,180,185]. This extends the growth phase and allows control of the particle size. Consequently, it can be concluded that unlike batch processes, membrane-assisted nanoprecipitation is a versatile procedure that enables to tune the size of the polymeric nanoparticles by varying the S1/S2 ratio, at a given range of shear stress.

3.3.2 Effect of organic solution flux

The effect of organic solution (stream 1) flow rate on particle size and particle-size distribution of PLGA-PEG nanoparticles has been investigated. Three different S1 flow rates were tested: 0.8, 3.2 and 100 mL min-1, corresponding to a range of flux from 15.3 to 1917 L $h^{-1}m^{-2}$ maintaining constant the shear stress in 2.8 Pa. Figure 3.4 reports Z-average and PDI of PLGA-PEG nanoparticles produced by pulsed cross-flow membrane-based process as a function of S1 flux. This very wide range of flow

rate values has been selected in order to investigate the suitability of MANA to control nanoparticles formation over a large interval of processing rates. The high-end values of S1 flux are sufficiently high to make the process attractive for industrial production. The results indicate that, for a given S1/S2 ratio, particle size was almost independent on stream 1 flow rate, giving a p-value >0.05 (Figure S3.1 in appendix). Z-average values of 250 and 224 nm were obtained in the range of flux investigated for S1/S2 ratios of 0.32 and 0.83, respectively. In addition, the PDI was always lower than 0.2, indicating a high uniformity on the PLGA-PEG nanoparticles irrespective of the S1 Flux (Figure S3.2 in appendix). This is in contrast with the usual results when membrane emulsification processes are used for particles production: the droplet size increases linearly with the stream 1 flow rate because a necking time is usually required before droplets detachment from the membrane surface. During this time, an additional amount of the polymer solution flows into the forming droplet [226]. However, as discussed above, our results indicate that in membrane-assisted nanoprecipitation, the formation of nanoparticle nuclei is practically instantaneous. This fast kinetics are able to accommodate the increased throughput (and the decreased contact time) as the flow rates of S1 and S2 are increased. Similar results were obtained in previous works [227,227]. On the contrary, Khayata et al. 2012 obtained that the greater pressure of S1 solution used (and then S2 flow rate), the greater was the mean size of nanocapsules because droplets coalescence occurred during droplets formation from the membrane pores, supposing a drop-by-drop mechanism for nanoprecipitation membrane-assisted as in conventional membrane emulsification [228].

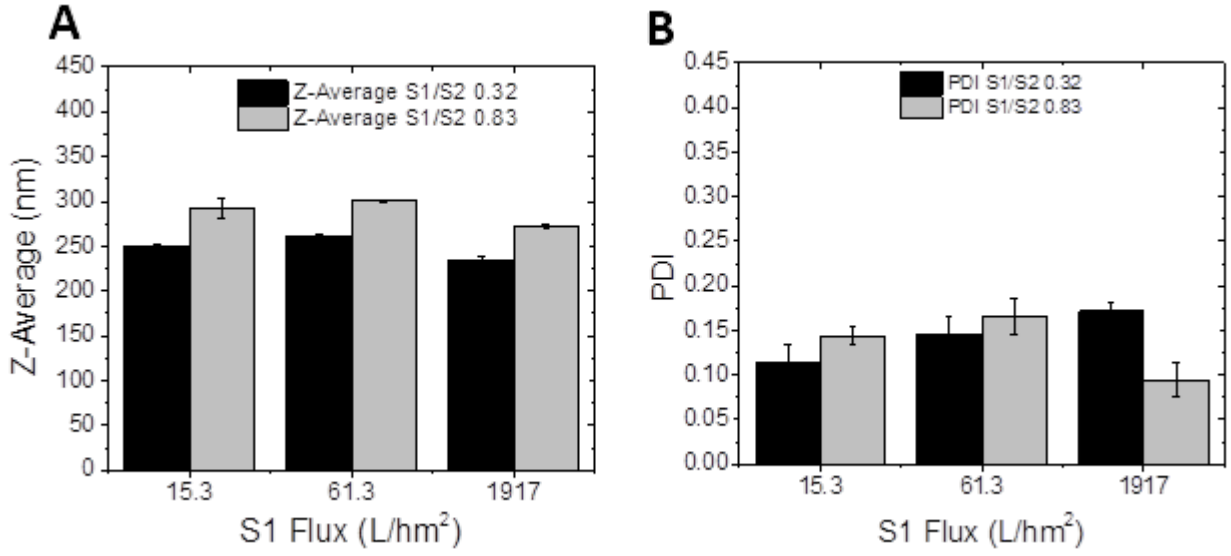

Figure 3.4. The effect of stream 1 flux on nanoparticle size and particle-size distribution of PLGA-PEG nanoparticles produced by membrane-assisted nanoprecipitation (Shear stress: 2.8 Pa).

To clarify the mechanism of NPs formation in MANA, we have evaluated the wettability of SPG membranes by the organic solution. Using PLGA-PEG in acetone at 10 mg mL^{-1}, the membrane was immediately wetted by the polymer solution and an accurate measurement of the contact angle was not possible (Figure 3.5-A). Only when the polymer concentration was sufficiently high (100 mg mL^{-1}) a contact angle of 130 °C was measured (Figure 3.5B). Because the membrane is highly wetted by the S1, we can conclude that under the conditions used in MANA, particle formation is not a result of a drop-by-drop mechanism but it is a consequence of phases micromixing at the pore level. This is also consistent with the results obtained in the previous section regarding the effect of the S1/S2 ratio.

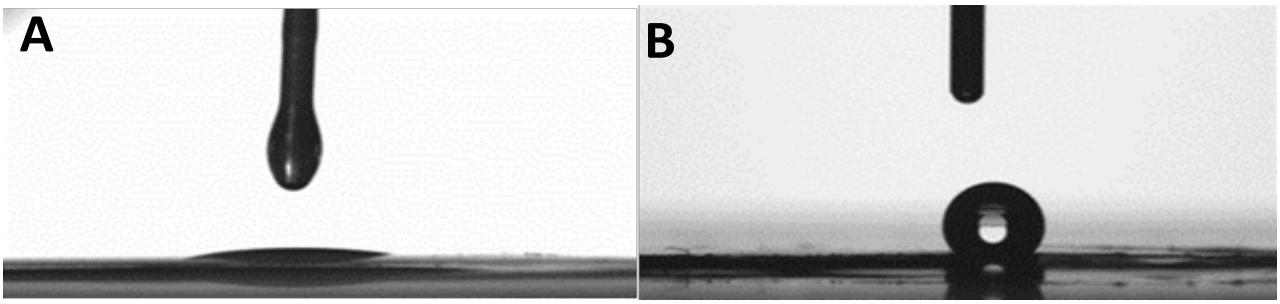

Figure 3.5. Contact angles of PLGA-PEG in acetone on SPG hydrophilic membrane A) PLGA-PEG 10 mg mL^{-1} B) PLGA-PEG 100 mg mL^{-1}

From our results, membrane-assisted nanoprecipitation emerges as a promising technology for nanoparticles production at large scale as demonstrated by increasing the organic solution flux over two orders of magnitude. A flux of 1917 L $h^{-1}m^{-2}$ (PLGA-PEG Mass Flux 192 g h-1m-2) could be employed without modifying the control over particles size and size distribution. This is in contrast with the results found when attempting to scale up membrane emulsification processes, where the stream 1 flux is strongly limited [150]. Membranes not wetted by the polymeric solution are usually required to obtain droplets with controlled size and size distribution, but the low polymeric solution flux obtained results in low productivity [229]. This limitation is overcome in case of membrane-assisted nanoprecipitation as shown above.

3.3.3 Effect of wall shear stress

The shear stress depends on the frequency and the amplitude of the pulsation along the lumen side of the membrane. Figure 3.6 reports Z-average and PDI of PLGA-PEG nanoparticles produced by pulsed cross-flow membrane-based process as a function of the shear stress. The experiments were

carried out by keeping constant the amplitude of the pulsation while increasing the frequency. Three different shear stresses were used 1.12; 2.48 and 4.16 Pa. The Z-Average and PDI were found approximately constant as the shear stress was increased (Figure 6 and Figure S3-S4 in supplementary information).

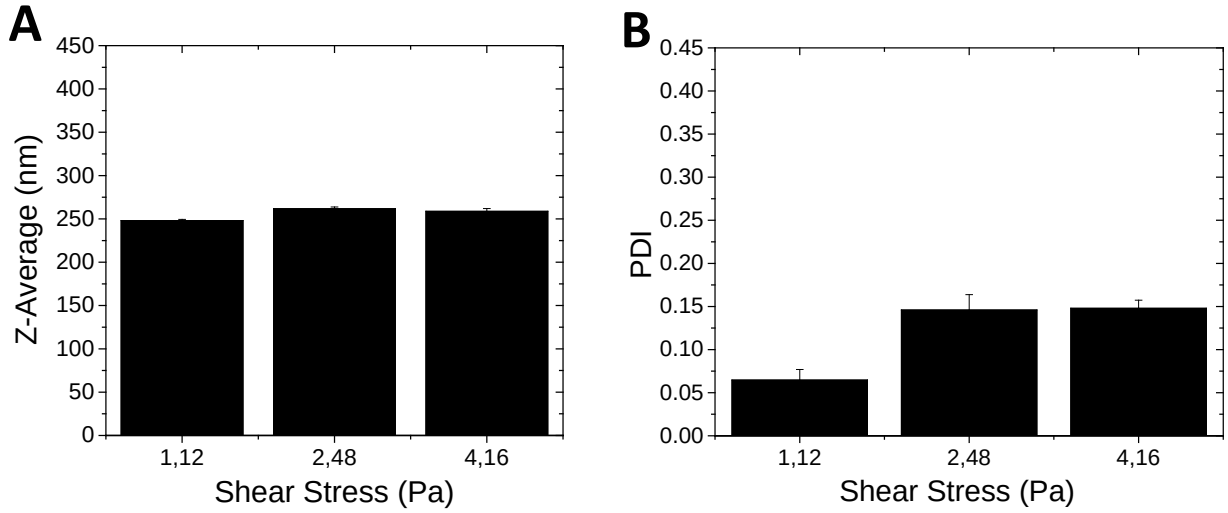

Figure 3.6. Influence of wall shear stress on nanoparticle size and particle-size distribution of PLGA-PEG nanoparticles produced by membrane-assisted nanoprecipitation (S1 flux: 61.3L/hm2; S1/S2 ratio: 0.32).

The same morphology was also observed for PLGA-PEG nanoparticles produced by using different shear stress value as shown in Figure 3.7. Similar results were reported in the production of PCL nanoparticles by Khayata et al. by using SPG membranes in a cross-flow membrane emulsification system [228]. In conventional membrane emulsification a decrease in terms of particles size is observed when the shear stress was increased [230,231]. The different trend can be explained considering that in nanoprecipitation the appropriate mixing between solvent and antisolvent controls the particles production instead of the balance between the shear force, exerted on the forming droplet by the aqueous phase, and the interfacial tension as in membrane emulsification. The range of value of the shear stress selected in the present work did not allow to improve the solvent-antisolvent mixing however PDI lower than 0.2 indicates high uniformity of PLG-PEG-nanoparticles produced.

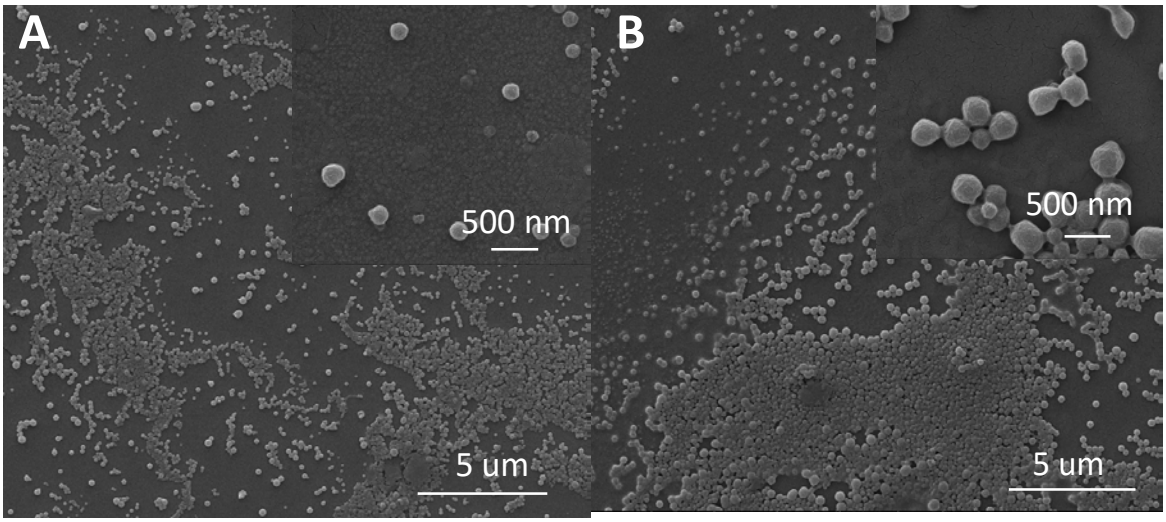

Figure 3.7. SEM images of PLGA-PEG nanoparticles produced by membrane-assisted nanoprecipitation at different shear stress values: A) 1.12 Pa B) 4.16 Pa.

3.3.4 Effect of membrane pore size

The effect of membrane pore size on the mean size of PLGA-PEG nanoparticles prepared by pulsed-cross flow MANA process is reported in

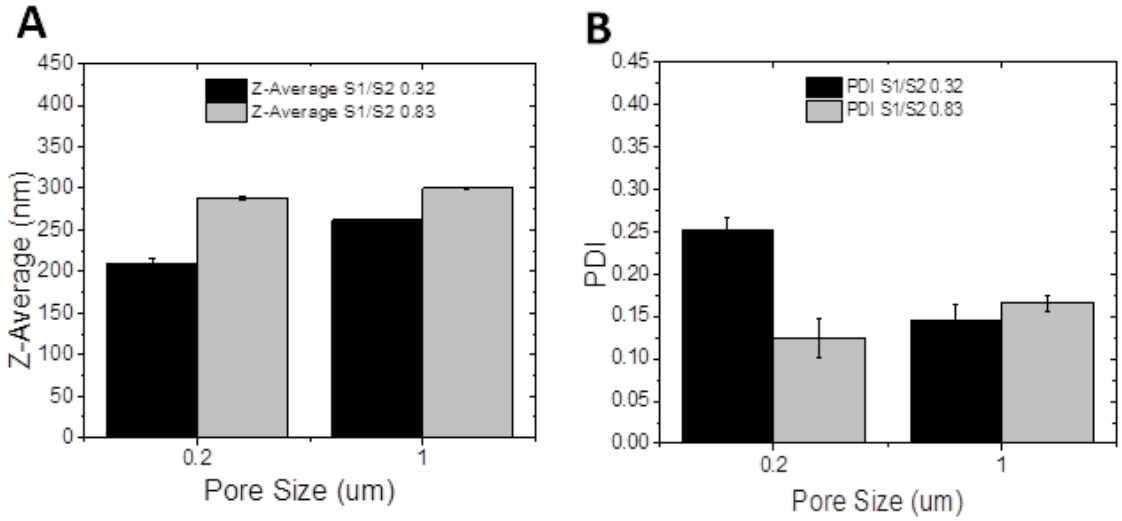

Figure 3.8. The mean nanoparticle size increased by increasing the membrane pore size, and the effect was more pronounced at low S1/S2 ratio (0.32). The average particle size increased from 210 to 288 nm (37%) and from 261 to 300 nm (15%), when membranes with pore sizes of 0.2 and 1 um were used, respectively. Z-average values also show to be significantly influenced by the pore size of the membrane (p value < 0.05 Figure S3.5) while PDI values were not significantly influenced by the pore size of the membrane (p value > 0.05 Figure S3.6). Although the results show that in

nanoprecipitation particle size is sensitive to the membrane pore size, it should be highlighted that the particle size did not varied linearly with the pore size, which is the general trend observed in membrane emulsification process. These findings are in agreement with the results obtained by Charcosset et al. and Othman et al. [112,215]. In conventional membrane emulsification, a linear relationship exists between the pore size of the membrane and the droplet size, and membranes with a mean pore size smaller than the target particle size are required. In contrast, the membrane-assisted nanoprecipitation technique enables the production of particles significantly smaller in size than the pore size of the membrane. The production of Polycaprolactone (PCL) nanoparticles by nanoprecipitation in the range of size between 100 to 300 nm was obtained by using membranes with the pore size in the range between 6 to 100 nm [112] and 20 to 40 □m [215]. These results can be explained by considering that the contact area between solvent and antisolvent is higher in case of big-pore membranes. Nucleation is extremely fast in nanoprecipitation (as discussed in section 3.1 above), therefore nuclei are quickly formed, as soon as the S1 comes into contact with the S2. In a small-pore membrane, the supply of polymer to the formed nuclei is slower, so the particle does not have time to grow much until it is entrained into the S2. Growth is limited to the sphere of diffusion around the nuclei. As the pore size increases, diffusion is faster and nuclei grow into larger particles before entrainment in the S2 (Figure 8).

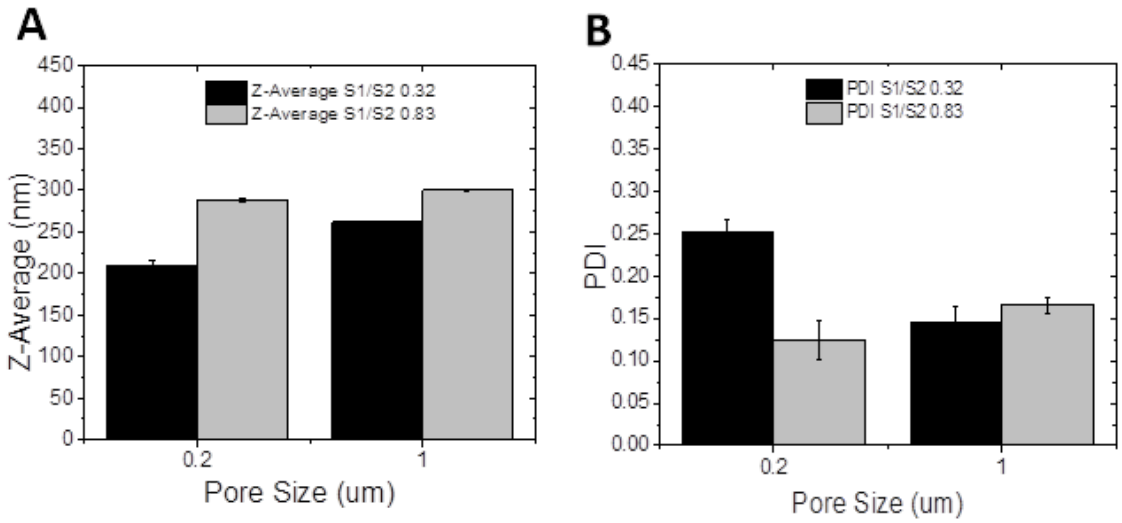

Figure 3.8. Influence of membrane pore size on nanoparticle size and particle size distribution of PLGA-PEG nanoparticles produced by membrane-assisted nanoprecipitation.

3.3.5 Reproducibility of nanoprecipitation membrane-assisted process

Figure 3.9 reports the reproducibility achieved in the production of nanoparticles prepared by pulsed-cross flow membrane-assisted nanoprecipitation technique. Once a manufacturing process has been developed and have a good performance, it is required to go further and study if the process is consistent "in control" or it is unpredictable "out of control" [232]. Control charts are an excellent tool to inspect the process performance and enable to measure, monitor and control the production process. These facts make the control charts being widely used in pharmaceutical and biopharmaceuticals manufacturing processes [232–234]. Control charts of nanoprecipitation membrane-assisted process (Z- Average and PDI) were performed using 6 lots with the following operative conditions: S1/S2 ratio of 0.32, shear stress of 2.48 Pa and S1 flux of 61.3 L $h^{-1}m^{-2}$ control chart methodology was employed and media, upper control limit (UCL) and the lower control limit (LCL) was calculated (see Appendix). Figure 3.9A, in which the Z-average is plotted against the different batches of nanoparticles produced, shows that there is no variability between the samples and all the range of measurements are fairly narrow and close to the mean (250 nm). On the other hand, the analysis of PDI variations between lots also confirms the reproducibility between lots, obtaining a narrow PDI variation (Figure 9-b).

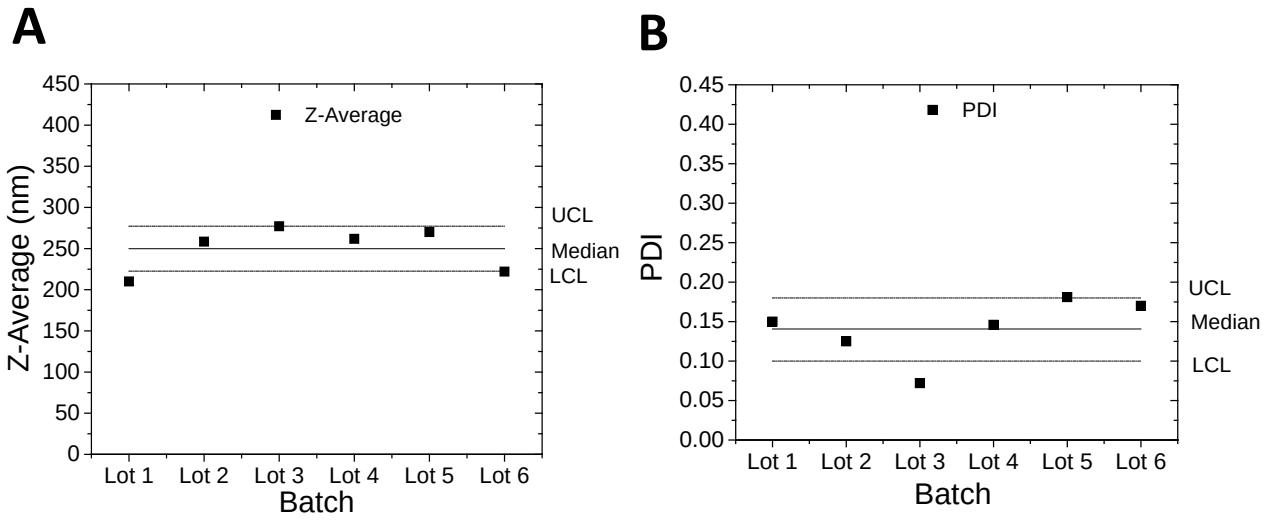

Figure 3.9: Control Chart of 6 nanoparticles lots produced by nanoprecipitation membrane-assisted process (operating conditions: S1/S2 ratio of 0.32, shear stress of 2.48 Pa and S1 flux of 61.3 L h-1m-2): A) Z-Average B) PDI

3.3.6 Encapsulation efficiency (EE) and drug loading efficiency (DLE)

Figure 3.10 depicts the effect of S1/S2 ratio on the dexamethasone encapsulation efficiency (EE) and drug loading efficiency (DLE) of PLGA-PEG nanoparticles produced by pulsed-cross flow MANA. DLE is highly relevant in drug delivery because achieving a high drug loading allows reducing the content of the carrier material [184]. However, in terms of productivity, EE has a relevant economic impact considering that drugs are usually the most expensive components of pharmaceutical formulations. Consequently, it is desirable to maximize both parameters, EE and DLE. According to the results obtained in this work, the EE decreases in the range from 52.3 % to 34 % as a function of the increase of S1/S2 ratio. The same trend was obtained in case of DLE. These insights about the S1/S2 influence are in agreement with previously reported data where a variety of drugs were encapsulated in different polymers by nanoprecipitation procedure [142,235–237]. A large volume of the non-solvent solution (i.e., a low S1/S2 ratio) provides a high concentration gradient of the organic solvent across the phase boundary, leading to fast solidification of the particles [238]. Conversely, at high S1/S2 ratio, the diffusion of acetone is delayed by the presence of the acetone in water. In addition, the solubility of dexamethasone in the water phase is an important parameter determining the maximum amount of drug that can be dissolved in the external phase, during the solidification step. Dexamethasone is a hydrophobic drug with a water solubility of 0.1 mg mL-1. The diffusion of acetone out of particle together with the drug occurs during polymer precipitation and the partition between the organic and the aqueous solutions continues until the equilibrium is reached, decreasing the entrapment into the nanoparticles [239]. Our results are in agreement with the data reported in literature by Campus et al. They obtained an EE of 48% for dexamethasone-loaded PLGA nanoparticles, using acetone as solvent and a S1/S2 ratio of 0.25. [18].

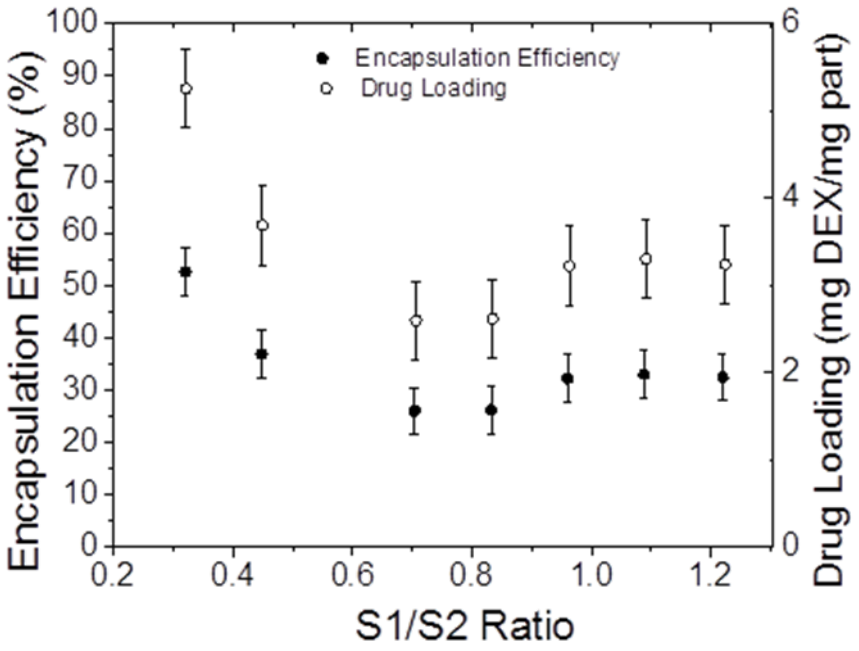

Figure 3.10. Influence of S1/S2 ratio on Encapsulation efficiency and Drug Loading of Dexamethasone encapsulated in PLGA-PEG nanoparticles produced by membrane-assisted nanoprecipitation.

3.3.7 Release studies from the drug loaded nanoparticles

In vitro release studies of dexamethasone from PLGA-PEG nanoparticles were carried out during 15 days. The delivery profile showed: 1) a low release of dexamethasone during the first 2 h (induction time) of the test that can be attributed to non-encapsulated drug or drug on the surface, 2) an increase of drug release for the following 4 days that can be attributed to drug diffusion through pores and 3) a constant release rate that could be related with the polymer degradation and a slow drug diffusion (Figure 3.11). The initial burst release is commonly observed for biodegradable polymeric systems, where a high percentage of the biomolecule is released [73]. Initial burst release is expected to increase for drugs with a higher solubility and also as the drug is located on the surface of the nanoparticles, where the diffusion paths are negligible. In this case the relatively low burst release observed is noteworthy since dexamethasone is not a highly hydrophobic drug, with a significant water solubility of 0.1 mg mL-1. For instance, in a previous work [17] with dexamethasone-loaded PLGA nanoparticles, a burst release of 60% in the first two days was found. This indicates a good distribution of dexamethasone in the PLGA-PEG nanoparticles, and also points

to the effectiveness of PEG to reduce burst release. The complete release of the drug in PLGA polymeric particles could require one month due to the polymer hydrolysis. However in this case release was performed during 15 days because this period is enough to study the kinetics of the system [40].

A variety of release models were selected and used to fit the experimental data. Table 1 summarizes the most important kinetic parameters for each model obtained from statistical data fitting: the release constant (K), release exponent (n), and regression coefficient (R2).

On the basis of best fit with the highest correlation value (R2), it is concluded that model that better fits the experimental data obtained from in vitro drug release studies is the Korsmeyer-Peppas model (R2 = 0.97). The magnitude of the release exponent n was found to be smaller than 0.5 (0.31), indicating that the mechanism of dexamethasone release from PLGA-PEG nanoparticles during 15 days preferentially followed a Fickian diffusion process. Fickian diffusional release occurs by the usual molecular diffusion of the drug due to a chemical potential gradient while non-Fickian predominates when there are also effects of swelling, erosion, degradation, stresses, structural changes and relaxation of the material [240,241]. The findings obtained are in agreement with literature, where Fickian diffusion was predominant at early times in PLGA-PEG systems. Vega et al [201], reported the cumulative in vitro release profile of flurbiprofen-loaded PLGA-PEG nanoparticles, achieving the best fitting with Korsmeyer-Peppas model (R2 =0.94, release exponent = 0.16). Assuming that Fickian diffusion is directing the dexamethasone release implies that PLGA-PEG nanoparticles were not substantially degraded during the release interval. In fact, after the release interval the amount of dexamethasone loaded in PLGA-PEG nanoparticles was higher that 40%. The initial release intervals in PLGAs based polymeric particles are normally associated to the Fickian transport and Non-Fickian is gradually predominant as the erosion and degradation phenomena are evident by the formation of new pores in the polymeric matrix. Higuchi model, a Fickian model, was also evaluated to fit the experimental release data, but a correlation factor R = 0.87 was obtained (Table 3.2). It implies that dexamethanose release from PLGA-PEG nanoparticles is not a pure diffusion process. This fact can be justified because the release analysis is usually made global, presenting always one transport type more predominant than the other [17].

Table 3.2. Interpretation of R2 values and rate constants of dexamethasone release kinetics of PLGA-PEG nanoparticles

Model	Release constant (K)	Release exponent (n)	Regression coefficient (R2)
Zero Order	3.99	-	0.73
First Order	0.06	-	0.53
Korsmeyer-Peppas	0.47	0.31	0.97
Higuchi	0.32	-	0.87

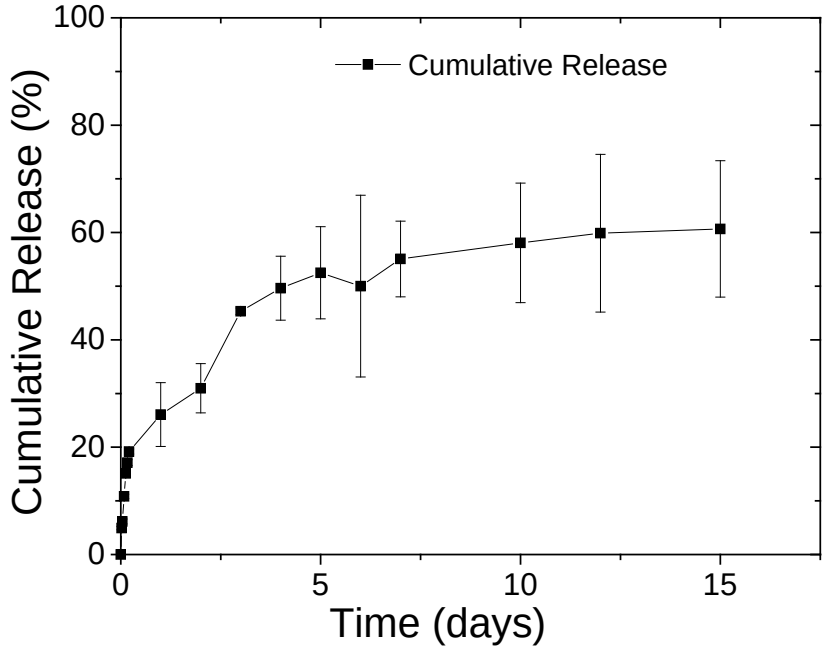

Figure 3.11. Dexamethasone release from PLGA-PEG nanoparticles produced by membrane-assisted nanoprecipitation.

3.4 Conclusions

In this phD work, the efficiency of membrane-assisted nanoprecipitation (MANA) process to tune PLGA-PEG nanoparticles size with high producibility has been demonstrated. PLGA-PEG nanoparticle size in the range from 250 to 400 nm and with a PDI lower than 0.2 were continuously obtained. The main role of the membrane was to govern nuclei formation and subsequent growth into

nanoparticles by controlling the mixing of solvent and non-solvent at the pore level. Particle size and particle size distribution have been demonstrated to be independent on the stream 1 flux. High fluxes of 1917 L $h^{-1}m^{-2}$ could be employed while maintaining control over particles size and size distribution, showing a high potential for large scale production.

The highest dexamethasone encapsulation efficiency (54 %) and drug loading (5.2 %) were achieved at the lower organic solution volume/ aqueous volume ratio, i.e., in the presence of a high concentration gradient of the solvent across the phase boundary, leading to fast solidification of the particles. The dexamethasone release from PLGA-PEG nanoparticles was found to preferentially follow a Fickian diffusion process. A comparatively low initial burst release was obtained.

In summary, MANA seems a highly promising alternative as a reproducible, productive and low-energy method for the continuous production of size-tuneable drug-loaded nanoparticles.

Chapter 4

Sustainable production of drug-loaded particles by membrane emulsification

This chapter is adapted with permission of American Chemical Society from A. Albisa et al, Sustainable production of drug-loaded particles by membrane emulsification, ACS Sustainable Chemistry & Engineering, March, 2018. Permission conveyed through Copyright Clearance Center, Inc.

4.1 Introduction

Among the new generation of pharmaceutical forms, polymeric particles have gained significant relevance due to their ability to deliver drugs at a controlled rate and toward a specific target (Albisa et al. 2016). Polymeric particles have been frequently used as drug delivery depots of drugs with low aqueous solubility. Approximately 40% of all new drug candidates in development, and about 70–80% in some therapeutic areas, are poorly absorbed orally, principally due to their low aqueous solubility. As the field of drug delivery is expanding into consumer products, it is essential to advance in the development of efficient synthesis technologies while preserving, at the same time, human health and the environment for future generations. The design of highly efficient particulate systems with high yield, minimizing solvent and energy consumption and with a reduced waste production is a significant challenge in particle engineering technologies. (Boodhoo et Harvey 2013; Etheridge et al. 2013; Frank Roschangar et al. 2017) Producers are making a big effort to create the basis to regulate process manufacturing procedures to reach high quality products, with high productivity and to fulfill also the requirements of the pharmacopeia (Sainz et al. 2015; Pramod et al. 2016).

Biodegradability or biocompatibility is an essential requirement for the polymer used for pharmaceutical applications (Li, Rouaud, et Poncelet 2008). Several drug delivery systems based on poly (D,L-lactide-co-glycolide) (PLGA) family are approved by the FDA and their ability to modulate drug release are strictly connected with the relative amount of lactic (PLA) and glycolic acids (PGA) [40,152]. The modification of PLGA with an hydrophilic and inert polymer like PEG (poly ethylene glycol) prolongs the circulation of the particles in the body and decreases the premature drug release increasing their therapeutic effect [80]. Dexamethasone (DEX) is currently used in many biomedical applications such as: cell culture, ophthalmology, proliferative vitreoretinopathy, subretinal neovascularization, arthritis and diabetic macular edema as anti-inflammatory and immunosuppressant drug [14]. The main limitations of this drug for pharmaceutical applications are its high hydrophobicity and high doses necessary to reach its therapeutic level (Cohen 1973; Urbańska, Karewicz, et Nowakowska 2014). Consequently, various delivery systems have been developed and the majority of them are based on its encapsulation within both natural and synthetic polymers (Krishnan et al. 2013; Urbańska, Karewicz, et Nowakowska 2014; Campos et al. 2014; Gu et Burgess 2015).

Microencapsulation by solvent evaporation is a widely applied technique for entrapping insoluble or poorly water-soluble drugs. Different aspects have to be taken into account to choose the most appropriate solvent for the preparation of polymeric particles by this technique: 1) the ability to

dissolve the polymer 2) a reduced solubility in the continuous phase 3) high volatility 4) low toxicity (Li, Rouaud, et Poncelet 2008).

Solvents used during polymer particle synthesis are often volatile organic compounds and their use is associated to some concerns about their potential environmental impact (some of them are able to form low-level ozone and smog through free radical air oxidation processes), their adverse health effects (ranging from carcinogenic properties to headaches and allergic skin reactions, eye irritations) and their hazardous properties (they are often highly flammable)(Roy 2014). Dichloromethane (DMC) is one of the most used solvents for the production of polymeric particles via emulsification and subsequent solvent-evaporation due to its high volatility, low boiling point and high immiscibility with water (Li, Rouaud, et Poncelet 2008). Ethyl acetate (EA) has been proven to be a potential substitute of DCM with less toxicity (Sah 1997; Bahl et Sah 2000; Soppimath et Aminabhavi 2002; Song et al. 2006; Li, Rouaud, et Poncelet 2008). It has been classified as "recommended" considering the safety, health and environmental scores while DCM is considered "problematic" or "hazardous" (Prat, Hayler, et Wells 2014; Byrne et al. 2016).

Microengineered technologies are emerging as promising particle fabrication methods for their ability to generate droplets individually by injecting the dispersed phase in the continuous phase through a single (i.e., microfluidic device) or a multitude of channel/pores (i.e., membranes) (Ortiz de Solorzano et al. 2016; Piacentini, Dragosavac, et Giorno 2017). These techniques allow the production of uniformly sized droplets with tuned sizes and improved encapsulation efficiency (Liu et al. 2006; Surh et al. 2007; G. T. Vladisavljević, Kobayashi, et Nakajima 2012; Matos et al. 2015). Polymeric particles can be obtained by combining membrane emulsification with additional physical (i.e., evaporation/solvent diffusion) or chemical (cross-linking, coacervation and interfacial polymerization) treatments. This allows controlling the physicochemical properties, size, size distribution and drug loading in the resulting particles. Membrane systems have been indicated as new "green process engineering" able to redesign traditional operations [242] however; to the best of our knowledge, the greenness of membrane emulsification has never been measured.

In the pHD work, PLGA-PEG microparticles were produced by membrane emulsification/solvent diffusion. The effect of the different solvents used for polymer dissolution (EA or DCM), fluid-dynamics and operating conditions applied during membrane emulsification and solidification steps, respectively, were investigated. In particular, the sustainability assessment of the process was evaluated by considering the properties of the polymeric particles produced (size, size uniformity, and drug encapsulation efficiency) together with the energy consumption. To determine the green

impact of the particle production method proposed, the metric based on the Green Aspiration Level™ (GAL) was used (F. Roschangar, Sheldon, et Senanayake 2015; Frank Roschangar et al. 2017). Many authors have dedicated their efforts to optimize membrane emulsification processes for manufacturing structured microparticles with tailored properties (Goran T. Vladisavljević 2015) however; to the best of our knowledge, this work is the first one in which the greenness of the process was measured. A comparison with previous research carried out for the production of DEX-loaded PLGA particles is also reported to emphasize the advances of the present work.

4.2 Materials and Method

4.2.1 Materials

The polymer used in this study was Resomer RGP d 5055 (Di-block PLGA (50:50) PEG (5kDa, 5%) (PLGA-PEG), EVONIK, Germany). Dexamethasone (DEX) supplied by SIGMA–Aldrich was used as model drug. Pluronic F127 was used as stabilizer in the external phase during the microencapsulation process and Ethyl acetate (EA) and Dichloromethane (DCM) were used as non-polar solvents. Surfactants and solvents (analytical grade) were purchased from SIGMA–Aldrich.

4.2.2 Dispersed Phase and continuous phase preparation

The dispersed phase used to produce the o/w emulsion was obtained by dissolving PLGA-PEG in EA at a polymer concentration of 10 mg mL^{-1}. The continuous phase was a water solution containing Pluronic F127 at 11.6 mg mL^{-1}. A continuous phase saturated in Ethyl Acetate was used during the emulsification step in order to avoid its diffusion from the formed droplets while a non-saturated continuous phase was used as dilution medium for the preparation of the particles by solvent diffusion, after emulsification.

To evaluate the dexamethasone encapsulation efficiency and drug loading, the dispersed phase was modified by including dexamethasone (1 mg mL^{-1}).

4.2.3 Membrane emulsification step

The o/w emulsion was prepared by using a Shirasu porous glass-based (SPG, Miyazaki, Japan), hydrophilic tubular membrane with a pore size of 1 μm having a membrane area of 31.30 cm^2. A schematic representation of the membrane and the membrane emulsification plant are reported in Figure 4.1. The dispersed phase was injected through the membrane under gas pressure using a

transmembrane pressure (P_{TM}) between 0.18 and 0.45 Pa, corresponding to a dispersed flux (J_d) between 1.16 and 30.67 $Lh^{-1}m^{-2}$. The dispersed phase flux (J_d) was determined as follows:

Equation 4.1: $J_d = \frac{Q_d}{A}$

Where, Q_d is the Dispersed Phase Flow ($L \cdot h^{-1}$) and A is the Membrane Area (m^2). It represents a measurement of membrane emulsification throughput.

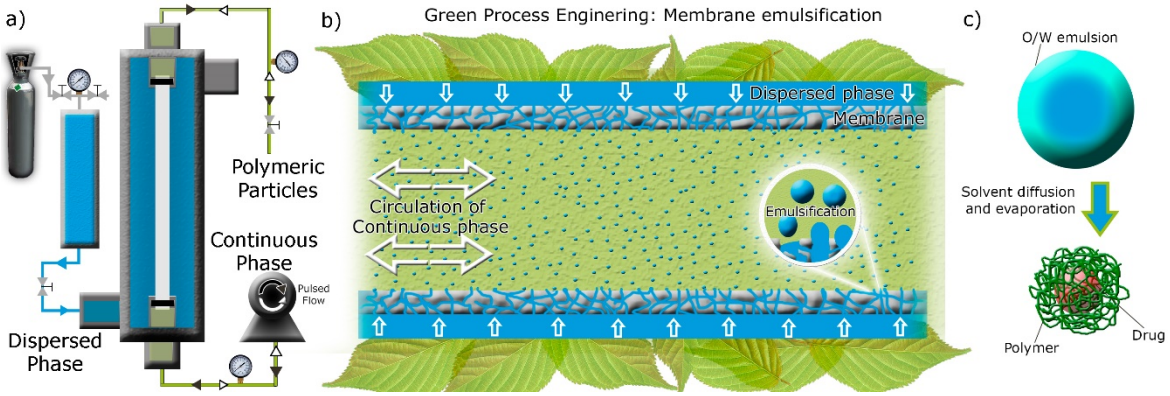

Figure 4.1. A) Schematic representation of the membrane emulsification set up. B) Schematic representation of membrane emulsification process. C) Schematic representation of solvent diffusion - evaporation process.

The continuous phase was agitated by means of a pulsed back-and-forward mode along the lumen side of the membrane by using a programmable peristaltic pump (Digi-Staltic double-Y Masterflex® pump Micropump, model GJ-N23.JF1SAB1). [221,243] The maximum shear stress (τ_{max}) [Pa] at the membrane surface depends on the frequency (f) [Hz] and on the amplitude (α) [m] of the continuous phase flow. The amplitude and the frequency of the oscillation were calculated considering the flow rate of the pump (Qc) [$m^3 \cdot s^{-1}$] and the volume of the continuous phase that was pumped inside the membrane before the flow direction was reversed (Vc) [L]. These parameters were calculated as follows:

Equation 4.2: $\tau_{max} = 2\alpha(\pi f)^{1.5}(\mu_c \rho_c)^{0.5}$

Equation 4.3: $\alpha = \frac{4Vc}{\pi d_h^2}$

Equation 4.4: $f = \frac{2Qc}{Vc}$

Where μ_c is the Continuous phase viscosity [Pa·s] and ρ_c is the Continuous phase density [$kg \cdot m^{-3}$]. The effect of amplitude was fixed at $4.7 \cdot 10^{-2}$m and frequency was modified between 1.48 and 3.57 Hz.

The volume ratio % of the dispersed phase obtained for each experiment respect to the continuous phase volume (DP/CP) was 20 %. The emulsification process was carried out at 20 ± 5°C.

The membrane was pre-wetted in the continuous phase solution before each experiment. After each experiment, a membrane cleaning step was carried out by using acetone and EA [244].

The water permeability of a brand new membrane before each experiment was measured to evaluate its recovery after the cleaning procedure and it was set at 7523.00 ± 80.00 $Lh^{-1}m^{-2}bar^{-1}$.

4.2.4 Solidification Step

The liquid droplets were precipitated as solid microparticles by the addition of a certain volume of non-saturated continuous phase (diffusion volume, V_d). The diffusion volume was selected taking into account the theoretical minimum volume (V_{th}) (i.e., the minimum theoretical amount of diffusion volume necessary to ensure the complete diffusion of solvent), calculated using equation 1. The V_d/Vt_h ratio was changed from 0 to 3 in order to control the solidification rate of the droplets. V_d/V_{th} = 0 corresponded to the case in which the solidification was carried out without the addition of the non-saturated continuous phase.

Equation 4.5: $V_{th} = \frac{V_{DP} + S_{solvent} * V_{CP}}{S_{solvent}}$

Where V_{th} (mL) is the theoretical minimum volume of the organic solvent, V_{DP} (mL) is the dispersed phase volume, $S_{solvent}$ (mL solvent/mL water) is the solubility of the organic solvent in water and V_{CP} (mL) is the continuous phase volume.

The organic solvent was removed by evaporation in a fume hood under stirring for 3 hours. The resulting particles were centrifuged at 2100 g for 10 min and the supernatant was stored for further analysis while the pellet was lyophilized using a LyoAlfa 10/15 from Telstar for 24h (0.01 bar, -40°C).

4.2.5 Particles characterization

4.2.5.1 Particle analysis

The particle size analysis of the resulting microparticles was performed by using laser diffraction in a Malvern Mastersizer 2000 (Malvern Instruments, Worcestershire, UK). The software used to collect and analyze the data was a Malvern 2000 Software 5.61 using a refractive index of 1.55 PLGA-PEG polymer.

Microparticles were also observed by Scanning Electron Microscopy (SEM) using an Inspect F50 SEM operated at 10–15 kV; FEI from Eindhoven, Netherlands at the LMA-INA-Universidad de Zaragoza facilities. To perform the measurement, the sample was stained with a phosphotungstic acid solution (75 mg mL^{-1}) and washed three times with distilled water. One drop of the particulate dispersion was placed on a glass slide, dried overnight and cover with platinum before observation.

The size distribution was expressed in terms of the surface weighed median diameter or Sauter diameter (D(3,2)) calculated according to Equation 4.6. Volume weighed median diameter or Brouckere diameter (D(4,3)) was calculated according Equation 4.7.

Equation 4.6: $D(3,2) = \frac{\sum D_i^3 n_i}{\sum D_i^2 n_i}$

Equation 4.7: $D(4,3) = \frac{\sum D_i^4 n_i}{\sum D_i^3 n_i}$

Where D_i is particle diameter of class i and ni is number of particles in class i.

The width of particle size distribution was expressed as Span number calculated by Equation 8

Equation 4.8: $Span = \frac{\mathrm{D(90)-D(10)}}{\mathrm{D(50)}}$

Where D(X) is the diameter corresponding to the percent of volume on a relative cumulative particle size curve.

4.2.5.2 Encapsulation Efficiency and Drug Loading

The encapsulation efficiency (EE) and drug loading (DL) were evaluated according to the following equations (Equation 4.9 and Equation 4.10):

Equation 4.9: $\mathrm{EE} = \frac{\mathrm{DEX\ encap}}{\mathrm{DEX\ total}} * 100$

Equation 4.10: $\mathrm{DL} = \frac{\mathrm{DEX\ encap}}{\mathrm{PLGA\ total}} * 100$

Where EE is the encapsulation efficiency (%), DEX_{encap} stands for Dexamethasone mass encapsulated (mg) measured by mass balance, DEX_{total} stands for the initial Dexamethasone mass in the dispersed phase (mg), DL represents the drug loading efficiency (%) and $PLGA_{total}$ stands for the initial PLGA mass in the dispersed phase (mg). The particles were separated from the liquid by centrifugation at 2100 g. DEX content in the supernatant was determined by HPLC. A reversed-phase C18 column (2.6 µm, 50x4.6mm Phenomenex kinetex) was used. The mobile phase was acetonitrile/water at a pH 3 (50/50 v/v). The flow rate was 0.4 mL min^{-1} and the detection was obtained at 260 nm with a UV detector. The linear regression coefficient (R2) was determined in the range 0.01–30 µg/mL as 0.9993 (n=10).

4.2.6 Green analysis and energy consumption

4.2.6.1 Energy consumption calculation

The energy consumption was evaluated considering the production with a DP/CP of 20%. The energy required was calculated in terms of energy density (Ev, J m^{-3}), according to the following equation [245]:

Equation 4.11: $\mathrm{Ev} = \frac{P}{Q_E}$

where P stands for the effective power input (J s-1) and QE stands for the volume flow rate of the emulsion ($m^3 s^{-1}$). Power input was calculated as follows:

Equation 4.12: $P = \left(\frac{\Delta P_{CP} * Q_{CP}}{\eta_{CP}}\right)$

Where ΔP_{CP} is the pressure drop along the membrane module, Q_{CP} is the flow rate of the pump used to generate the pulsed flow and η_{CP} is the pump efficiency.

4.2.6.2 Green factor calculation

E factor is a simple analysis used to calculate the greenness of a process. Process waste was determined via complete E factor calculation based on a simple mass-balance [165]. Two factors were determined: simple E factor (sEF) and complete E factor (cEF) (in which solvent and water consumed during the process are also included) using equation 4.13 and equation 4.14, respectively, adapted to the specific case of particle production:

Equation 4.13: $\mathrm{sEF} = \frac{\sum \mathrm{m(Raw\ Materials)} + \sum \mathrm{m(Reagents)} - \mathrm{m(Product)}}{\mathrm{m(Product)}} = \frac{\mathrm{m(Polymer)} + \mathrm{m(Drug)} + \mathrm{m(surfactant)} - \mathrm{m(particles)}}{\mathrm{m(particles)}}$

Equation 4.14: $\frac{\sum \mathrm{m(Raw\ Materials)} + \sum \mathrm{m(Reagents)} + \sum \mathrm{m(Solvents)} + \sum \mathrm{(Water)} - \mathrm{m(Product)}}{\mathrm{m(Product)}} = \frac{\mathrm{m(Polymer)} + \mathrm{m(Drug)} + \mathrm{m(surfactant)} + \mathrm{m(solvent)} + \mathrm{m(water)} - \mathrm{m(particles)}}{\mathrm{m(particles)}}$

Where Σm(Raw Materials) represents the total mass of polymer and drug used for producing a batch of product. Σm(Reagent) represents the total mass of the reagents used in the process, principally the surfactant. m(Product), Σm(solvent) and Σm(water) represent the masses of particles produced, mass of solvent and mass of water, respectively. cEF is used in GAL-based analysis enabling organizations to calculate their green performance scores.

The process mass intensity (PMI), calculated as the ratio of the total mass of materials to the mass of the product, has been selected from ACS Green Chemistry Institute Pharmaceutical Roundtable as indicator of sustainability for the pharmaceutical sector:

Equation 4.15: $\mathrm{PMI} = \frac{\sum \mathrm{m(\ Materials\ \ input)}}{\mathrm{m(Product)}} = \ \mathrm{cEF} + 1$

Where the Σm(Materials input) includes the total mass of polymer, drug, reagents used in the process (i.e., surfactant), mass of solvent and mass of water. The cEF and PMI can be used interchangeably in the GAL methodology [163] and in this article, we will refer to it as cEF.

Percent's relation (%cEF and % solvent+water) was calculated using equation 4.16 and 4.17:

Equation 4.16: $\%cEF = \frac{sEF}{cEF} * 100\%$

Equation 4.17: $\%solvent + water = \frac{m(solvent)+m(water)}{m(total)}$

4.3 Results and Discussion

4.3.1 Effect of fluid-dynamic conditions during membrane emulsification process

The fluid-dynamic conditions play an important role during particle manufacturing by membrane emulsification, determining the droplet size and droplet size distribution of the emulsion before the solidification step. The influence of the dispersed phase flux and shear stress on PLGA-PEG particle sizes and size distributions have been studied in order to identify the operation conditions that provide the smaller droplets with the highest uniformity and productivity. On the other hand, the dispersed phase flux and shear stress are strictly correlated with the throughput and energy consumption, respectively. These two parameters have also been evaluated in order to demonstrate the sustainability of the productive process.

4.3.1.1 Effect of dispersed phase flux

The effect of dispersed phase flux on PLGA-PEG particle size and particle size distribution has also been investigated. Figure 2A describes the resulting particle sizes for D[4,3], D[3,2] and span of PLGA-PEG microparticles produced by pulsed back-and-forward ME as a function of the dispersed phase flux in the range from 1.15 to 30.67 $Lh^{-1}m^{-2}$, keeping constant the maximum shear stress (2.48 Pa).

Results demonstrated that the dispersed phase flux does not have a significant influence on particle size and span in the range from 1.15 to 12.84 $Lh^{-1}m^{-2}$. An average diameter (D[3,2]) and a span of distribution equal to 1.10 µm and 0.50 were obtained, respectively. This flux range is identified as

"dripping" regime [213,244]. The droplets are rapidly detached from the membrane surface and the contribution of the inertial force from the dispersed phase to the droplet sizes was negligible respect to the viscous drag and capillary forces. SEM images of the particles produced in this range are reported in Figure 4.2 (C1). The images reveal the homogenous size distributions and spherical shapes. An approximately linear increase in the particle size and span was observed when the dispersed phase flux was further increased in the range from 12.84 to 30.67 $Lh^{-1}m^{-2}$. A similar trend was previously reported in the literature for the production of other polymeric particles and emulsions.[27,221,244] The formation of larger droplets was the result of the faster increase in the droplet growth as the dispersed phase flux was increased. At 18.02 L $h^{-1}m^{-2}$ droplets were sheared off from the membrane surface before coalescence at the pore level. Uniform droplets (span = 0.8) were then produced although a slight increase in the droplet sizes was obtained (D[3,2]= 1.65 μm) (Figure 4.2, C2). The further increase of the dispersed phase flux generated less uniform (span = 1.6) and larger particles (D[3,2]= 3.6 μm) (Figure 2, C3).

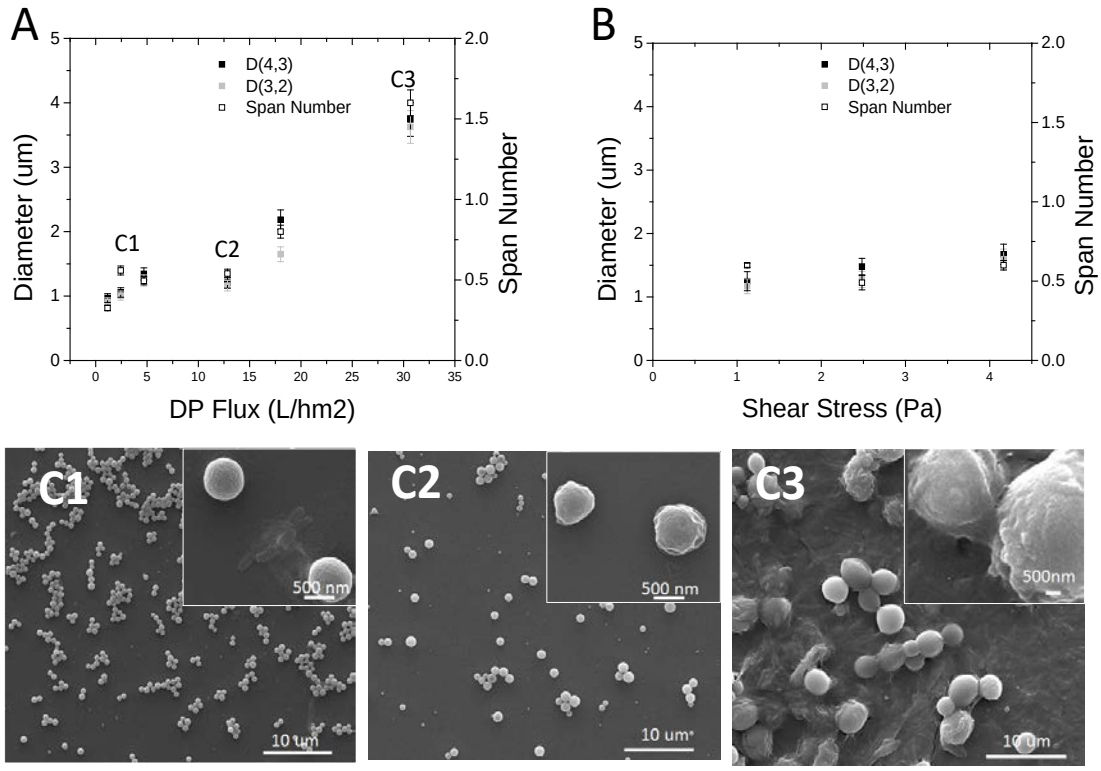

Figure 4.2. Effect of maximum shear stress and dispersed phase flux on particle size and particle size distribution at lower. A) Modification of dispersed phase flux at maximum shear stress of 2.48 Pa. B) Modification maximum shear stress at dispersed phase flux of 2.5 $Lh^{-1}m^{-2}$. C1, C2, C3 SEM images of the particles represented in the graph

Results demonstrate that PLGA-PEG particles with sufficiently narrow distribution in the droplet size (span lower than 0.55) and mean diameter tending to the membrane pore diameter can be produced for dispersed phase fluxes in the range of 1.15 to 12.84 $Lh^{-1}m^{-2}$. The increase in the dispersed phase flow determines an increase in the throughput from 36.18 mg h^{-1} to 402 mg h^{-1} reducing the operation time from 1.38 to 0.12 h. Data indicate that membrane emulsification can satisfy the demand of advanced manufacturing processes for industrial scale production by connecting efficiency and productivity. With their easy scale-up and large operational flexibility, membrane operations have been developed to the stage of large scale manufacture [242] and membrane emulsification has also demonstrated its capability for large scale industrial operations [246].

4.3.1.2 Effect of maximum shear stress

In pulsed back-and-forward ME, the shear stress is a function of the frequency and the amplitude of the pulsation along the lumen side of the membrane. The amplitude of the pulsation was kept constant (47.1 mm) while the increase of the continuous phase flow rate in the range from 500 to 1200 mL min^{-1} determined an increase in the frequency from 1.49 to 3.57 Hz. Figure 2B shows the effect of the maximum wall shear stress on PLGA-PEG particle size and particle-size distribution. Particle size (mean droplet diameter = 1.25 ± 0.13 μm) was not significantly influenced as the shear stress was increased in the range of values investigated (from 1.12 to 4.16 Pa). Typically, the mean particle decreases sharply as the wall shear stress increases and reaches a size where it becomes more or less independent of the shear. This effect is decreased in case of the production of submicron droplets and relatively small droplets are produced at lower shear stress.

The development of environmentally benign methods for manufacturing processes has become increasingly relevant in the last years determining a significant expansion in the development of more energy-efficient methodologies. Unutilized energy may be considered as a waste and the design of manufacturing processes that do not require intensive energy use is highly desirable. Membrane emulsification is a valuable technology to asses this goal. In the present work, the energy consumption used during the membrane emulsification process was reduced in the range from 9.50 10^5 to 3.90 10^5 Jm^{-3} as the maximum shear stress was decreased from 4.16 and 1.12 Pa. Considering that a shear stress of 1.12 Pa was enough to produce uniform particles (span = 0.6) with D[3,2] of 1.17 μm (tending to the membrane pore size), the further increase of the shear stress was not needed minimizing also energy consumption. Furthermore, traditional emulsification techniques

are known to be rather energy consuming[115,247]. The energy consumption associated with the use of an homogenizer, a sonicator and a magnetic stirrer is 10^6-10^8 Jm^{-3} [248] that is 1-3 orders of magnitude higher that the value measured in the present work.

Results clearly indicate that membrane emulsification allows operating under mild conditions to generate uniform droplets with mean diameters tending to the pore diameter reducing, at the same time, energy consumption.

4.3.2 Effect of process conditions used in the solidification step

In the production of PLGA-PEG microparticles by membrane emulsification- solvent diffusion method, both the organic solvent phase, in which the polymer is dissolved, and the aqueous continuous phase saturated with the organic solvent, are in the state of thermodynamic equilibrium. The addition of a certain volume of continuous phase to the system destabilizes the equilibrium. It causes the organic solvent to diffuse to the external phase and precipitates the polymer to form the solidified particles. Solvent removal determines droplet volume reduction by a shrinkage factor given by the chemical composition of the organic phase and defined as the ratio between the liquid droplet diameter and the solidified particle diameter [249] .

The effect of the type of organic phase solvents (EA or DCM) and solidification diffusion velocity on PLGA-PEG mean particle size, size distribution and particle morphology were investigated. On the other hand, for drug encapsulation, it is required that all the chemicals are used (such as solvents, polymer, and reagents) reducing or eliminating the generation of undesirable products that could be harmful both for human health and the environment. For that reason, sEF and cEF were evaluated for each chemical used in the production of PLGA-PEG microparticles.

4.3.2.1 Effect of organic solvent phase

Variations in particle size and particle morphology were observed when different organic solvents were used in the preparation of PLGA-PEG microparticles by the membrane emulsification/solvent diffusion method. Figure 4.3A reports the average diameter and span of PLGA-PEG particles produced by using EA or DCM as polymer solvent while SEM images of PLGA-PEG particles are reported in Figure 4.3C. More heterogeneous particles (span = 0.95) with an average diameter of three times the pore size of the membrane (D[3,2] =3.15 □m) were obtained when DCM was used. SEM images confirmed the heterogeneous distribution of the particles and revealed the presence of large holes and protuberances on the particles (Figure 4.3C1). On the contrary, uniform particles (span = 0.62) with an average diameter close to the pore size of the membrane (D[3,2] =1.25 μm)

were produced by using EA. SEM images show a dense and slightly rough surface without pores (Figure 4.3 C2). The differences observed in terms of particle-size distribution and morphology are strictly correlated with the solvent solubility in the water phase. The miscibility of the solvent in water influences the diffusion velocity and has a direct impact on the final size of the particles [143]. EA has a water miscibility (S_{EA}=9.7 wt%) 4.5 times higher than DCM and, as a result, EA-Water interfacial tension (6.8 ±0.6mN m^{-1}) is significant lower than DCM-Water interfacial tension (28.28 ± 0.40 m Nm^{-1}) [250,251]. In addition, since PLGA-PEG microparticles are formed from the emulsion droplets after organic solvent diffusion, emulsion droplets stability plays an important role to tune the properties of the structured particles. Uniform and smaller particles produced by using EA resulted from both the ability of the emulsifier (Pluronic P127) to prevent droplet coalescence, and the low interfacial tension between the aqueous and the organic phases, due to the partially water-soluble nature of EA. On the contrary, the boiling point of DCM is lower than the one of EA, allowing a flash solvent evaporation. Its miscibility with water is also lower, delaying solvent diffusion and increasing the solidification time. This determines the formation of pores and holes (Figure 4.3C1) as well as droplet aggregation probably responsible for the production of larger mean particle sizes. Similar results were found by Song et al. using PLGA as polymer, EA and DCM as solvents and Dimethylamine borane (DMAB) as surfactant [143].

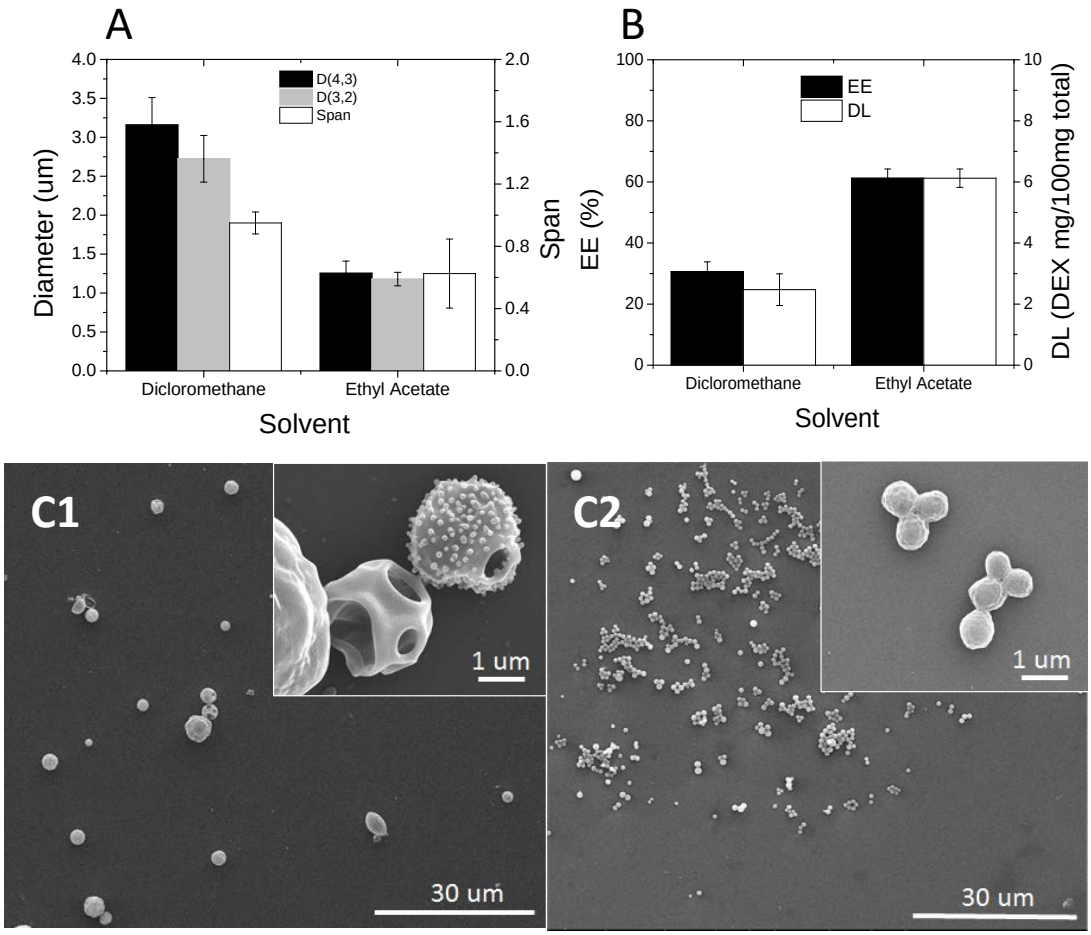

Figure 4.3**.** The effect of organic solvent type on A) particle size, particle-size distribution of particles. B) EE and DL (membrane emulsification/ solvent diffusion) and on particles morphology. C) (Polymer: PLGA-PEG, Surfactant: Pluronic, Vd/Vth= 3, PTM/Pc= 1.20, Shear stress: 2.48Pa). C1) SEM image of the particles PLGA-PEG particles produced with DCM. C2) SEM image of the particles PLGA-PEG particles produced with EA.

EE and DL were also evaluated (Figure 4.3B). The use of EA improves the encapsulation efficiency up to 50% respect to the use of DCM. The analysis of the particle morphology previously discussed can suggest that the porous surface of PLGA-PEG particles produced with DCM determined the enhanced leakage of the dexamethasone into the continuous phase. Similar results were previously reported by Imbrogno et al. for porous particles produced by using Polycaprolactone as polymer and DCM as solvent [231]. The use of EA also improved DL up to 50% reducing the content of the carrier material [184] minimizing waste generation and improving production profitability. For that reason, sEF and cEF values and particle costs were evaluated in this section (Table 1).

The generation of any material that does not have realizable value, such as the non-encapsulated drug, can be considered as a waste. The non-encapsulated drug may affect the environment

differently depending on its nature, toxicity or dose. On the other hand, maximizing the use of raw materials (such as drugs and carrier materials) so that the final formulation contains the maximum number of atoms coming from the reactants is the key point to design an efficient and sustainable manufacturing process.

sEF and cEF values were calculated when EA or DCM were used as organic solvents (Table 4.1). The evaluation of sEF and cEF plays a major role when focusing the attention on the problem of waste generation in pharmaceutical particle manufacturing and provides the impetus for developing cleaner and more sustainable processes. sEF and cEF values were reduced by 80%, when EA was used compared to DCM.

Table 4.1. The effect of organic solvent type and solidification velocity on green metric factors in memrane emulsification/solvent diffusion

	Solvent	**DCM**	**EA**	**EA**	**EA**	**EA**
	Vd/Vth	**3**	**3**	**1**	**0.5**	**0**
Green Analysis	sEF (mg/mg)	290.99	59.18	23.66	14.78	5.90
	cEF	25503.38	5237.41	2140.03	1365.69	591.35
	% cEF litd	1.14%	1.13%	1.11%	1.08%	1.00%
	% solvent + water	98.86%	98.85%	98.85%	98.85%	98.84%
Economic Analysis	Polymer Price (Euros/g product)	50.00				
	Drug Price(Euros/g product)	34.50				
	Surfactant Price (Euros/g product)	581.78	118.15	47.12	29.36	11.60
	Solvent Price (Euros/g product)	0.57	0.54			
	Water Price (Euros/g product)	25.07	5.04	1.98	1.22	0.45
	Total (Euros/g product)	691.92	208.23	134.14	115.61	97.09

Table 1 summarizes the economic analysis and the breakdown of the chemical reagents involved in the production of Dexamethasone loaded PLGA-PEG particles. Particle cost was reduced by 70%, when EA was used compared to DCM using V_d/V_{th} =3 (Table 4.1) as a result of the low amount of water and emulsifier required to obtain particle solidification when using EA. When particle solidification occurs by solvent diffusion, solvent solubility strictly influences the amount of non-solvent (i.e., water) and surfactant required for solvent-non-solvent exchange [140]. EA is more

soluble in water than DCM and the amount of water and surfactant required for droplet solidification is lower (Table 4.1). This difference is the main reason to explain why costs were reduced for PLGA-PEG particles produced at the same Vd/Vth ratio with EA (208.23 Euros/g product) and DCM (691.92 Euros/g product). In addition, EA results to be a greener solvent for the production of drug delivery systems based on PLGA-PEG considering both its E factor and its low toxicity. Several researchers have analyzed the toxicity on human cell lines of PLGA-PEG particles produced using EA as a solvent, observing that particles do not alter cell proliferation. This indicates that the PLGA delivery systems prepared by using EA are nontoxic at the doses used [121,252,253].

4.3.2.2 Solidification diffusion velocity

The influence of V_d/V_{th} ratio on PLGA-PEG particle size and span is presented in Figure 4.4. The solidification rate of the emulsion droplets is directly related to the solvent diffusion volume. Results indicate that particle sizes were almost independent on V_d/V_{th} ratio. Uniform particles (span <0.60) with an average diameter of 1.25 μm were produced (Figure 4A, 4C). EA has a low vapour pressure that makes its evaporation very fast (EA Vapor Pressure: 0.13 bar at 25°C). This promotes the solidification process because the emulsification-diffusion method guarantees the free solvent diffusion as long as the organic solvent solubility condition is satisfied [142]. Considering the partially water-soluble nature of EA, its fast diffusion from the droplets was expected.

DEX EE was decreased from 61.22 (±3.00)% to 57.12(±3.56)% when the V_{th}/V_o was increased from 0 to 3 (Figure 4B) as a result of the increase in the concentration gradient of the encapsulated DEX toward the external aqueous phase during the solidification process [254].

Green metric factors were calculated and are presented in Table 4.1. sEF and cEF values were reduced by 90.03%, when V_d/Vt_h =0 (no diffusion solution added) was used compared to V_d/Vt_h =3. Data indicate that the use of EA allowed reducing the water consumption and the surfactant amount used in the solidification step. This determines also a cost reduction of 53.38% as a function of V_d/Vt_h (from 3 to 0). (Table 4.1).

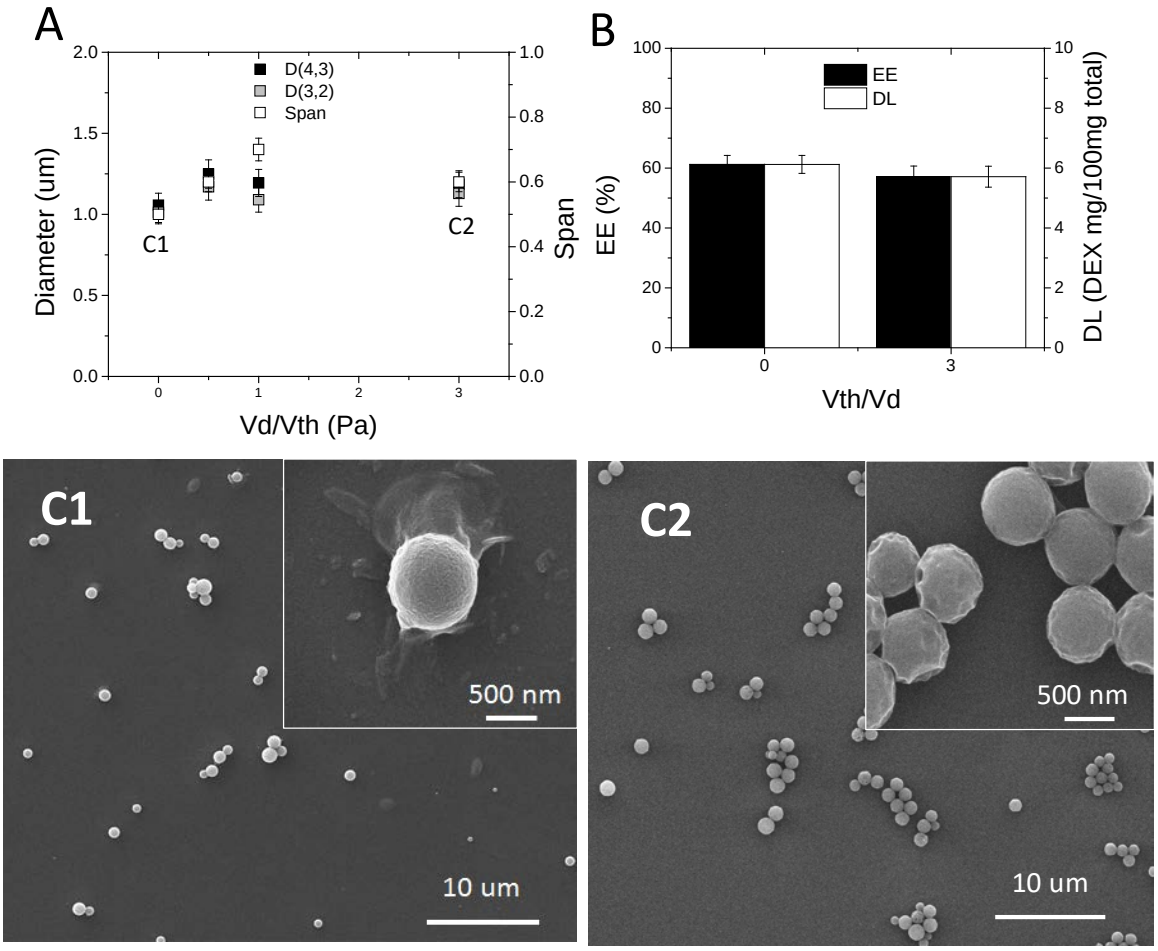

Figure 4.4. The effect of solidification velocity on A) particle size, particle-size distribution of particles, B) EE and DL (membrane emulsification/ solvent diffusion) and on particles morphology C) (Polymer: PLGA-PEG, Surfactant: Pluronic, Organic solvent: EA, PTM/Pc= 1.2, Shear stress: 2.48Pa). C1) SEM image of the particles PLGA-PEG particles produced with Vt/Vo =0. C2) SEM image of the particles PLGA-PEG particles produced with Vt/Vo =3.

In the present work, the production of PLGA-PEG particles as potential drug delivery vectors was assessed by using membrane emulsification/solvent diffusion method. The optimized operative conditions during the emulsification (DP flux = 12.84 $Lh^{-1}m^{-2}$, shear stress = 1.12 Pa) and the solidification steps (solvent= EA, Vd/Vth = 0) allowed to produce uniform particles (span = 0.62) with an average particle size of 1.25 μm and an EE of 61.22%. High throughput was achieved by increasing the dispersed phase flux to 12.84 $Lh^{-1}m^{-2}$ in mild operative conditions (shear stress = 1.12 Pa) reducing at the same time the energy consumption ($3.96.10^5$ Jm^{-3}). EA resulted to be a valuable alternative solvent for PLGA particle production as being a greener solvent considering both green metric factors and toxicity compared to the use of DCM. The use of EA makes the particle production

process more sustainable reducing the volume of water consumed and the amount of emulsifier used. This allowed also decreasing the economic impact of these components.

4.3.3 A comparison with the literature

Recent works on the production of PLGA-PEG particles by emulsification-solvent diffusion method is analysed in this section with the aim to demonstrate the sustainability of the manufacturing method used in the present work. The use of membrane-emulsification in the preparation of PLGA particles has been previously reported [255–258] however; the greenness of this process has not been measured.

Energy density and process throughput obtained in the present work are compared with data calculated from previous works in which membrane-based processes [255,258] and also conventional emulsification methods [40,140,142] have been used during PLGA particle production (Table 2). Considering the similar physicochemical properties of PLGA and PLGA-PEG polymers [142], literature data about PLGA particles manufacturing were used for the comparison according to the availability of all the information required for throughput and energy density calculations (see Appendix Table S4.1 – S4.10).

One of the frequently mentioned advantages of membrane emulsification over conventional emulsification methods is the lower energy density requirement[259]. The concept of energy density has been previously applied to compare different mechanical emulsifying processes [259,260]. The comparison illustrates that, given equal energy densities, different emulsifying equipment (rotor-stator systems, ultrasound systems, high-pressure homogenizers and membrane emulsifiers) produces very different droplet sizes. In membrane emulsification, particles with a mean diameter approximately equal to were produced with an energy density in the range of 10^3-10^6 Jm^{-3} which is 1-2 orders of magnitude smaller than in high-pressure valve homogenizers [259]. In the present work, we compared the energy density required for the production of PLGA particles by using different mechanical emulsifying processes. The comparison illustrates that only the pulsed back-and-forward method allowed decreasing effectively the energy density respect to the other conventional emulsification methods. It is well known that higher energy densities are needed to produce smaller droplets[259,260]. For that reason, results obtained in the present work by using the pulsed back-and-forward method are more relevant if we consider that the mean particle size (1.25 μm) is significantly smaller that the size reported by other membrane emulsification methods (60-120 μm) [255] or by conventional emulsification methods (15-80 μm) [16,78,261]. Slightly

smaller particles (mean particle size = 0.4-0.6 μm) with high throughput (3 10^{-7} m^3s^{-1}) were produced by using the sonicator in the emulsification step but with a significant increase in the energy consumption (from 10^5 Jm^{-3} by using pulsed-back-and-forward membrane emulsification to 10^8 Jm^{-3} by using a sonicator). [248] Pulsed back-and-forward membrane emulsification appears to be an alternate valuable method with low energy consumption (3 orders of magnitude lower) respect to other membrane emulsification methods of operation for the production of particles in the same range of sizes[258] although the process throughput was one order of magnitude lower than those associated with the conventional emulsification methods.

Table 2. Comparison between the membrane emulsification/solvent diffusion process and processes described in the literature

		MEMBRANE EMULSIFICATION			CONVENTIONAL EMULSIFICATION METHOD			
		Present Work	Ho et al, 2013 [258]	Gasparini et al, 2008 [255]	Kim and Martin, 2006 [17]	Gu and Burgess, 2015 [16]	Park et al, 2009 [261]	Goodfriend et al, 2016 [78]
Chemical Composition	Polymer	PLGA-PEG	PLGA	PLGA	PLGA	PLGA	PLGA	PLGA
	Drug	DEX	curcumin	N/A	DEX	DEX	DEX	DEX
	Solvent	EA	Chloroform	DCM	DCM/Acetone	DCM	DCM	Tetrahydrofuran
	Surfactant	Pluronic F127	PVA	PVA	PVA	PVA	PVA	Pluronic F127
	Dispersed Phase/Continuous Phase ratio	0.20	0.10	0.07	0.20	0.20	0.10	1.00
	Total Volume (mL)	30.00	6.60	160.00	180.00	137.00	330.00	10.00
Emulsification Process	Membrane	SPG Membrane D_p= 1um	Silicon nitride membrane D_p= 2um	Metallic membrane D_p= 40um	-	-	-	-
	Emulsification Device	Cross-Flow pulsed back-and-forward	Cross-Flow	Stirred	Sonicator (Fisher 500)	T 25 digital ULTRA-TURRAX homogenizer	Magnetic stirrer	Vortexed stirrer
	Throughput (m3 s-1)	$1.32*10^{-08}$	$2.20*10^{-08}$	$1.33*10^{-07}$	$3.00*10^{-07}$	$2.00*10^{-07}$	$5.50*10^{-07}$	$5.56*10^{-09}$
Formulation Properties	Mean Particle size (um)	1.25	2.30	60.00	0.40–0.60	15.00	20.00	50.00
	EE %	61.20	32.00	N/A	79.00±5.00	70-95	N/A	60.00
	DL %	6.16	2.00	N/A	13.00±3.00	10	N/A	N/A
Energy Consumption	Energy density (Jm-3)	$3.96*10^{-05}$	$2.29*10^{-08}$	$2.25*10^{-08}$	$2.00*10^{-08}$	$1.60*10^{-09}$	$1.09*10^{-08}$	$2.52*10^{-08}$
Green Analysis	sEF	5.90				0.71		
	cEF	591.35				313.17		
	% cEF litd	1.00%				0.23%		
	% solvent + water	98.84%				99.45%		
Economic Analysis	Polymer Price (Euros/g product)	50.00	50.00	50.00	50.00	50.00	50.00	50.00
	Drug Price(Euros/g product)	34.50	34.50	N/A	86.25	70.38	3.45	215.63
	Total Cost (Euros/g product)	97.09	106.09	52.14	155.35	121.73	56.56	265.68

Green metric factors obtained for the method developed in the present work were compared with the same data calculated for the method described by Gu and Burgess [16]. This paper was the only one that included data referred to both emulsification and solvent diffusion steps, while other papers analysed in this section only referred to the emulsification step [17,78,255,258,261] sEF and cEF resulted to be quite similar and the most important difference was attributed to the amount of polymer and drug used. The ratio between sEF and cEF values (% cEF litd) is a helpful indicator for relative solvent usage and thus waste reduction potential. The low % cEF litd value (lower than 1%) and the relative value of solvent and water percentages higher than 95% indicated that, solvents (organic solvent and water) are the most utilized material in the production of polymer particles via emulsification and solvent diffusion.

Similar analysis previously conducted in the pharmaceutical field confirms the higher contribution of solvents to the cumulative PMI. The relative value of solvent and water percentages associated with the production of active ingredients from a survey of several pharmaceutical companies was estimated to be 88% by the Pharmaceutical Roundtable [262]. In contrast, the results for the commercial route show a lower relative value of solvent and water percentage solvent of 78% [263]. Anyway, the environmental impact of the solvent depends on the environmental factor and the solvent type as previously discussed. Solvents used for the production of PLGA particles included in Table 4.2 are DCM [17,255,261] and chloroform [258]. Both, Chloroform and DCM have been classified as Class 2 with a permissible concentration of 60 ppm for Chloroform and (lower than that allowed for DCM) [154]. EA is classified as a Class 3 solvent and then it results a greener solvent respect to the solvents previously used in PLGA particles production. EQ-factor (environmental quotient factor) was proposed as a valuable extension of E-factor in order to consider the toxicity of materials and it is obtained by multiplying the E factor with an arbitrarily assigned unfriendliness quotient, Q. However, the magnitude of Q is currently debatable and difficult to quantify and this hampers the correct assessment of a green analysis. [264] Several general purpose solvents, [265] analyzing the most conventional solvents taking into account the European regulation concerning the 'Registration, Evaluation, Authorisation and Restriction of Chemicals' (REACH) and the recommendations of pharmaceutical industry solvent selection guides identified EA as recommended/preferred solvent while Chloroform and DCM as undesirable.

The economic analysis performed demonstrates that the cost of the microparticles was 97.09euro/g of particles produced. It is important to point out that in the calculation only the raw material costs are included, however, the calculation helps to identify the components influencing most significantly the cost of particle production. Main cost components result to be the polymer (51.15%) and the drug (35.45%) as reported also in previous works [16,17,78,255,258,261].

About the formulation properties, it is notable that EE and DL for DEX encapsulation previously reported in Table 4.2 were close to those obtained in the present work. This indicates that the encapsulation efficiency is not correlated with the emulsification method used. EE and DL are highly dependent on the polymer and drug initial amounts, surfactant type, concentration and solvent type[16,142]. A low initial amount of drug used in the present work (1 mg L^{-1}) is responsible for a lower EE obtained respect to other data reported in Table 4.2 (EE = 70%, initial drug concentration = 6.66 mg L^{-1} [17] and 44.93 mg L^{-1} [16]).
The simplicity and versatility of the membrane emulsification method combined with the use of green solvents hold much promise for the development of a sustainable chemical manufacturing industry. Considering that a broad spectrum of micro-nanostructured materials with predictable and controllable sizes, different chemical compositions, morphologies, and functionalities can be produced by using the proposed method, membrane-based technologies result the best green process choice.

4.4 Conclusion

In the pHD work, the sustainable production of PLGA-PEG particles as potential drug delivery vectors was assessed by using membrane emulsification/solvent diffusion method. The optimized operative conditions during the emulsification (DP flux = 12.84 $Lh^{-1}m^{-2}$, shear stress = 1.12 Pa) and the solidification steps (solvent= EA, V_d/Vt_h = 0) allowed to produce uniform particles (span = 0.62) with an average particle size of 1.25 μm and an EE of 61.2%. High throughput was achieved by increasing the dispersed phase flux to 12.84 $Lh^{-1}m^{-2}$ in mild operative conditions (shear stress = 1.12 Pa) reducing at the same time the energy consumption (3.96E+05 Jm-3). EA resulted to be a valuable alternative solvent for PLGA particle production as being a greener solvent considering both green metric factors and toxicity compared to the use of DCM. The use of EA makes the particles production process more sustainable reducing the volume of water consumed and the amount of emulsifier used. This allowed also decreasing the economic impact of these components.
The simplicity and versatility of the membrane emulsification method combined with the use of green solvents hold much promise for the development of a sustainable chemical manufacturing industry. Considering that a broad spectrum of micro-nanostructured materials with predictable and controllable sizes, different chemical compositions, morphologies, and functionalities can be produced by using the proposed method, membrane-based technologies result a best green process choice.

Chapter 5

Production of catechol loaded PVA particle by membrane emulsification combined with glutaraldehyde crosslinking reaction

Reduced version of chapter 5

Colloidal systems, such as liposomes, particles, and emulsions, have generally been reported in the literature as carriers of hydrophobic drugs. [97,166]. However, the delivery of hydrophilic molecules is also a challenging goal and their encapsulation has received increased interest over recent years. [266]. Many drugs are hydrophilic, and many of them are low-molecular-weight molecules (less than 500 Da). Hydrophilic drugs are often subject to low intracellular absorption, enzymatic degradation, rapid clearance, suboptimal distribution, development of resistance, poor pharmacokinetics, low therapeutic index and, in the case of antitumoral drugs, failure to accumulate and be retained within the tumor. [267] The inclusion of hydrophilic drug in water in oil (W/O) emulsion, also used as a template for the production of polymeric particles, is advantageous because it permits: (i) drug protection, (ii) drug solubilization in the core, (iii) sustained drug release (iv) to reduce polymer content [266]. The main disadvantage is the low stability of the W/O emulsion, that is solved with the combination of this process with a crosslinking or other secondary reaction to produce solidified particle.

Polyvinyl alcohol (PVA) is a biocompatible polymer, approved by the FDA for the use in several medical applications including transdermal patches[153]. Table 5.1 shows some drug delivery systems based on this polymer. The production of fibers and membranes based on PVA has been extensively reported [268–274], on the contrary, only few examples are available for the production of PVA particles [69,70,275]. Glutaraldehyde (GA)-cross-linked PVA particles demonstrated modulated drug-release properties as a function of cross-linking density [69]. PVA particles produced by combining PVA with other polymers such as chitosan or alginate demonstrated pH sensitive properties.

Table 5.1: Examples of drug delivery systems based on PVA polymer.

Polymer	Blending Copolypmer	Drug	Emulsification	Solidification	Physical Aparience	Application	Reference
Membranes and fibers							
PVA	Chitosan	Ampicillin sodium	Electrospinning	GA cosslinking	nanofiber	bactericide-transdermal	[269]
PVA	-	aspirin and BSA	Electrospinning		fibers	-	[274]
PVA	-	sodium salicylate	Electrospinning		nanofibers	pain disease	[272]
PVA	-	diclofenac sodium	Electrospinning		nanofibers	pain disease	[272]
PVA	-	indomethacin	Electrospinning		nanofibers	pain disease	[272]
PVA	-	naproxen	Electrospinning		nanofibers	pain disease	[272]
PVA	chitosan	ibuprofen	phase inversion method		membrane	pain disease	[270]
PVA	Polycaprolactone	Cefuroxime Sodium	freeze / thawing process		nano composite membrane	bactericide-transdermal	[273]
PVA	Chitosan	glutathione	Casting method		membrane	cancers and diabetes	[268]
PVA	-	oxprenolol	Casting method		membrane	Gastrointestinal diseases	[271]
Nanoparticles and microparticles							
PVA	silk fibroin	doxorubicin hydrochloride	Electrospraying		nanoparticles	anticancer	[276]
PVA	-	Diltiazem	W/O emulsion produced by stirring	GA crosslinking	microparticle	cardiovascular diseases	[275]
PVA	-	Aspirin	W/O emulsion produced by stirring	GA crosslinking	microparticle	pain disease	[69]
PVA	Chitosan	Cupper	W/O membrane emulsification	GA crosslinking	microparticle	pH modulated release	[70]
PVA	-	Biophenols	W/O membrane emulsification	-	microparticle	antioxidants	[27]

PVA particles could be obtained starting from a W/O emulsion where the dispersed phase is the polymeric solution. The W/O emulsion can be produced by using different emulsification devices as high-pressure systems, high speed system, ultrasonic system, microfluidic systems [115]. As it was stated in Chapter I, membrane emulsification is emerging as a promising tool for the production of emulsions and solidified particles with tailored properties in many fields. The process has many advantages for the design of pharmaceutical particles: i) the production of uniform, reproducible and size-controlled droplets; ii) process flexibility for the production of a variety of solid and advanced particles formulations for drug protection or controlled release at lab scale as well as at large scale; iii) high encapsulation and loading efficiencies of bioactive ingredient and iv) maintenance of the bioactivity of protein/peptide drugs due to mild fluid-dynamic conditions.[136]

In the present work, the production of Catechol encapsulated PVA particles by membrane emulsification/crosslinking has been investigated. Catechol due to its well-known hydrophilic characteristic has been selected as a model drug to be encapsulated. Catechol is phenol derivative mainly used as raw material for the synthesis of polymerization inhibitors, perfumes, drugs, pesticides, dyes, in fur dyeing and leather tanning, as well as in photographic developers, deoxygenating agents, and analytical reagents. [22]. Interestingly, Zheng et.al found a correlation between its neuroprotective and anti-inflammatory effects with a huge potential anti-inflammatory activity suggesting its potential use as bioactive ingredient for pharmaceutical formulations [23]. However, Catechol is susceptible to oxidative deterioration, when exposed to oxygen, light, moisture, and temperature affecting its quality and shelf life. For this purpose, this biocomponent needs to be encapsulated in order to be used as pharmaceutical product [24]. It has been successfully encapsulated into carbon nanotubes [25], hyaluronic acid hydrogels [26] and water-in-oil emulsion [27].

The aim of this chapter is to develop an effective drug delivery system based on PVA microparticles with potential application in pharmaceutical field. The production of the PVA microparticles is divided in two steps: membrane emulsification and glutaraldehyde crosslinking reaction. Membrane emulsification was performed using the optimized procedure for W/O emulsion production [27,277]. Glutaraldehyde crosslinking process was optimized to produce PVA microparticles with sustained release properties. Process development and drug release aspects essential for the potential clinic translation of PVA microparticles have been studied. In particular, encapsulation efficiency and drug loading efficiency of Catechol in PVA particles and its delivery profile as a function of GA:PVA ratio have been studied. Cytotoxicity assessment of the produced microparticles was also carried out to evaluate their biocompatibility and safety performance, showing their suitability for potential biological applications.

Membrane emulsification combined with glutaraldehyde crosslinking process was successfully applied to prepare uniform catechol-loaded PVA microparticles. The optimization of the cross-linking solidification process and chemical parameters was carried out and microparticles with an average diameter and a span of distribution equal to 2.48 µm and 0.50 for 15% PVA concentration; 1.75 µm and 0.4 for 7% PVA concentration were produced, respectively. The swelling was modulated using GA:PVA ratios between 0.05 to 2, being able to modulate also the catechol release. PVA microparticles did not modify significantly cell metabolism, cell membrane or cell cycle at the concentrations used and on the cell lines tested, showing their suitability for potential biological applications after stabilizing them as colloidal suspensions.

Chapter 6

Overall Conclusions

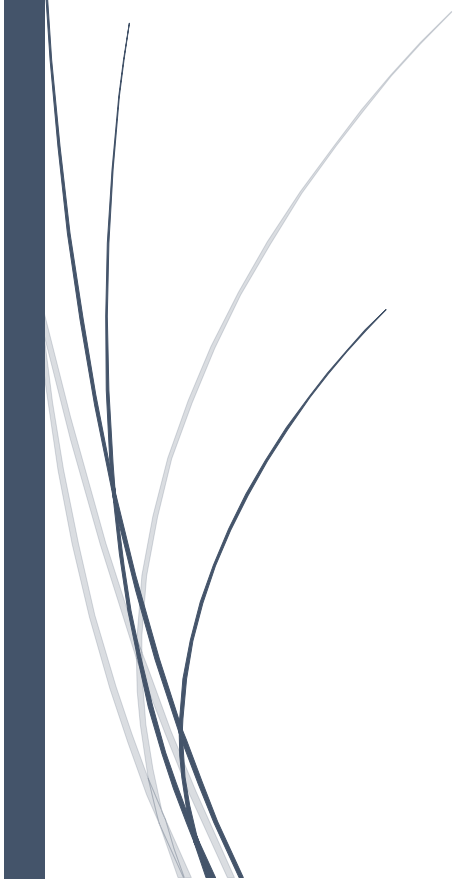

6.1 Overall Conclusion

A solid methodology for the production of a variety of particles (nano and microparticles) following different synthesis mechanisms (emulsification and nanoprecipitation) by two promising production approaches (membrane and microfluid device) was obtained.

The nanoprecipitation using a millimixer for production of nanoparticles was evaluated in **Chapter 2**. The nanoprecipitation process of PLGA-PEG was studied, evaluating the precipitation mechanism by ternary phase diagram (PLGA-PEG/acetone/water) and finding the area where the particles obtained by precipitation are in nanorange size scale, and have a narrow size distribution and spherical shape. PLGA-PEG nanoparticle size in the range from 77 to 160nm and with a PDI lower than 0.1 were continuously obtained. Encapsulation mechanism of dexamethasone is through solubilization in the polymer particles obtaining a maximum encapsulation efficiency of 45.04 ± 2.42% and drug loading efficiency of DLE: 4.74 ± 0.2% when DEX/PLGA ratio is 10% and $f_{PLGA\text{-}PEG}$ is $2.56*10^{-3}$ .The work provides the explanation for encapsulation of DEX where the dexamethasone does not coprecipitate together with the PLGA-PEG. Instead of this, dexamethasone encapsulation mechanism is through solubilization in the polymer particles. Also, PLGA-PEG precipitates faster than DEX, promoting the formation of separated crystals.

The production of PLGA-PEG nanoparticles by membrane-assisted nanoprecipitation has been investigated for the first time in **Chapter 3**. Tubular Shirasu porous glass (SPG) membranes with pore diameters of 1 µm and 0.2 µm were used to control the mixing process during the nanoprecipitation reaction. The size of the resulting PLGA-PEG nanoparticles was readily tuned in the range from 250 to 400 nm with high homogeneity (PDI lower than 0.2) by controlling the dispersed phase volume/continuous phase volume (DP/CP) ratio. Dexamethasone was successfully encapsulated in a continuous process, achieving an encapsulation efficiency (EE) and drug loading efficiency (DLE) of 50% and 5%, respectively. The dexamethasone was released from the nanoparticles following Fickian kinetics.

Chapter 4 presents the production of PLGA-PEG microparticle by membrane emulsification/solvent diffusion as example of sustainable production process. The impact of solvent used for polymer particle synthesis on size distribution, particles morphology and green performance scores was demonstrated. More uniform particles, with dense and slightly rough surface, high encapsulation efficiency and drug loading were obtained by replacing dichloromethane with ethyl acetate. The E factor was also decreased by 80%. Results demonstrated that membrane emulsification is an environmentally improved method for the production of drug delivery systems with enormous impact in the pharmaceutical industry not only in terms of formulation quality but also for energy consumption reduction and waste minimization

Membrane emulsification combined with glutaraldehyde crosslinking process was successfully applied to prepare uniform catechol encapsulated PVA microparticles in **Chapter 5**. Microparticles with an average diameter and a span of distribution equal to 2.48 µm and 0.50 for 15% PVA concentration; 1.75 µm and 0.4 for 7% PVA concentration were produced, respectively. Particles swelling was modulated using GA:PVA ratios between 0.05 to 2, being able to modulate also the catechol release. PVA microparticles did not significantly damage cell metabolism, cell membrane or cell cycle at the concentrations and with cell lines tested, showing their suitability for potential biological applications after stabilizing them as colloidal suspensions.

From this work, new opportunities in the pharmaceutical area can be opened through the design of polymeric particles as drug delivery systems by using membrane emulsification and millifluidic systems. The high-quality standards of the particulate products in terms of tuned size, uniform size distribution, particles morphology, drug encapsulation/loading as well as the low energy consumption and the continuous mode of operations make the developed methodologies extremely attractive for the pharmaceutical industry.

6.2 Conclusiones Generales

Se ha obtenido una metodología sólida para la producción de una variedad de partículas (nano y micropartículas) siguiendo diferentes procesos de síntesis (emulsificación y nanoprecipitación) mediante dos enfoques de producción prometedores (membrana y dispositivo de reactores millifluidicos).

El proceso nanoprecipitación utilizando un reactor de microfluidca para producción de nanopartículas se evaluó en el **Capítulo 2**. Se estudió el proceso de nanoprecipitación de PLGA-PEG, evaluando el mecanismo de precipitación por diagrama ternario de fases (PLGA-PEG / acetona / agua) y encontrando el área donde se obtuvieron las partículas por precipitación están en rango nanométrico, y tienen una distribución de tamaño estrecho y forma esférica. Se obtuvieron tamaños de nanopartículas de PLGA-PEG en el rango de 77 a 160 nm y con un PDI inferior a 0,1. El mecanismo de encapsulación de la dexametasona es a través de la solubilización dentro de las partículas poliméricas, obteniendo una eficiencia de encapsulación máxima de 45.04 ± 2.42% y capacidad de carga de DLE: 4.74 ± 0.2% cuando la relación DEX / PLGA es 10% y $f_{PLGA-PEG}$ es 2.56 * 10^{-3}. El trabajo proporciona la explicación de la encapsulación de dexamethasona donde el fármaco no coprecipita junto con el PLGA-PEG. En lugar de esto, el mecanismo de encapsulación de dexametasona es a través de la solubilización en las partículas de polímero. Además, PLGA-PEG precipita más rápido que DEX, promoviendo la formación de cristales separados.

La producción de nanopartículas de PLGA-PEG por nanoprecipitación asistida por membrana se ha investigado por primera vez en el Capítulo 3. Las membranas SPG (del ingles Tubular Shirasu porous glass) con diámetros de poro de 1 µm y 0.2 µm se usaron para controlar el proceso de mezcla durante la reacción de nanoprecipitación. Las nanopartículas de PLGA-PEG resultantes tienen un tamaño de particula en el intervalo de 250 a 400 nm con alta homogeneidad (PDI inferior a 0,2) y se obtuvo controlando la relación volumetrica de fase dispersada / fase continua. La dexametasona se encapsuló con éxito en un proceso continuo, logrando una eficacia de encapsulación (EE) y capacidad de carga (DLE) del 50% y 5%, respectivamente. La dexametasona se liberó de las nanopartículas siguiendo la cinética de Fickian.

El **Capítulo 4** presenta la producción de micropartículas de PLGA-PEG por emulsificacion por membrana / difusión de solvente como ejemplo de proceso de producción sostenible. Se demostró el impacto del disolvente utilizado para la síntesis de partículas poliméricas en la distribución del tamaño, la morfología de las partículas y del rendimiento en ecológico. Se obtuvieron partículas más uniformes, con una superficie densa y ligeramente rugosa, alta eficacia de encapsulación y carga de fármaco mediante la sustitución de diclorometano por acetato de etilo. El factor E también se redujo en un 80%. Los resultados demostraron que la emulsificación por membrana es un método ambientalmente mejorado para la

producción de sistemas de liberación controlada con un enorme impacto en la industria farmacéutica no solo en términos de calidad de formulación, sino también para la reducción del consumo de energía y la minimización de residuos

La emulsificación por membranas combinada con el proceso de entrecruzamiento utilizando glutaraldehído se aplicó con éxito para preparar micropartículas de PVA encapsulando catecol y se presenta en el Capítulo 5. Micropartículas con un diámetro promedio y homogeneidad igual a 2,48 µm y 0,50 para una concentración de PVA del 15%; Se produjeron 1,75 µm y 0,4 para una concentración de PVA del 7%, respectivamente. El hinchamiento de las partículas se moduló usando relaciones GA: PVA entre 0,05 y 2, pudiendo modular también la liberación de catecol. Las micropartículas de PVA no dañaron significativamente el metabolismo celular, la membrana celular o el ciclo celular en las concentraciones y con las líneas celulares probadas, lo que demuestra su idoneidad para aplicaciones farmacéuticas.

A partir de este trabajo, se pueden abrir nuevas oportunidades en el área farmacéutica a través del diseño de partículas poliméricas como sistemas de liberación controlada mediante el uso de emulsificación por membrana y sistemas milifluídicos. Los altos estándares de calidad de los productos particulados en términos de tamaño ajustado, distribución de tamaño uniforme, morfología de partículas, encapsulación / carga de fármacos, así como el bajo consumo de energía y el modo continuo de operaciones hacen que las metodologías desarrolladas sean extremadamente atractivas para la industria farmacéutica.

6.3 Conclusioni generali

Nel presente lavoro di tesi è stata sviluppata una solida metodologia per la produzione di una varietà di particelle polimeriche (nano e microparticelle) ottenute con diversi metodi di sintesi (emulsificazione e nanoprecipitazione) mediante due promettenti approcci di produzione (membrana e sistemi microfluidici).

La nanoprecipitazione mediante sistema microfluidico per la produzione di nanoparticelle è stata studiata nel Capitolo 2. In particolare, è stato studiato il processo di nanoprecipitazione del PLGA-PEG, valutando il meccanismo di precipitazione mediante il diagramma di fase ternario (PLGA-PEG / acetone / acqua) e individuando l'area in cui le particelle ottenute per precipitazione sono di dimensioni nanometriche ed hanno una distribuzione uniforme e forma sferica. Nanoparticelle di PLGA-PEG nel range da 77 a 160 nm e con un PDI inferiore a 0.1 sono state ottenute in un processo continuo. Si è ottenuta un'efficienza massima di incapsulamento del 45,04 ± 2,42% e di carico del 4,74 ± 0,2% quando il rapporto DEX / PLGA-PEG è del 10% e $f_{PLGA-PEG}$ è 2,56 * 10^{-3}. Il lavoro condotto ha permesso di dimostrare che l'incapsulamento di DEX non avviene per coprecipitate insieme al PLGA-PEG ma attraverso la solubilizzazione nelle particelle di polimero. Inoltre, il PLGA-PEG precipita più velocemente del DEX, promuovendo la formazione di cristalli separati.

La produzione di nanoparticelle di PLGA-PEG mediante nanoprecipitazione assistita da membrana è stata valuata per la prima volta nel Capitolo 3. Le membrane tubolari in vetro poroso ottenute da lava vulcanica (SPG) con diametro dei pori di 1 µm e 0.2 µm sono state utilizzate per controllare il processo di miscelazione durante la reazione di nanoprecipitazione. La dimensione delle nanoparticelle di PLGA-PEG variava nel range da 250 a 400 nm mantenendo elevato grado di omogeneità (PDI inferiore a 0.2) quando è stato variato il rapporto volume di fase dispersa / volume di fase continua (DP / CP). Il desametasone è stato incapsulato con successo in un processo continuo, ottenendo un'efficienza di incapsulamento (EE) e efficienza di carico del farmaco (DLE) rispettivamente del 50% e del 5%. Il desametasone è stato rilasciato dalle nanoparticelle seguendo la cinetica di Fick.

Il capitolo 4 presenta la produzione di microparticelle PLGA-PEG mediante emulsificazione a membrana / diffusione del solvente come esempio di processo produttivo sostenibile. È stato dimostrato l'impatto del solvente utilizzato per la sintesi di particelle polimeriche sulla distribuzione delle dimensioni, sulla morfologia delle particelle e sulla base dei "green performance scores". Particelle più uniformi, con superficie densa e leggermente ruvida, elevata efficienza di incapsulamento del farmaco sono state ottenute sostituendo diclorometano con etilacetato. Anche il fattore E è diminuito dell'80%. I risultati

hanno dimostrato che l'emulsificazione a membrana è un metodo altamente efficiente per la produzione di sistemi di somministrazione di farmaci basati su particelle permettendo di ottenere la riduzione del consumo energetico e della produzione di rifiuti e garantendo al contempo un'elevata qualità delle formulazioni prodotte.

L' emulsificazione a membrana combinata con il processo di reticolazione della glutaraldeide è stata applicata con successo nel Capitolo 5 per la preparazione di microparticelle uniformi di PVA contenenti catecolo. Microparticelle con un diametro medio e un'ampiezza della distribuzione pari a 2.48 µm e 0.50 sono state ottenute con una concentrazione di PVA pari al 15% e di 1.75 µm e 0.4 con una concentrazione di PVA del 7%. Lo "swelling" delle particelle è stato modulato utilizzando un rapporto GA: PVA tra 0.05 e 2 dimostrando una significativa influenza anche sul il rilascio del catecolo. In test di tossicità cellulare, le microparticelle di PVA non hanno dimostrato di danneggiare in modo significativo il metabolismo cellulare, la membrana cellulare o il ciclo cellulare alle concentrazioni e con le linee cellulari testate, mostrando la loro idoneità per potenziali applicazioni biologiche dopo averle stabilizzate come sospensioni colloidali.

Il presente lavoro di tesi offre nuove opportunità nel settore farmaceutico attraverso la progettazione di particelle polimeriche come sistemi di veicolazione di farmaci prodotti mediante emulsificazione di membrane e sistemi microfluidici. Gli elevati standard qualitativi dei prodotti in termini di dimensioni ottimizzate, distribuzione uniforme delle dimensioni, morfologia delle particelle, incapsulamento / carico del farmaco nonché il basso consumo energetico e la modalità operativa continua rendono le metodologie sviluppate estremamente interessanti per l'industria farmaceutica.

6.4 Conclusion générale

Une méthodologie solide pour la production d'une diversité de particules (nano et microparticules) en suivant différents mécanismes de synthèse (émulsification et nanoprécipitation) par deux approches de production prometteuses (outils de membrane et de microfluidique) a été obtenue.

La nanoprécipitation en utilisant un milli-mélangeur pour la production de nanoparticules a été évaluée dans le Chapitre 2. Le procédé de nano-précipitation du PLGA-PEG a été étudié, en évaluant le mécanisme de précipitation par un diagramme de phase ternaire (PLGA-PEG/acétone/eau) et en trouvant la zone dans laquelle les particules obtenues par précipitation sont dans la gamme nano, et ont une distribution en taille resserrée et une forme sphérique. Une taille de nanoparticule de PLGA-PEG dans la gamme 77-160 nm et avec un PDI inférieur à 0.1 ont été obtenus de manière continue. Le mécanisme d'encapsulation du dexamethasone obtient, à travers la solubilisation dans les particules de polymère, une efficacité maximale d'encapsulation de 45.04 ± 2.42% et une efficacité de charge en médicament de DLE: 4.74 ± 0.2% lorsque le ratio DEX/PLGA vaut 10% et fPLGA-PEG vaut 2.56*10-3. Le travail fournit une explication pour l'encapsulation de DEX lorsque le dexamethasone ne co-précipite pas avec le PLGA-PEG. Au lieu de cela, le mécanisme d'encapsulation du dexamethasone se fait par solubilisation dans les particules de polymères. En outre, le PLGA-PEG précipite plus rapidement que le DEX, ce qui favorise la formation de cristaux séparés.

La production de nanoparticules de PLGA-PEG par nanoprécipitation assistée par membrane a été investiguée pour la première fois dans le Chapitre 3. Des membranes tubulaires en verre poreux Shirasu (SPG) avec des diamètres de pore de 1 µm et 0.2 µm ont été utilisées pour contrôler le procédé de mélange durant la réaction de nanoprécipitation. La taille des nanoparticules de PLGA-PEG résultantes a été facilement réglée dans la gamme de 250 à 400 nm avec une grande homogénéité (PDI inférieur à 0.2) en contrôlant le ratio de volume de phase dispersée/phase continue (PD/PC). Le dexamethasone a été encapsulé avec succès dans un procédé continu, en atteignant une efficacité d'encapsulation (EE) et une efficacité de charge en médicament (DLE) de 50% et 5%, respectivement. Le dexamethasone a été libéré des nanoparticules suivant des cinétiques de Fickian.

Le Chapitre 4 présente la production de microparticules de PLGA-PEG par émulsification membranaire/diffusion de solvant en tant qu'exemple de procédé de production durable. L'impact du solvant utilisé pour la synthèse de particules de polymères sur la distribution de taille, la morphologie des particules et le degré de performance environnementale a été démontré. Des particules plus uniformes, avec une surface dense et légèrement rugueuse, une efficacité d'encapsulation et de charge en

médicament élevées, ont été obtenues en remplaçant le dichlorométhane par de l'acétate d'éthyle. Le facteur E a également été diminué de 80%. Les résultats ont montré que l'émulsification membranaire est une méthode améliorée d'un point de vue environnemental pour la production de systèmes d'administration de médicaments avec un énorme impact sur l'industrie pharmaceutique, non seulement en termes de qualité de formulation mais également pour la réduction de la consommation énergétique et la minimisation des déchets. L'émulsification membranaire combinée avec le procédé de réticulation de glutaraldéhyde a été appliquée avec succès pour préparer des microparticules uniformes de PVA encapsulées avec du catechol dans le Chapitre 5. Des microparticules avec un diamètre moyen et une largeur de distribution de 2.48 µm et 0.50 pour une concentration en PVA de 15% et 1.75 µm et 0.4 pour une concentration en PVA de 7%, respectivement, ont été produites. Le gonflement des particules a été modulé en utilisant des ratios GA :PVA entre 0.05 et 2, ce qui permet de moduler également la libération de catechol. Les microparticules de PVA n'ont pas significativement endommagé le métabolisme cellulaire, les membranes cellulaires ou les cycles cellulaires aux concentrations et avec les lignes cellulaires testées, ce qui montre leur pertinence pour des potentielles applications biologiques après qu'elles aient été stabilisées en suspensions colloïdales.

A partir de ce travail, de nouvelles opportunités dans le domaine pharmaceutique peuvent être ouvertes à travers la conception de particules de polymères comme systèmes d'administration de médicaments en utilisant l'émulsification membranaire et des systèmes milli-fluidiques. Les critères de qualité élevés pour les particules produites en termes de taille réglée, uniformité de la distribution en taille, morphologie des particules, encapsulation/charge du médicament de même que la faible consommation énergétique et le caractère continu des opérations rendent les méthodologies développées extrêmement attractives pour l'industrie pharmaceutique.

References

7.1 References

[1] R. Mulligan, The basic science of gene therapy, Science. 260 (1993) 926–932. doi:10.1126/science.8493530.

[2] C.W. Pouton, L.W. Seymour, Key issues in non-viral gene delivery, Adv. Drug Deliv. Rev. 34 (1998) 3–19. doi:10.1016/S0169-409X(98)00048-9.

[3] K.E. Uhrich, S.M. Cannizzaro, R.S. Langer, K.M. Shakesheff, Polymeric Systems for Controlled Drug Release, Chem. Rev. 99 (1999) 3181–3198. doi:10.1021/cr940351u.

[4] W.-C. Shen, Oral peptide and protein delivery: unfulfilled promises?, Drug Discov. Today. 8 (2003) 607–608.

[5] T.M. Allen, Drug Delivery Systems: Entering the Mainstream, Science. 303 (2004) 1818–1822. doi:10.1126/science.1095833.

[6] M. Moritz, M. Geszke-Moritz, Recent Developments in Application of Polymeric Nanoparticles as Drug Carriers, Adv. Clin. Exp. Med. 24 (2015) 749–758. doi:10.17219/acem/31802.

[7] S. Fredenberg, M. Wahlgren, M. Reslow, A. Axelsson, The mechanisms of drug release in poly(lactic-co-glycolic acid)-based drug delivery systems—A review, Int. J. Pharm. 415 (2011) 34–52. doi:10.1016/j.ijpharm.2011.05.049.

[8] R.P. Batycky, J. Hanes, R. Langer, D.A. Edwards, A Theoretical Model of Erosion and Macromolecular Drug Release from Biodegrading Microspheres, J. Pharm. Sci. 86 (1997) 1464–1477. doi:10.1021/js9604117.

[9] L. Wang, Y. Liu, W. Zhang, X. Chen, T. Yang, G. Ma, Microspheres and microcapsules for protein delivery: strategies of drug activity retention, Curr. Pharm. Des. 19 (2013) 6340–6352.

[10] D.Y. Arifin, L.Y. Lee, C.-H. Wang, Mathematical modeling and simulation of drug release from microspheres: Implications to drug delivery systems, Adv. Drug Deliv. Rev. 58 (2006) 1274–1325. doi:10.1016/j.addr.2006.09.007.

[11] J. Siepmann, K. Elkharraz, F. Siepmann, D. Klose, How Autocatalysis Accelerates Drug Release from PLGA-Based Microparticles: A Quantitative Treatment, Biomacromolecules. 6 (2005) 2312–2319. doi:10.1021/bm050228k.

[12] T. Rhen, J.A. Cidlowski, Antiinflammatory Action of Glucocorticoids — New Mechanisms for Old Drugs, N. Engl. J. Med. 353 (2005) 1711–1723. doi:10.1056/NEJMra050541.

[13] E.M. Cohen, Dexamethasone, in: Anal. Profiles Drug Subst., Elsevier, 1973: pp. 163–197. http://linkinghub.elsevier.com/retrieve/pii/S0099542808600398 (accessed November 30, 2016).

[14] J. Urbańska, A. Karewicz, M. Nowakowska, Polymeric delivery systems for dexamethasone, Life Sci. 96 (2014) 1–6. doi:10.1016/j.lfs.2013.12.020.

[15] G. Soleimani, A. Daryadel, A. Ansari Moghadam, M.R. Sharif, The Comparison of Oral and IM Dexamethasone Efficacy in Croup Treatment, J. Compr. Pediatr. 4 (2013) 175–8. doi:10.17795/compreped-4528.

[16] B. Gu, D.J. Burgess, Prediction of dexamethasone release from PLGA microspheres prepared with polymer blends using a design of experiment approach, Int. J. Pharm. 495 (2015) 393–403. doi:10.1016/j.ijpharm.2015.08.089.

[17] D.-H. Kim, D.C. Martin, Sustained release of dexamethasone from hydrophilic matrices using PLGA nanoparticles for neural drug delivery, Biomaterials. 27 (2006) 3031–3037. doi:10.1016/j.biomaterials.2005.12.021.

[18] I.M.F. Campos, T.M. Santos, G.M.F. Cunha, K.M.M.N. Silva, R.Z. Domingues, A. da Silva Cunha Júnior, K.C. de Souza Figueiredo, Preparation and release characteristics of dexamethasone acetate loaded organochlorine-free poly(lactide- *co* -glycolide) nanoparticles, J. Appl. Polym. Sci. 131 (2014) 1–6. doi:10.1002/app.41199.

[19] S. Fialho, Dexamethasone-loaded poly(ε-caprolactone) intravitreal implants: A pilot study, Eur. J. Pharm. Biopharm. 68 (2008) 637–646. doi:10.1016/j.ejpb.2007.08.004.
[20] L.B. Rodrigues, H.F. Leite, M.I. Yoshida, J.B. Saliba, A.S.C. Junior, A.A.G. Faraco, In vitro release and characterization of chitosan films as dexamethasone carrier, Int. J. Pharm. 368 (2009) 1–6. doi:10.1016/j.ijpharm.2008.09.047.
[21] CTI Reviews, Organic Chemistry: Chemistry, Organic chemistry, Edition 3, Cram101 Textbook Reviews, 2016.
[22] H. Fiege, H.-W. Voges, T. Hamamoto, S. Umemura, T. Iwata, H. Miki, Y. Fujita, H.-J. Buysch, D. Garbe, W. Paulus, Phenol Derivatives, in: Wiley-VCH Verlag GmbH & Co. KGaA (Ed.), Ullmanns Encycl. Ind. Chem., Wiley-VCH Verlag GmbH & Co. KGaA, Weinheim, Germany, 2000. doi:10.1002/14356007.a19_313.
[23] L.T. Zheng, G.-M. Ryu, B.-M. Kwon, W.-H. Lee, K. Suk, Anti-inflammatory effects of catechols in lipopolysaccharide-stimulated microglia cells: Inhibition of microglial neurotoxicity, Eur. J. Pharmacol. 588 (2008) 106–113. doi:10.1016/j.ejphar.2008.04.035.
[24] Z. Fang, B. Bhandari, Encapsulation of polyphenols – a review, Trends Food Sci. Technol. 21 (2010) 510–523. doi:10.1016/j.tifs.2010.08.003.
[25] A. Senthil Kumar, P. Swetha, Electrochemical-Assisted Encapsulation of Catechol on a Multiwalled Carbon Nanotube Modified Electrode, Langmuir. 26 (2010) 6874–6877. doi:10.1021/la100462r.
[26] J. Shin, J.S. Lee, C. Lee, H.-J. Park, K. Yang, Y. Jin, J.H. Ryu, K.S. Hong, S.-H. Moon, H.-M. Chung, H.S. Yang, S.H. Um, J.-W. Oh, D.-I. Kim, H. Lee, S.-W. Cho, Tissue Adhesive Catechol-Modified Hyaluronic Acid Hydrogel for Effective, Minimally Invasive Cell Therapy, Adv. Funct. Mater. 25 (2015) 3814–3824. doi:10.1002/adfm.201500006.
[27] E. Piacentini, T. Poerio, F. Bazzarelli, L. Giorno, Microencapsulation by Membrane Emulsification of Biophenols Recovered from Olive Mill Wastewaters, Membranes. 6 (2016) 25. doi:10.3390/membranes6020025.
[28] A. Vyas, S. Saraf, S. Saraf, Cyclodextrin based novel drug delivery systems, J. Incl. Phenom. Macrocycl. Chem. 62 (2008) 23–42. doi:10.1007/s10847-008-9456-y.
[29] B. Sarmento, A. Ribeiro, F. Veiga, P. Sampaio, R. Neufeld, D. Ferreira, Alginate/Chitosan Nanoparticles are Effective for Oral Insulin Delivery, Pharm. Res. 24 (2007) 2198–2206. doi:10.1007/s11095-007-9367-4.
[30] Y. Wu, W. Yang, C. Wang, J. Hu, S. Fu, Chitosan nanoparticles as a novel delivery system for ammonium glycyrrhizinate, Int. J. Pharm. 295 (2005) 235–245. doi:10.1016/j.ijpharm.2005.01.042.
[31] A.M. De Campos, A. Sánchez, M.J. Alonso, Chitosan nanoparticles: a new vehicle for the improvement of the delivery of drugs to the ocular surface. Application to cyclosporin A, Int. J. Pharm. 224 (2001) 159–168.
[32] P. Aramwit, N. Jaichawa, J. Ratanavaraporn, T. Srichana, A comparative study of type A and type B gelatin nanoparticles as the controlled release carriers for different model compounds, Mater. Express. 5 (2015) 241–248. doi:10.1166/mex.2015.1233.
[33] J.K. Li†, N. Wang†, X.S. Wu, Gelatin nanoencapsulation of protein/peptide drugs using an emulsifier-free emulsion method, J. Microencapsul. 15 (1998) 163–172. doi:10.3109/02652049809006846.
[34] Z. Lu, Paclitaxel-Loaded Gelatin Nanoparticles for Intravesical Bladder Cancer Therapy, Clin. Cancer Res. 10 (2004) 7677–7684. doi:10.1158/1078-0432.CCR-04-1443.
[35] A. Kaur, S. Jain, A. Tiwary, Mannan-coated gelatin nanoparticles for sustained and targeted delivery of didanosine: In vitro and in vivo evaluation, Acta Pharm. 58 (2008). doi:10.2478/v10007-007-0045-1.

[36] A.K. Bajpai, J. Choubey, Design of gelatin nanoparticles as swelling controlled delivery system for chloroquine phosphate, J. Mater. Sci. Mater. Med. 17 (2006) 345–358. doi:10.1007/s10856-006-8235-9.
[37] G.W. Hastings, Structural considerations and new polymers for biomedical applications, Polymer. 26 (1985) 1331–1335. doi:10.1016/0032-3861(85)90308-8.
[38] J.C. Middleton, A.J. Tipton, Synthetic biodegradable polymers as orthopedic devices, Biomaterials. 21 (2000) 2335–2346. doi:10.1016/S0142-9612(00)00101-0.
[39] I. Vroman, L. Tighzert, Biodegradable Polymers, Materials. 2 (2009) 307–344. doi:10.3390/ma2020307.
[40] H.K. Makadia, S.J. Siegel, Poly Lactic-co-Glycolic Acid (PLGA) as Biodegradable Controlled Drug Delivery Carrier, Polymers. 3 (2011) 1377–1397. doi:10.3390/polym3031377.
[41] R. Gref, Y. Minamitake, M. Peracchia, V. Trubetskoy, V. Torchilin, R. Langer, Biodegradable long-circulating polymeric nanospheres, Science. 263 (1994) 1600–1603. doi:10.1126/science.8128245.
[42] S. Hosseininasab, R. Pashaei-Asl, A.A. Khandaghi, H.T. Nasrabadi, K. Nejati-Koshki, A. Akbarzadeh, S.W. Joo, Y. Hanifehpour, S. Davaran, Synthesis, Characterization, and *In vitro* Studies of PLGA-PEG Nanoparticles for Oral Insulin Delivery, Chem. Biol. Drug Des. 84 (2014) 307–315. doi:10.1111/cbdd.12318.
[43] S. Gogolewski, A.J. Pennings, Biodegradable materials of polylactides, 4. Porous biomedical materials based on mixtures of polylactides and polyurethanes, Makromol. Chem. Rapid Commun. 3 (1982) 839–845. doi:10.1002/marc.1982.030031201.
[44] W. Chen, F. Meng, R. Cheng, C. Deng, J. Feijen, Z. Zhong, Advanced drug and gene delivery systems based on functional biodegradable polycarbonates and copolymers, J. Controlled Release. 190 (2014) 398–414. doi:10.1016/j.jconrel.2014.05.023.
[45] P. Ojer, L. Neutsch, F. Gabor, J.M. Irache, A. López de Cerain, Cytotoxicity and cell interaction studies of bioadhesive poly(anhydride) nanoparticles for oral antigen/drug delivery, J. Biomed. Nanotechnol. 9 (2013) 1891–1903.
[46] J. Pajak, M. Ziemski, B. Nowak, Poly(vinyl alcohol) – biodegradable vinyl material, Chem. 2010. 64 (2010) 523–530.
[47] R. Chandra, Biodegradable polymers, Prog. Polym. Sci. 23 (1998) 1273–1335. doi:10.1016/S0079-6700(97)00039-7.
[48] C. Pinto Reis, R.J. Neufeld, A.J. Ribeiro,, F. Veiga, Nanoencapsulation I. Methods for preparation of drug-loaded polymeric nanoparticles, Nanomedicine Nanotechnol. Biol. Med. 2 (2006) 8–21. doi:10.1016/j.nano.2005.12.003.
[49] A. Kumari, S.K. Yadav, S.C. Yadav, Biodegradable polymeric nanoparticles based drug delivery systems, Colloids Surf. B Biointerfaces. 75 (2010) 1–18. doi:10.1016/j.colsurfb.2009.09.001.
[50] O. Wichterle, D. LíM, Hydrophilic Gels for Biological Use, Nature. 185 (1960) 117–118. doi:10.1038/185117a0.
[51] S.K. H. Gulrez, S. Al-Assaf, G. O, Hydrogels: Methods of Preparation, Characterisation and Applications, in: A. Carpi (Ed.), Prog. Mol. Environ. Bioeng. - Anal. Model. Technol. Appl., InTech, 2011. http://www.intechopen.com/books/progress-in-molecular-and-environmental-bioengineering-from-analysis-and-modeling-to-technology-applications/hydrogels-methods-of-preparation-characterisation-and-applications (accessed April 17, 2016).
[52] A. Kumar, S.S. Han, PVA-based hydrogels for tissue engineering: A review, Int. J. Polym. Mater. Polym. Biomater. 66 (2017) 159–182. doi:10.1080/00914037.2016.1190930.
[53] C. Gong, T. Qi, X. Wei, Y. Qu, Q. Wu, F. Luo, Z. Qian, Thermosensitive Polymeric Hydrogels As Drug Delivery Systems, Curr. Med. Chem. 20 (2012) 79–94. doi:10.2174/092986731130201000 9.

[54] D. Schmaljohann, Thermo- and pH-responsive polymers in drug delivery☆, Adv. Drug Deliv. Rev. 58 (2006) 1655–1670. doi:10.1016/j.addr.2006.09.020.
[55] J.P. Gong, T. Nitta, Y. Osada, Electrokinetic Modeling of the Contractile Phenomena of Polyelectrolyte Gels. One-Dimensional Capillary Model, J. Phys. Chem. 98 (1994) 9583–9587. doi:10.1021/j100089a036.
[56] A. Mamada, T. Tanaka, D. Kungwatchakun, M. Irie, Photoinduced phase transition of gels, Macromolecules. 23 (1990) 1517–1519. doi:10.1021/ma00207a046.
[57] J.J. Kim, K. Park, Modulated insulin delivery from glucose-sensitive hydrogel dosage forms, J. Control. Release Off. J. Control. Release Soc. 77 (2001) 39–47.
[58] X. Zhong, Y.-X. Wang, S.-C. Wang, Pressure dependence of the volume phase-transition of temperature-sensitive gels, Chem. Eng. Sci. 51 (1996) 3235–3239. doi:10.1016/0009-2509(95)00344-4.
[59] T. Miyata, N. Asami, T. Uragami, Preparation of an Antigen-Sensitive Hydrogel Using Antigen−Antibody Bindings, Macromolecules. 32 (1999) 2082–2084. doi:10.1021/ma981659g.
[60] H.M. Creque, R. Langer, J. Folkman, One month of sustained release of insulin from a polymer implant, Diabetes. 29 (1980) 37–40.
[61] Z. Gu, A.A. Aimetti, Q. Wang, T.T. Dang, Y. Zhang, O. Veiseh, H. Cheng, R.S. Langer, D.G. Anderson, Injectable Nano-Network for Glucose-Mediated Insulin Delivery, ACS Nano. 7 (2013) 4194–4201. doi:10.1021/nn400630x.
[62] B.P. Timko, M. Arruebo, S.A. Shankarappa, J.B. McAlvin, O.S. Okonkwo, B. Mizrahi, C.F. Stefanescu, L. Gomez, J. Zhu, A. Zhu, J. Santamaria, R. Langer, D.S. Kohane, Near-infrared-actuated devices for remotely controlled drug delivery, Proc. Natl. Acad. Sci. 111 (2014) 1349–1354. doi:10.1073/pnas.1322651111.
[63] R. Skouri, F. Schosseler, J.P. Munch, S.J. Candau, Swelling and Elastic Properties of Polyelectrolyte Gels, Macromolecules. 28 (1995) 197–210. doi:10.1021/ma00105a026.
[64] R.J. Phillips, W.M. Deen, J.F. Brady, Hindered transport of spherical macromolecules in fibrous membranes and gels, AIChE J. 35 (1989) 1761–1769. doi:10.1002/aic.690351102.
[65] W. Shen, K. Zhang, J.A. Kornfield, D.A. Tirrell, Tuning the erosion rate of artificial protein hydrogels through control of network topology, Nat. Mater. 5 (2006) 153–158. doi:10.1038/nmat1573.
[66] M. Yamamoto, Y. Takahashi, Y. Tabata, Controlled release by biodegradable hydrogels enhances the ectopic bone formation of bone morphogenetic protein, Biomaterials. 24 (2003) 4375–4383.
[67] S.-A. Oh, H.-Y. Lee, J.H. Lee, T.-H. Kim, J.-H. Jang, H.-W. Kim, I. Wall, Collagen Three-Dimensional Hydrogel Matrix Carrying Basic Fibroblast Growth Factor for the Cultivation of Mesenchymal Stem Cells and Osteogenic Differentiation, Tissue Eng. Part A. 18 (2012) 1087–1100. doi:10.1089/ten.tea.2011.0360.
[68] Q. Wang, J. Zhang, A. Wang, Preparation and characterization of a novel pH-sensitive chitosan-g-poly (acrylic acid)/attapulgite/sodium alginate composite hydrogel bead for controlled release of diclofenac sodium, Carbohydr. Polym. 78 (2009) 731–737. doi:10.1016/j.carbpol.2009.06.010.
[69] B.C. Thanoo, M.C. Sunny, A. Jayakrishnan, Controlled release of oral drugs from cross-linked polyvinyl alcohol microspheres, J. Pharm. Pharmacol. 45 (1993) 16–20.
[70] S. Morelli, R.G. Holdich, M.M. Dragosavac, Chitosan and Poly (Vinyl Alcohol) microparticles produced by membrane emulsification for encapsulation and pH controlled release, Chem. Eng. J. 288 (2016) 451–460. doi:10.1016/j.cej.2015.12.024.
[71] S. Hua, H. Ma, X. Li, H. Yang, A. Wang, pH-sensitive sodium alginate/poly(vinyl alcohol) hydrogel beads prepared by combined Ca2+ crosslinking and freeze-thawing cycles for controlled release of diclofenac sodium, Int. J. Biol. Macromol. 46 (2010) 517–523. doi:10.1016/j.ijbiomac.2010.03.004.

[72] S.Ø. Andreasen, S.-F. Chong, B.M. Wohl, K.N. Goldie, A.N. Zelikin, Poly(vinyl alcohol) Physical Hydrogel Nanoparticles, Not Polymer Solutions, Exert Inhibition of Nitric Oxide Synthesis in Cultured Macrophages, Biomacromolecules. 14 (2013) 1687–1695. doi:10.1021/bm400369u.
[73] A.N. Ford Versypt, D.W. Pack, R.D. Braatz, Mathematical modeling of drug delivery from autocatalytically degradable PLGA microspheres — A review, J. Controlled Release. 165 (2013) 29–37. doi:10.1016/j.jconrel.2012.10.015.
[74] J. Bile, M.-A. Bolzinger, C. Vigne, O. Boyron, J.-P. Valour, H. Fessi, Y. Chevalier, The parameters influencing the morphology of poly(ε-caprolactone) microspheres and the resulting release of encapsulated drugs, Int. J. Pharm. 494 (2015) 152–166. doi:10.1016/j.ijpharm.2015.07.068.
[75] P. Karuppuswamy, J. Reddy Venugopal, B. Navaneethan, A. Luwang Laiva, S. Ramakrishna, Polycaprolactone nanofibers for the controlled release of tetracycline hydrochloride, Mater. Lett. 141 (2015) 180–186. doi:10.1016/j.matlet.2014.11.044.
[76] R. Sun, X.-J. Du, C.-Y. Sun, S. Shen, Y. Liu, X.-Z. Yang, Y. Bao, Y.-H. Zhu, J. Wang, A block copolymer of zwitterionic polyphosphoester and polylactic acid for drug delivery, Biomater. Sci. 3 (2015) 1105–1113. doi:10.1039/C4BM00430B.
[77] M. Frounchi, S. Shamshiri, Magnetic nanoparticles-loaded PLA/PEG microspheres as drug carriers: MAGNETIC NANOPARTICLES-LOADED PLA/PEG MICROSPHERES AS DRUG CARRIERS, J. Biomed. Mater. Res. A. 103 (2015) 1893–1898. doi:10.1002/jbm.a.35317.
[78] A.C. Goodfriend, T.R. Welch, K.T. Nguyen, R.F. Johnson, V. Sebastian, S.V. Reddy, J. Forbess, A. Nugent, Thermally processed polymeric microparticles for year-long delivery of dexamethasone, Mater. Sci. Eng. C. 58 (2016) 595–600. doi:10.1016/j.msec.2015.09.003.
[79] S. Feng, L. Nie, P. Zou, J. Suo, Effects of drug and polymer molecular weight on drug release from PLGA-mPEG microspheres, J. Appl. Polym. Sci. 132 (2015) n/a-n/a. doi:10.1002/app.41431.
[80] Q. Xu, L.M. Ensign, N.J. Boylan, A. Schön, X. Gong, J.-C. Yang, N.W. Lamb, S. Cai, T. Yu, E. Freire, J. Hanes, Impact of Surface Polyethylene Glycol (PEG) Density on Biodegradable Nanoparticle Transport in Mucus *ex Vivo* and Distribution *in Vivo*, ACS Nano. 9 (2015) 9217–9227. doi:10.1021/acsnano.5b03876.
[81] M. Guada, V. Sebastián, S. Irusta, E. Feijoó, M. del Carmen Dios-Viéitez, M.J. Blanco-Prieto, Lipid nanoparticles for cyclosporine A administration: development, characterization, and in vitro evaluation of their immunosuppression activity, Int. J. Nanomedicine. 10 (2015) 6541.
[82] B. Lasa-Saracíbar, M. Guada, V. Sebastián, M.J. Blanco-Prieto, In vitro intestinal co-culture cell model to evaluate intestinal absorption of edelfosine lipid nanoparticles, Curr. Top. Med. Chem. 14 (2014) 1124–1132.
[83] V.P. Torchilin, Recent advances with liposomes as pharmaceutical carriers, Nat. Rev. Drug Discov. 4 (2005) 145–160. doi:10.1038/nrd1632.
[84] S.K. Sriraman, V.P. Torchilin, Recent Advances with Liposomes as Drug Carriers, in: A. Tiwari, A.N. Nordin (Eds.), Adv. Biomater. Biodevices, John Wiley & Sons, Inc., Hoboken, NJ, USA, 2014: pp. 79–119. doi:10.1002/9781118774052.ch3.
[85] F. Meunier, H.G. Prentice, O. Ringdén, Liposomal amphotericin B (AmBisome): safety data from a phase II/III clinical trial, J. Antimicrob. Chemother. 28 Suppl B (1991) 83–91.
[86] P.S. Gill, J. Wernz, D.T. Scadden, P. Cohen, G.M. Mukwaya, J.H. von Roenn, M. Jacobs, S. Kempin, I. Silverberg, G. Gonzales, M.U. Rarick, A.M. Myers, F. Shepherd, C. Sawka, M.C. Pike, M.E. Ross, Randomized phase III trial of liposomal daunorubicin versus doxorubicin, bleomycin, and vincristine in AIDS-related Kaposi's sarcoma., J. Clin. Oncol. 14 (1996) 2353–2364. doi:10.1200/JCO.1996.14.8.2353.
[87] N.M. Bressler, S.B. Bressler, Photodynamic therapy with verteporfin (Visudyne): impact on ophthalmology and visual sciences, Invest. Ophthalmol. Vis. Sci. 41 (2000) 624–628.

[88] S. Phuphanich, B. Maria, R. Braeckman, M. Chamberlain, A pharmacokinetic study of intra-CSF administered encapsulated cytarabine (DepoCyt®) for the treatment of neoplastic meningitis in patients with leukemia, lymphoma, or solid tumors as part of a phase III study, J. Neurooncol. 81 (2006) 201–208. doi:10.1007/s11060-006-9218-x.

[89] B. Carvalho, L.M. Roland, L.F. Chu, V.A. Campitelli, E.T. Riley, Single-dose, extended-release epidural morphine (DepoDur) compared to conventional epidural morphine for post-cesarean pain, Anesth. Analg. 105 (2007) 176–183. doi:10.1213/01.ane.0000265533.13477.26.

[90] A.H. Sarris, F. Hagemeister, J. Romaguera, M.A. Rodriguez, P. McLaughlin, A.M. Tsimberidou, L.J. Medeiros, B. Samuels, O. Pate, M. Oholendt, H. Kantarjian, C. Burge, F. Cabanillas, Liposomal vincristine in relapsed non-Hodgkin's lymphomas: early results of an ongoing phase II trial, Ann. Oncol. Off. J. Eur. Soc. Med. Oncol. 11 (2000) 69–72.

[91] FDA, Press Announcements - FDA approves new treatment for advanced pancreatic cancer., (2015). https://www.fda.gov/NewsEvents/Newsroom/PressAnnouncements/ucm468654.htm.

[92] A. Kumano, T. Kajiyama, M. Takayanagi, T. Kunitake, Y. Okahata, Phase Transition Behavior and Permeation Properties of Cationic and Anionic Artificial Lipids with Two Alkyl Chains, Berichte Bunsenges. Für Phys. Chem. 88 (1984) 1216–1222. doi:10.1002/bbpc.198400051.

[93] H.-Y. Chang, Y.-J. Sheng, H.-K. Tsao, Structural and mechanical characteristics of polymersomes, Soft Matter. 10 (2014) 6373. doi:10.1039/C4SM01092B.

[94] Y. Zhang, K. Zhang, Z. Wu, T. Guo, B. Ye, M. Lu, J. Zhao, C. Zhu, N. Feng, Evaluation of transdermal salidroside delivery using niosomes via in vitro cellular uptake, Int. J. Pharm. 478 (2015) 138–146. doi:10.1016/j.ijpharm.2014.11.018.

[95] S. Moghassemi, A. Hadjizadeh, Nano-niosomes as nanoscale drug delivery systems: An illustrated review, J. Controlled Release. 185 (2014) 22–36. doi:10.1016/j.jconrel.2014.04.015.

[96] L. Guan, L. Rizzello, G. Battaglia, Polymersomes and their applications in cancer delivery and therapy, Nanomed. 10 (2015) 2757–2780. doi:10.2217/nnm.15.110.

[97] C. Vauthier, K. Bouchemal, Methods for the Preparation and Manufacture of Polymeric Nanoparticles, Pharm. Res. 26 (2009) 1025–1058. doi:10.1007/s11095-008-9800-3.

[98] K.A. Howard, J. Kjems, Polycation-based nanoparticle delivery for improved RNA interference therapeutics, Expert Opin. Biol. Ther. 7 (2007) 1811–1822. doi:10.1517/14712598.7.12.1811.

[99] S. Daoud-Mahammed, C. Ringard-Lefebvre, N. Razzouq, V. Rosilio, B. Gillet, P. Couvreur, C. Amiel, R. Gref, Spontaneous association of hydrophobized dextran and poly-β-cyclodextrin into nanoassemblies., J. Colloid Interface Sci. 307 (2007) 83–93. doi:10.1016/j.jcis.2006.10.072.

[100] R. Gref, C. Amiel, K. Molinard, S. Daoud-Mahammed, B. Sébille, B. Gillet, J.-C. Beloeil, C. Ringard, V. Rosilio, J. Poupaert, P. Couvreur, New self-assembled nanogels based on host–guest interactions: Characterization and drug loading, J. Controlled Release. 111 (2006) 316–324. doi:10.1016/j.jconrel.2005.12.025.

[101] S. Schubert, J.T. Delaney, Jr, U.S. Schubert, Nanoprecipitation and nanoformulation of polymers: from history to powerful possibilities beyond poly(lactic acid), Soft Matter. 7 (2011) 1581–1588. doi:10.1039/C0SM00862A.

[102] S.A. Galindo-Rodríguez, F. Puel, S. Briançon, E. Allémann, E. Doelker, H. Fessi, Comparative scale-up of three methods for producing ibuprofen-loaded nanoparticles, Eur. J. Pharm. Sci. 25 (2005) 357–367. doi:10.1016/j.ejps.2005.03.013.

[103] R. Karnik, F. Gu, P. Basto, C. Cannizzaro, L. Dean, W. Kyei-Manu, R. Langer, O.C. Farokhzad, Microfluidic Platform for Controlled Synthesis of Polymeric Nanoparticles, Nano Lett. 8 (2008) 2906–2912. doi:10.1021/nl801736q.

[104] J.B. Knight, A. Vishwanath, J.P. Brody, R.H. Austin, Hydrodynamic Focusing on a Silicon Chip: Mixing Nanoliters in Microseconds, Phys. Rev. Lett. 80 (1998) 3863–3866. doi:10.1103/PhysRevLett.80.3863.

[105] V. Hessel, ed., Chemical micro process engineering: processing and plants, Wiley-VCH, Weinheim, 2005.
[106] S. Ding, N. Anton, T.F. Vandamme, C.A. Serra, Microfluidic nanoprecipitation systems for preparing pure drug or polymeric drug loaded nanoparticles: an overview, Expert Opin. Drug Deliv. 13 (2016) 1447–1460. doi:10.1080/17425247.2016.1193151.
[107] S. Schwolow, J. Hollmann, B. Schenkel, T. Röder, Application-Oriented Analysis of Mixing Performance in Microreactors, Org. Process Res. Dev. 16 (2012) 1513–1522. doi:10.1021/op300107z.
[108] S. Dev, K.S. Iyer, C.L. Raston, Nanosized drug formulations under microfluidic continuous flow, Lab. Chip. 11 (2011) 3214. doi:10.1039/c1lc20666d.
[109] N. Anton, F. Bally, C.A. Serra, A. Ali, Y. Arntz, Y. Mely, M. Zhao, E. Marchioni, A. Jakhmola, T.F. Vandamme, A new microfluidic setup for precise control of the polymer nanoprecipitation process and lipophilic drug encapsulation, Soft Matter. 8 (2012) 10628. doi:10.1039/c2sm25357g.
[110] V. Hessel, H. Löwe, F. Schönfeld, Micromixers—a review on passive and active mixing principles, Chem. Eng. Sci. 60 (2005) 2479–2501. doi:10.1016/j.ces.2004.11.033.
[111] I. Ortiz de Solorzano, L. Uson, A. Larrea, M. Miana, V. Sebastian, M. Arruebo, Continuous synthesis of drug-loaded nanoparticles using microchannel emulsification and numerical modeling: Effect of passive mixing, Int. J. Nanomedicine. 11 (2016) 3397–3416. doi:10.2147/IJN.S108812.
[112] C. Charcosset, H. Fessi, Preparation of nanoparticles with a membrane contactor, J. Membr. Sci. 266 (2005) 115–120. doi:10.1016/j.memsci.2005.05.016.
[113] A. Basile, C. Charcosset, eds., Integrated membrane systems and processes, John Wiley & Sons Inc, Chichester, West Sussex, United Kingdom, 2016.
[114] Z. Jia, Y. Zhao, L. Liu, F. He, Z. Liu, A membrane reactor intensifying micromixing: Effects of parameters on segregation index, J. Membr. Sci. 276 (2006) 295–300. doi:10.1016/j.memsci.2005.10.003.
[115] D.J. McClements, Food emulsions: principles, practices, and techniques, 2nd ed, CRC Press, Boca Raton, 2005.
[116] Z. Li, T. Ming, J. Wang, T. Ngai, High Internal Phase Emulsions Stabilized Solely by Microgel Particles, Angew. Chem. Int. Ed. 48 (2009) 8490–8493. doi:10.1002/anie.200902103.
[117] S. Giovagnoli, P. Blasi, A. Schoubben, C. Rossi, M. Ricci, Preparation of large porous biodegradable microspheres by using a simple double-emulsion method for capreomycin sulfate pulmonary delivery, Int. J. Pharm. 333 (2007) 103–111. doi:10.1016/j.ijpharm.2006.10.005.
[118] A. Dingler, R. P. Blum, H. Niehus, Solid lipid nanoparticles (SLNTM/LipopearlsTM) a pharmaceutical and cosmetic carrier for the application of vitamin E in dermal products, J. Microencapsul. 16 (1999) 751–767. doi:10.1080/026520499288690.
[119] J.-L. Capelo-Martínez, ed., Ultrasound in chemistry: analytical applications, Wiley-VCH, Weinheim, 2009.
[120] A. Patist, D. Bates, Ultrasonic innovations in the food industry: From the laboratory to commercial production, Innov. Food Sci. Emerg. Technol. 9 (2008) 147–154. doi:10.1016/j.ifset.2007.07.004.
[121] L. Español, A. Larrea, V. Andreu, G. Mendoza, M. Arruebo, V. Sebastian, M.S. Aurora-Prado, E.R.M. Kedor-Hackmann, M.I.R.M. Santoro, J. Santamaria, Dual encapsulation of hydrophobic and hydrophilic drugs in PLGA nanoparticles by a single-step method: drug delivery and cytotoxicity assays, RSC Adv. 6 (2016) 111060–111069. doi:10.1039/C6RA23620K.
[122] A.C. Silva, E. González-Mira, M.L. García, M.A. Egea, J. Fonseca, R. Silva, D. Santos, E.B. Souto, D. Ferreira, Preparation, characterization and biocompatibility studies on risperidone-loaded solid lipid nanoparticles (SLN): High pressure homogenization versus ultrasound, Colloids Surf. B Biointerfaces. 86 (2011) 158–165. doi:10.1016/j.colsurfb.2011.03.035.

[123] V. Gall, M. Runde, H. Schuchmann, Extending Applications of High-Pressure Homogenization by Using Simultaneous Emulsification and Mixing (SEM)—An Overview, Processes. 4 (2016) 46. doi:10.3390/pr4040046.
[124] M. Rayner, P. Dejmek, eds., Engineering Aspects of Food Emulsification and Homogenization, CRC Press, 2015. doi:10.1201/b18436.
[125] A. Calvör, B.W. McIller, Production of Microparticles by High-Pressure Homogenization, Pharm. Dev. Technol. 3 (1998) 297–305. doi:10.3109/10837459809009857.
[126] V. Jenning, A. Lippacher, S.H. Gohla, Medium scale production of solid lipid nanoparticles (SLN) by high pressure homogenization, J. Microencapsul. 19 (2002) 1–10. doi:10.1080/713817583.
[127] C. Schwarz, W. Mehnert, J.S. Lucks, R.H. Müller, Solid lipid nanoparticles (SLN) for controlled drug delivery. I. Production, characterization and sterilization, J. Controlled Release. 30 (1994) 83–96. doi:10.1016/0168-3659(94)90047-7.
[128] T. Kawakatsu, Y. Kikuchi, M. Nakajima, Regular-sized cell creation in microchannel emulsification by visual microprocessing method, J. Am. Oil Chem. Soc. 74 (1997) 317–321.
[129] I. Kobayashi, K. Uemura, M. Nakajima, Formulation of monodisperse emulsions using submicron-channel arrays, Colloids Surf. Physicochem. Eng. Asp. 296 (2007) 285–289. doi:10.1016/j.colsurfa.2006.09.015.
[130] I. Kobayashi, M.A. Neves, Y. Wada, K. Uemura, M. Nakajima, Large microchannel emulsification device for mass producing uniformly sized droplets on a liter per hour scale, Green Process. Synth. 1 (2012). doi:10.1515/gps-2012-0023.
[131] I. Kobayashi, S. Mukataka, M. Nakajima, Novel Asymmetric Through-Hole Array Microfabricated on a Silicon Plate for Formulating Monodisperse Emulsions, Langmuir. 21 (2005) 7629–7632. doi:10.1021/la050915x.
[132] C.-X. Zhao, A.P.J. Middelberg, Two-phase microfluidic flows, Chem. Eng. Sci. 66 (2011) 1394–1411. doi:10.1016/j.ces.2010.08.038.
[133] G.T. Vladisavljević, I. Kobayashi, M. Nakajima, Production of uniform droplets using membrane, microchannel and microfluidic emulsification devices, Microfluid. Nanofluidics. 13 (2012) 151–178. doi:10.1007/s10404-012-0948-0.
[134] I. Kobayashi, S. Ichikawa, M.A. Neves, T. Kuroiwa, M. Nakajima, FORMULATION OF LIPID MICRO/NANODISPERSION SYSTEMS, in: Lipids Nanotechnol., Elsevier, 2012: pp. 95–134. doi:10.1016/B978-0-9818936-7-9.50008-1.
[135] S. Sugiura, M. Nakajima, S. Iwamoto, M. Seki, Interfacial Tension Driven Monodispersed Droplet Formation from Microfabricated Channel Array, Langmuir. 17 (2001) 5562–5566. doi:10.1021/la010342y.
[136] E. Piacentini, M. Dragosavac, L. Giorno, Pharmaceutical particles design by membrane emulsification: preparation methods and applications in drug delivery, Curr. Pharm. Des. 23 (2017) 302–318.
[137] G. Vladisavljevic, M. Shimizu, T. Nakashima, Permeability of hydrophilic and hydrophobic Shirasu-porous-glass (SPG) membranes to pure liquids and its microstructure, J. Membr. Sci. 250 (2005) 69–77. doi:10.1016/j.memsci.2004.10.017.
[138] J.P. Rao, K.E. Geckeler, Polymer nanoparticles: Preparation techniques and size-control parameters, Spec. Issue Compos. 36 (2011) 887–913. doi:10.1016/j.progpolymsci.2011.01.001.
[139] J.W. Vanderhoff, M.S. El-Aasser, J. Ugelstad, Polymer emulsification process, Google Patents, 1979.
[140] M. Li, O. Rouaud, D. Poncelet, Microencapsulation by solvent evaporation: State of the art for process engineering approaches, Int. J. Pharm. 363 (2008) 26–39. doi:10.1016/j.ijpharm.2008.07.018.

[141] M. Trotta, M. Gallarate, F. Pattarino, S. Morel, Emulsions containing partially water-miscible solvents for the preparation of drug nanosuspensions, J. Controlled Release. 76 (2001) 119–128. doi:10.1016/S0168-3659(01)00432-1.
[142] C.E. Mora-Huertas, H. Fessi, A. Elaissari, Influence of process and formulation parameters on the formation of submicron particles by solvent displacement and emulsification–diffusion methods, Adv. Colloid Interface Sci. 163 (2011) 90–122. doi:10.1016/j.cis.2011.02.005.
[143] K.C. Song, H.S. Lee, I.Y. Choung, K.I. Cho, Y. Ahn, E.J. Choi, The effect of type of organic phase solvents on the particle size of poly(d,l-lactide-co-glycolide) nanoparticles, Colloids Surf. Physicochem. Eng. Asp. 276 (2006) 162–167. doi:10.1016/j.colsurfa.2005.10.064.
[144] H.-Y. Kwon, J.-Y. Lee, S.-W. Choi, Y. Jang, J.-H. Kim, Preparation of PLGA nanoparticles containing estrogen by emulsification–diffusion method, Colloids Surf. Physicochem. Eng. Asp. 182 (2001) 123–130. doi:10.1016/S0927-7757(00)00825-6.
[145] L.M. Delgado, Y. Bayon, A. Pandit, D.I. Zeugolis, To Cross-Link or Not to Cross-Link? Cross-Linking Associated Foreign Body Response of Collagen-Based Devices, Tissue Eng. Part B Rev. 21 (2015) 298–313. doi:10.1089/ten.teb.2014.0290.
[146] K.-J. Kim, S.-B. Lee, N.-W. Han, Kinetics of crosslinking reaction of PVA membrane with glutaraldehyde, Korean J. Chem. Eng. 11 (1994) 41–47. doi:10.1007/BF02697513.
[147] H. Wen, H. Jung, X. Li, Drug Delivery Approaches in Addressing Clinical Pharmacology-Related Issues: Opportunities and Challenges, AAPS J. 17 (2015) 1327–1340. doi:10.1208/s12248-015-9814-9.
[148] F. Wood-Black, Considerations for Scale-Up – Moving from the Bench to the Pilot Plant to Full Production, in: M.K. Moore, E.B. Ledesma (Eds.), ACS Symp. Ser., American Chemical Society, Washington, DC, 2014: pp. 37–45. doi:10.1021/bk-2014-1163.ch003.
[149] V. Sebastian, M. Arruebo, J. Santamaria, Reaction Engineering Strategies for the Production of Inorganic Nanomaterials, Small. 10 (2014) 835–853. doi:10.1002/smll.201301641.
[150] F. Spyropoulos, D.M. Lloyd, R.D. Hancocks, A.K. Pawlik, Advances in membrane emulsification. Part B: recent developments in modelling and scale-up approaches, J. Sci. Food Agric. 94 (2014) 628–638. doi:10.1002/jsfa.6443.
[151] X.Y. Lawrence, Pharmaceutical quality by design: product and process development, understanding, and control, Pharm. Res. 25 (2008) 781–791.
[152] J.M. Chan, P.M. Valencia, L. Zhang, R. Langer, O.C. Farokhzad, Polymeric Nanoparticles for Drug Delivery, in: S.R. Grobmyer, B.M. Moudgil (Eds.), Cancer Nanotechnol., Humana Press, Totowa, NJ, 2010: pp. 163–175. http://link.springer.com/10.1007/978-1-60761-609-2_11 (accessed February 22, 2015).
[153] C.. DeMerlis, D.. Schoneker, Review of the oral toxicity of polyvinyl alcohol (PVA), Food Chem. Toxicol. 41 (2003) 319–326. doi:10.1016/S0278-6915(02)00258-2.
[154] Guideline, I. H. T., Impurities: Guideline for residual solvents Q3C (R5), Curr. Step. 4 (2005) 509.
[155] W.H. De Jong, P.J. Borm, Drug delivery and nanoparticles: applications and hazards, Int. J. Nanomedicine. 3 (2008) 133.
[156] A. Sharma, S.V. Madhunapantula, G.P. Robertson, Toxicological considerations when creating nanoparticle-based drugs and drug delivery systems, Expert Opin. Drug Metab. Toxicol. 8 (2012) 47–69. doi:10.1517/17425255.2012.637916.
[157] V. Sainz, J. Conniot, A.I. Matos, C. Peres, E. Zupančič, L. Moura, L.C. Silva, H.F. Florindo, R.S. Gaspar, Regulatory aspects on nanomedicines, Biochem. Biophys. Res. Commun. (2015) 504–510. doi:10.1016/j.bbrc.2015.08.023.
[158] D.J. Burgess, A.S. Hussain, T.S. Ingallinera, M.-L. Chen, Assuring quality and performance of sustained and controlled release parenterals: AAPS workshop report, co-sponsored by FDA and USP, Pharm. Res. 19 (2002) 1761–1768.

[159] P. Muralidhar, E. Bhargav, CONTROLLED RELEASE INJECTABLE DRUG DELIVERY: AN OVER VIEW, Asian J. Biomater. Res. 3 (2017) 6–15.
[160] K. Boodhoo, A. Harvey, Process intensification technologies for green chemistry engineering solutions for sustainable chemical processing, Wiley, Chichester, 2013.
[161] R.A. Sheldon, The E factor 25 years on: the rise of green chemistry and sustainability, Green Chem. (2017) 18–43. doi:10.1039/C6GC02157C.
[162] C.A.M. Afonso, ed., Green separation processes: fundamentals and applications, WILEY-VCH, Weinheim, 2005.
[163] D.J.C. Constable, A.D. Curzons, V.L. Cunningham, Metrics to 'green' chemistry—which are the best?, Green Chem. 4 (2002) 521–527. doi:10.1039/B206169B.
[164] B. Trost, The atom economy--a search for synthetic efficiency, Science. 254 (1991) 1471–1477. doi:10.1126/science.1962206.
[165] F. Roschangar, J. Colberg, P.J. Dunn, F. Gallou, J.D. Hayler, S.G. Koenig, M.E. Kopach, D.K. Leahy, I. Mergelsberg, J.L. Tucker, R.A. Sheldon, C.H. Senanayake, A deeper shade of green: inspiring sustainable drug manufacturing, Green Chem. (2017) 281–285. doi:10.1039/C6GC02901A.
[166] D. Bennet, S. Kim, Polymer Nanoparticles for Smart Drug Delivery, in: A.D. Sezer (Ed.), Appl. Nanotechnol. Drug Deliv., InTech, 2014. http://www.intechopen.com/books/application-of-nanotechnology-in-drug-delivery/polymer-nanoparticles-for-smart-drug-delivery (accessed October 31, 2015).
[167] E. Luque-Michel, E. Imbuluzqueta, V. Sebastián, M.J. Blanco-Prieto, Clinical advances of nanocarrier-based cancer therapy and diagnostics, Expert Opin. Drug Deliv. (2016) 1–18. doi:10.1080/17425247.2016.1205585.
[168] F. Danhier, E. Ansorena, J.M. Silva, R. Coco, A. Le Breton, V. Préat, PLGA-based nanoparticles: An overview of biomedical applications, J. Controlled Release. 161 (2012) 505–522. doi:10.1016/j.jconrel.2012.01.043.
[169] A. Fahr, X. Liu, Drug delivery strategies for poorly water-soluble drugs, Expert Opin. Drug Deliv. 4 (2007) 403–416. doi:10.1517/17425247.4.4.403.
[170] R.A. Kudgus, C.A. Walden, R.M. McGovern, J.M. Reid, J.D. Robertson, P. Mukherjee, Tuning Pharmacokinetics and Biodistribution of a Targeted Drug Delivery System Through Incorporation of a Passive Targeting Component, Sci. Rep. 4 (2015). doi:10.1038/srep05669.
[171] B.S. Zolnik, Á. González-Fernández, N. Sadrieh, M.A. Dobrovolskaia, Minireview: Nanoparticles and the Immune System, Endocrinology. 151 (2010) 458–465. doi:10.1210/en.2009-1082.
[172] S. Dhar, N. Kolishetti, S.J. Lippard, O.C. Farokhzad, Targeted delivery of a cisplatin prodrug for safer and more effective prostate cancer therapy in vivo, Proc. Natl. Acad. Sci. 108 (2011) 1850–1855. doi:10.1073/pnas.1011379108.
[173] A. Albisa, L. Español, M. Prieto, V. Sebastian, Polymeric Nanomaterials as Nanomembrane Entities for Biomolecule and Drug Delivery, Curr. Pharm. Des. 23 (2016) 263–280.
[174] K. Avgoustakis, Pegylated Poly(Lactide) and Poly(Lactide-Co-Glycolide) Nanoparticles: Preparation, Properties and Possible Applications in Drug Delivery, Curr. Drug Deliv. 1 (2004) 321–333. doi:10.2174/1567201043334605.
[175] Q. Wang, P. Wu, W. Ren, K. Xin, Y. Yang, C. Xie, C. Yang, Q. Liu, L. Yu, X. Jiang, B. Liu, R. Li, L. Wang, Comparative studies of salinomycin-loaded nanoparticles prepared by nanoprecipitation and single emulsion method, Nanoscale Res. Lett. 9 (2014) 351. doi:10.1186/1556-276X-9-351.
[176] Z. Zhu, Flash Nanoprecipitation: Prediction and Enhancement of Particle Stability via Drug Structure, Mol. Pharm. 11 (2014) 776–786. doi:10.1021/mp500025e.
[177] S.A. Vitale, J.L. Katz, Liquid Droplet Dispersions Formed by Homogeneous Liquid−Liquid Nucleation: "The Ouzo Effect," Langmuir. 19 (2003) 4105–4110. doi:10.1021/la026842o.

[178] M. Beck-Broichsitter, J. Nicolas, P. Couvreur, Solvent selection causes remarkable shifts of the “Ouzo region” for poly(lactide-co-glycolide) nanoparticles prepared by nanoprecipitation, Nanoscale. 7 (2015) 9215–9221. doi:10.1039/C5NR01695A.
[179] J. Aubry, F. Ganachaud, J.-P. Cohen Addad, B. Cabane, Nanoprecipitation of Polymethylmethacrylate by Solvent Shifting:1. Boundaries, Langmuir. 25 (2009) 1970–1979. doi:10.1021/la803000e.
[180] B.K. Johnson, R.K. Prud’homme, Mechanism for Rapid Self-Assembly of Block Copolymer Nanoparticles, Phys. Rev. Lett. 91 (2003). doi:10.1103/PhysRevLett.91.118302.
[181] J. Sun, Y. Xianyu, M. Li, W. Liu, L. Zhang, D. Liu, C. Liu, G. Hu, X. Jiang, A microfluidic origami chip for synthesis of functionalized polymeric nanoparticles, Nanoscale. 5 (2013) 5262. doi:10.1039/c3nr01289a.
[182] B.K. Johnson, R.K. Prud’homme, Flash NanoPrecipitation of Organic Actives and Block Copolymers using a Confined Impinging Jets Mixer, Aust. J. Chem. 56 (2003) 1021. doi:10.1071/CH03115.
[183] J.-M. Lim, A. Swami, L.M. Gilson, S. Chopra, S. Choi, J. Wu, R. Langer, R. Karnik, O.C. Farokhzad, Ultra-High Throughput Synthesis of Nanoparticles with Homogeneous Size Distribution Using a Coaxial Turbulent Jet Mixer, ACS Nano. 8 (2014) 6056–6065. doi:10.1021/nn501371n.
[184] A. Villaverde, ed., Nanoparticles in translational science and medicine, Elsevier, Acad. Press, Amsterdam, 2011.
[185] B.K. Johnson, R.K. Prud’homme, Chemical processing and micromixing in confined impinging jets, AIChE J. 49 (2003) 2264–2282. doi:10.1002/aic.690490905.
[186] M. Jasińska, Test Reactions to Study Efficiency of mixing, Chem. Process Eng. 36 (2015). doi:10.1515/cpe-2015-0013.
[187] J. Baldyga, J.R. Bourne, B. Walker, Non-isothermal micromixing in turbulent liquids: Theory and experiment, Can. J. Chem. Eng. 76 (1998) 641–649. doi:10.1002/cjce.5450760336.
[188] P.W. Atkins, J. De Paula, Elements of physical chemistry, 5th ed, Oxford University Press, Oxford ; New York, 2009.
[189] G.L. Barthauer, F.V. Jones, A.V. Metler, Determination of Acetone An Ultraviolet Spectrophotometric Method, Ind. Eng. Chem. Anal. Ed. 18 (1946) 354–355. doi:10.1021/i560154a004.
[190] C. Pucci, F. Cousin, F. Dole, J.-P. Chapel, C. Schatz, Impact of the Formulation Pathway on the Colloidal State and Crystallinity of Poly-ε-caprolactone Particles Prepared by Solvent Displacement, Langmuir. (2018). doi:10.1021/acs.langmuir.7b04198.
[191] E. Lepeltier, C. Bourgaux, P. Couvreur, Nanoprecipitation and the “Ouzo effect”: Application to drug delivery devices, Adv. Drug Deliv. Rev. 71 (2014) 86–97. doi:10.1016/j.addr.2013.12.009.
[192] M. Beck-Broichsitter, Stability-limit □Ouzo region□ boundaries for poly(lactide-co-glycolide) nanoparticles prepared by nanoprecipitation, Int. J. Pharm. 511 (2016) 262–266. doi:10.1016/j.ijpharm.2016.07.010.
[193] J.G.J.L. Lebouille, R. Stepanyan, J.J.M. Slot, M.A. Cohen Stuart, R. Tuinier, Nanoprecipitation of polymers in a bad solvent, Colloids Surf. Physicochem. Eng. Asp. 460 (2014) 225–235. doi:10.1016/j.colsurfa.2013.11.045.
[194] C. Reichardt, T. Welton, Solvents and solvent effects in organic chemistry., Wiley-VCH, Weinheim, 2011.
[195] R.L. Adelman, I.M. Klein, Effects of solvent structure in polyvinyl chloride-solvent systems, J. Polym. Sci. 31 (1958) 77–94. doi:10.1002/pol.1958.1203112209.
[196] J.H.W. Coover, J.B. Dickey, Mixtures comprising polyacrylonitrile and polymeric ester-lactones, Google Patents, 1951.

[197] L. Lindfors, P. Skantze, U. Skantze, J. Westergren, U. Olsson, Amorphous Drug Nanosuspensions. 3. Particle Dissolution and Crystal Growth, Langmuir. 23 (2007) 9866–9874. doi:10.1021/la700811b.
[198] L. Lindfors, S. Forssén, J. Westergren, U. Olsson, Nucleation and crystal growth in supersaturated solutions of a model drug, J. Colloid Interface Sci. 325 (2008) 404–413. doi:10.1016/j.jcis.2008.05.034.
[199] C. Gomezgaete, N. Tsapis, M. Besnard, A. Bochot, E. Fattal, Encapsulation of dexamethasone into biodegradable polymeric nanoparticles, Int. J. Pharm. 331 (2007) 153–159. doi:10.1016/j.ijpharm.2006.11.028.
[200] C.G. Madsen, A. Skov, S. Baldursdottir, T. Rades, L. Jorgensen, N.J. Medlicott, Simple measurements for prediction of drug release from polymer matrices – Solubility parameters and intrinsic viscosity, Eur. J. Pharm. Biopharm. 92 (2015) 1–7. doi:10.1016/j.ejpb.2015.02.001.
[201] E. Vega, Egea, Calpena, Espina, García, Role of hydroxypropyl-β-cyclodextrin on freeze-dried and gamma-irradiated PLGA and PLGA–PEG diblock copolymer nanospheres for ophthalmic flurbiprofen delivery, Int. J. Nanomedicine. (2012) 1357. doi:10.2147/IJN.S28481.
[202] M. Chacón, L. Berges, J. Molpeceres, M.R. Aberturas, M. Guzman, Optimized preparation of poly d,l (lactic-glycolic) microspheres and nanoparticles for oral administration, Int. J. Pharm. 141 (1996) 81–91. doi:10.1016/0378-5173(96)04618-2.
[203] C.W. Noorlander, M.W. Kooi, A.G. Oomen, M.V. Park, R.J. Vandebriel, R.E. Geertsma, Horizon scan of nanomedicinal products, Nanomed. 10 (2015) 1599–1608. doi:10.2217/nnm.15.21.
[204] N. Faisant, J. Siepmann, J.P. Benoit, PLGA-based microparticles: elucidation of mechanisms and a new, simple mathematical model quantifying drug release, Eur. J. Pharm. Sci. 15 (2002) 355–366. doi:10.1016/S0928-0987(02)00023-4.
[205] Mona Noori Koopaeia, Seyed Hossein Mostafavib, Mohsen Aminid, Mohammad Reza Khorramizadehe, Mahmood Jeddi Tehranif, Mona Noori Koopaei, Docetaxel Loaded PEG-PLGA Nanoparticles: Optimized Drug Loading, In-vitro Cytotoxicity and In-vivo Antitumor Effect, Iran. J. Pharm. Res. 13 (2014) 819–883.
[206] S. Xu, F. Yang, X. Zhou, Y. Zhuang, B. Liu, Y. Mu, X. Wang, H. Shen, G. Zhi, D. Wu, Uniform PEGylated PLGA Microcapsules with Embedded Fe_3O_4 Nanoparticles for US/MR Dual-Modality Imaging, ACS Appl. Mater. Interfaces. 7 (2015) 20460–20468. doi:10.1021/acsami.5b06594.
[207] A.A. Ghahremankhani, F. Dorkoosh, R. Dinarvand, PLGA-PEG-PLGA Tri-Block Copolymers as In Situ Gel-Forming Peptide Delivery System: Effect of Formulation Properties on Peptide Release, Pharm. Dev. Technol. 13 (2008) 49–55. doi:10.1080/10837450701702842.
[208] D. Vllasaliu, R. Fowler, S. Stolnik, PEGylated nanomedicines: recent progress and remaining concerns, Expert Opin. Drug Deliv. 11 (2014) 139–154. doi:10.1517/17425247.2014.866651.
[209] R. Rietscher, C. Thum, C.-M. Lehr, M. Schneider, Semi-Automated Nanoprecipitation-System—An Option for Operator Independent, Scalable and Size Adjustable Nanoparticle Synthesis, Pharm. Res. 32 (2015) 1859–1863. doi:10.1007/s11095-014-1612-z.
[210] I.Y. Perevyazko, J.T. Delaney, A. Vollrath, G.M. Pavlov, S. Schubert, U.S. Schubert, Examination and optimization of the self-assembly of biocompatible, polymeric nanoparticles by high-throughput nanoprecipitation, Soft Matter. 7 (2011) 5030. doi:10.1039/c1sm05079f.
[211] A. Imbrogno, E. Piacentini, E. Drioli, L. Giorno, Preparation of uniform poly-caprolactone Microparticles by membrane emulsification/solvent diffusion process, J. Membr. Sci. 467 (2014) 262–268. doi:10.1016/j.memsci.2014.05.037.
[212] E. Piacentini, E. Drioli, L. Giorno, Membrane emulsification technology: Twenty-five years of inventions and research through patent survey, J. Membr. Sci. 468 (2014) 410–422. doi:10.1016/j.memsci.2014.05.059.

[213] G.T. Vladisavljević, Structured microparticles with tailored properties produced by membrane emulsification, Adv. Colloid Interface Sci. 225 (2015) 53–87. doi:10.1016/j.cis.2015.07.013.
[214] E. Piacentini, M.. Dragosavac, L. Giorno, Pharmaceutical Particles Design by Membrane Emulsification, Curr. Pharm. Des. in press (2016).
[215] R. Othman, G.T. Vladisavljević, H. Shahmohamadi, Z.K. Nagy, R.G. Holdich, Formation of size-tuneable biodegradable polymeric nanoparticles by solvent displacement method using micro-engineered membranes fabricated by laser drilling and electroforming, Chem. Eng. J. (2016). doi:10.1016/j.cej.2016.07.010.
[216] A. Laouini, C. Charcosset, H. Fessi, R.G. Holdich, G.T. Vladisavljević, Preparation of liposomes: a novel application of microengineered membranes - investigation of the process parameters and application to the encapsulation of vitamin E, RSC Adv. 3 (2013) 4985. doi:10.1039/c3ra23411h.
[217] A. Laouini, K.P. Koutroumanis, C. Charcosset, S. Georgiadou, H. Fessi, R.G. Holdich, G.T. Vladisavljević, pH-Sensitive Micelles for Targeted Drug Delivery Prepared Using a Novel Membrane Contactor Method, ACS Appl. Mater. Interfaces. 5 (2013) 8939–8947. doi:10.1021/am4018237.
[218] I. Limayem Blouza, C. Charcosset, S. Sfar, H. Fessi, Preparation and characterization of spironolactone-loaded nanocapsules for paediatric use, Int. J. Pharm. 325 (2006) 124–131. doi:10.1016/j.ijpharm.2006.06.022.
[219] R. Othman, G.T. Vladisavljević, Z.K. Nagy, R.G. Holdich, Encapsulation and Controlled Release of Rapamycin from Polycaprolactone Nanoparticles Prepared by Membrane Micromixing Combined with Antisolvent Precipitation, Langmuir. 32 (2016) 10685–10693. doi:10.1021/acs.langmuir.6b03178.
[220] S. Agustina, M. Tokuda, H. Minami, C. Boyer, P.B. Zetterlund, Synthesis of polymeric nano-objects of various morphologies based on block copolymer self-assembly using microporous membranes, React Chem Eng. (2017). doi:10.1039/C7RE00032D.
[221] E. Piacentini, E. Drioli, L. Giorno, Pulsed back-and-forward cross-flow batch membrane emulsification with high productivity to obtain highly uniform and concentrate emulsions, J. Membr. Sci. 453 (2014) 119–125. doi:10.1016/j.memsci.2013.10.063.
[222] J. Cheng, B. Teply, I. Sherifi, J. Sung, G. Luther, F. Gu, E. Levynissenbaum, A. Radovicmoreno, R. Langer, O. Farokhzad, Formulation of functionalized PLGA–PEG nanoparticles for in vivo targeted drug delivery, Biomaterials. 28 (2007) 869–876. doi:10.1016/j.biomaterials.2006.09.047.
[223] F. Ganachaud, J.L. Katz, Nanoparticles and Nanocapsules Created Using the Ouzo Effect: Spontaneous Emulsification as an Alternative to Ultrasonic and High-Shear Devices, ChemPhysChem. 6 (2005) 209–216. doi:10.1002/cphc.200400527.
[224] S. Stainmesse, A.-M. Orecchioni, E. Nakache, F. Puisieux, H. Fessi, Formation and stabilization of a biodegradable polymeric colloidal suspension of nanoparticles, Colloid Polym. Sci. 273 (1995) 505–511. doi:10.1007/BF00656896.
[225] M. Beck-Broichsitter, E. Rytting, T. Lebhardt, X. Wang, T. Kissel, Preparation of nanoparticles by solvent displacement for drug delivery: A shift in the “ouzo region” upon drug loading, Eur. J. Pharm. Sci. 41 (2010) 244–253. doi:10.1016/j.ejps.2010.06.007.
[226] G.T. Vladisavljevic, Integrated Membrane Processes for the Preparation of Emulsions, Particles and Bubbles, Integr. Membr. Syst. Process. (2015) 79.
[227] A. Laouini, C. Jaafar-Maalej, S. Sfar, C. Charcosset, H. Fessi, Liposome preparation using a hollow fiber membrane contactor—Application to spironolactone encapsulation, Int. J. Pharm. 415 (2011) 53–61. doi:10.1016/j.ijpharm.2011.05.034.
[228] N. Khayata, W. Abdelwahed, M.F. Chehna, C. Charcosset, H. Fessi, Preparation of vitamin E loaded nanocapsules by the nanoprecipitation method: From laboratory scale to large scale using a membrane contactor, Int. J. Pharm. 423 (2012) 419–427. doi:10.1016/j.ijpharm.2011.12.016.

[229] E. Piacentini, A. Imbrogno, E. Drioli, L. Giorno, Membranes with tailored wettability properties for the generation of uniform emulsion droplets with high efficiency, J. Membr. Sci. 459 (2014) 96–103. doi:10.1016/j.memsci.2014.01.075.
[230] E. Piacentini, L. Giorno, M.M. Dragosavac, G.T. Vladisavljević, R.G. Holdich, Microencapsulation of oil droplets using cold water fish gelatine/gum arabic complex coacervation by membrane emulsification, Food Res. Int. 53 (2013) 362–372. doi:10.1016/j.foodres.2013.04.012.
[231] A. Imbrogno, M.. Dragosavac, E. Piacentini, G.T. Vladisavljević, R.G. Holdich, L. Giorno, Polycaprolactone multicore-matrix particle for the simultaneous encapsulation of hydrophilic and hydrophobic compounds produced by membrane emulsification and solvent diffusion processes, Colloids Surf. B Biointerfaces. 135 (2015) 116–125. doi:10.1016/j.colsurfb.2015.06.071.
[232] C. Kahraman, S. Yanık, eds., Intelligent Decision Making in Quality Management, Springer International Publishing, Cham, 2016. http://link.springer.com/10.1007/978-3-319-24499-0 (accessed September 14, 2016).
[233] J. Ermer, H.-J. Ploss, Validation in pharmaceutical analysis, J. Pharm. Biomed. Anal. 37 (2005) 859–870. doi:10.1016/j.jpba.2004.06.018.
[234] L. Zhang, ed., Nonclinical Statistics for Pharmaceutical and Biotechnology Industries, Springer International Publishing, Cham, 2016. http://link.springer.com/10.1007/978-3-319-23558-5 (accessed September 14, 2016).
[235] M. Chorny, I. Fishbein, H.D. Danenberg, G. Golomb, Lipophilic drug loaded nanospheres prepared by nanoprecipitation: effect of formulation variables on size, drug recovery and release kinetics, J. Controlled Release. 83 (2002) 389–400. doi:10.1016/S0168-3659(02)00211-0.
[236] A. Budhian, S.J. Siegel, K.I. Winey, Haloperidol-loaded PLGA nanoparticles: Systematic study of particle size and drug content, Int. J. Pharm. 336 (2007) 367–375. doi:10.1016/j.ijpharm.2006.11.061.
[237] S.A. Guhagarkar, V.C. Malshe, P.V. Devarajan, Nanoparticles of Polyethylene Sebacate: A New Biodegradable Polymer, AAPS PharmSciTech. 10 (2009) 935–942. doi:10.1208/s12249-009-9284-4.
[238] R. Dhakar, FROM FORMULATION VARIABLES TO DRUG ENTRAPMENT EFFICIENCY OF MICROSPHERES: A TECHNICAL REVIEW, J. Drug Deliv. Ther. 2 (2012). http://jddtonline.info/index.php/jddt/article/view/160.
[239] T. Govender, S. Stolnik, M.C. Garnett, L. Illum, S.S. Davis, PLGA nanoparticles prepared by nanoprecipitation: drug loading and release studies of a water soluble drug, J. Control. Release Off. J. Control. Release Soc. 57 (1999) 171–185.
[240] P.L. Ritger, N.A. Peppas, A simple equation for description of solute release I. Fickian and non-fickian release from non-swellable devices in the form of slabs, spheres, cylinders or discs, J. Controlled Release. 5 (1987) 23–36. doi:10.1016/0168-3659(87)90034-4.
[241] M. Grassi, G. Grassi, Mathematical Modelling and Controlled Drug Delivery: Matrix Systems, Curr. Drug Deliv. 2 (2005) 97–116. doi:10.2174/1567201052772906.
[242] E. Drioli, A. Brunetti, G. Di Profio, G. Barbieri, Process intensification strategies and membrane engineering, Green Chem. 14 (2012) 1561. doi:10.1039/c2gc16668b.
[243] R.G. Holdich, M.M. Dragosavac, G.T. Vladisavljević, E. Piacentini, Continuous Membrane Emulsification with Pulsed (Oscillatory) Flow, Ind. Eng. Chem. Res. (2012) 507–515. doi:10.1021/ie3020457.
[244] A. Imbrogno, E. Piacentini, E. Drioli, L. Giorno, Micro and nano polycaprolactone particles preparation by pulsed back-and-forward cross-flow batch membrane emulsification for parenteral administration, Int. J. Pharm. 477 (2014) 344–350. doi:10.1016/j.ijpharm.2014.10.049.

[245] F. Bazzarelli, E. Piacentini, L. Giorno, Biophenols-loaded solid lipid particles (SLPs) development by membrane emulsification, J. Membr. Sci. 541 (2017) 587–594. doi:10.1016/j.memsci.2017.07.029.
[246] R.A. Williams, S.J. Peng, D.A. Wheeler, N.C. Morley, D. Taylor, M. Whalley, D.W. Houldsworth, Controlled Production of Emulsions Using a Crossflow Membrane, Chem. Eng. Res. Des. 76 (1998) 902–910. doi:10.1205/026387698525702.
[247] H. Karbstein, H. Schubert, Developments in the continuous mechanical production of oil-in-water macro-emulsions, Chem. Eng. Process. Process Intensif. 34 (1995) 205–211. doi:10.1016/0255-2701(94)04005-2.
[248] S. Schultz, G. Wagner, K. Urban, J. Ulrich, High-Pressure Homogenization as a Process for Emulsion Formation, Chem. Eng. Technol. 27 (2004) 361–368. doi:10.1002/ceat.200406111.
[249] I.D. Rosca, F. Watari, M. Uo, Microparticle formation and its mechanism in single and double emulsion solvent evaporation, J. Controlled Release. 99 (2004) 271–280. doi:10.1016/j.jconrel.2004.07.007.
[250] H.H.. Girault, D.. Schiffrin, B.D.. Smith, The measurement of interfacial tension of pendant drops using a video image profile digitizer, J. Colloid Interface Sci. 101 (1984) 257–266. doi:10.1016/0021-9797(84)90026-2.
[251] J. Drelich, C. Fang, C. White, Measurement of interfacial tension in fluid-fluid systems, Encycl. Surf. Colloid Sci. 3 (2002) 3158–3163.
[252] F. Lagarce, E. Garcion, N. Faisant, O. Thomas, P. Kanaujia, P. Menei, J.P. Benoit, Development and characterization of interleukin-18-loaded biodegradable microspheres, Int. J. Pharm. 314 (2006) 179–188. doi:10.1016/j.ijpharm.2005.07.029.
[253] P. Verderio, P. Bonetti, M. Colombo, L. Pandolfi, D. Prosperi, Intracellular Drug Release from Curcumin-Loaded PLGA Nanoparticles Induces G2/M Block in Breast Cancer Cells, Biomacromolecules. 14 (2013) 672–682. doi:10.1021/bm3017324.
[254] R. Liu, S.-S. Huang, Y.-H. Wan, G.-H. Ma, Z.-G. Su, Preparation of insulin-loaded PLA/PLGA microcapsules by a novel membrane emulsification method and its release in vitro, Colloids Surf. B Biointerfaces. 51 (2006) 30–38. doi:10.1016/j.colsurfb.2006.05.014.
[255] G. Gasparini, S.R. Kosvintsev, M.T. Stillwell, R.G. Holdich, Preparation and characterization of PLGA particles for subcutaneous controlled drug release by membrane emulsification, Colloids Surf. B Biointerfaces. 61 (2008) 199–207. doi:10.1016/j.colsurfb.2007.08.011.
[256] F. Ito, H. Honnami, H. Kawakami, K. Kanamura, K. Makino, Preparation and properties of PLGA microspheres containing hydrophilic drugs by the SPG (shirasu porous glass) membrane emulsification technique, Colloids Surf. B Biointerfaces. 67 (2008) 20–25. doi:10.1016/j.colsurfb.2008.07.008.
[257] Y. Yu, S. Tan, S. Zhao, X. Zhuang, Q. Song, Y. Wang, Q. Zhou, Z. Zhang, Antitumor activity of docetaxel-loaded polymeric nanoparticles fabricated by Shirasu porous glass membrane-emulsification technique, Int. J. Nanomedicine. 8 (2013) 2641–2652.
[258] T.H. Ho, T.P. Tuyen Dao, T.A. Nguyen, D.D. Le, M.C. Dang, Cross-flow membrane emulsification technique for fabrication of drug-loaded particles, Adv. Nat. Sci. Nanosci. Nanotechnol. 4 (2013) 045008. doi:10.1088/2043-6262/4/4/045008.
[259] H. Schubert, K. Ax, Engineering Food Emulsions en McKenna, BM, Texture Foods Semisolids. (2003).
[260] H. Schubert, H. Karbstein, Mechanical Emulsification, in: T. Yano, R. Matsuno, K. Nakamura (Eds.), Dev. Food Eng., Springer US, Boston, MA, 1994: pp. 9–14. doi:10.1007/978-1-4615-2674-2_2.
[261] J.S. Park, K. Na, D.G. Woo, H.N. Yang, K.-H. Park, Determination of dual delivery for stem cell differentiation using dexamethasone and TGF-β3 in/on polymeric microspheres, Biomaterials. 30 (2009) 4796–4805. doi:10.1016/j.biomaterials.2009.05.054.

[262] C. Jimenez-Gonzalez, C.S. Ponder, Q.B. Broxterman, J.B. Manley, Using the Right Green Yardstick: Why Process Mass Intensity Is Used in the Pharmaceutical Industry To Drive More Sustainable Processes, Org. Process Res. Dev. 15 (2011) 912–917. doi:10.1021/op200097d.
[263] D. Cespi, E.S. Beach, T.E. Swarr, F. Passarini, I. Vassura, P.J. Dunn, P.T. Anastas, Life cycle inventory improvement in the pharmaceutical sector: assessment of the sustainability combining PMI and LCA tools, Green Chem. 17 (2015) 3390–3400. doi:10.1039/C5GC00424A.
[264] M. Lancaster, Green chemistry: an introductory text, 3rd edition, Royal Society of Chemistry, Cambridge, UK, 2016.
[265] F.P. Byrne, S. Jin, G. Paggiola, T.H.M. Petchey, J.H. Clark, T.J. Farmer, A.J. Hunt, C. Robert McElroy, J. Sherwood, Tools and techniques for solvent selection: green solvent selection guides, Sustain. Chem. Process. 4 (2016) 1–24. doi:10.1186/s40508-016-0051-z.
[266] S. Vrignaud, J.-P. Benoit, P. Saulnier, Strategies for the nanoencapsulation of hydrophilic molecules in polymer-based nanoparticles, Biomaterials. 32 (2011) 8593–8604. doi:10.1016/j.biomaterials.2011.07.057.
[267] S. Arpicco, L. Battaglia, P. Brusa, R. Cavalli, D. Chirio, F. Dosio, M. Gallarate, P. Milla, E. Peira, F. Rocco, S. Sapino, B. Stella, E. Ugazio, M. Ceruti, Recent studies on the delivery of hydrophilic drugs in nanoparticulate systems, J. Drug Deliv. Sci. Technol. 32 (2016) 298–312. doi:10.1016/j.jddst.2015.09.004.
[268] G. Chen, C. Bunt, J. Wen, Mucoadhesive polymers-based film as a carrier system for sublingual delivery of glutathione: Glutathione delivery via sublingual route, J. Pharm. Pharmacol. 67 (2015) 26–34. doi:10.1111/jphp.12313.
[269] Z. Cui, Z. Zheng, L. Lin, J. Si, Q. Wang, X. Peng, W. Chen, Electrospinning and crosslinking of polyvinyl alcohol/chitosan composite nanofiber for transdermal drug delivery, Adv. Polym. Technol. (2017). doi:10.1002/adv.21850.
[270] P.I. Morgado, P.F. Lisboa, M.P. Ribeiro, S.P. Miguel, P.C. Simões, I.J. Correia, A. Aguiar-Ricardo, Poly(vinyl alcohol)/chitosan asymmetrical membranes: Highly controlled morphology toward the ideal wound dressing, J. Membr. Sci. 469 (2014) 262–271. doi:10.1016/j.memsci.2014.06.035.
[271] N.A. Peppas, N.K. Mongia, Ultrapure poly(vinyl alcohol) hydrogels with mucoadhesive drug delivery characteristics, Eur. J. Pharm. Biopharm. 43 (1997) 51–58. doi:10.1016/S0939-6411(96)00010-0.
[272] P. Taepaiboon, U. Rungsardthong, P. Supaphol, Drug-loaded electrospun mats of poly(vinyl alcohol) fibres and their release characteristics of four model drugs, Nanotechnology. 17 (2006) 2317–2329. doi:10.1088/0957-4484/17/9/041.
[273] T. Wan, G.K. Stylios, M. Giannoudi, P.V. Giannoudis, Investigating a new drug delivery nano composite membrane system based on PVA/PCL and PVA/HA(PEG) for the controlled release of biopharmaceuticals for bone infections, Injury. 46 (2015) S39–S43. doi:10.1016/S0020-1383(15)30053-X.
[274] C. Zhang, X. Yuan, L. Wu, Y. Han, J. Sheng, Study on morphology of electrospun poly(vinyl alcohol) mats, Eur. Polym. J. 41 (2005) 423–432. doi:10.1016/j.eurpolymj.2004.10.027.
[275] D. Shah, Y. Shah, R. Pradhan, Development and Evaluation of Controlled-Release Diltiazem HCl Microparticles Using Cross-Linked Poly(Vinyl Alcohol), Drug Dev. Ind. Pharm. 23 (1997) 567–574. doi:10.3109/03639049709149821.
[276] Y. Cao, F. Liu, Y. Chen, T. Yu, D. Lou, Y. Guo, P. Li, Z. Wang, H. Ran, Drug release from core-shell PVA/silk fibroin nanoparticles fabricated by one-step electrospraying, Sci. Rep. 7 (2017). doi:10.1038/s41598-017-12351-1.
[277] N. Cardillo, Microincapsulamento di molecole farmacologicamente attive in microsfere di PVA preparate tramite emulsificazione a membrana, Università della Calabria, 2016.

[278] V.G. Babak, F. Baros, O. Boulanouar, F. Boury, M. Fromm, N.R. Kildeeva, N. Ubrich, P. Maincent, Impact of bulk and surface properties of some biocompatible hydrophobic polymers on the stability of methylene chloride-in-water mini-emulsions used to prepare nanoparticles by emulsification–solvent evaporation, Colloids Surf. B Biointerfaces. 59 (2007) 194–207. doi:10.1016/j.colsurfb.2007.05.010.
[279] R. Zarzycki, Z. Modrzejewska, K. Nawrotek, Drug release from hydrogel matrices, Ecol Chem Enginer S. 17 (2010) 117–136.
[280] J. Li, D.J. Mooney, Designing hydrogels for controlled drug delivery, Nat. Rev. Mater. 1 (2016) 16071. doi:10.1038/natrevmats.2016.71.

Appendix

8.1 Appendix 1 (Related to chapter 1)

Not applicable (N/A)

8.2 Appendix 2 (Related to chapter 2)

Table S2.1: Operative conditions of the formulations for the Block 1

Table S2.2: Operative conditions of the formulations for Block 2 Experiment 1

Table S2.3: Operative conditions for the formulations for the Block 2 Experiment 3:

Figure S2.1. Statistical analysis of the effect of contact time on EE of DEX leaded PLGA-PEG nanoparticles produced by nanoprecipitation using millifluidic systems. Statistical analysis was performed using Origin Software. The relationship EE against operative conditions was explored using an analysis of variance (ANOVA) with a significance level of $p < 0.05$

Figure S2.2. Statistical analysis of the effect of contact time on DLE of DEX loaded PLGA-PEG nanoparticles produced by nanoprecipitation using millifluidic systems. Statistical analysis was performed using Origin Software. The relationship DLE against operative conditions was explored using an analysis of variance (ANOVA) with a significance level of $p < 0.05$

Table S2.1: Operative conditions of the formulations for the Block 1

	Stream 1					Stream 2			Result					
	Acetone			PLGA-PEG Polymer		Water			Flow			Fractions		
Sample	Fstream1 (Acetone Flow rate)	Acetone Density	Acetone Mass Flow	Conc Polymer	PLGA-PEG Mass Flow	Fstream2 (Water Flow rate)	Water Density	Water Mass Flow	S1/S2	Total Volume Flow	Total Mass Flow	fraction Acetone	fraction Water	fraction PLGA-PEG
-	mL	g/mL	g	mg/mL	g	mL/min	g/mL	g/min	-	mL/min	g/min	-	-	-
1	22.20	0.790	17.54	2.00	0.04	69.00	1.00	69.00	0.32	91.20	86.58	0.203	0.797	5.13E-04
2	22.20	0.790	17.54	4.00	0.09	69.00	1.00	69.00	0.32	91.20	86.63	0.202	0.797	1.03E-03
3	22.20	0.790	17.54	10.00	0.22	69.00	1.00	69.00	0.32	91.20	86.76	0.202	0.795	2.56E-03
4	33.30	0.790	26.31	5.70	0.19	66.60	1.00	66.60	0.50	99.90	93.10	0.283	0.715	2.04E-03
5	33.30	0.790	26.31	20.00	0.67	66.60	1.00	66.60	0.50	99.90	93.57	0.281	0.712	7.12E-03
6	11.10	0.790	8.77	70.00	0.78	100.00	1.00	100.00	0.11	111.10	109.55	0.080	0.913	7.09E-03
7	90.00	0.790	71.10	10.50	0.95	25.00	1.00	25.00	3.60	115.00	97.05	0.733	0.258	9.74E-03
8	90.00	0.790	71.10	145.00	13.05	25.00	1.00	25.00	3.60	115.00	109.15	0.651	0.229	1.20E-01

Table S2.2: Operative conditions of the formulations for Block 2 Experiment 1

	Stream 1							Stream 2			Result						
	Acetone			PLGA-PEG Polymer		DEX		Water			Flows			Fractions			
Sample	Fstream1 (Acetone Flow rate)	Acetone Density	Acetone Mass Flow	Conc Polymer	PLGA-PEG Mass Flow	Conc DEX	DEX Mass Flow	Fstream2 (Water Flow rate)	Water Density	Water Mass Flow	S1/S2	Total Volume Flow	Total Mass Flow	fraction Acetone	fraction Water	fraction PLGA-PEG	fraction DEX
	mL	g/mL	g	mg/mL	g	mg/mL	g	mL/min	g/mL	g/min	-	mL/min	g/min	-	-	-	-
1	11.10	0.790	8.77	20.00	0.22	10.00	0.11	100.00	1.00	100.00	0.11	108.77	108.99	0.080	0.918	2.04E-03	1.02E-03
2	33.30	0.790	26.31	20.00	0.67	10.00	0.33	66.60	1.00	66.60	0.50	92.91	93.57	0.281	0.712	7.12E-03	3.56E-03
3	22.20	0.790	17.54	20.00	0.44	10.00	0.22	69.36	1.00	69.36	0.32	86.90	87.34	0.201	0.794	5.08E-03	2.54E-03
4	33.30	0.790	26.31	5.70	0.19	2.85	0.09	66.60	1.00	66.60	0.50	92.91	93.10	0.283	0.715	2.04E-03	1.02E-03
5	44.40	0.790	35.08	13.75	0.61	6.80	0.30	50.00	1.00	50.00	0.89	85.08	85.69	0.409	0.584	7.12E-03	3.52E-03
6	22.20	0.790	17.54	2.00	0.04	1.00	0.02	69.00	1.00	69.00	0.32	86.54	86.58	0.203	0.797	5.13E-04	2.56E-04

Table S2.3: Operative conditions for the formulations for the Block 2 Experiment 3:

	Stream 1							Stream 2			Result						
	Acetone			PLGA-PEG Polymer		DEX		Water			Flows			Fractions			
Sample	Fstream1 (Acetone Flow rate)	Acetone Density	Acetone Mass Flow	Conc Polymer	PLGA-PEG Mass Flow	Conc DEX	DEX Mass Flow	Fstream2 (Water Flow rate)	Water Density	Water Mass Flow	S1/S2	Total Volume Flow	Total Mass Flow	fraction Acetone	fraction Water	fraction PLGA-PEG	fraction DEX
	mL/min	g/mL	g	mg/mL	g	mg/mL	g	mL/min	g/mL	g/min	-	mL/min	g/min	-	-	-	-
1	22.20	0.790	17.54	2.00	0.04	1.00	0.02	69.00	1.00	69.00	0.32	86.54	86.58	0.203	0.797	5.13E-04	2.56E-04
2	22.20	0.790	17.54	4.00	0.09	1.00	0.02	69.00	1.00	69.00	0.32	86.54	86.63	0.202	0.797	1.03E-03	2.56E-04
3	22.20	0.790	17.54	10.00	0.22	1.00	0.02	69.00	1.00	69.00	0.32	86.54	86.76	0.202	0.795	2.56E-03	2.56E-04
4	22.20	0.790	17.54	28.00	0.62	1.00	0.02	69.00	1.00	69.00	0.32	86.54	87.16	0.201	0.792	7.13E-03	2.55E-04

ANOVAOneWay (2/9/2018 11:09:14)

Descriptive Statistics

	N Analysis	N Missing	Mean	Standard Deviation	SE of Mean
0.17	3	0	43.5	1.865	1.07676
0.5	3	0	47	1.91	1.10274
2	3	0	42.8	1.8	1.03923
24	3	0	45.3	2.18	1.25862
Control	3	0	46.6	2.33	1.34523

One Way ANOVA

Overall ANOVA

	DF	Sum of Squares	Mean Square	F Value	Prob>F
Model	4	41.196	10.299	2.50613	0.1088
Error	10	41.09525	4.10953		
Total	14	82.29125			

Null Hypothesis: The means of all levels are equal.
Alternative Hypothesis: The means of one or more levels are different.
At the 0.05 level, the population means are not significantly different.

Fit Statistics

	R-Square	Coeff Var	Root MSE	Data Mean
	0.50061	0.04501	2.0272	45.04

Figure S2.1. Statistical analysis of the effect of contact time on EE of DEX leaded PLGA-PEG nanoparticles produced by nanoprecipitation using millifluidic systems. Statistical analysis was performed using Origin Software. The relationship EE against operative conditions was explored using an analysis of variance (ANOVA) with a significance level of $p < 0.05$

ANOVAOneWay (2/9/2018 11:09:18)

Input Data

	Data	Range
Dependent Variable	[Book1]"Data full EE and DLE"!D"DLE"	[1*:15*]
Factor	[Book1]"Data full EE and DLE"!I1"Contact Time"	[1*:15*]

Descriptive Statistics

	N Analysis	N Missing	Mean	Standard Deviation	SE of Mean
0.17	3	0	4.7	0.185	0.10681
0.5	3	0	4.8	0.19	0.1097
2	3	0	4.6	0.18	0.10392
24	3	0	4.9	0.22	0.12702
Control	3	0	4.7	0.245	0.14145

One Way ANOVA

Overall ANOVA

	DF	Sum of Squares	Mean Square	F Value	Prob>F
Model	4	0.156	0.039	0.92351	0.48773
Error	10	0.4223	0.04223		
Total	14	0.5783			

Null Hypothesis: The means of all levels are equal.
Alternative Hypothesis: The means of one or more levels are different.
At the 0.05 level, the population means are not significantly different.

Fit Statistics

	R-Square	Coeff Var	Root MSE	Data Mean
	0.26976	0.04335	0.2055	4.74

Figure S2.2. Statistical analysis of the effect of contact time on DLE of DEX loaded PLGA-PEG nanoparticles produced by nanoprecipitation using millifluidic systems. Statistical analysis was performed using Origin Software. The relationship DLE against operative conditions was explored using an analysis of variance (ANOVA) with a significance level of $p < 0.05$

8.3 Appendix 3 (Related to chapter 3)

S3.1 Control Charts

S3.2: Kinetic Release Models

S3.3 ANOVA Test

Figure S3.1. Statistical analysis of the effect of dispersed phase flux on nanoparticle size (Z-Average) of PLGA-PEG nanoparticles produced by membrane-assisted nanoprecipitation.

Figure S3.2. Statistical analysis of the effect of dispersed phase flux on particle-size (PDI) distribution of PLGA-PEG nanoparticles produced by membrane-assisted nanoprecipitation.

Figure S3.3. Statistical analysis of the influence of wall shear stress on nanoparticle size (Z-Average) of PLGA-PEG nanoparticles produced by membrane-assisted nanoprecipitation.

Figure S3.4. Statistical analysis of the influence of wall shear stress on particle-size distribution (PDI) of PLGA-PEG nanoparticles produced by membrane-assisted nanoprecipitation.

Figure S3.5. Statistical analysis of influence of membrane pore size on nanoparticle size (Z-Average) of PLGA-PEG nanoparticles produced by membrane-assisted nanoprecipitation.

Figure S3.6. Statistical analysis of influence of membrane pore size on particle size distribution (PDI) of PLGA-PEG nanoparticles produced by membrane-assisted nanoprecipitation.

S3.1 Control Charts

Control Charts was obtained by calculation media, upper control limit (UCL) and lower control limit (LCL) as following:

$Equation$ S3.1 $$\bar{X} = \frac{X_1 + X_2 + \cdots\ldots + X_n}{n}$$

$Equation$ S3.2 $$\mathrm{LCL} = \bar{X} - \sigma$$

$Equation$ S3.3 $$\mathrm{UCL} = \bar{X} + \sigma$$

Where X is quality characteristic (Z-average or PDI) and σ is standard deviation.

S3.2: Kinetic Release Models

Zero-order release, in which the drug is released at a constant rate (independent of the initial drug concentration), is described by equation S4.

$$\boldsymbol{Equation\ S3.4 \quad Qt = Qo + Ko * t}$$

Where Q_t is amount of dexamethasone dissolved in time t (mg), Q_0 is the initial amount of drug in the solution (mg), t is the time (days) and k_0 is zero order grate constant (mg days^{-1}). This model is generally used for transdermal systems and matrix tablets with low solubility drugs (Dash et al., 2010).

On the other hand, the *first order release model* describes a release process in which the drug rate increases linearly with the increase of drug concentration loaded in the nanoparticle. This model is described by equation S5:

$$Equation\ S3.5 \qquad LOG\ (Qt) = LOG(Qo) + K1 * t$$

Where K1 is the first order rate constant (mg days^{-1}).

This relationship is used to describe the drug release of water-soluble drugs in porous matrices (Dash et al., 2010).

Equation S6 describes the Korsmeyer–Peppas model release. This model describes the drug release in systems where several simultaneous processes occur (i.e. swelling, erosion, dissolution, etc.).

$$\boldsymbol{Equation\ S3.6 \qquad Mt/M_{\infty} = KP * t^{n}}$$

Where Mt/M_{∞} is the fraction of drug released at time t, KP is the rate constant (mg days^{-1}) and n is the release exponent (-). The "n" value is used to characterize the release mechanism of drug: for a Fickian diffusion "n" is about 0.45 while for non-Fickian mechanism "n" in the range between 0.45 and 0.89 (Hines and Kaplan, 2013; Ritger and Peppas, 1987).

Finally, Higuchi model, described by equation 6 is based on Fickian drug diffusion. This model assumes that initial drug concentration in the matrix is much higher than the drug solubility; edge effect, swelling and dissolution of the matrix are negligible, the drug diffusivity is constant and perfect sink conditions are always attained in the release environment. (Dash et al., 2010)

$$Equation\ S3.7 \qquad Mt/M_{\infty} = KH * t^{0.5}$$

Where KH is the dissolution rate constant (mg·days^{-1}).

S3.3 ANOVA Test

Statistical analysis was performed using Origin Software. The relationship Z-Average or PDI against operative conditions was explored using an analysis of variance (ANOVA) with a significance level of $p < 0.05$

Input Data

	Data	Range
Dependent Variable	[Book1]Analysis!C"Z-Average"	[1:18]
Factor A	[Book1]Analysis!A"DP Flux"	[1:18]
Factor B	[Book1]Analysis!B"DP/CP"	[1:18]

Descriptive Statistics

DP Flux

	N	Mean	SD	SEM	Variance	Missing	NonMissing
15.3	6	259.7	34.57022	14.11323	1195.1	0	6
61.3	6	281.11667	21.21673	8.66169	450.14967	0	6
1971	6	254.01667	20.77522	8.48145	431.60967	0	6

DP/CP

	N	Mean	SD	SEM	Variance	Missing	NonMissing
0.32	9	249.17778	11.73028	3.91009	137.59944	0	9
0.83	9	280.71111	30.1241	10.04137	907.46111	0	9

Overall

N	Mean	SD	SEM	Variance	Missing	NonMissing
18	264.94444	27.47733	6.47647	755.00379	0	18

ANOVA

Overall ANOVA

	DF	Sum of Squares	Mean Square	F Value	P Value
DP Flux	2	2450.76778	1225.38389	2.90291	0.08818
DP/CP	1	4474.58	4474.58	10.60019	0.00575
Model	3	6925.34778	2308.44926	5.46867	0.01064
Error	14	5909.71667	422.12262	--	--
Corrected Total	17	12835.06444	--	--	--

At the 0.05 level, the population means of **DP Flux** are **not significantly** different.
At the 0.05 level, the population means of **DP/CP** are **significantly** different.

Figure S3.1. Statistical analysis of the effect of dispersed phase flux on nanoparticle size (Z-Average) of PLGA-PEG nanoparticles produced by membrane-assisted nanoprecipitation.

Input Data

	Data	Range
Dependent Variable	[Book1]Analysis!D"PDI"	[1:18]
Factor A	[Book1]Analysis!A"DP Flux"	[1:18]
Factor B	[Book1]Analysis!B"DP/CP"	[1:18]

Descriptive Statistics

DP Flux

	N	Mean	SD	SEM	Variance	Missing	NonMissing
15.3	6	0.13	0.04627	0.01889	0.00214	0	6
61.3	6	0.15583	0.01664	0.00679	2.76967E-4	0	6
1971	6	0.13317	0.04652	0.01899	0.00216	0	6

DP/CP

	N	Mean	SD	SEM	Variance	Missing	NonMissing
0.32	9	0.14478	0.02892	0.00964	8.36444E-4	0	9
0.83	9	0.13456	0.04761	0.01587	0.00227	0	9

Overall

	N	Mean	SD	SEM	Variance	Missing	NonMissing
	18	0.13967	0.03857	0.00909	0.00149	0	18

ANOVA

Overall ANOVA

	DF	Sum of Squares	Mean Square	F Value	P Value
DP Flux	2	0.00238	0.00119	0.7431	0.49349
DP/CP	1	4.70222E-4	4.70222E-4	0.29335	0.5966
Model	3	0.00285	9.50852E-4	0.59318	0.62968
Error	14	0.02244	0.0016	--	--
Corrected Total	17	0.02529	--	--	--

At the 0.05 level, the population means of **DP Flux** are **not significantly** different.
At the 0.05 level, the population means of **DP/CP** are **not significantly** different.

Figure S3.2. Statistical analysis of the effect of dispersed phase flux on particle-size (PDI) distribution of PLGA-PEG nanoparticles produced by membrane-assisted nanoprecipitation.

ANOVAOneWay (11/19/2016 12:26:06)

Input Data

	Data	Range
Dependent Variable	[Book1]Analysis!C"Z-Average"	[1*:9*]
Factor	[Book1]Analysis!A"ShearStress"	[1*:9*]

Descriptive Statistics

	N Analysis	N Missing	Mean	Standard Deviation	SE of Mean
1.12	3	0	248	11.40526	6.58483
2.48	3	0	261.8	1.96977	1.13725
4.16	3	0	258.73333	3.23161	1.86577

One Way ANOVA

Overall ANOVA

	DF	Sum of Squares	Mean Square	F Value	Prob>F
Model	2	315.04889	157.52444	3.27259	0.1094
Error	6	288.80667	48.13444		
Total	8	603.85556			

Null Hypothesis: The means of all levels are equal.
Alternative Hypothesis: The means of one or more levels are different.
At the 0.05 level, the population means are not significantly different.

Figure S3.3. Statistical analysis of the influence of wall shear stress on nanoparticle size (Z-Average) of PLGA-PEG nanoparticles produced by membrane-assisted nanoprecipitation.

ANOVAOneWay (11/19/2016 12:26:51)

Input Data

	Data	Range
Dependent Variable	[Book1]Analysis!D"PDI"	[1*:9*]
Factor	[Book1]Analysis!A"ShearStress"	[1*:9*]

Descriptive Statistics

	N Analysis	N Missing	Mean	Standard Deviation	SE of Mean
1.12	3	0	0.06467	0.01222	0.00706
2.48	3	0	0.146	0.01778	0.01026
4.16	3	0	0.601	0.78724	0.45451

One Way ANOVA

Overall ANOVA

	DF	Sum of Squares	Mean Square	F Value	Prob>F
Model	2	0.50129	0.25065	1.2124	0.36122
Error	6	1.24041	0.20674		
Total	8	1.74171			

Null Hypothesis: The means of all levels are equal.
Alternative Hypothesis: The means of one or more levels are different.
At the 0.05 level, the population means are not significantly different.

Figure S3.4. Statistical analysis of the influence of wall shear stress on particle-size distribution (PDI) of PLGA-PEG nanoparticles produced by membrane-assisted nanoprecipitation.

Input Data

	Data	Range
Dependent Variable	[Book1]Analysis!D"Z-Average"	[1:12]
Factor A	[Book1]Analysis!B"Memb Pore"	[1:12]
Factor B	[Book1]Analysis!C"DP/CP"	[1:12]

Descriptive Statistics

Memb Pore

	N	Mean	SD	SEM	Variance	Missing	NonMissing
1 um	6	281.11667	21.21673	8.66169	450.14967	0	6
0.2 um	6	249.16667	42.99998	17.55467	1848.99867	0	6

DP/CP

	N	Mean	SD	SEM	Variance	Missing	NonMissing
0.32	6	235.95	28.63241	11.68913	819.815	0	6
0.83	6	294.33333	6.82984	2.78827	46.64667	0	6

Overall

N	Mean	SD	SEM	Variance	Missing	NonMissing
12	265.14167	36.3795	10.50186	1323.46811	0	12

ANOVA

Overall ANOVA

	DF	Sum of Squares	Mean Square	F Value	P Value
Memb Pore	1	3062.4075	3062.4075	21.7038	0.00119
DP/CP	1	10225.84083	10225.84083	72.47225	1.34262E-5
Model	2	13288.24833	6644.12417	47.08802	1.70996E-5
Error	9	1269.90083	141.10009	--	--
Corrected Total	11	14558.14917	--	--	--

At the 0.05 level, the population means of **Memb Pore** are **significantly** different.
At the 0.05 level, the population means of **DP/CP** are **significantly** different.

Figure S3.5. Statistical analysis of influence of membrane pore size on nanoparticle size (Z-Average) of PLGA-PEG nanoparticles produced by membrane-assisted nanoprecipitation.

Input Data

	Data	Range
Dependent Variable	[Book1]Analysis!E"PDI"	[1:12]
Factor A	[Book1]Analysis!B"Memb Pore"	[1:12]
Factor B	[Book1]Analysis!C"DP/CP"	[1:12]

Descriptive Statistics

Memb Pore

	N	Mean	SD	SEM	Variance	Missing	NonMissing
1 um	6	0.15583	0.01664	0.00679	2.76967E-4	0	6
0.2 um	6	0.1885	0.0716	0.02923	0.00513	0	6

DP/CP

	N	Mean	SD	SEM	Variance	Missing	NonMissing
0.32	6	0.199	0.0598	0.02441	0.00358	0	6
0.83	6	0.14533	0.0272	0.0111	7.39867E-4	0	6

Overall

	N	Mean	SD	SEM	Variance	Missing	NonMissing
	12	0.17217	0.05241	0.01513	0.00275	0	12

ANOVA

Overall ANOVA

	DF	Sum of Squares	Mean Square	F Value	P Value
Memb Pore	1	0.0032	0.0032	1.56791	0.24207
DP/CP	1	0.00864	0.00864	4.23177	0.0698
Model	2	0.01184	0.00592	2.89984	0.10665
Error	9	0.01838	0.00204	--	--
Corrected Total	11	0.03022	--	--	--

At the 0.05 level, the population means of **Memb Pore** are **not significantly** different.
At the 0.05 level, the population means of **DP/CP** are **not significantly** different.

Figure S3.6. Statistical analysis of influence of membrane pore size on particle size distribution (PDI) of PLGA-PEG nanoparticles produced by membrane-assisted nanoprecipitation.

8.4 Appendix 4 (Related to chapter 4)

An intensification analysis was made dividing the analysis in Mass balance, economic, green analysis and energy consumption.

Table S4.1: Intensification analysis from our work using EA as solvent and Vsd/Vtho equal 0

Table S4.2: Intensification analysis from our work using EA as solvent and Vsd/Vtho equal 0.5

Table S4.3: Intensification analysis from our work using EA as solvent and Vsd/Vtho equal 1

Table S4.4: Intensification analysis from our work using EA as solvent and Vsd/Vtho equal 3

Table S4.5: Intensification analysis from our work using DCM as solvent and Vsd/Vtho equal 3

Table S4.6: Intensification analysis using data from Kim and Martin, 2006 (Kim et Martin 2006)

Table S4.7: Intensification analysis using data from Gu and Burgess, 2015 (Gu et Burgess 2015)

Table S4.8: Intensification analysis using data from Park et al, 2009 (Park et al. 2009)

Table S4.9: Intensification analysis using data from Goodfriend et al, 2016 (Goodfriend et al. 2016)

Table S4.10: Intensification analysis using data from Ho et al, 2013 (Ho et al. 2013)

Table S4.11: Intensification analysis using data from Gasparini et al, 2008 (Gasparini et al. 2008)

References

Gasparini, G., S.R. Kosvintsev, M.T. Stillwell, et R.G. Holdich. 2008. « Preparation and Characterization of PLGA Particles for Subcutaneous Controlled Drug Release by Membrane Emulsification ». *Colloids and Surfaces B: Biointerfaces* 61 (2): 199-207. https://doi.org/10.1016/j.colsurfb.2007.08.011.

Goodfriend, Amy C., Tré R. Welch, Kytai T. Nguyen, Romaine F. Johnson, Vinod Sebastian, Surendranath Veeram Reddy, Joseph Forbess, et Alan Nugent. 2016. « Thermally Processed Polymeric Microparticles for Year-Long Delivery of Dexamethasone ». *Materials Science and Engineering: C* 58 (janvier): 595-600. https://doi.org/10.1016/j.msec.2015.09.003.

Gu, Bing, et Diane J. Burgess. 2015. « Prediction of Dexamethasone Release from PLGA Microspheres Prepared with Polymer Blends Using a Design of Experiment Approach ». *International Journal of Pharmaceutics* 495 (1): 393-403. https://doi.org/10.1016/j.ijpharm.2015.08.089.

Ho, Thanh Ha, Thi Phuong Tuyen Dao, Tuan Anh Nguyen, Duy Dam Le, et Mau Chien Dang. 2013. « Cross-flow membrane emulsification technique for fabrication of drug-loaded particles ». *Advances in Natural Sciences: Nanoscience and Nanotechnology* 4 (4): 045008. https://doi.org/10.1088/2043-6262/4/4/045008.

Kim, Dong-Hwan, et David C. Martin. 2006. « Sustained Release of Dexamethasone from Hydrophilic Matrices Using PLGA Nanoparticles for Neural Drug Delivery ». *Biomaterials* 27 (15): 3031-37. https://doi.org/10.1016/j.biomaterials.2005.12.021.

Park, Ji S., Kun Na, Dae G. Woo, Han N. Yang, et Keun-Hong Park. 2009. « Determination of Dual Delivery for Stem Cell Differentiation Using Dexamethasone and TGF-B3 in/on Polymeric Microspheres ». *Biomaterials* 30 (27): 4796-4805. https://doi.org/10.1016/j.biomaterials.2009.05.054.

Table S4.1: Intensification analysis from our work using EA as solvent and Vsd/Vtho equal 0

		EA; Vsd/Vtheo :0			
Materials			**Phases Components**		
Raw Materials			**Dispersed Phase**	**Continuous Phase**	
Polymer	PLGA		PLGA	Water	
Drug	DEX		DEX	Pluronic F127	
Reagent			EA		
Surfactant	Pluronic F127				
Solvent			**Phases Volumens (mL)**		
Solvent 1	EA		Dispersed Phase	5	
Water			Continuous Phase	25	
			Ratio DP/CP	0.20	
EA Solubility (mL EA/mL T)			Total Emulsion Volume	30.00	
EA Solubility	0.097		Vtho	76.55	
			Buffer Volume (Vsd)	0.00	
Vsd/Vtheo			Total Volume	30.00	
Vsd/Vtheo	0		EA	7.43	
			Water	22.58	
Mass Balance					
Classification	**Material**	**Volume (mL)**	**Mass (mg)**	**Concentration or Density (mg/mL)**	
Raw Materials	PLGA	5.00	50.00	10.00	
	DEX	5.00	5.00	1.00	
Reagent	Pluronic F127	25.00	290.00	11.60	
	Pluronic F127	0.00	0.00	11.60	
Solvent	EA	7.43	6697.35	902.00	
Water	Water	22.58	22575.00	1000.00	
Green Analysis					
m(Raw Materials) mg	5.50E+01		**sEF**	5.90	
m(Reagents) mg	2.90E+02		**cEF**	591.35	
m(Solvents) mg	6.70E+03		**% cEF litd**	1.00%	
m(Water) mg	2.26E+04		**% solvent + water**	98.84%	
Total	2.96E+04				
m(Product) mg	5.00E+01				
Economic Analysis					
Material	**Mass (mg)**	**Cost (Euros/mg)**	**Total Cost (Euros)**	**Euros/g product**	
PLGA	50.00	5.00E-02	2.50	50.00	
DEX	5.00	3.45E-01	1.73	34.50	
Pluronic F127	290.00	2.00E-03	0.58	11.60	
EA	6697.35	4.00E-06	0.03	0.54	
Water	22575.00	1.00E-06	0.02	0.45	
	Total (Euros)		4.85		
	Total (Euros/mg product)		97.09		
Energy Consumption					
DP Flow (L/hm2)	2.52		**Productivity (m3/S)**	1.32E-08	
CP Flow (m3/s)	8.33E-06		**Energy pump (W)**	5.21E-03	
Time (s)	2280.00		**Energy Density (J/m3)**	3.96E+05	
Volume (m3)	3.00E-05				
CP Presure (Pa)	500.00				
Efficiency pump	0.8				

Table S4.2: Intensification analysis from our work using EA as solvent and Vsd/Vtho equal 0.5

EA; Vsd/Vtheo :0.5				
Materials			**Phases Components**	
Raw Materials			**Dispersed Phase**	**Continuous Phase**
Polymer	PLGA		PLGA	Water
Drug	DEX		DEX	Pluronic F127
Reagent			EA	
Surfactant	Pluronic F127			
Solvent			**Phases Volumens (mL)**	
Solvent 1	EA		Dispersed Phase	5.00
Water			Continuous Phase	25.00
			Ratio DP/CP	0.20
EA Solubility (mL EA/mL T)			Total Emulsion Volume	30.00
EA Solubility	0.097		Vtho	76.55
			Buffer Volume (Vsd)	38.27
Vsd/Vtheo			Total Volume	68.27
Vsd/Vtheo	0.50		EA	7.43
			Water	60.85

Mass Balance

Classification	Material	Volume (mL)	Mass (mg)	Concentration or Density (mg/mL)
Raw Materials	PLGA	5.00	50.00	10.00
	DEX	5.00	5.00	1.00
Reagent	Pluronic F127	25.00	290.00	11.60
	Pluronic F127	38.27	443.97	11.60
Solvent	EA	7.43	6697.35	902.00
Water	Water	60.85	60848.20	1000.00

Green Analysis

m(Raw Materials) mg	5.50E+01		**sEF**	14.78
m(Reagents) mg	7.34E+02		**cEF**	1365.69
m(Solvents) mg	6.70E+03		**% cEF litd**	1.08%
m(Water) mg	6.08E+04		**% solvent + water**	98.85%
Total	6.83E+04			
m(Product) mg	5.00E+01			

Economic Analysis

Material	Mass (mg)	Cost (Euros/mg)	Total Cost (Euros)	Euros/g product
PLGA	50.00	5.00E-02	2.50	50.00
DEX	5.00	3.45E-01	1.73	34.50
Pluronic F127	733.97	2.00E-03	1.47	29.36
EA	6697.35	4.00E-06	0.03	0.54
Water	60848.20	1.00E-06	0.06	1.22
	Total (Euros)		5.78	
	Total (Euros/mg product)		115.61	

Energy Consumption

DP Flow (L/hm2)	2.52		**Productivity (m3/S)**	1.32E-08
CP Flow (m3/s)	8.33E-06		**Energy pump (W)**	5.21E-03
Time (s)	2280.00		**Energy Density (J/m3)**	3.96E+05
Volume (m3)	3.00E-05			
CP Presure (Pa)	500.00			
Efficiency pump	0.80			

Table S4.3: Intensification analysis from our work using EA as solvent and Vsd/Vtho equal 1

		EA; Vsd/Vtheo :1		
Materials			**Phases Components**	
Raw Materials			**Dispersed Phase**	**Continuous Phase**
Polymer	PLGA		PLGA	Water
Drug	DEX		DEX	Pluronic F127
Reagent			EA	
Surfactant	Pluronic F127			
Solvent			**Phases Volumens (mL)**	
Solvent 1	EA		Dispersed Phase	5.00
Water			Continuous Phase	25.00
			Ratio DP/CP	0.20
EA Solubility (mL EA/mL T)			Total Emulsion Volume	30.00
EA Solubility	0.097		Vtho	76.55
			Buffer Volume (Vsd)	76.55
Vsd/Vtheo			Total Volume	106.55
Vsd/Vtheo	1		EA	7.43
			Water	99.12

Mass Balance

Classification	Material	Volume (mL)	Mass (mg)	Concentration or Density (mg/mL)
Raw Materials	PLGA	5.00	50.00	10.00
	DEX	5.00	5.00	1.00
Reagent	Pluronic F127	25.00	290.00	11.60
	Pluronic F127	76.55	887.94	11.60
Solvent	EA	7.43	6697.35	902.00
Water	Water	99.12	99121.39	1000.00

Green Analysis

m(Raw Materials) mg	5.50E+01	**sEF**	23.66
m(Reagents) mg	1.18E+03	**cEF**	2140.03
m(Solvents) mg	6.70E+03	**% cEF litd**	1.11%
m(Water) mg	9.91E+04	**% solvent + water**	98.85%
Total	1.07E+05		
m(Product) mg	5.00E+01		

Economic Analysis

Material	Mass (mg)	Cost (Euros/mg)	Total Cost (Euros)	Euros/g product
PLGA	50.00	5.00E-02	2.50	50.00
DEX	5.00	3.45E-01	1.73	34.50
Pluronic F127	1177.94	2.00E-03	2.36	47.12
EA	6697.35	4.00E-06	0.03	0.54
Water	99121.39	1.00E-06	0.10	1.98
	Total (Euros)		6.71	
	Total (Euros/mg product)		134.14	

Energy Consumption

DP Flow (L/hm2)	2.52	**Productivity (m3/S)**	1.32E-08
CP Flow (m3/s)	8.33E-06	**Energy pump (W)**	5.21E-03
Time (s)	2280.00	**Energy Density (J/m3)**	3.96E+05
Volume (m3)	3.00E-05		
CP Presure (Pa)	500.00		
Efficiency pump	0.80		

Table S4.4: Intensification analysis from our work using EA as solvent and Vsd/Vtho equal 3

		EA; Vsd/Vtheo :3		
Materials			**Phases Components**	
Raw Materials			**Dispersed Phase**	**Continuous Phase**
Polymer	PLGA		PLGA	Water
Drug	DEX		DEX	Pluronic F127
Reagent			EA	
Surfactant	Pluronic F127			
Solvent			**Phases Volumens (mL)**	
Solvent 1	EA		Dispersed Phase	5.00
Water			Continuous Phase	25.00
			Ratio DP/CP	0.20
EA Solubility (mL EA/mL T)			Total Emulsion Volume	30.00
EA Solubility	0.097		Vtho	76.55
			Buffer Volume (Vsd)	229.64
Vsd/Vtheo			Total Volume	259.64
Vsd/Vtheo	3		EA	7.43
			Water	252.21

Mass Balance

Classification	**Material**	**Volume (mL)**	**Mass (mg)**	**Concentration or Density (mg/mL)**
Raw Materials	PLGA	5.00	50.0	10.00
	DEX	5.00	5.0	1.00
Reagent	Pluronic F127	25.00	290.0	11.60
	Pluronic F127	229.64	2663.8	11.60
Solvent	EA	7.43	6697.4	902.00
Water	Water	252.21	252214.2	1000.00

Green Analysis

m(Raw Materials) mg	5.50E+01	**sEF**	59.18
m(Reagents) mg	2.95E+03	**cEF**	5237.41
m(Solvents) mg	6.70E+03	**% cEF litd**	1.13%
m(Water) mg	2.52E+05	**% solvent + water**	98.85%
Total	2.62E+05		
m(Product) mg	5.00E+01		

Economic Analysis

Material	**Mass (mg)**	**Cost (Euros/mg)**	**Total Cost (Euros)**	**Euros/g product**
PLGA	50.00	5.00E-02	2.50	50.00
DEX	5.00	3.45E-01	1.73	34.50
Pluronic F127	2953.81	2.00E-03	5.91	118.15
EA	6697.35	4.00E-06	0.03	0.54
Water	252214.18	1.00E-06	0.25	5.04
	Total (Euros)		10.41	
	Total (Euros/mg product)		208.23	

Energy Consumption

DP Flow (L/hm2)	2.52	**Productivity (m3/S)**	1.32E-08
CP Flow (m3/s)	8.33E-06	**Energy pump (W)**	5.21E-03
Time (s)	2280.00	**Energy Density (J/m3)**	3.96E+05
Volume (m3)	3.00E-05		
CP Presure (Pa)	500.00		
Efficiency pump	0.80		

Table S4.5: Intensification analysis from our work using DCM as solvent and Vsd/Vtho equal 3

DCM; Vsd/Vtheo :3				
Materials			**Phases Components**	
Raw Materials			**Dispersed Phase**	**Continuous Phase**
Polymer	PLGA		PLGA	Water
Drug	DEX		DEX	Pluronic F127
Reagent			DCM	
Surfactant	Pluronic F127			
Solvent			**Phases Volumens (mL)**	
Solvent 1	DCM		Dispersed Phase	5.00
Water			Continuous Phase	25.00
			Ratio DP/CP	0.20
DCM Solubility (mL EA/mL T)			Total Emulsion Volume	30.00
DCM Solubility	0.013		Vtho	409.62
			Buffer Volume (Vsd)	1228.85
Vsd/Vtheo			Total Volume	1258.85
Vsd/Vtheo	3		DCM	5.33
			Water	1253.52

Mass Balance

Classification	Material	Volume (mL)	Mass (mg)	Concentration or Density (mg/mL)
Raw Materials	PLGA	5.00	50	10.00
	DEX	5.00	5	1.00
Reagent	Pluronic F127	25.00	290	11.60
	Pluronic F127	1228.85	14254.61538	11.60
Solvent	DCM	5.33	7098.225	1333.00
Water	Water	1253.52	1253521.154	1000.00

Green Analysis

m(Raw Materials) mg	5.50E+01		**sEF**	290.99
m(Reagents) mg	1.45E+04		**cEF**	25503.38
m(Solvents) mg	7.10E+03		**% cEF litd**	1.14%
m(Water) mg	1.25E+06		**% solvent + water**	98.86%
Total	1.28E+06			
m(Product) mg	5.00E+01			

Economic Analysis

Material	Mass (mg)	Cost (Euros/mg)	Total Cost (Euros)	Euros/g product
PLGA	50.00	5.00E-02	2.50	50.00
DEX	5.00	3.45E-01	1.73	34.50
Pluronic F127	14544.62	2.00E-03	29.09	581.78
DCM	7098.23	4.00E-06	0.03	0.57
Water	1253521.15	1.00E-06	1.25	25.07
	Total (Euros)		34.60	
	Total (Euros/g product)		691.92	

Energy Consumption

DP Flow (L/hm2)	2.52	**Productivity (m3/S)**	1.32E-08
CP Flow (m3/s)	8.33E-06	**Energy pump (W)**	5.21E-03
Time (s)	2280.00	**Energy Density (J/m3)**	3.96E+05
Volume (m3)	3.00E-05		
CP Presure (Pa)	500.00		
Efficiency pump	0.80		

Table S4.6: Intensification analysis using data from Kim and Martin, 2006 (Kim et Martin 2006)

(Kim and Martin 2006)				
Materials			**Phases Components**	
Raw Materials			**Dispersed Phase**	**Continuous Phase**
Polymer	PLGA		PLGA	Water
Drug	DEX		DEX	PVA
Reagent			DCM	
Surfactant	PVA		Acetone	
Solvent				
Solvent 1	DCM			
Solvent 2	Acetone		**Phases Volumens (mL)**	
Water			Dispersed Phase	30.00
			Continuous Phase	150.00
			Ratio DP/CP	0.20
m(Product) mg	800.00		Total Volume	180.00

Mass Balance				
Classification	**Material**	**Volume (mL)**	**Mass (mg)**	**Concentration or Density (mg/mL)**
Raw Materials	PLGA	30.00	800.00	26.67
	DEX	30.00	200.00	6.67
Reagent	PVA	150.00	7500.00	50.00
Solvent	DCM	15.00	19950.00	1330.00
	Acetone	15.00	11865.00	791.00
Water	Water	150.00	150000.00	1000.00

Energy Consumption			
Power (W)	60.00	**Productivity (m3/S)**	3.00E-07
Time (s)	600.00	**Energy Density (J/m3)**	2.00E+08
Volume (m3)	1.80E-04		

Economic Analysis				
Material	**Mass (mg)**	**Cost (Euros/mg)**	**Total Cost (Euros)**	**Material Cost (Euros/g product)**
PLGA	800.00	5.00E-02	40.00	50.00
DEX	200.00	3.45E-01	69.00	86.25
PVA	7500.00	2.00E-03	15.00	18.75
DCM	19950.00	4.00E-06	0.08	0.10
Acetone	11865.00	4.00E-06	0.05	0.06
Water	150000.00	1.00E-06	0.15	0.19
	Total (Euros)		124.28	
	Total (Euros/g product)		155.35	

Product Obtained			
Size and Distribution um	0.4–0.6	**DL %**	13±3
EE %	79±5	**Polydispersity**	N/A

Assumptions

The nanoparticles preparation was only the PLGA process, not the alginate hydrogel preparation

The ratio DP/CP =0.2

Mass the product (mg) is equal mass of polymer (mg)

The energy consumtion was calculated taken into account only the emulsion production

Table S4.7: Intensification analysis using data from Gu and Burgess, 2015 (Gu et Burgess 2015)

(Gu and Burgess 2015)				
Materials			**Phases Components**	
Raw Materials			**Dispersed Phase**	**Continuous Phase**
Polymer	PLGA		PLGA	Water
Drug	DEX		DEX	PVA
Reagent			Methylene choride	
Surfactant	PVA			
Solvent				
Solvent 1	Methylene choride		**Phases Volumens (mL)**	
Water			Dispersed Phase	2.00
			Continuous Phase	10.00
			Ratio DP/CP	0.20
			Total Emulsion Volume	12.00
m(Product) mg	440.54		Solidif Buffer	125.00
			Total Volume	137.00

Mass Balance

Classification	Material	Volume (mL)	Mass (mg)	Concentration or Density (mg/mL)
Raw Materials	PLGA	2.00	440.54	220.27
	DEX	2.00	89.87	44.94
Reagent	PVA	10.00	100.00	10.00
	PVA	125.00	125.00	1.00
Solvent	Methylene choride	2.00	2650.00	1325.00
Water	Water	135.00	135000.00	1000.00

Green Analysis

m(Raw Materials) mg	5.30E+02		**sEF**	0.7
m(Reagents) mg	2.25E+02		**cEF**	313.2
m(Solvents) mg	2.65E+03		**% cEF litd**	0.23%
m(Water) mg	1.35E+05		**% solvent + water**	99.45%
Total	1.38E+05			
m(Product) mg	4.41E+02			

Energy Consumption

Power (W)	320.00		**Productivity (m3/S)**	2.00E-07
Time (s)	60.00		**Energy Density (J/m3)**	1.60E+09
Volume (m3)	1.20E-05			

Economic Analysis

Material	Mass (mg)	Cost (Euros/mg)	Total Cost (Euros)	Material Cost (Euros/g product)
PLGA	440.54	5.00E-02	22.03	50.00
DEX	89.87	3.45E-01	31.01	70.38
PVA	100.00	2.00E-03	0.20	0.45
PVA	125.00	2.00E-03	0.25	0.57
Methylene choride	2650.00	4.00E-06	0.01	0.02
Water	135000.00	1.00E-06	0.14	0.31
	Total (Euros)		53.63	
	Total (Euros/g product)		121.73	

Product Obtained

Size and Distribution um	15		**DL %**	15.9
EE %	93.8		**Polydispersity**	N/A

Maximun Drug Loading and EE was selected (CCD-18)
Mass the product (mg) is equal mass of polymer (mg)
The energy consumtion was calculated taken into account only the emulsion production
The power of the homogenizer was adjusted to the rpm used in the process

Table S4.8: Intensification analysis using data from Park et al, 2009 (Park et al. 2009)

		(Park et al. 2009)		
Materials			**Phases Components**	
Raw Materials			**Dispersed Phase**	**Continuous Phase**
Polymer	PLGA		PLGA	Water
Drug	DEX		DEX	PVA
Reagent			DCM	
Surfactant	PVA			
Solvent				
Solvent 1	DCM			
Water			**Phases Volumens (mL)**	
			Dispersed Phase	30.00
			Continuous Phase	300.00
			Ratio DP/CP	0.10
m(Product) mg	4000.00		Total Volume	330.00

Mass Balance

Classification	Material	Volume (mL)	Mass (mg)	Concentration or Density (mg/mL)
Raw Materials	PLGA	30.00	4000.00	133.33
	DEX	30.00	40.00	1.33
Reagent	PVA	300.00	6000.00	20.00
Solvent	DCM	30.00	39900.00	1330.00
Water	Water	300.00	300000.00	1000.00

Energy Consumption

Power (W)	60.00	**Productivity (m3/S)**	5.50E-07
Time (s)	600.00	**Energy Density (J/m3)**	1.09E+08
Volume (m3)	3.30E-04		

Economic Analysis

Material	Mass (mg)	Cost (Euros/mg)	Total Cost (Euros)	Material Cost (Euros/g product)
PLGA	4000.00	5.00E-02	200.00	50.00
DEX	40.00	3.45E-01	13.80	3.45
PVA	6000.00	2.00E-03	12.00	3.00
DCM	39900.00	4.00E-06	0.16	0.04
Water	300000.00	1.00E-06	0.30	0.08
	Total (Euros)		226.26	
	Total (Euros/g product)		56.56	

Product Obtained

Size and Distribution um	20.0	**DL %**	N/A
EE %	N/A	**Polydispersity**	N/A

Assumptions

The nanoparticles preparation was only the PLGA process, not wash and other steps

The ratio DP/CP =0.2

Mass the product (mg) is equal mass of polymer (mg)

The energy consumtion was calculated taken into account only the emulsion production

Table S4.9: Intensification analysis using data from Goodfriend et al, 2016 (Goodfriend et al. 2016)

(Goodfriend et al. 2016)				
Materials			**Phases Components**	
Raw Materials			**Dispersed Phase**	**Continuous Phase**
Polymer	PLGA		PLGA	Water
Drug	DEX		DEX	Pluronic F127
Reagent			Tetrahydrofloran	
Surfactant	Pluronic F127			
Solvent				
Solvent 1	Tetrahydrofloran			
Water			**Phases Volumens (mL)**	
			Dispersed Phase	5.00
			Continuous Phase	5.00
			Ratio DP/CP	1.00
m(Product) mg	1000.00		Total Volume	10.00

Mass Balance

Classification	Material	Volume (mL)	Mass (mg)	Concentration or Density (mg/mL)
Raw Materials	PLGA	5.00	1000.00	200.00
	DEX	5.00	625.00	125.00
Reagent	Pluronic F127	5.00	17.50	3.50
Solvent	Tetrahydrofloran	5.00	4445.00	889.00
Water	Water	5.00	5000.00	1000.00

Energy Consumption

Power (W)	140.00	**Productivity (m3/S)**	5.56E-09
Time (s)	1800.00	**Energy Density (J/m3)**	2.52E+10
Volume (m3)	1.00E-05		

Economic Analysis

Material	Mass (mg)	Cost (Euros/mg)	Total Cost (Euros)	Material Cost (Euros/g product)
PLGA	1000.00	5.00E-02	50.00	50.00
DEX	625.00	3.45E-01	215.63	215.63
Pluronic F127	17.50	2.00E-03	0.04	0.04
Tetrahydrofloran	4445.00	4.00E-06	0.02	0.02
Water	5000.00	1.00E-06	0.01	0.01
	Total (Euros)		265.68	
	Total (Euros/mg product)		265.68	

Product Obtained

Size and Distribution um	50.00	**DL %**	N/A
EE %	60.00	**Polydispersity**	N/A

Assumptions

The nanoparticles preparation was only the PLGA process, not wash and other steps

The sonication bath potency was assumed as 140W (average values of differences commercial equipment

Mass the product (mg) is equal mass of polymer (mg)

The energy consumtion was calculated taken into account only the emulsion production

Table S4.10: Intensification analysis using data from Ho et al, 2013 (Ho et al. 2013)

(Ho et al. 2013)				
Materials			**Phases Components**	
Raw Materials			**Dispersed Phase**	**Continuous Phase**
Polymer	PLGA		PLGA	Water
Drug	curcumin		DEX	PVA
Reagent			Cloroform	
Surfactant	PVA			
Solvent			**Phases Flow (mL/s)**	
Solvent 1	Cloroform		Dispersed Phase	0.002
Water				
			Phases Volumens (mL)	
Time (s)	300.00		Dispersed Phase	0.60
			Continuous Phase	6.00
m(Product) mg	6.00		Ratio DP/CP	0.10
			Total Volume	6.60

Mass Balance

Classification	Material	Volume (mL)	Mass (mg)	Concentration or Density (mg/mL)
Raw Materials	PLGA	0.60	6.00	10.00
	curcumin	0.60	0.60	1.00
Reagent	PVA	6.00	60.00	10.00
Solvent	Cloroform	0.60	888.00	1480.00
Water	Water	6.00	6000.00	1000.00

Energy Consumption

Power (W)	5.04	**Productivity (m3/S)**	2.20E-08
Time (s)	300.00	**Energy Density (J/m3)**	2.29E+08
Volume (m3)	6.60E-06		

Economic Analysis

Material	Mass (mg)	Cost (Euros/mg)	Total Cost (Euros)	Material Cost (Euros/g product)
PLGA	6.00	5.00E-02	0.30	50.00
curcumin	0.60	3.45E-01	0.21	34.50
PVA	60.00	2.00E-03	0.12	20.00
Cloroform	888.00	4.00E-06	0.00	0.59
Water	6000.00	1.00E-06	0.01	1.00
	Total (Euros)		0.64	
	Total (Euros/mg product)		106.09	

Product Obtained

Size and Distribution um	2.3	**DL %**	2
EE %	32	**Polydispersity**	N/A

Assumptions

The nanoparticles preparation was only the PLGA process, not wash and other steps

The pump used was HF-8367 from Headon with Voltaje: 24V and Amp:0.21A = 5.04W

Mass the product (mg) is equal mass of polymer (mg)

The energy consumtion was calculated taken into account only the emulsion production

Table S4.11: Intensification analysis using data from Gasparini et al, 2008 (Gasparini et al. 2008)

(Gasparini et al. 2008)				
Materials			**Phases Components**	
Raw Materials			**Dispersed Phase**	**Continuous Phase**
Polymer	PLGA		PLGA	Water
Drug	N/A		DCM	PVA
Reagent				
Surfactant	PVA			
Solvent			**Phases Flow (mL/s)**	
Solvent 1	DCM		Dispersed Phase	0.0083
Water				
			Phases Volumens (mL)	
Time (s)	1200.00		Dispersed Phase	10.00
			Continuous Phase	150.00
m(Product) mg	1500.00		Ratio DP/CP	0.07
			Total Volume	160.00

Mass Balance

Classification	Material	Volume (mL)	Mass (mg)	Concentration or Density (mg/mL)
Raw Materials	PLGA	10.00	1500.00	150.00
	N/A	0.00	0.00	0.00
Reagent	PVA	150.00	1500.00	10.00
Solvent	DCM	10.00	13300.00	1330.00
Water	Water	150.00	150000.00	1000.00

Energy Consumption

Power (W)	30.00	**Productivity (m3/S)**	1.33E-07
Time (s)	1200.00	**Energy Density (J/m3)**	2.25E+08
Volume (m3)	1.60E-04		

Economic Analysis

Material	Mass (mg)	Cost (Euros/mg)	Total Cost (Euros)	Material Cost (Euros/g product)
PLGA	1500.00	5.00E-02	75.00	50.00
N/A	0.00	3.45E-01	0.00	0.00
PVA	1500.00	2.00E-03	3.00	2.00
DCM	13300.00	4.00E-06	0.05	0.04
Water	150000.00	1.00E-06	0.15	0.10
	Total (Euros)		78.20	
	Total (Euros/mg product)		52.14	

Product Obtained

Size and Distribution um	60	**DL %**	N/A
EE %	N/A	**Polydispersity**	N/A

Assumptions

The nanoparticles preparation was only the PLGA process, not wash and other steps

The PLGA concentration was selected as 15%, using the best condition obtained

Mass the product (mg) is equal mass of polymer (mg)

The potency of dispersion cell from Micropore Technology (Stirrer PSU 130 Adjustable Benchtop)